Ultrasound-Guided Peripheral Nerve Blocks

Enzo Silvestri
Fabio Martino
Filomena Puntillo
Editors

Springer

Ultrasound-Guided Peripheral Nerve Blocks

Enzo Silvestri · Fabio Martino
Filomena Puntillo
Editors

Ultrasound-Guided Peripheral Nerve Blocks

Springer

Editors
Enzo Silvestri
Department of Radiology
Ospedale Evangelico Internazionale
Genova, Italy

Fabio Martino
Radiology Department
Distretto Socio Sanitario
Mola di Bari, Bari, Italy

Filomena Puntillo
Department of Emergency and Organ
Transplants
University of Bari Aldo Moro
Piazza Umberto, Bari, Italy

ISBN 978-3-319-71019-8 ISBN 978-3-319-71020-4 (eBook)
https://doi.org/10.1007/978-3-319-71020-4

Library of Congress Control Number: 2018935293

Printed on acid-free paper

This Springer imprint is published by the registered company Springer International Publishing AG part of Springer Nature.
The registered company address is: Gewerbestrasse 11, 6330 Cham, Switzerland

Foreword

It is my great pleasure and privilege to introduce another volume on peripheral nervous system ultrasound anatomy, peripheral nerve pathology imaging, and ultrasound-aided regional anesthesia and pain management edited by Enzo Silvestri, Fabio Martino, and Filomena Puntillo.

Ultrasound is an emergent imaging modality that is widely used to assess peripheral nerve neuropathies. Among its many features, it is the only imaging modality that is able to perform dynamic evaluations of the soft tissues related to the musculoskeletal system and without patient exposure to ionizing radiation. Also, in expert hands, ultrasound enables the precise guidance of needles within soft tissues and joints, for use in regional anesthesia for a wide range of nerve blocks and for interventional pain management for relief of acute, chronic non-cancer, and cancer pain.

The book consists of three parts. In the first one, general knowledge on ultrasonography and peripheral nervous system ultrasound anatomy is presented. In the second part, concepts of nerve pathology and nerve entrapment syndromes are discussed with an emphasis on the most appropriate use of each imaging modality. In the third part, ultrasound-guided nerve blocks are pictorially presented offering point-by-point checklists for each procedure together with detailed anatomic schemes.

I would also like to emphasize that this handbook is based both on data obtained from the literature and the daily experience of authors who are all recognized opinion leaders in radiology, anesthesiology, and pain medicine. It therefore describes different approaches for the same procedure, allowing the reader to select the most suitable for the particular application.

I would like to thank and to congratulate most sincerely the editors and the authors for their efforts, which have resulted in this comprehensive but well-balanced and very readable text, completed with a remarkable ultrasound-guided nerve blocks section and a large series of dedicated didactic schemes.

This book will be of great value to both anaesthesiologists and radiologists, with a different level of experience, ranging from the physician in training to the one who already performs the treated procedures with traditional technique and want to become familiar with US guidance. It will provide

them with the state-of-the-art knowledge in the specific fields of peripheral nerve sonoanatomy and ultrasound-aided regional anesthesia and pain management.

I am confident that it will meet the same success with the readers as the previous volumes published in this series.

Genova, Italy Giacomo Garlaschi

Contents

Contributors

Marco Baciarello Department of Medicine and Surgery, University of Parma, Parma, Italy

Silvia Perugin Bernardi, M.D. Postgraduate School of Radiology, Genoa University, Genova, Italy

Laura Bertini Anaethesia and Pain Unit, Santa Caterina Hospital, Rome, Italy

Mario Bosco Anaesthesia and Intensive Care Unit, Santo Spirito Hospital, Rome, Italy

Angelo Corazza, M.D. Department of Diagnostic and Interventional Radiology, IRCCS Istituto Ortopedico Galeazzi, Milano, Italy

Gianluigi Martino, M.D. Department of Radiology, Ospedale di Venere, Bari, Italy

Fabio Martino, M.D. Medico Radiologo Ambulatoriale, ASL, BA, Bari, Italy

Elena Massone, M.D. Postgraduate school of Radiology, Genoa University, Genova, Italy

Alessandro Muda, M.D. Department of Radiology, IRCCS Policlinico San Martino-IST, Genova, Italy

Davide Orlandi, M.D., Ph.D. Department of Radiology, Ospedale Evangelico Internazionale, Genova, Italy

Ernesto La Paglia, M.D. Department of Radiology, Ospedale di Alessandria, Alessandria, Italy

Filomena Puntillo Department of Emergency and Organ Transplantation, University of Bari, Bari, Italy

Riccardo Sartoris, M.D. Postgraduate School of Radiology, Genoa University, Genova, Italy

Luca Maria Sconfienza, M.D., Ph.D. Department of Diagnostic and Interventional Radiology, IRCCS Istituto Ortopedico Galeazzi, Milano, Italy

Department of Biomedical Sciences for Health, Università degli Studi di Milano, Milan, Italy

Enzo Silvestri, M.D. Department of Radiology, Ospedale Evangelico Internazionale, Genova, Italy

Mario Tedesco Pain Therapy Unit, Mater Day Hospital, Bari, Italy

Fundamentals

1

Enzo Silvestri, Silvia Perugin Bernardi,
Elena Massone, and Riccardo Sartoris

1.1 Basic Principles

Ultrasonography (US) is one of the most widely used imaging technologies in the first-level study of each human body structure, including soft tissue components of the musculoskeletal system and nerves. It is quick, portable and free of radiation risk, and, thanks to its high sensitivity and image resolution, its applications are continuously increasing.

Furthermore, US allows to acquire the images in 'real time', thus providing instantaneous visual guidance for many interventional procedures and reducing the risk of complications.

Rapid advances in transducer technology (broadband and high-definition probes), development of tissue harmonic imaging (THI) systems, new dedicated software and reconstruction algorithms (compound imaging, steering-based imaging, extended field-of-view imaging, three-dimensional imaging, sonoelastography), together with the possibility of a dynamic analysis of tendons, muscular structures and nerves, resulted in increased diagnostic performances and have opened new fields of applications in interventional procedures including those for regional anaesthesia and pain management.

US examination is relatively operator dependent, and it presumes a good knowledge of the physical principles on which it is based and the technical properties of the available equipment.

In this chapter, we describe some of the fundamental principles and physics underlying US technology.

1.1.1 Ultrasound Wave Properties

Ultrasonography is based on the use of acoustic waves with frequencies higher than the human hearing range (>20 kHz).

Sound waves can be described in terms of their **amplitude** (measured in decibel), **frequency** (measured in cycles per second or hertz), **wavelength** (measured in millimetre), **period** (the time interval in which each oscillatory phenomenon is reproduced), **velocity** (greater in rigid or less compressible materials, lower in air, water and soft tissues), **power** (measured in watts) and **intensity** (measured in watts per square centimetre) (Fig. 1.1).

E. Silvestri, M.D. (✉)
Department of Radiology, Ospedale Evangelico Internazionale, Genova, Italy

S. P. Bernardi, M.D. • E. Massone, M.D.
R. Sartoris, M.D.
Postgraduate School of Radiology, Genoa University, Genova, Italy

E. Silvestri et al. (eds.), *Ultrasound-Guided Peripheral Nerve Blocks*,
https://doi.org/10.1007/978-3-319-71020-4_1

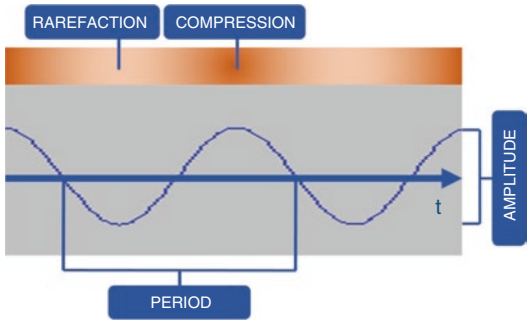

Fig. 1.1 The graphic demonstrates the oscillatory behaviour of the ultrasound waves propagating in tissues

1.1.2 Interactions Between US and Anatomical Structures

In ultrasonography, high-frequency sound waves are generated and transmitted through the body by a transducer.

Ultrasound transducers (or probes) contain multiple piezoelectric crystals which are electronically interconnected and vibrate in response to an applied electric current (piezoelectric effect). So, it produces not only the US but is also able to detect the returning echo produced by the interaction with tissue target, converting them back into electrical signals and then encoding into images.

Crossing anatomical structure, sound wave is subjected to varying phenomena that contribute to US image formation: attenuation, absorption, reflection, diffusion, refraction and divergence.

Attenuation (expressed in units of decibels per centimetre): it is reduction in the intensity of a signal through tissue. It depends on US frequency (MHz) and the distance travelled (cm): the higher the frequency and the distance, the greater the attenuation. So, the high-frequency US allows a better image resolution, but the beam is more attenuated. The implication, in the clinical practice, is that the high-frequency linear-array probes (7–13 MHz) are used for the study of superficial structures (tendons, muscles, ligaments) and the low frequency curved-array probes (2.5–5 MHz) for deep organ evaluation. The main causes of attenuation are absorption, reflection, refraction, diffusion and divergence.

Absorption: the acoustic energy is transformed into thermal energy of the tissue, according to US beam frequency and intrinsic characteristics of the medium (low in liquids, intermediate in soft tissues, high in bones and air).

Reflection and refraction: these are the deviation of the transmitted beam from the incident beam direction. The energy can be reflected back to the transducer (reflection) or deviated through the interface (refraction). These phenomena depend on the angle of incidence (the orientation of sound wave relative to the surface) and the different acoustic impedances between two materials.

The reflection increases when the US beam approximates to the angle of incidence, that is, equals to zero (when the US beam is perpendicular to the surface) while the refraction decreases and vice versa.

The acoustic impedance is an intrinsic property of tissues which expresses their resistance to the passage of the US beam (expressed in units of Rayls = kilogrammes per square metre per second).

So, we have the strongest detected returning echoes in clinical sonograms (*specular reflection*) when the angle of incidence equalled to zero and the difference in acoustic impedance between two materials is high.

Diffusion: according to the characteristics of the interface (homogeneous or irregular), the reflection can be *specular* (mirror-like) or *diffuse.* The latter one is the scattering of the reflected US beam in all directions because we have multiple interfaces (i.e. parenchymal organs).

Divergence: when the US beam is not focused, it diverges distally with consequent reduction of the depth resolution (Fig. 1.2).

1.1.3 Images Formation

A pulse-echo type of measurement allows to obtain ultrasonographic images.

The transducer is composed by a number of piezoelectric crystals assembled in a linear or curved disposition. Each crystal is excited by electrical pulses (*reverse piezoelectric effect*) and converts electricity (electrical energy) into sound (mechanical energy). The combination of these

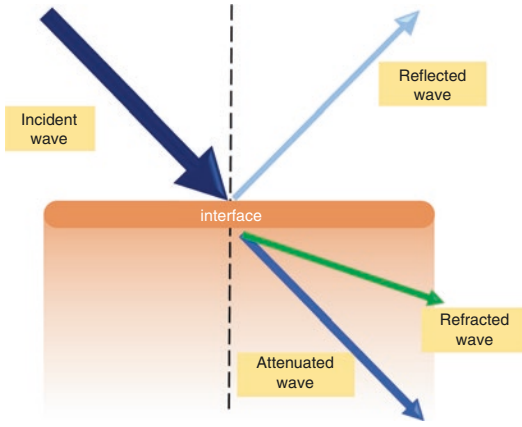

Fig. 1.2 Scheme of the physical phenomena contributing to US image formation

multiple beams generates the US beam. When the latter one is reflected to the transducer by tissue structures (returning echoes), it is converted back into electrical pulses (*piezoelectric effect*) and then in the image presented on the screen.

Currently, transducers contain a range of ultrasound frequencies (bandwidth) instead of a single fundamental frequency.

The generation of US images requires a complicated acquisition and display of ultrasound pulse-echo data. The broadband transducer generates a sequential series of focused beams all in the same plane (scan plane). Each set of target data from a single pulse transmission is placed in the image, as acquired along a line. All tissues in the scan plane are interrogated by these beams, and each real-time image frame is composed of a set of parallel or sector lines representing the positions of the interrogating beams in the patient. Computer algorithms are used to fill in between the image lines so that the image appears continuous.

When the transmitted US pulse encounters internal tissue targets, part of its energy is deflected (reflected or scattered) back to the transducer (the echo). Because pulse-echo imaging techniques employ the same transducer for both sending and receiving US pulses, only echoes travelling in the direction of the transducer have any chance of being detected.

The main pulse-echo parameters used in the formation of images include echo amplitude and target spatial position. Echo amplitude is encoded into shades of grey (greyscale imaging), with the lighter shades representing higher amplitude echoes.

The depth of the target along the direction of the beam is accurately calculated from a pulse time-of-flight measurement. Assuming US propagation velocity is fairly constant from tissue to tissue (1540 m/s), the time between beam transmission and echo reception is used to determine the exact internal spatial location of all tissue targets.

The image quality is represented by two important parameters: *spatial* and *temporal resolutions.*

The first one refers to the capability to distinguish two adjacent points, along (*axial resolution*) or perpendicular to the axis of the beam (*lateral resolution*).

Temporal resolution is linked to real-time identification of anatomical structures according to the pulse repetition frequency (PRF) and the frame (number of encoded images per time unit).

Visualization Systems:

- Amplitude mode (*A-mode*): it is the simplest form of display. It is a diagram in which echo amplitude is shown according to tissue depth (echo time of flight).
- Time-motion mode (*TM-mode*): echoes returning from moving structures are displayed depending on the time. It is used in cardiac US evaluation.
- Brightness mode (*B-mode*): it is a greyscale tomographic imaging (Fig. 1.3).

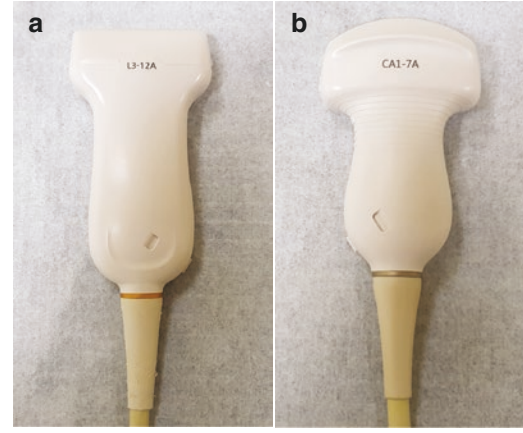

Fig. 1.3 **(a)** Linear-array probe (5–12 MHz). **(b)** Convex-array probe (2–5 MHz)

1.1.4 Artefacts

A detailed description of US artefacts lies outside the aim of our handbook. However, the errors in image display are important to know because it can be induced in an uncorrected interpretation of clinical findings.

The artefact can be linked to improper scanning technique or the physical characteristic of the US beam.

Anisotropy is an artefact that originates from a loss of echogenicity in structure. It is strictly related to US beam angle of incidence. If the US beam is not perpendicular to linear structures, the reflection is not specular, and so the returning echoes have low intensity: the structure wrongly appears more hypoechoic. The knowledge and the capability to correct the anisotropy artefacts are very important in order to achieve a high diagnostic accuracy and ultimately an optimal management of patients.

US Equipment: Hands On

If the tissue target is superficial and small (i.e. nerve), we have the necessity to increase the spatial resolution and image definition.

So, in order to improve image quality and diagnostic performances, some important parameters can be adjusted before and during US examination.

1. *Probe selection*: high-frequency linear-array probes, operating with frequencies of 10 MHz or more.
2. *US beam focusing*: it determines the number and pattern of focal zones. The zone in which the width and thickness of the US beam are reduced dynamically.
3. *Gain adjustment*: it optimizes echo intensity at different levels of depth.
4. *Zoom*: it better visualizes small and thin structures.
5. *Dynamic range adjustment*: it must be reduced in order to enhance the contrast resolution. In fact the dynamic range is inversely proportional to contrast resolution.

1.2 Doppler and Sonoelastographic Imaging

1.2.1 Doppler Imaging

Doppler effect is a change in frequency of the reflected ultrasound waves backscattered from the structure that is in motion, and it is based on an essential principle: the sound frequency of a target changes as the target travels towards or away from a point of reference. In particular, when the US beam, produced by the probe, is transmitted into a vessel, the frequency of the received wave is different from that of the transmitted wave because the source (red cells) moves relative to the given receiver (probe). Doppler ultrasound describes a frequency shift between an emitted ultrasound beam and the received echo.

The change of frequency detected between the transmitted and the received US frequencies is named 'Doppler shift'. The received US frequency would be higher if the direction is towards the receiver and lower if the direction is opposite. The equation which describes this phenomenon is:

$$\Delta f = (2\, fo\, v/c) \times \cos \alpha.$$

C: speed of ultrasound in soft tissues
V: speed of erythrocytes
fo: emitted frequency
$f1$: the frequency of the reflected ultrasound
$\Delta f = fo - f1$: Doppler shift
α: angle between the direction of the movement and the direction of the US beam

From the Doppler equation seen above, we see that the Doppler shift is influenced by the following factors:

1. The frequency of the ultrasound beam (*f*) used to interrogate flow
2. The angle of the ultrasound beam to flow direction (α)
3. The velocity of flowing red blood cell aggregates (*V*)

The Doppler shift of the moving red blood cells is continuously monitored to produce the Doppler signal; it is in the audible range and can thus be heard. The resulting sound is distinct and provides feedback to the operator.

In Doppler measurement, the Doppler angle is very important: the beam incidence should be from 0 to 89° because at 90° there is no signal (cos 90° = 0). Practically, 30–60° offers the best Doppler angle (Fig. 1.4).

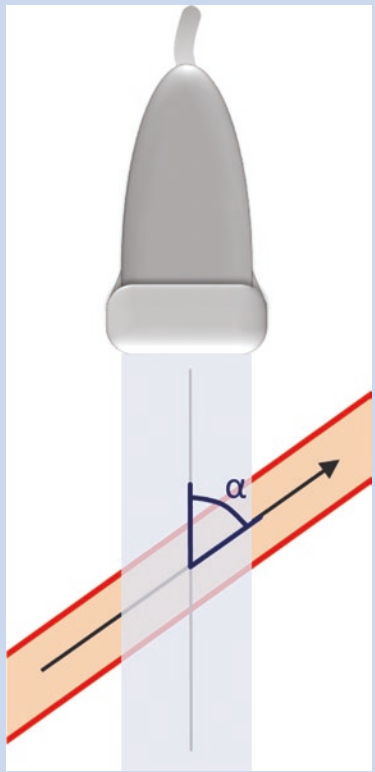

Fig. 1.4 Angle of Doppler insonation (α). Given a flow direction, ideally the transducer should be parallel to blood vessel but that is not possible. 30–60° offers the best Doppler angle

1.2.1.1 Signal Processing

Changes in frequency are expressed in a graphic mode with spectral representation which comprise the feedback signal frequency (longitudinal axis) versus time (transverse axis). The analysis of the frequency is performed using the fast Fourier transform, a physical phenomenon that allows variations in the amplitude of the wavelength obtained by the device to be displayed in the range of frequencies.

Some parameters that the radiologist must know and adjust influence the quality of the spectral analysis (Figs. 1.5, 1.6 and 1.7):

- *Pulse repetition frequency*: determines the number of pulses originated in the machine; they differ if we use B-mode or Doppler at the examination. High PRF detects high speed; low PRF detects slow flow, and if it detects high flows, aliasing occurs.
- *Size of the sample box*: the modification of the volume of the sample produces effects on the spectrum; if the size is too big, you get signal record below the spectrum. It marks the point at which the flow rate is determined. Sample volume should be 1/3 diameter of the artery. For very small blood vessels and veins, expanding sample volume is used. Too wide sample volume in the arteries causes spectral expansion.
- *Gain control*: if it is augmented, it can increase noise in the spectrum background and overestimate the velocity, and on the other hand, if it is reduced, the spectral record is not well demonstrated and can underestimate the velocity.
- *Angle control*: the angle of insonation is critical in estimating the correct velocity of the vessel of interest. When the angle is correctly adjusted under 60°, the spectrum is better delineated. When the insonation includes an angle greater than 60°, there is spectral broadening.
- *Wall filter use*: it annuls the signals on the wall or out of the blood vessels, ignores frequencies below a threshold and can be controlled by the operator. When a low-speed flow is explored by a very high filter, it could suppress the Doppler signal.

- *Flow parameters*: they provide diagnostic thresholds and are derived from the spectral frequency. The major representatives are resistive index (RI) and pulsatility index (PI) not influenced by the angle of insonation but useful to determine flow resistance in the vascular system. The operator can calculate them using the spectrum (Fig. 1.8).

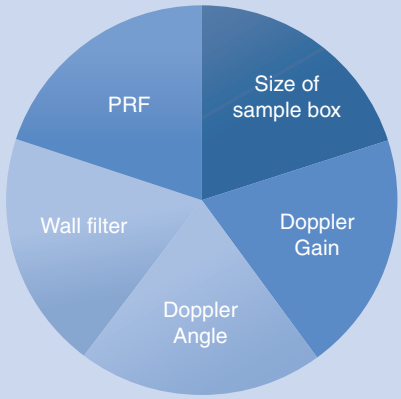

Fig. 1.5 Technical factors influencing the quality of the Doppler spectrum

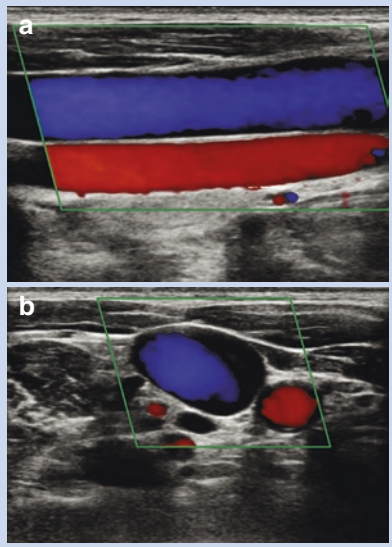

Fig. 1.6 Colour Doppler imaging shows the carotid artery (red) and jugular vein (blue) at the level of the neck in a longitudinal scan (**a**) and in a transverse scan (**b**). Especially in imaging soft tissues, identifying neurovascular bundles with US colour Doppler technique can be very useful to correctly localize tendinous and muscular structures

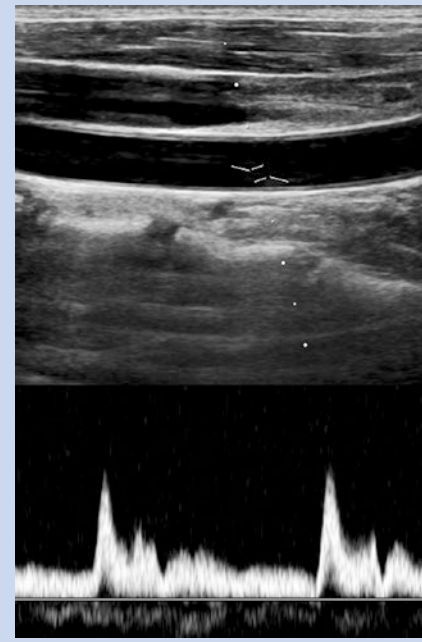

Fig. 1.7 Ultrasound spectral examination of the flow of the carotid artery

Resistive Index (RI)

$$RI = \frac{\text{max V} - \text{min V}}{\text{Max V}} = \frac{\text{S-D}}{\text{S}}$$

Pulsatility Index (PI)

$$PI = \frac{\text{max V} - \text{min V}}{\text{Mean V}} = \frac{\text{S-D}}{\text{Mean}}$$

Fig. 1.8 Resistive index and pulsatility index equation. *MaxV* maximum velocity, *minV* minimum velocity, *S*, sistole; *D* diastole

Doppler ultrasound is an imaging technique that combines anatomical information derived using US pulse-echo techniques with velocity information derived using Doppler techniques to generate colour-coded maps of tissue velocity superimposed on greyscale images of tissue anatomy.

The most common use of the technique is to do the accurate noninvasive evaluation of the blood flow movement through the heart, arteries and veins, but it may also be used to image the motion of solid tissues such as the heart walls. As the name implies, US Doppler technique uses the Doppler effect to assess how blood flows through the major blood vessels.

There are three methods of analysis:

- *Qualitative analysis*: evaluating the presence, site and direction of the blood flow
- *Quantitative analysis*: evaluating flow velocity and flow rate
- *Semi-quantitative analysis*: evaluating the spectrum of the wave frequencies

There are two types of technical mode of Doppler imaging in medicine:

- *Continuous-wave Doppler* (CW Doppler): it uses two separate crystals, one transmitting and the other one receiving the reflected waves. The first crystal transmits a continuous signal at a known frequency, and the other crystal receives the returning echoes and records their frequency. Consequently, the US machine cannot determine which sound pulse was frequency shifted and, therefore, cannot precisely define the location of the moving target. In conclusion, this technique is employed in detection of blood flow but does not give information about direction, depth and velocity of flow.
- *Pulsed wave Doppler* (PW Doppler): one transducer is used as a transmitter and as a receiver. The probe produces US beams in pulses, alternating the transmission and reception. This has provided the means of detecting the depth at which a returning signal has originated. The depth can be positioned at any point along the axis of US beam referred to as the 'sample volume'. The position of the sample volume is decided by the operator. When the US beam is transmitted into tissues, it travels for a given time until it is reflected by a moving red cell; then, it returns to the probe over the same time interval but at a shifted frequency. Calculating the total transit time, the US machine is able to measure the distance of the sample volume. In respect to the CW Doppler, PW Doppler is able to evaluate the depth from which the returning echoes originate, but it cannot correctly depict higher velocities (blood flow velocity measurements are limited to the physiologic range, usually around 1.5 m/s).
  PW is based on three technical parameters: *high pulse repetition frequency* (the difference between successive burst of incidence ultrasound beam), the optimum *transducer frequency* (low frequency for deeper structures and high frequency for superficial structures) and the correct *insonation angle* (<60°).

PW Doppler is usually combined with a 2D, real-time, B-mode scanner to form what is known as a duplex scanner.

PRF scale (repeated pulsing frequency) is the number of pulses per unit of time that is transmitted to the blood vessel, and when it is too long relative to the velocity of the blood flow and it will not be possible to determine the direction of blood flow, we have the aliasing phenomena. In particular, aliasing occurs when the velocity is more than one half of the PRF; in this case, velocities above this limit will be displayed on the tracing opposite to the true direction of blood flow. To correct for aliasing, the operator can increase the PRF or increase the angle between the US beam and the flow direction towards perpendicularity.

Colour Doppler: It is an ultrasound system in which the echo signals received along a series of locations in an ultrasound beam width by applying transmit-receive pulse signals are called pulse packets. The energy of the returning echoes is displayed as an assigned colour; by convention, red for echoes that flow towards the probe and blue for echoes that flow in the opposite direction, away from the transducer. US machine displays coloured blood flow superimposed on a greyscale image, thus allowing simultaneous visualization of anatomy and flow dynamics. Brighter shades in colour conventionally depict faster flow.

To optimize the colour Doppler evaluation, it is crucial to set the US beam at an optimal angulation <60° in respect to the vessel, basing on the physical Doppler equation (cos 90° = 0).

Power Doppler: It is a type of colour Doppler, more sensitive to blood flow compared with conventional colour Doppler, ignores the velocity and the direction of flow and simply estimates the strength/amplitude of the Doppler signal detected from each location. Power Doppler shows small vessels and slow flow rates; indeed it is most commonly used to evaluate low-velocity microvascular flow in soft tissue imaging. Power Doppler is extremely sensitive to the movement of the probe, which produces a flash artefact.

So the advantages of power Doppler versus colour Doppler imaging are:

- More sensitive to flow states.
- Angle effects are ignored.
- Aliasing artefact is not applicable to power Doppler imaging.

The disadvantages are:

- Values of velocity and the direction of blood flow cannot be assessed.
- Flash artefact: because of more averaging of information at slower frame rates, slow-moving soft tissue signals appear as flash artefact.

Power Doppler should be optimized while the probe is not in contact with patient's skin. The gain should be set at maximum level and then decreased up to the disappearance of all artefacts. Further, it is important to set low wall filters (WF) and pulse repetition frequency (PRF) between 700 and 1000 Hz in order to better evaluate low-velocity blood flows.

Combining with greyscale ultrasound, colour Doppler imaging and power Doppler imaging allow unique real-time evaluation of the regional blood flow, enabling a wide range of applications for the evaluation of soft tissues.

Often blood vessels are used in musculoskeletal imaging as anatomical landmarks. Colour Doppler and power Doppler are very helpful in detecting inflammatory diseases and neovascularity, possibly related to malignancy, and so they represent a useful tool also for the quick assessment of vascular anomalies and post-traumatic vascular lesions. It is also important to use colour Doppler imaging during a biopsy to ensure that major vessels are avoided.

1.2.2 Sonoelastography (SEL)

Sonoelastography (SEL) is a recently developed imaging technique which allows for qualitative visual or quantitative measurements of the mechanical properties of tissues. It is based on the principle for which, applying an extrinsic (mechanical or physical) stress, it is possible to induce changes in a determined tissue, depending on the elastic properties of the tissue itself; hence, qualitative and/or quantitative measurements of the elastic changes induced through the tissue could be obtained, usually by mean of an ultrasound transducer in clinical practice. The recent diffusion of SEL into commercially available ultrasound systems has promoted the development of many studies regarding the potential clinical applications of this technique in different clinical fields and, in particular, in the musculoskeletal system.

1.2.2.1 Elasticity: Basics Principles

The elasticity of a material represents its tendency to resume its original shape and size after being subjected to a deforming force or stress. Fluids resist a change in volume but not in shape: they have only 'volume elasticity'. Solids instead resist changes in volume and shape: they present

rigidity or 'shear elasticity', as well as volume elasticity. Viscoelastic fluids also exhibit elasticity in certain conditions.

It is essential that the terms stress and strain be defined because the elasticity of a material is described in terms of a stress-strain relation: the 'strain' is the relative deformation in volume or shape, produced by a force per unit area (called 'stress').

For a homogeneous isotropic solid, the ratio of stress-strain is a constant, called the 'modulus of elasticity'. A modulus measures the amount of force per unit area (stress) needed to achieve a given amount of deformation and usually is expressed in units of Pa. A higher modulus typically indicates that the material is harder to deform.

Three moduli are commonly used to define elasticity:

- *Young's modulus* (E) represents longitudinal elasticity and is defined by the ratio between the stress and the strain.
  Young modulus $E = S/e$.
- *Shear or torsion modulus* (G) represents transverse elasticity.
- Bulk or volume modulus (K) represents volume elasticity.

A stress determines two types of mechanical waves in the tissue:

1. *Compression wave* that compresses tissue little by little, inducing a displacement parallel to the propagation direction
2. *Shear wave* that is responsible of a slip of different tissue layers, relative to each other, inducing a displacement perpendicular to the wave propagation direction

The ultrasound elastography quantitative techniques do not directly measure the Young's modulus but the speed V of shear wave propagation.

The velocity V of the shear wave is related to shear modulus μ (shear):

$$\mu = r V^2 \text{ with } r = \text{tissue density}$$

The shear modulus μ is itself connected to the elastic modulus:

$$E = 3\mu$$

The measurement of the shear wave propagation velocity V (in m/s) allows to assess the elastic modulus E according to the formula:

$$E = 3\rho V^2$$

For computations, the tissue density is assumed to be constant and equal to 1000 kg/mm^3.

The shear modulus describes the response to shear forces, Young's modulus describes the response to linear stress (tensile stress) and bulk modulus represents the response (in all directions) to uniform compression; it is usual for values of shear and Young's modulus to be reported in the studies regarding the investigation of elastic properties of tissues by means of ultrasound.

So the aim of elastography is to assess tissue stiffness based on three steps:

1. Excitation: transmission of stress in a tissue (mechanical, vibrational, shear)
2. Acquisition: recording the signal induced by the tissue deformation due to the stress (RF or B-mode data)
3. Analysis/post-treatment: analysis of tissue strain induced by the propagation of the stress

Human body has a mechanical behaviour similar to a soft homogeneous and isotropic linear elastic material.

1.2.2.2 Modalities

There are several elastographic techniques depending on the difference in the stress application and the method used to detect tissue displacement and build the image (Figs. 1.9 and 1.10).

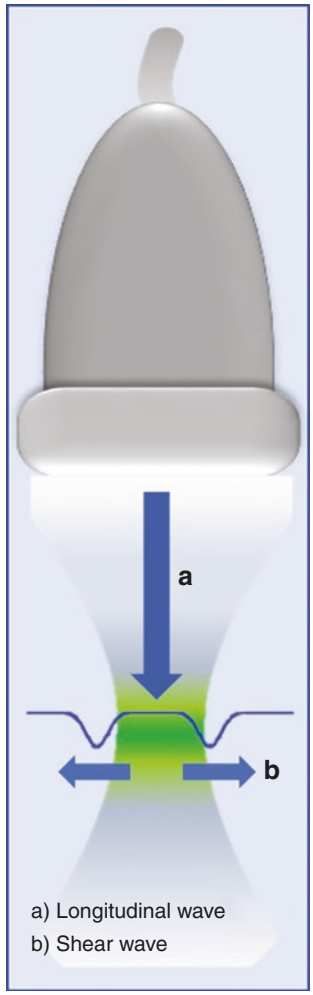

Fig. 1.9 Two different types of mechanical wave. (**a**) longitudinal wave; (**b**), shear wave

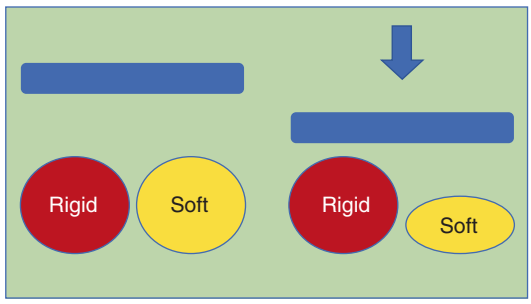

Fig. 1.10 The elasticity of rigid and soft materials

Two main types of SEL have become established in clinical practice, in particular for soft tissue evaluation:

- *Strain elastography*: it is also described as 'quasi-static elastography', 'compression elastography' and 'real-time elastography'. The stress is applied by repeated manual compression of the transducer, and the amount of tissue deformation (strain) relative to the surrounding normal tissue is measured, usually with a tracking algorithm working on the radio frequency data. The resulting data can then be used to form an image that is coded in colour or greyscale to show the pattern of strain, which is inversely related to tissue stiffness and can be assessed subjectively. These are qualitative data; however, regions of interest (ROIs) can be positioned over target areas in the screen in order to obtain semi-quantitative analysis (Fig. 1.11).
- *Shear wave elastography*: it is a very potential technique for the noninvasive quantification of tissue stiffness. Shear waves in the body can be induced by various methods, including physiological motion, external mechanical excitation or acoustic radiation force (by a focused ultrasound beam). Shear waves are transverse, they are rapidly attenuated by tissue, they travel much more slowly (between 1 and 10 m/s) and they are not supported by liquids of low viscosity. Using a real-time imaging modality such as ultrasound (but also magnetic resonance), the underlying tissue stiffness can be estimated measuring the produced shear wave speeds. Their speed is commonly expressed in metres per second (m/s); it is closely related to the modulus of elasticity of the tissue, and there is a simplified formula for converting between the shear wave speed and the elastic modulus of the tissue to locally quantify its stiffness in kilopascals (kPa). In contrast to strain elastography, this technique allows for the performance of quantitative analysis of the tissue stiffness. There are some

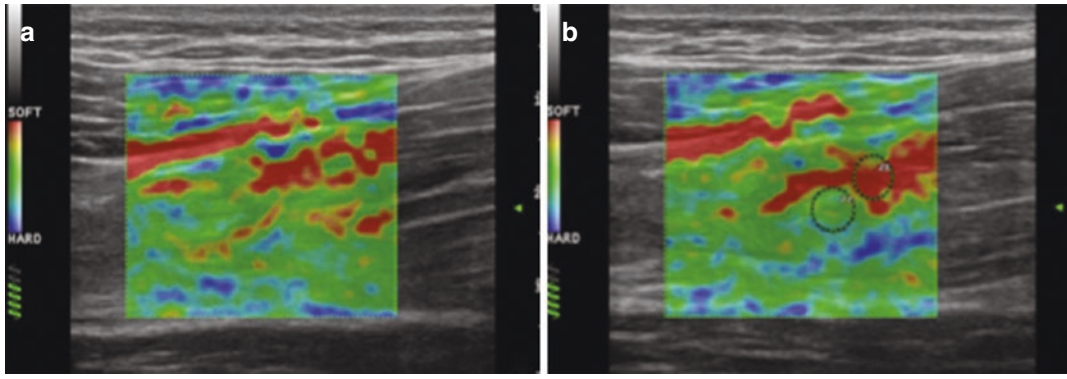

Fig. 1.11 Strain elastography. (**a**) Qualitative analysis: the modulus of elasticity of the soft tissue scanned in the B-mode image is represented by a superimposed colour-coded map in which (in this case) the lower values are depicted in red and the higher ones in blue; (**b**) it shows the possibility to perform also a semi-quantitative analysis of the strain elastogram with placement of two ROIs in order to take definite measurements of the Young's modulus of elasticity of the targeted tissue. The green-coloured spring-shaped figure shown in the left bottom of both the elastograms indicates that the pressure the operator performed with the transducer was appropriate to produce an adequate stress to get the elastogram

variations of this method in clinical practice, depending on the difference in the modality of stress application:

- *Transient elastography* (TE): it is a system developed and commonly used for liver fibrosis assessment, in which a mechanical piston within an ultrasound transducer is used to apply a push to the skin over an intercostal space. The speed of the produced shear waves into the liver, along the direction of the ultrasound beam, is measured in a way similar to M-mode.
- *Acoustic radiation force imaging (ARFI)*: in this technique, a focused ultrasound 'pushing' beam (with intensity below the threshold for bio-effects) is used to induce tiny displacements in soft tissue along its direction and generate orthogonal shear waves that propagate sideways in tissue. The shear wave speed or amplitude is detected by conventional ultrasound using tracking algorithms and is used to quantify the underlying tissue stiffness. Shear wave speed measurement could be made by a single small measurement box positioned by the operator within the tissue adjacent to the pushing beam (Fig. 1.12) and/or could be extended to sequential multiple pushing and measurement points in order to construct a colour-coded map of the shear wave speed, which is also quantitative with positionable ROIs (Fig. 1.13). ARFI images represent the spatial distribution of tissue stiffness.
- *Supersonic shear imaging (SSI):* it is a similar system which uses multiple acoustic radiation force impulses focused at different depths to create an extended cylindrical wavefront. These excitations are applied supersonically so that the shear waves generated from different depths constructively interfere adding each other's and dedicated ultrasound transducers could detect and measure them.

An overview of the different elastographic techniques is shown in Fig. 1.14, Tables 1.1 and 1.2.

1.2.2.3 Technical Considerations

In strain elastography, data acquisition and interpretation of elasticity images are largely dependent on the operators' experience and skills. SEL soft-

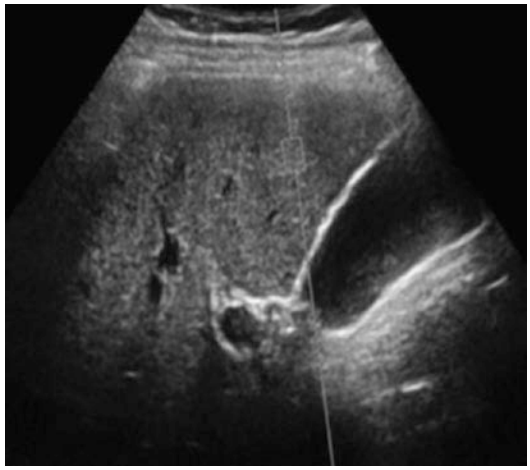

Fig. 1.12 Acoustic radiation force imaging (ARFI): shear wave speed quantification is obtained by a single small measurement box positioned by the operator within the tissue (fifth segment of the liver in this case) along the direction of the pushing beam. Data regarding liver segment, depth of the box placement and shear wave speed expressed in meters per second are represented right to the B-mode image

ware derive elastograms which usually depend on the changing probe pressure experienced during freehand scanning and on the individual capability of images' interpretation: consequently possible significant intra- and interobserver variability has to be taken in consideration. Further, this technique provides only qualitative and/or semi-quantitative analysis with elasticity data resulting from the relative stiffness of the targeted region and the remaining tissue area. Hence, this technical feature may significantly influence the clinical use of strain elastography in terms of reproducibility and accuracy.

In contrast, the quantitative nature of shear wave elastography is an advantage and seems to let this technique be more reproducible; the fact that the system displaces the tissue could improve consistency since the examiner does not need to move the transducer. The localized nature of the applied force should also improve the relationship between displacement and elasticity com-

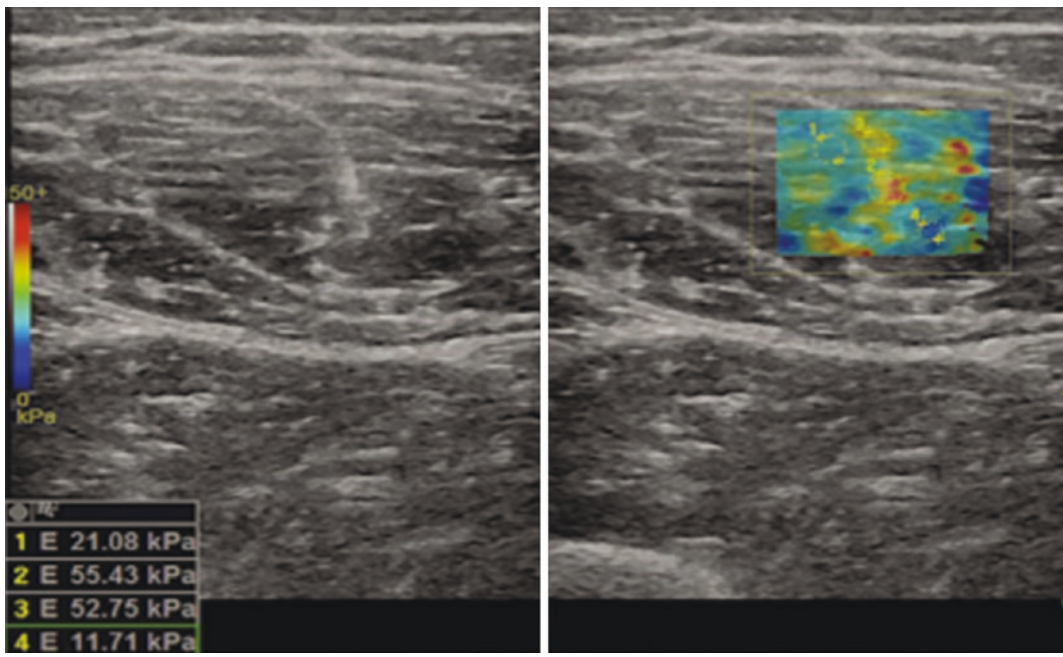

Fig. 1.13 Shear wave elastography of rectus femoris muscle: after the generation of the 'pushing' beam by the transducer, the values of the shear modulus in the targeted area are represented by mean of a colour-coded map set as represented by the coloured bar on the left of the screen. It is possible to get also a quantitative analysis of the investigated tissue by placing some ROIs (with modifiable dimensions) over the map and get the corresponding value at the left bottom angle of the screen. Note that, on the right elastographic map, the stiffer areas in the centre of the map correspond to the central rectus femoris aponeurosis

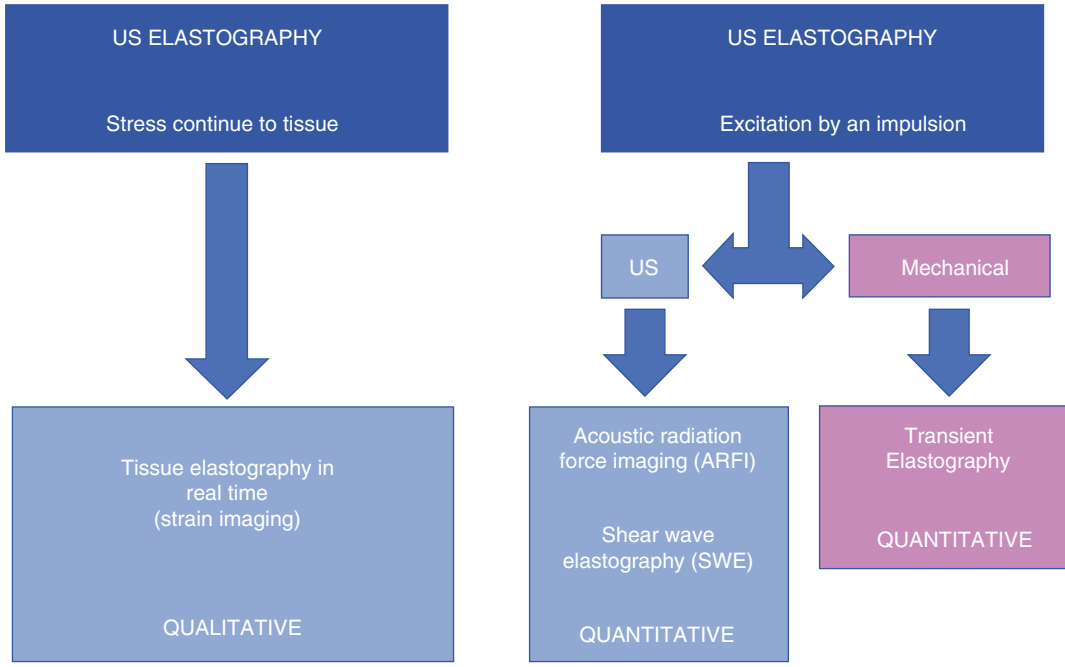

Fig. 1.14 Several elastographic techniques depending on the difference in the stress application and the method used to detect tissue displacement and build the image

Table 1.1 The technical characteristics of the different elastography modes

Elastography	Quasi-static		Dynamic	
Method	Strain imaging	ARFI	TE transient elastography	Ultra-fast shear wave elastography
Excitation mode	Mechanical (external compression) or physiological	Ultrasonic (radiation force)	Mechanical (pulse by an external vibrator)	Ultrasonic (radiation force)
Stress application	Surface or internal structure	Different depths	Surface	Different depths
Involved modulus	Young	Shear	Shear	Shear
Measured parameters	Displacement → strain	Shear wave velocity	Shear wave velocity	Shear wave velocity
Visualization	Temporal strain map	One fixed image	One measure (no image)	Temporal images (several/s)
Quantification	No	Yes	Yes	Yes

pared with applying the force at the surface, as well as improve contrast and spatial resolution. Despite the overall promising features of shear wave sonoelastography, in particular if compared with those of the strain elastography, some limitations have to be mentioned. Shear wave speed measurements using radiation force produced by a focused ultrasound beam can be dependent on transducer geometry, focusing depth, lateral tracking range and frequency of the shear wave used for imaging. Further, the shear wave speed in tissue is dependent on the shear modulus and its density, usually calculated by making some conventional assumptions which not always reflect the actual characteristics of the investigated tissue.

Sonoelastography is a very promising tool in addition to B-mode sonography and colour/

Table 1.2 Advantages and drawbacks of quasi-static and dynamic elastography

Elastography	Method	Advantages	Drawbacks
Quasi-static	*Strain imaging*	Easy	Operator dependent Applicable for superficial organ Qualitative method
Dynamic	*TE (transient elastography)* *Arfi Swe* *SWE (share wave elastography)*	Quantitative method Easy Validated for liver fibrosis Quantitative method Short breath hold Quantitative method Elasticity map	Limits for overweight and ascites Depth limited to 8 cm Longer breath hold

power Doppler techniques to evaluate stiffness changes in various soft tissue structures. Strain elastography provides quick, easier and qualitative or semi-quantitative measurements of such structures; shear wave elastography adds a more precise quantitative characterization with a much more difficult learning curve and a longer examination time.

1.3 Normal Anatomy

1.3.1 Peripheral Nerves

Peripheral nerves are usually made of nervous fibres (containing axons, myelin sheaths and Schwann cells) grouped in fascicles and loose connective tissue (containing elastic fibres and vessels). Each fascicle is encased by a proper connective sheath called *perineurium*. Inside the fascicle are a group of axons bathed in *endoneurial fluid*. Each axon has an insulating lining of *myelin*—a fatty material inside the *Schwann cells*. Between the fascicles and the outer nerve sheath, there is a fatty material called the *interfascicular epineurium* which houses the nerve vascular structure. The nerve is then wrapped in the main *outer epineurium*—an external sheath.

Clinical experience with ultrasound and improvements in technology have been helpful in the evaluation of peripheral nerve, and the improvements in Doppler sensitivity and power Doppler have made it possible to assess vascular changes within major nerve segments.

Peripheral nerve ultrasound, when compared to electrodiagnostic testing, adds the possibility to provide anatomic detail of the affected site without any discomfort. In fact ultrasound is a low-cost, quick and noninvasive imaging method, providing an excellent view of peripheral nerve anatomy as well as of surrounding structures. US provides high spatial resolution and the ability to explore long segments of nerve trunks in a single study, also allowing nerves examination in both static and dynamic conditions, during passive or active movements of the extremities.

US enables the identification of post-traumatic changes of nerves, neuropathies secondary to compression syndromes and inflammatory or neoplastic nerve lesions as well as the evaluation of postoperative complications, and it is increasingly used in anaesthesiology for regional anaesthesia.

Nerves present cable-like structures and have a distinct architecture consisting of fascicles and surrounding epineurium (Fig. 1.15).

In the transverse plane, the echo pattern is described as a ‘honeycomb’ aspect because tiny round and hypoechogenic areas representing the nerve bundles with hyperechogenic rims of the epineurium are visible.

In the longitudinal plane, nerves present as long, slim structures with a mixture of parallel

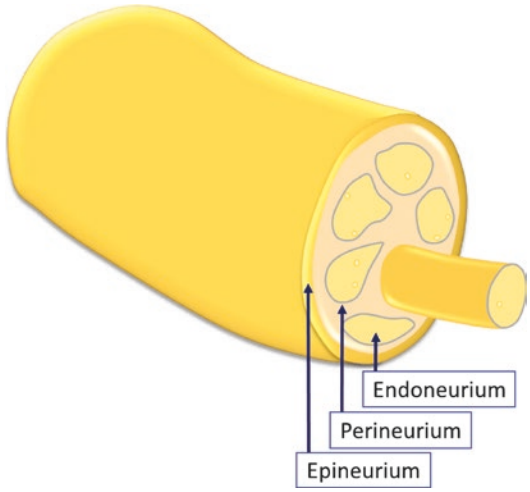

Fig. 1.15 Scheme of peripheral nerve illustrating its inner structure

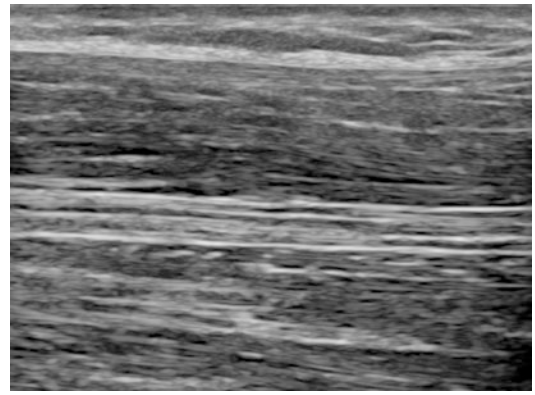

Fig. 1.16 Peripheral nerves. Longitudinal 3–16 MHz US image obtained over the median nerve (white arrows) at the middle third of the forearm. The nerve is made of parallel linear hypoechoic areas, the fascicles, separated by hyperechoic bands, the interfascicular epineurium

hyperechogenic lines, representing the perineurium, between two more prominent and also hyperechogenic layers of the epineurium. This image resembles that of an electric cable (Figs. 1.16 and 1.17).

The transverse image is much more frequently used in clinical practice, as it allows for the nerve to be examined by the so-called *elevator technique* which consists of finding the set nerve at a characteristic anatomic point and 'tracking it' either proximally or distally. In this way, it is possible to assess the nerve's shape, echogenicity and thickness and its relation to the surrounding tissues, the surface area of the nerve and its vasculature. If an abnormality is seen in the transverse view, the nerve should be examined in the longitudinal view.

The US aspect of nerves changes from hypo- to hyperechogenic as they are followed more peripherally for an increasing amount of connective tissue between the nerve bundles. It has been assumed that nerves are not anisotropic even if the property of anisotropy is seen in cases of nerves with large cross sections.

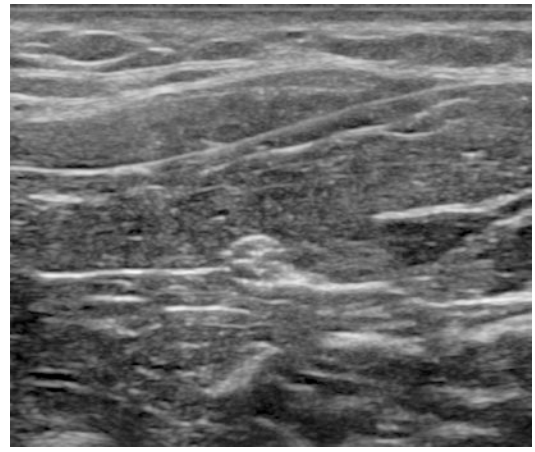

Fig. 1.17 Nerve echotexture. Transverse US image of the median nerve at the middle third of forearm. The nerve (white arrowhead) is characterized by a honeycombing appearance made of round hypoechoic areas in a homogeneous hyperechoic background

Anisotropy is a typical characteristic of tendon and refers to the sound reflection properties of tissue: tissues with low anisotropy tend to backscatter sound reflection, and those with high anisotropy

tend to reflect sound such that the angle of incidence equals the angle of reflection, making them much brighter with perpendicular insonation. So the angle of insonation does not alter the appearance of a nerve in the way that they alter the appearance of tendons. Tendons are more homogenously hyperechoic than nerves and have a distinctive fibrillary composition, and additionally, tendons, if followed proximally or distally, lead to muscle.

The shape of a nerve may also be different and vary between individuals, round, oval, triangular or irregularly shaped, which may change under compression by the probe or with the movement of a neighbouring muscle. Nerve may change its shape along its course, for example, from a triangular to a round cross section, or may present anatomic variants (e.g. bifid or trifid variants of the median nerve).

Knowledge of regional anatomy and topography is needed for the sonographic assessment of peripheral nerves and for localizing fine and deep nerves, and so characteristic anatomic reference points are used (often large vessels accompanying the nerves, which may be seen via Doppler imaging). The following anatomical landmarks are useful: the brachial artery for the median nerve in the upper arm, the superficial and deep flexor muscles for the median nerve in the forearm, the contents of the carpal tunnel for the median nerve at the wrist, the ulnar artery for the ulnar nerve at the wrist, the medial epicondyle for the ulnar nerve at the elbow, the radial groove for the radial nerve, the anterior and middle scalene muscles and the proximal subclavian artery for the brachial plexus, the popliteal artery for the distal sciatic nerve, the fibular head for the fibular nerve and the posterior tibial artery for the tibial nerve at the ankle.

Motor and motor-sensory nerves may be evaluated indirectly analysing the skeletal muscles which they innervate: we can evaluate muscular atrophy in case of chronic denervation as a decrease of the muscle's volume and fatty infiltration, which increases its echogenicity.

Ultrasound measurement of nerve size is very important because nerve enlargement is the most important diagnostic marker of an abnormal nerve: *cross-sectional area* and *swelling ratio* (the ratio between the cross-sectional area of the nerve at the site of maximal enlargement and that at an unaffected site) can be measured on transverse images, and diameter can be measured on longitudinal images.

For correct measurement, the transducer should be perpendicular to the nerve, with minimal pressure, and the site of maximal enlargement should be selected for the measurement of nerve size. Variability within a measurement can be reduced doing multiple measures. Measuring just inside the echogenic rim of the nerve is the preferred technique.

Placing the power Doppler box over the nerve and slowly increasing the gain can be useful to evaluate the vascularity of the peripheral nerves. No colour Doppler signal will be observed in the normal nerve.

Nerve mobility can be routinely assessed to exclude nerve entrapments.

1.3.2 Technique for Ultrasonographic Imaging of Peripheral Nerves

For the imaging of peripheral nerves, the patient lies with the 'region of interest' on the examination table.

Usually a linear probe with a frequency greater than 12–18 MHz is used. In the case of obese patients or the evaluation of deeply located nerves, a convex probe may be used, for a deeper penetration of the ultrasound waves.

For the evaluation of superficial nerves, using a thick layer of US gel or a stand-off pad can be helpful. In particular, such adjuncts are useful in the evaluation of fine nerves of the wrist.

Suggested Readings

Arda K, Ciledag N, Aktas E, Kadri Arıbas B, Köse K. Quantitative assessment of normal soft-tissue elasticity using shear-wave ultrasound elastography. AJR. 2011;197(3):532–6.

Christopher R. Doppler US: the basics. Radiographics. 1991;11:109–19.

Mitchell DG. Color doppler imaging: principles, limitations, and artifacts. Radiology. 1990;177:1–10.

Drakonaki EE, Allen GM, Wilson DJ. Ultrasound elastography for musculoskeletal applications. Br J Radiol. 2012;85(1019):1435–45.

Evan J. AAPM/RSNA physics tutorial for residents: topics in US doppler US techniques: concepts of blood flow detection and flow dynamics. Radiographics. 2003;23:1315–27.

Klauser AS, Miyamoto H, Bellmann-Weiler R, Feuchtner GM, Wick MC, Jaschke WR. Sonoelastography: musculoskeletal applications. Radiology. 2014;272(3):622–33.

Kot BC, Zhang ZJ, Lee AW, Leung VY, Fu SN. Elastic modulus of muscle and tendon with shear wave ultrasound elastography: variations with different technical settings. PLoS One. 2012;7(8):e44348.

Kot Wing BC, Zhi Jie Z, Chun Lee AW, Fong Leung VY, Ngor FS. Elastic modulus of muscle and tendon with shear wave ultrasound elastography: variations with different technical settings. PLoS One. 2012;7(8):e44448.

Martinoli C, Bianchi S. Ultrasound of the musculoskeletal system. Berlin/New York: Springer; 2007.

O'Neill J. Musculoskeletal ultrasound: anatomy and technique. New York: Springer; 2008.

Pavčec Z, Žokalj I, Saghir H, Pal A, Roić G. Doppler ultrasound in the diagnosis and follow-up of the muscle rupture and an arteriovenous fistula of the thigh in 12 year boy. Radiol Oncol. 2006;40(4):211–5.

Silvestri E, Martinoli C, Derchi LE, et al. Echotexture of peripheral nerves: correlation between US and histologic findings and criteria to differentiate tendons. Radiology. 1995;197:291–6.

Taylor KJ, Holland S. Doppler US part I. Basic principles, instrumentation, and pitfalls. Radiology. 1990;174:297–307.

Normal US Anatomy and Scanning Technique

2

Fabio Martino, Luca Maria Sconfienza, Alessandro Muda, and Davide Orlandi

2.1 Ultrasonography: Basic Principles and Techniques

Ultrasonography is an established method for peripheral nerves imaging. It enables the identification of post-traumatic changes of nerves, neuropathies secondary to compression syndromes, inflammatory or neoplastic nerve lesions as well as the evaluation of postoperative complications. It is increasingly used in anesthesiology for regional anesthesia. The examination of peripheral nerves is noninvasive, well-tolerated by patients, and relatively inexpensive.

F. Martino, M.D. (✉)
Medico Radiologo Ambulatoriale, ASL BA, Bari, Italy

L. M. Sconfienza, M.D., Ph.D.
Department of Diagnostic and Interventional Radiology, IRCCS Istituto Ortopedico Galeazzi, Milano, Italy

Department of Biomedical Sciences for Health, Università degli Studi di Milano, Milan, Italy

A. Muda, M.D.
Department of Radiology, IRCCS Policlinico San Martino-IST, Genova, Italy

D. Orlandi, M.D., Ph.D.
Department of Radiology, Ospedale Evangelico Internazionale, Genova, Italy

2.1.1 Ultrasound of Normal Nerves

In the short axis, the nerve has a honeycomb-like appearance, with multiple rounded hypoechoic areas in a homogeneous hyperechoic background (Fig. 2.1a).

In the long axis, it has a striated appearance composed of multiple parallel hypoechoic and hyperechoic bands. This image resembles that of an electric cable (Fig. 2.1b). This type of US appearance can be defined as fascicular structure.

It is also important to distinguish the other anatomical components that surround peripheral nerves and know what their normal echotexture is.

Skeletal muscle: Ultrasound anatomy reflects the proportion between connective tissue and muscle. In the short axis, the intramuscular tendons appear as hyperechoic strands, and the epimysium (the outer muscle fascia) appears as a well-delineated echogenic envelope surrounding the hypoechoic muscle (Fig. 2.2a).

In the long axis, the echotexture of muscle fibers is relatively hypoechoic, while the fibroadipose septa (perimysium) appear like hyperechoic lines presenting a broadly parallel disposition (Fig. 2.2b).

E. Silvestri et al. (eds.), *Ultrasound-Guided Peripheral Nerve Blocks*,
https://doi.org/10.1007/978-3-319-71020-4_2

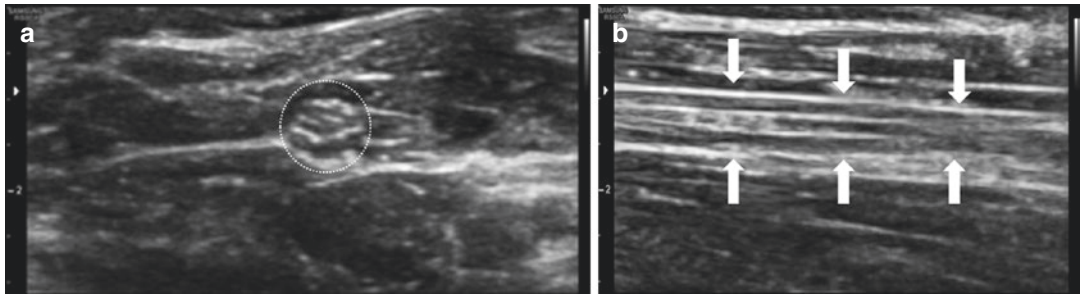

Fig. 2.1 Ultrasound anatomy of normal nerve: (**a**) short axis; (**b**) long axis

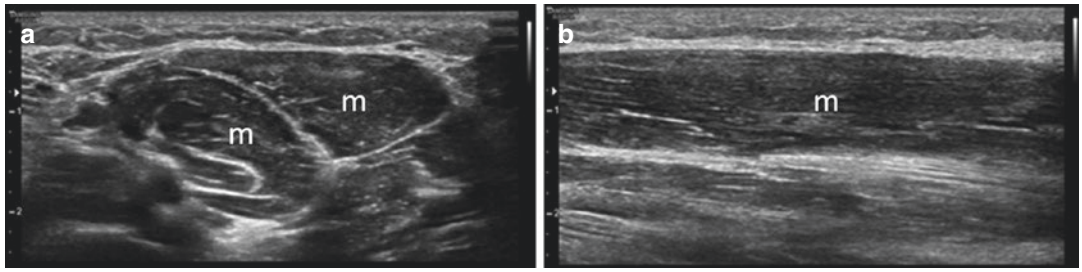

Fig. 2.2 Ultrasound anatomy of normal muscle: (**a**) short axis; (**b**) long axis

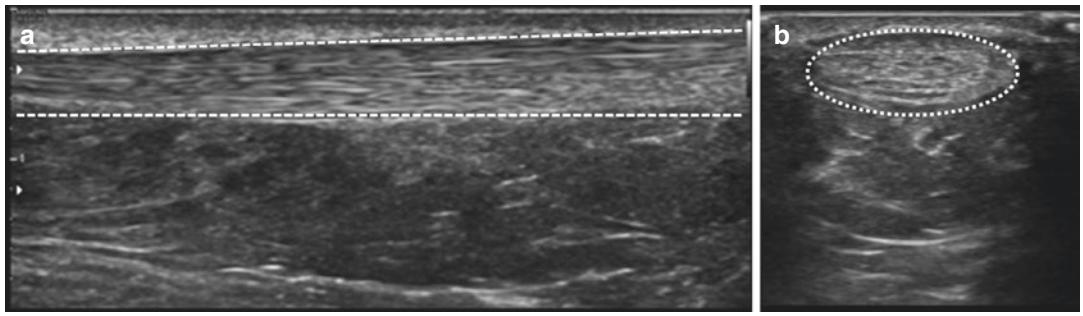

Fig. 2.3 Ultrasound anatomy of normal tendon: (**a**) long axis; (**b**) short axis

- *Tendon*: Tendons consist of linear fibrils of collagen with a supporting matrix. The normal echotexture reflects this model called fibrillar pattern.
- In long axis, the tendon appears as a hyperechoic ribbon-like structure (Fig. 2.3a). The tendon has a succession of thin hyperechoic fibrillar bands, which tend to grow apart from one another when the tendon is released and to move closer when the tendon is tense. This fibrillar echotexture is caused by the specular reflections within the tendon, determined by the existing acoustic interface between the endotenon septa. The tendon is surrounded by hyperechoic bands that correspond to the paratenon.
- In a transverse view (short axis), the tendons appear as round- or oval-shaped structures, characterized by several homogeneously scattered spotty echoes (Fig. 2.3b).
- *Vessels*: In short and long axes, the vessel appears like an anechoic round or tubular structure, respectively (Fig. 2.4).

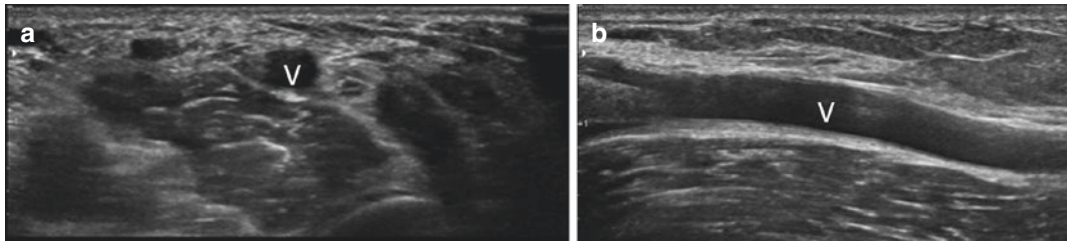

Fig. 2.4 Ultrasound anatomy of normal vessel: (**a**) short axis; (**b**) long axis

Tool box: Anisotropy is an artifact produced by the linear conFiguration of tendons, whereby hypoechoic change is seen if the transducer is slightly angulated. This artifact can mimic hypoechoic tendinopathy, but careful minor changes to the transducer angulation make anisotropy disappear, whereas true pathologic findings do not disappear.

Investigation with power Doppler technique is performed if tendon abnormalities are seen, although the exact significance of neovascularity is not clear. Power Doppler settings are optimized to detect low blood flow, and gain is reduced or increased until signal from adjacent bone is eliminated. Excessive transducer pressure and tendon tension can compress and artificially eliminate neovascularity, so, during Doppler assessment, the tendon should be in a relaxed position.

2.1.1.1 Ultrasound: Scanning Technique

All these anatomical structures can be assessed with a high-frequency linear transducer (9–18 MHz) with a thick layer of coupling gel.

Systematic scanning on short-axis planes is essential to follow the nerves contiguously throughout the limbs.

Tool box: The "elevator" technique consists in localizing a nerve at a characteristic anatomic reference point (usually bony landmarks) and following it proximally or distally. In this way it is possible to assess the nerve's echogenicity, thickness, shape, and its relation to the surrounding tissues.

Color Doppler can help to assess perineural vascularity and differentiate nerves fascicles from small vessels.

2.2 Brachial Plexus

2.2.1 Anatomy

The brachial plexus is a network of nerve fibers that supplies the skin and musculature of the upper limb. It is formed by the merging of the ventral roots of **C5–C8 and T1 nerves** and extends from the neck to the apex of the axilla (variable contributions may also come from the fourth cervical (C4) and the second thoracic (T2) nerves).

These roots join to form three trunks between the scalenus anterior and medius muscles:

- **Superior trunk** (C5–C6)
- **Middle trunk** (C7)
- **Lower trunk** (C8–T1)

The three trunks undergo primary anatomic separation, at the lateral border of the first rib, into **anterior** and **posterior** divisions.

The anterior divisions of the superior and middle trunks form the **lateral cord** of the plexus, the

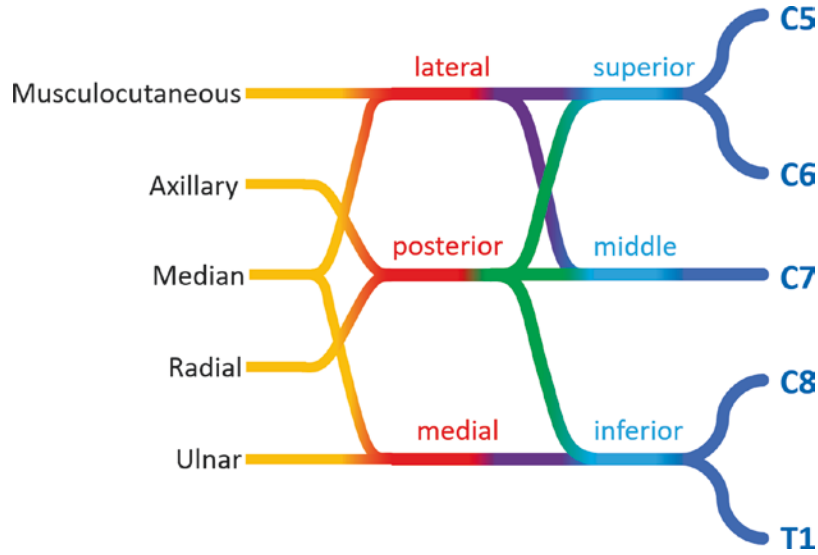

Fig. 2.5 Brachial plexus scheme

posterior divisions of all three trunks form the **posterior cord**, and the anterior division of the inferior trunk forms the **medial cord**.

In the axilla and the proximal aspect of the upper limb, the three cords divide and give rise to the terminal branches of the plexus, with each cord possessing two major terminal branches and a variable number of minor intermediary branches (Fig. 2.5).

The five major branches are listed below:

- **Musculocutaneous nerve** (roots, C5, C6, C7; cord, lateral)
- **Axillary nerve** (roots, C5, C6; cord, posterior)
- **Median nerve** (roots, C6–T1; cord, lateral and medial)
- **Radial nerve** (roots, C5–C8 and T1; cord, posterior)
- **Ulnar nerve** (roots, C8 and T1; cord, medial)

In addition to the five major branches of the brachial plexus, there are a number of smaller nerves that arise.

The brachial plexus provides sensory and motor innervation to the upper limb.

2.2.2 Topographic Anatomy

The ventral roots of the brachial plexus emerge from the vertebral foramina C5–T1.

The roots, along their course, enter the interscalene groove (between the anterior and middle scalene muscles, deep to the sternocleidomastoid muscle, lateral to the carotid artery, and internal jugular vein), where they pass the subclavian artery, before regrouping into trunks.

Distally, the trunks are redistributed into cords at the level of the costoclavicular gap.

In the sagittal plane, the cords are superior and posterior to the subclavian artery, forming a "Phrygian cap" over it.

In the axial plane, the cords are lateral to the subclavian artery, which is itself lateral to the subclavian vein.

After passing through the tunnel formed by the pectoralis minor, the cords give rise to the terminal nerve branches (Fig. 2.6).

2.2.3 Brachial Plexus: Technique

Based on topographic anatomy, some anatomical regions can be identified when we want study the different components of the brachial plexus:

- **Paravertebral region**
- **Interscalene region**
- **Supraclavear region**
- **Retropectoral and infraclavicular/axillary regions**

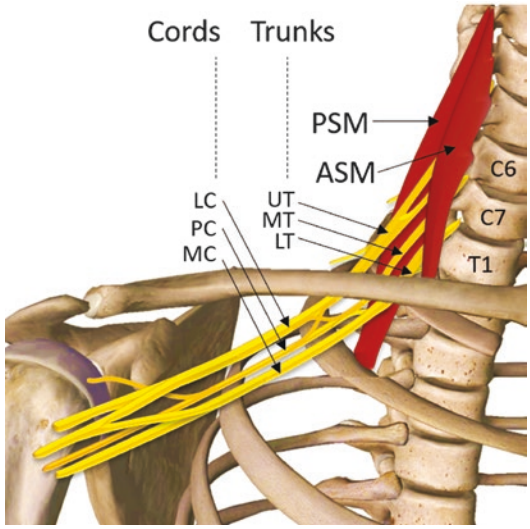

Fig. 2.6 Anatomical scheme of the brachial plexus. *PSM* posterior scalene muscle, *ASM* anterior scalene muscle, *UT* upper trunk, *MT* middle trunk, *LT* lower trunk, *LC* lateral cord, *PC* posterior cord, *MC* medial cord

Exploration of the brachial plexus requires a high-frequency probe, generally between 10 and 18 MHz.

2.2.4 The Paravertebral Region

It is important to have some landmarks that will help find the actual level of the roots:

- Thyroid gland
- The transverse process of C7
- Vertebral artery

The probe is positioned in a horizontal plane at the level of the thyroid gland.

Move the probe laterally and find the transverse processes of the cervical vertebrae; from this position, drag the probe from the top downward to see the different roots (Fig. 2.7a). The most caudal roots (C8–T1 level) may be difficult to visualize in short and thick necks, even with careful scanning technique.

Each root leaves the intervertebral foramen sliding on the transverse process of its corresponding vertebral level.

Because there are eight cervical nerves and only seven cervical vertebrae, the C8 root lies at the level of the T1 vertebra.

TIPS AND TRICKS: C6 is "V" shaped, C5 is like a "U" for the presence of two branches (anterior and posterior), and T1 doesn't have a tubercle (Fig. 2.7b, c).

The transverse process of C7, instead, not only lacks an anterior tubercle but also, in most cases, the foramen for the vertebral artery. Therefore, it is possible to identify it anterior to the most prominent processes (Fig. 2.7d).

In the coronal plane, the landmarks are the vertebral vessels (artery and vein), well detectable by color Doppler sonography (Fig. 2.8).

Landmarks of the interscalene triangle:

- *Superficially*: the junctional fibrous layer of the omohyoid muscle
- *Anteriorly and medially*: the anterior scalene muscle
- *Posteriorly and laterally*: the middle scalene muscle
- *Inferiorly*: the subclavian artery

Another important landmark for the detection of the roots-trunks is:

- The deep cervical artery that arises from subclavian artery and generally passes between C7 and C8 cervical nerves.

2.2.5 The Interscalene Region

Start with axial slices of the roots using the **"elevator technique"** along the omohyoid muscle. Using the anatomical landmarks

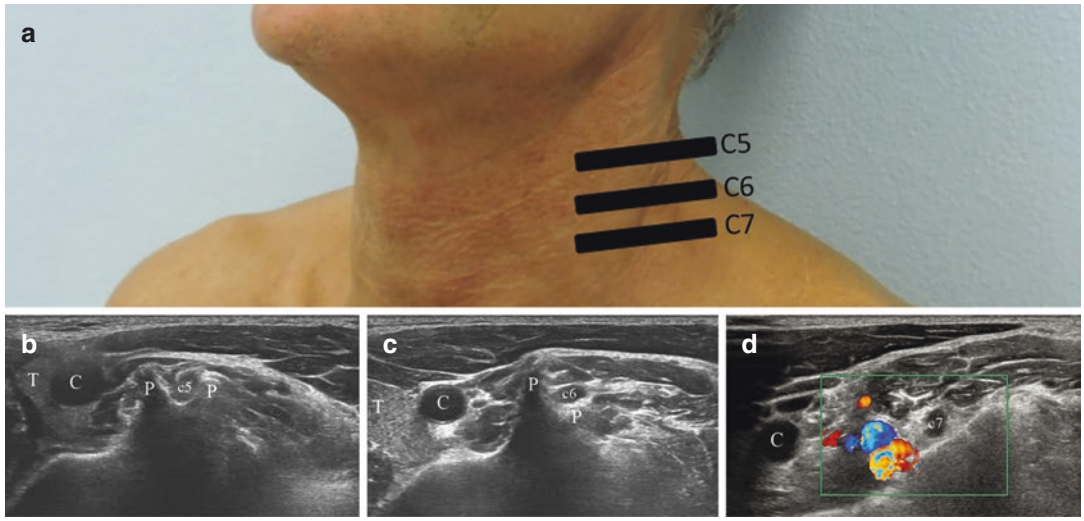

Fig. 2.7 (**a**) Positioning of the probe to analyze the extraforaminal part of nerve roots; (**b**) *T* thyroid, *C* carotid artery, *P* articular process, *c5* c5 nerve root; (**c**) *T* thyroid, *C* carotid artery, *P* articular process, *c6* c6 nerve root; (**d**) *C* carotid artery, *c7* c7 nerve root, *with color Doppler* vertebral vessels

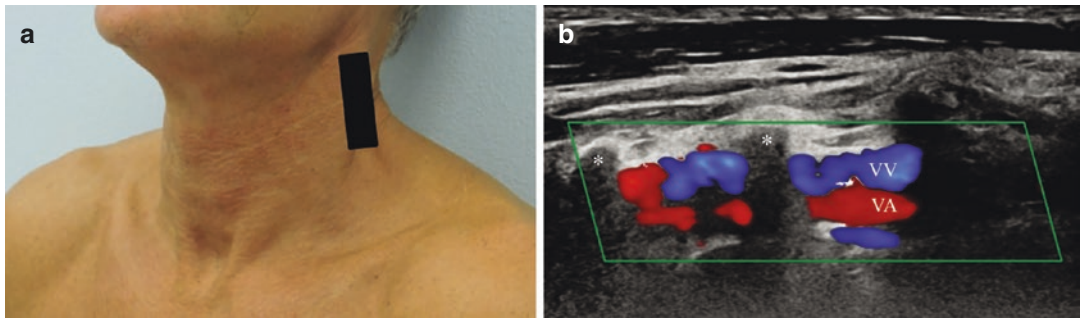

Fig. 2.8 (**a**) Positioning of the probe to analyze the vertebral vessels; (**b**) *VV* vertebral vein, *VA* vertebral artery

previously described, the roots and then the trunks can be identified in the interscalene groove. C5 is the most superficial root, T1 the deepest (Fig. 2.9).

Focus on: The subclavian artery passes at the base of the anterior scalene. Roots C8 and T1 are posterior to the subclavian artery so this deep position making their visualization more difficult.

Roots C5, C6, and C7 are situated above the subclavian artery.

Tool box: The long thoracic nerve innervates the serratus anterior muscle. This nerve arises from the anterior rami of C5, C6, and C7 of the brachial plexus. It runs posterior to the roots of the brachial plexus and anterior to the scalenus posterior muscle, then descends inferiorly on the chest wall along the mid axillary line, and

eventually lies on the superficial surface of the serratus anterior muscle.

Based on topographic anatomy, it's possible to check the long thoracic nerve in the US interscalene region scan, on the surface of the scalenus posterior muscle.

Longitudinal US scan shows the C5, C6, C7, and C8 nerve roots at the interscalene triangle in their long axis.

The use of color Doppler allows showing the deep cervical artery separating C7 and C8 cervical nerves.

2.2.6 The Supraclavear Region

Landmarks:
- Subclavian artery
- Transverse cervical artery
- First rib (hyperechoic cortex with a shadow cone)
- The apex of the lung (hyperechoic pleura moving with breathing)

The probe is oriented in a sagittal-oblique plane (slowly tilted medially and inferiorly), with the long axis of the probe that leans on the clavicle. In this region we find the division and the initial part of the cords that appear like a round hypoechoic cluster (Fig. 2.10). A supraclavicular approach is possible to detect the subclavian artery and the transverse cervical artery (Fig. 2.11).

2.2.7 Retropectoral and Infraclavicular/Axillary Regions

Landmarks:
- Axillary artery (continuation of the subclavian artery distal to the costoclavicular gap)

This region can be studied in sagittal or axial transverse slices by translating the probe from a sub-clavicular slice or from a slice passing through the coracoids process (proximal insertion of the pectoralis minor).

The pectoralis major muscle is superficially with the pectoralis minor, and the axillary artery is deeper than the latter, and the cords of the brachial plexus surround it.

The cords are grouped posterior and lateral to the axillary artery, forming a "Phrygian cap" (Mercedes sign) (Fig. 2.12):

- *Posteriorly and laterally*: the posterior cord
- *Superficially*: the lateral cord
- *Medially and deeply*: the medial cord

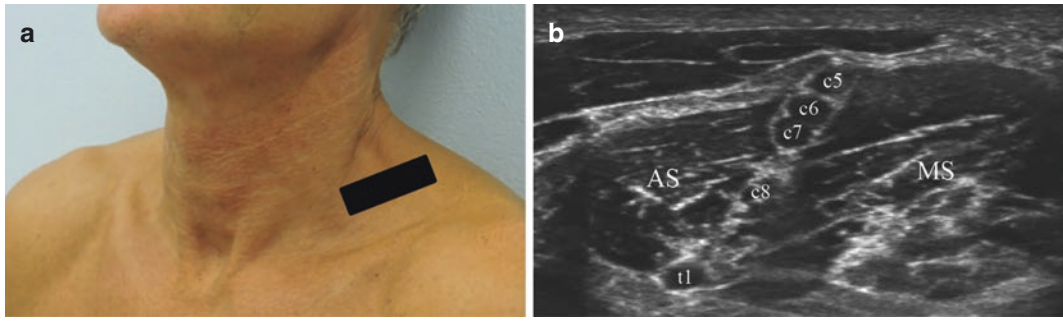

Fig. 2.9 (**a**) Positioning of the probe to analyze the nerve roots and the trunks at the interscalene triangle; (**b**) *AS* anterior scalene muscle, *MS* middle scalene muscle, *c5-c6* superior trunk, *c7* middle trunk, *c8-t1* lower trunk

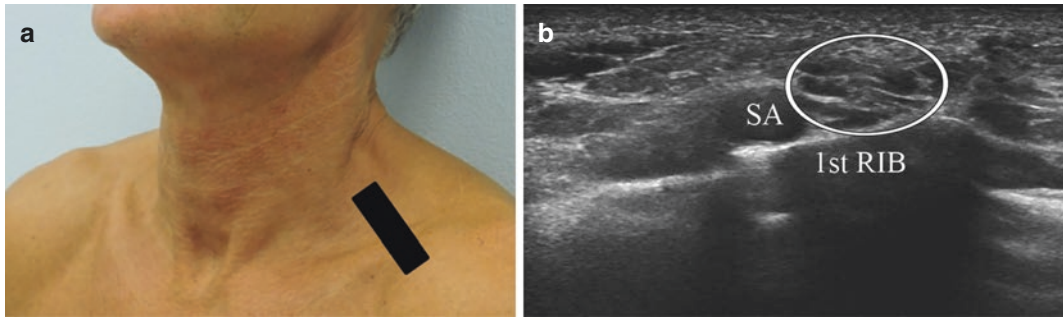

Fig. 2.10 (**a**) Positioning of the probe to analyze the cords of the brachial plexus by a supraclavicular approach; (**b**) *SA* subclavian artery, white circle brachial plexus

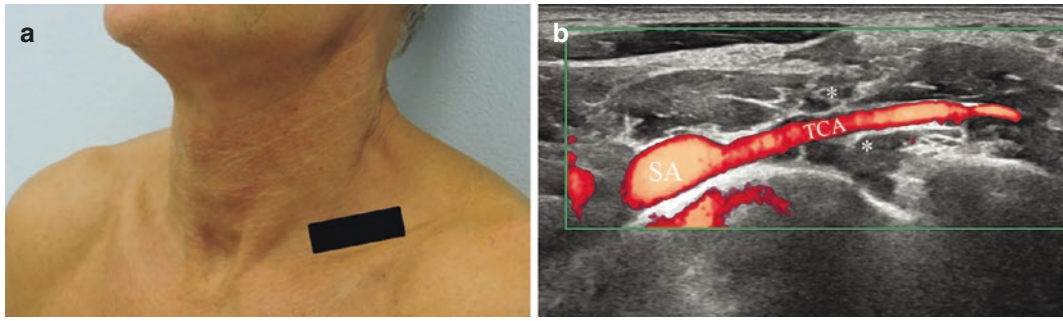

Fig. 2.11 (**a**) Positioning of the probe by a supraclavicular approach; (**b**) *SA* subclavian artery, *TCA* transverse cervical artery

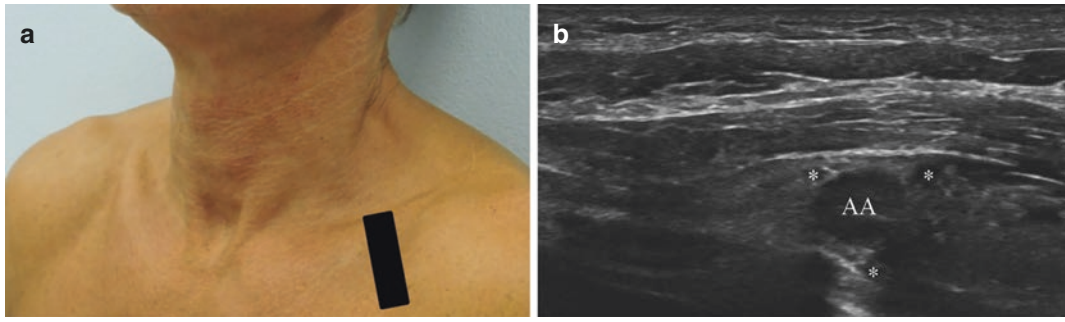

Fig. 2.12 (**a**) Positioning of the probe to analyze the cords of the brachial plexus at the retropectoralis minor space; (**b**) *AA* axillary artery, asterisks cords of the brachial plexus

Tips and Tricks: To study the cords under the axilla, raise the arm of the patient, and start from the proximal third of the arm, where the median, ulnar, and radial nerves are easy to find surrounding the brachial artery. Then follow them back to the axilla using the elevator technique (distal to proximal, short-axis scan).

2.3 Upper Limb Peripheral Nerves

2.3.1 Median Nerve

2.3.1.1 Median Nerve: Anatomy

The median nerve is a major **peripheral nerve** of the upper limb (Table 2.1).

2.3.1.2 Medial Nerve: Topographic Anatomy

The median nerve descends in the arm on the posteromedial side of the biceps and accompanies the brachial artery (Fig. 2.13).

It crosses the elbow anteriorly and, in the upper forearm, passes between the two heads of the pronator teres (Fig. 2.14).

After the median nerve leaves the pronator teres muscles, the anterior interosseous nerve arises.

It lies deep on the anterior surface of the interosseous membrane (Fig. 2.15).

At the level of the wrist, it lies just under the retinaculum and runs superficial and parallel to the second flexor tendon and medial to the flexor pollicis longus tendon, inside the carpal tunnel (Fig. 2.16).

Distal to the transverse carpal ligament, the median nerve divides into the recurrent motor branch and the common palmar digital branch.

2.3.1.3 Median Nerve: Technique

1. High-frequency linear transducer (9–17 MHz) with a thick layer of coupling gel.
2. Systematic scanning on short-axis planes of the nerve.
3. Based on topographic anatomy, some anatomical regions are of a particular relevance when we want study the course of the median nerve:
   - **Medial and anterior sides of the arm**
   - **Medial elbow and forearm**
   - **Wrist: carpal tunnel**
   - **Palm and fingers**

2.3.1.4 Medial and Anterior Sides of the Arm

Landmarks:
- Brachial artery

The probe is positioned on the short axis of the median nerve, on the medial side of the arm (Fig. 2.17a).

Table 2.1 The median nerve

Roots	C6-C7 (sometimes it contains fibres from C5)
Cords	Lateral and medial
Sensory innervation	• The lateral aspect of the palm (by the palmar cutaneous branch) • The skin of the palmar side of the index, thumb and middle finger, half of the ring finger and the nail bed (by digital cutaneous branch)
Motor innervation	• The flexor muscles in the anterior compartment of the forearm (except the flexor carpi ulnaris and part of the flexor digitorum profundus, innervated by the ulnar nerve). • The thenar muscles and the first and second lumbricals in the hand
Branches	• Anterior interosseous nerve • Palmar cutaneous nerve • Recurrent branch • Palmar digital branch

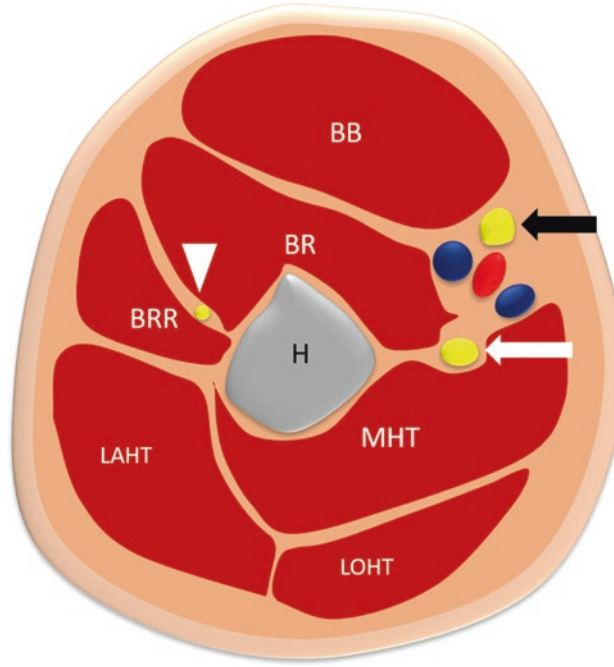

Fig. 2.13 Axial anatomical scheme of the median nerve (black arrow), ulnar nerve (white arrow), and radial nerve (white arrowhead) at the level of the diaphysis of the humerus (H). *BB* biceps brachii muscle, *BR* brachialis muscle, *BRR* brachioradialis muscle, *MHT* medial head of the triceps muscle, *LAHT* lateral head of the triceps muscle, *LOHT* posterior long head of the triceps

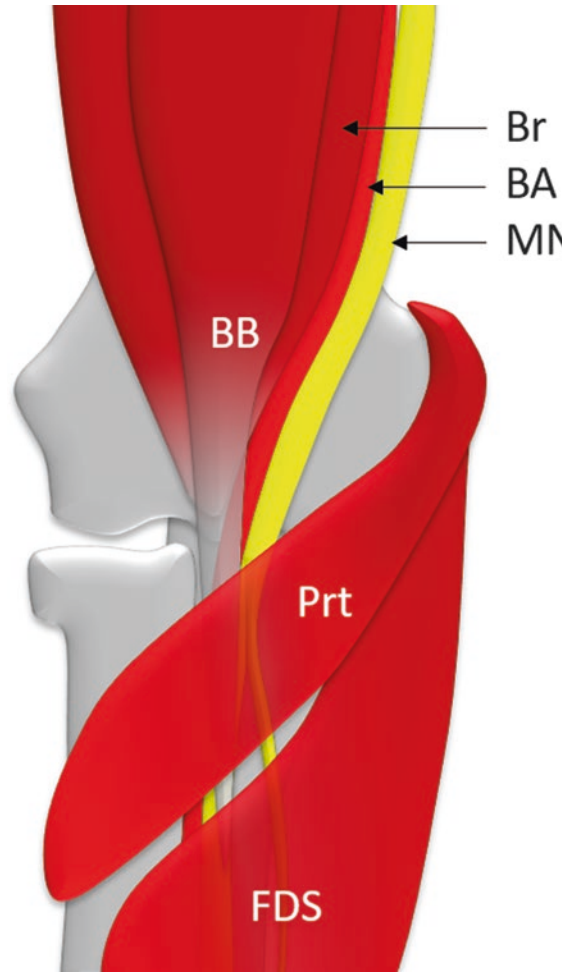

Fig. 2.14 Anatomical scheme of the median nerve (MN) at the level of the elbow, adjacent to the brachial artery (BA). *BB* biceps brachialis muscle, *Br* brachialis muscle, *Prt* pronator teres muscle, *FDS* flexor digitorum superficialis muscle

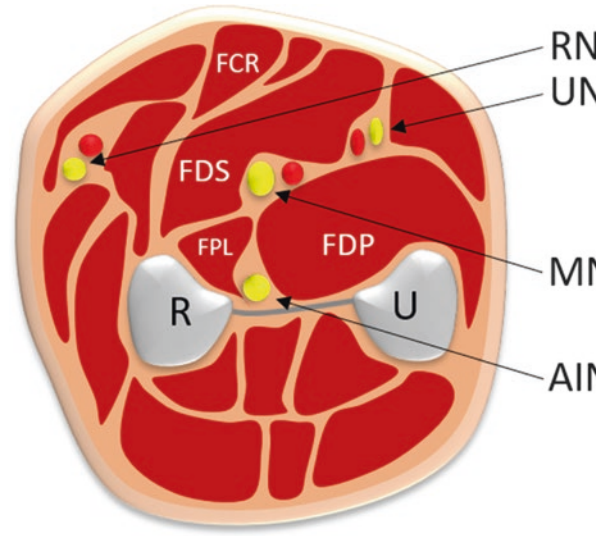

Fig. 2.15 Axial scheme of the forearm, showing the radial nerve (RN), the ulnar nerve (UN), the medial nerve (MN), and the anterioris interosseous nerve (AIN) and their relationships with muscles and bones. *FCR* flexor carpi radialis, *FDS* flexor digitorum superficialis, *FDP* flexor digitorum profundis, *FPL* flexor pollicis longus

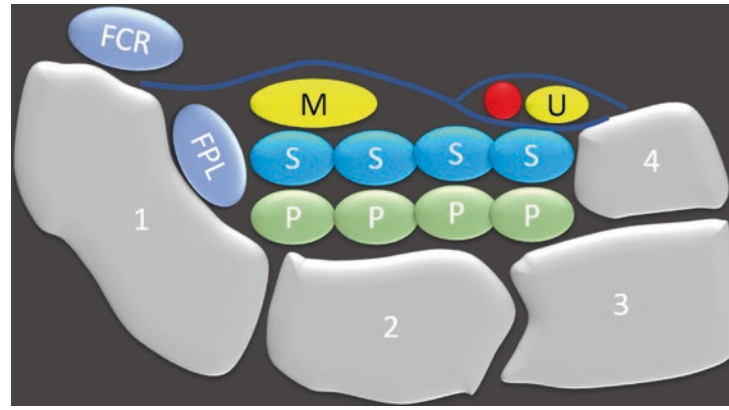

Fig. 2.16 Axial simplified scheme of the carpal tunnel. *1* scaphoid carpal bone, *2* lunate bone, *3* triquetrum bone, *4* pisiform carpal bone, *FCR* flexor carpi radialis, *FPL* flexor pollicis longus, *S* flexor digitorum superficialis tendons, *P* flexor digitorum profundus tendons, *M* median nerve, *U* ulnar nerve

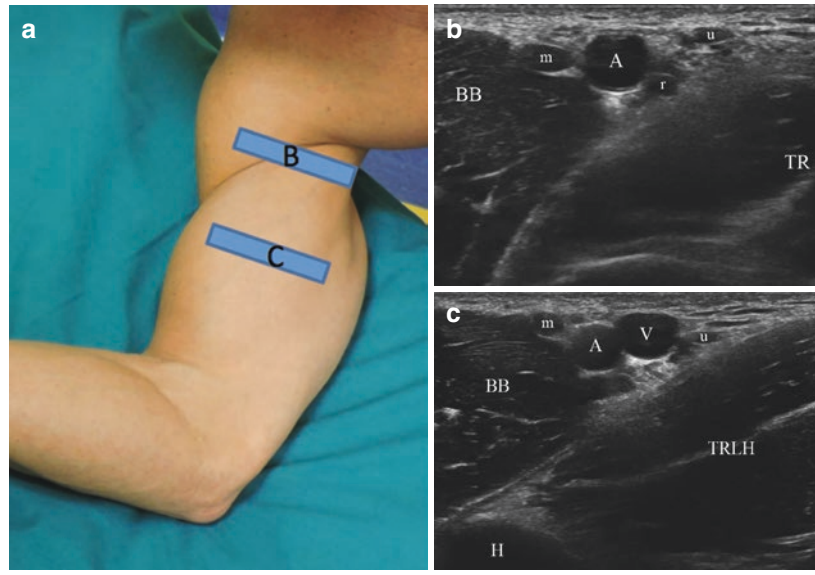

Fig. 2.17 (**a**) Positioning of the probe to analyze the median nerve at the proximal third of the arm (**b**) and on middle third of the arm (**c**); (**b**) *BB* biceps brachii muscle, *TR* triceps brachii muscle, *A* brachial artery, *m* median nerve, *u* ulnar nerve, *r* radial nerve, (**c**) *TRLH* triceps brachii muscle, *BB* biceps brachii muscle, *A* brachial artery, *V* brachial Vein, *u* ulnar nerve, *m* median nerve

At the proximal third of the arm, the median, ulnar, and radial nerves surround the brachial artery as shown in Fig. 2.17b.

At the middle third of the arm, before entering the antecubital fossa, the median nerve crosses above the artery and runs medial and parallel to the vessel (Fig. 2.17c).

2.3.1.5 Medial Elbow and Forearm

Landmarks:
- Humeral head
- Ulnar head
- Brachial artery
- Pronator teres muscle

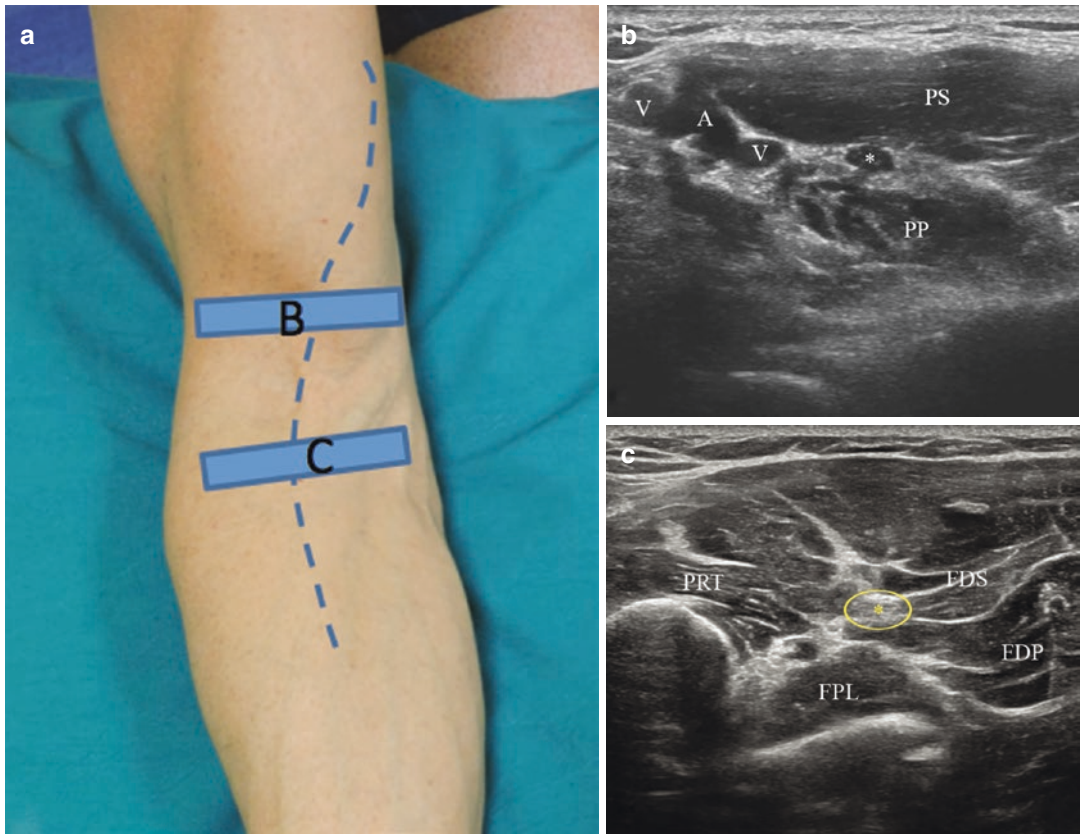

Fig. 2.18 (**a**) Positioning of the probe to analyze the median nerve at the level of elbow (**b**) and the forearm (**c**). (**b**) *A* brachial artery, *V* brachial vein, *PS* pronator teres superficialis muscle, *PP* pronator teres profundus muscle, asterisk median nerve, (**c**) *PRT* pronator teres, *FPL* flexor pollicis longus muscle, *FDS* flexor digitorum superficialis, *FDP* flexor digitorum profundus of hand muscle, asterisk median nerve

Place the upper limb on a flat surface with the palm of the hand facing upward (Fig. 2.18a).

At the level of the elbow, the median nerve courses downward between the humeral and ulnar head of pronator teres muscle (Fig. 2.18b), and then, at the level of forearm, it runs deep to the tendinous bridge connecting the humero-ulnar and radial heads of the flexor digitorum superficialis muscle (Fig. 2.18c).

Tool box: At the distal third of the forearm, it is possible to detect the anterior interosseous nerve, which courses deeply on the interosseous membrane between flexor digitorum profundus (II–III), flexor pollicis longus, and pronator quadratus (Fig. 2.19a, b).

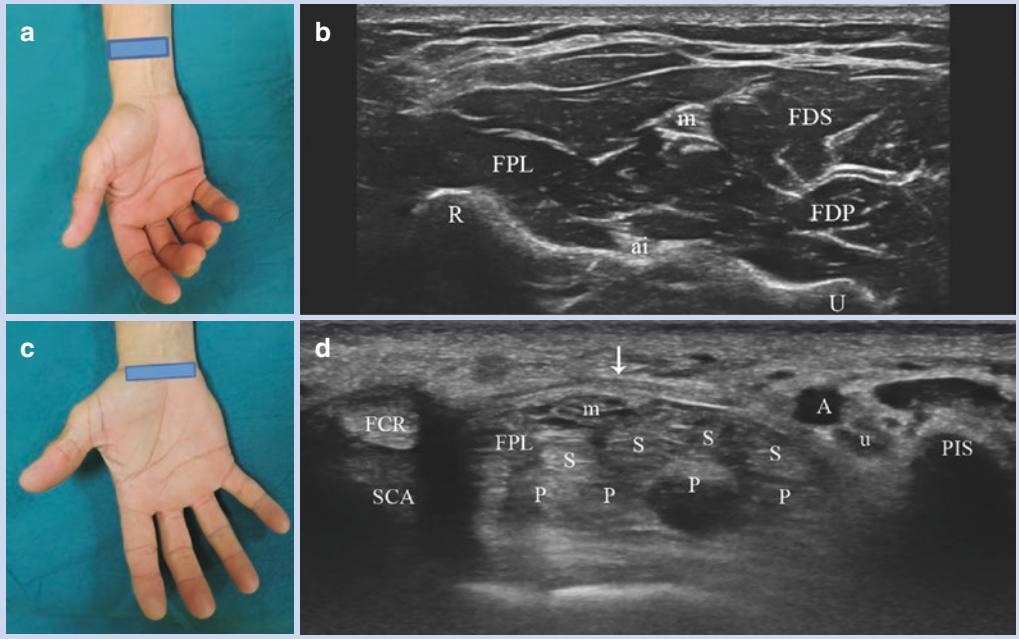

Fig. 2.19 (**a**) Positioning of the probe to analyze the median nerve at the level of distal third of the forearm; (**b**) *R* radius, *U* ulna, *ai* anterior interosseous nerve, *m* median nerve, *FPL* flexor pollicis longus muscle, *FDP* flexor digitorum profondus of hand muscle, *FDS* flexor digitorum superficialis of hand muscle; (**c**) positioning of the probe to analyze the median nerve at the level of carpal tunnel; (**d**) *FCR* flexor carpi radialis, *SCA* scaphoid, *FPL* flexor pollicis longus, *m* median nerve, *S* flexor digitorum superficialis tendons, *P* flexor digitorum profundus tendons, *A* ulnar artery, *u* ulnar nerve, *PIS* pisiform

2.3.1.6 Wrist: Carpal Tunnel

Landmarks:

- Flexor retinaculum
- Pisiform bone
- Scaphoid bone
- Flexor tendons

Place the upper limb on a flat surface with the palm of the hand facing upward (Fig. 2.19c).

The median nerve, at the level of carpal tunnel, courses under the retinaculum and between the flexor tendons like shown in Fig. 2.19d.

2.3.1.7 Palm and Fingers

Landmarks:
- Flexor digitorum tendons
- Palmar digital arteries

Following the median nerve distally, it is possible to see the division of the nerve into common palmar digital branches that course between the flexor tendons and close to the arteries.

2.3.2 Ulnar Nerve

2.3.2.1 Ulnar Nerve: Anatomy

The ulnar nerve is one of the major peripheral nerves of the upper limb (Table 2.2).

2.3.2.2 Ulnar Nerve: Topographic Anatomy

After arising from the brachial plexus, the ulnar nerve descends in the arm on the medial side, posterior to the **humeral artery** (Fig. 2.20), and then it runs in the posterior compartment, closely to the **medial head of the triceps**, posterior to the **medial intermuscular septum**.

At the level of the elbow, the ulnar nerve passes posterior to the medial epicondyle of the humerus, in a osteofibrous canal, **the cubital tunnel**, entering the forearm.

Focus on: the cubital tunnel:
The *cubital tunnel* is formed on the medial side by the medial epicondyle and the olecranon, bridged by the cubital tunnel retinaculum (*Osborne ligament*). The medial collateral ligament is the floor of this tunnel.

Distal to the condylar groove, the ulnar nerve enters in a tunnel formed between the ulnar and humeral heads of the **flexor carpi ulnaris muscle**, which are connected by the **arcuate ligament** and travel alongside the ulna (Fig. 2.21).

Table 2.2 The ulnar nerve

Roots	C8-T1
Cord	Medial
Sensory innervation	• The fifth digit, the medial half of the fourth digit, and the corresponding part of the palm (with nails by the palmar branch) • Dorsal medial hand and the dorsum of the medial 1.5 fingers (by the dorsal cutaneous branch)
Motor innervation	• The flexor carpi ulnaris • The flexor digitorum profundus (medial half) • Opponens digiti minimi • Abductor digiti minimi • Flexor digiti minimi brevis • Third and fourth lumbrical muscles • Dorsal and palmar interossei • Adductor pollicis • Deep head of the flexor pollicis brevis • Palmaris brevis
Branches	• Muscular • Palmar • Dorsal • Superficial • Deep

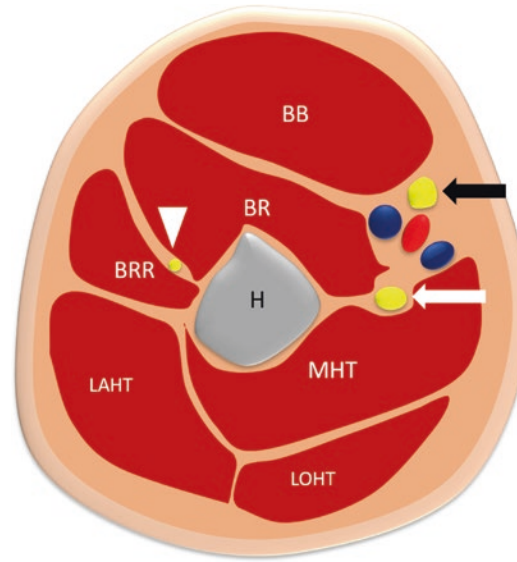

Fig. 2.20 Axial anatomical scheme of the median nerve (black arrow), ulnar nerve (white arrow), and radial nerve (white arrowhead) at the level of the diaphysis of the humerus (H). *BB* biceps brachii muscle, *BR* brachialis muscle, *BRR* brachioradialis muscle, *MHT* medial head of the triceps muscle, *LAHT* lateral head of the triceps muscle, *LOHT* posterior long head of the triceps

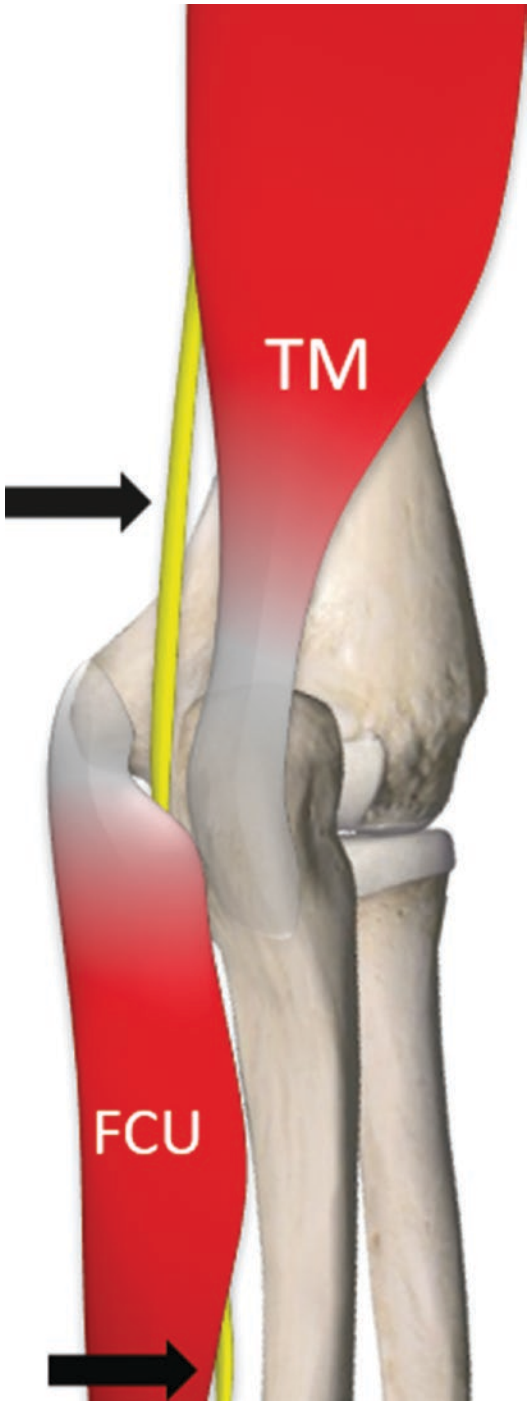

Fig. 2.21 Anatomical scheme of the ulnar nerve (black arrows) at the level of the elbow. *TM* triceps muscle, *FCU* flexor carpi ulnaris MUSCLE

Three branches arise in the forearm: muscular, palmar cutaneous, and dorsal cutaneous branches.

At the wrist, the ulnar nerve runs superficially to the **flexor retinaculum.** It enters the hand through the Guyon's canal.

Focus on: the Guyon's canal (Fig. 2.22): The walls of the Guyon tunnel consist of the pisiform medially and the hook of the hamate laterally:

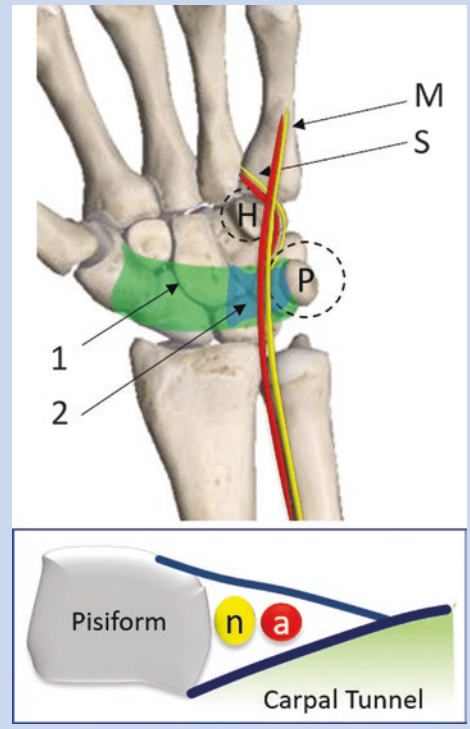

Fig. 2.22 Simplified scheme of the passage of the ulnar nerve and the ulnar artery at the level of pisiform bone. *1* flexor retinaculum, *2* palmar carpal ligament, *P* pisiform bone, *H* hamate, *M* deep motor branch of the radial nerve, *S* superficial sensory branch of the radial nerve, *n* nerve, *a* artery

- *Floor* → flexor retinaculum.
- *Roof* → palmar carpal ligament.
- The Guyon tunnel houses the ulnar nerve and the ulnar artery.

In the distal tunnel, the ulnar nerve bifurcates into a superficial sensory branch and a deep motor branch, which passes across the palm, distributing to intrinsic hand muscles.

2.3.2.3 Ulnar Nerve: Technique

1. High-frequency linear transducer (9–17 MHz) with a thick layer of coupling gel.
2. Systematic scanning on short-axis planes of the nerve following the elevator technique.
3. Based on topographic anatomy, some anatomical regions can be identified when we want to study the course of the medial nerve:
   - **Medial and posterior sides of the arm**
   - **Posterior elbow: cubital tunnel**
   - **Wrist: Guyon's tunnel**

2.3.2.4 Medial and Posterior Sides of the Arm

Landmarks:
- Humeral artery
- Medial head of the triceps
- Medial intermuscular septum

Start the examination placing the upper limb on a flat surface with the palm of the hand facing upward and the arm flexed by 90°.

The probe is positioned on the short axis of the ulnar nerve, at the proximal third of the arm (Fig. 2.23a).

The ulnar nerve is located posterior to the humeral artery and anterior to the medial intermuscular septum.

At the distal third, the probe is positioned on the posterior side of the arm.

The ulnar nerve is in close contact with the triceps and lies posteriorly to the intermuscular septum (Fig. 2.23b).

2.3.2.5 Posterior Elbow: Cubital Tunnel

Landmarks:
- Medial epicondyle
- Olecranon

The upper limb is positioned on a flat surface, with joint flexed by 90°, and the forearm slightly extrarotated (Fig. 2.23a).

The ulnar nerve is located between the medial epicondyle and the olecranon (Fig. 2.23c, d).

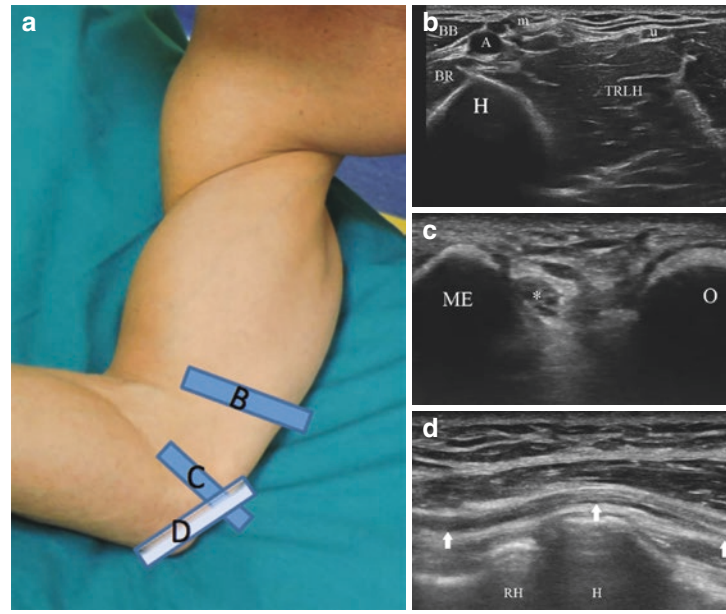

Fig. 2.23 (**a**) Positioning of the probe to analyze the ulnar nerve at the middle third of the arm (**b**) and at the level of the cubital tunnel (C-D); (**b**) *TRLH* triceps brachii muscle, *BB* biceps brachii muscle, *A* brachial artery, *u* ulnar nerve, *m* median nerve, *H* humerus; (**c**) asterisk ulnar nerve, *ME* medial epicondyle of the humerus, *O* olecranon; (**d**) *RH* radial head bone, *H* humerus, white arrows ulnar nerve in the long axis

Tool box: The Osborne retinaculum retains the ulnar nerve posterior to the medial epicondyle during elbow flexion.

In case of trauma or congenital laxity/absence of the retinaculum, dynamic scan during elbow flexion can depict intermittent subluxation or dislocation of the nerve over the medial epicondyle (Fig. 2.24).

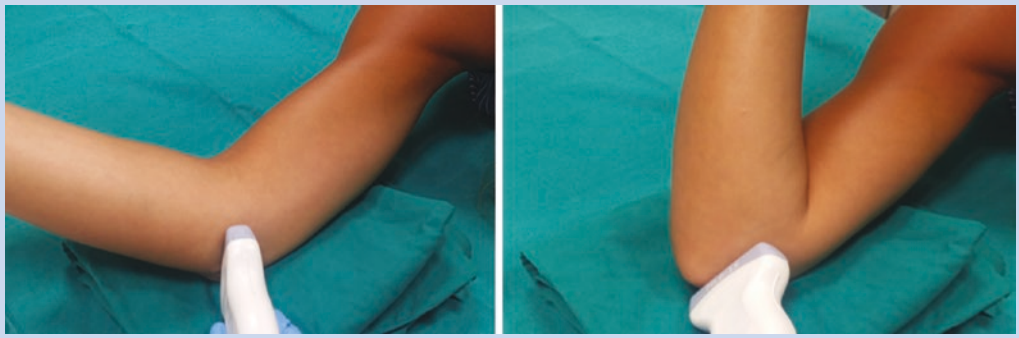

Fig. 2.24 Dynamic scan during elbow flexion

In some cases in combination with dislocation of the ulnar nerve, we can have the dislocation of the medial head of the triceps. So we have "two snaps," and this condition is known as double snapping syndrome.

2.3.2.6 Wrist: Guyon's Canal

Landmarks:
- Ulnar artery
- Pisiform
- Flexor retinaculum
- Palmar carpal ligament

The palm of the hand is faced upward (Fig. 2.25a).

The ulnar nerve, at the level of Guyon's canal, courses over the flexor retinaculum and under the palmar carpal ligament, near the ulnar artery (Fig. 2.25b, c).

In the distal tunnel, the ulnar nerve bifurcates into a superficial sensory branch and a deep motor branch.

2.3.3 Radial Nerve

2.3.3.1 Radial Nerve: Anatomy

The radial nerve is one of the main nerves of the upper limb. It is an extension of the **posterior cord** of the brachial plexus containing fibers from nerve roots C5 to T1 (Table 2.3).

2.3.3.2 Radial Nerve: Topographic Anatomy

After leaving the axilla, the radial nerve winds closely around the posterior aspect of the shaft of the humerus in the spiral groove, passing between the medial and lateral heads of the triceps muscle, and supplies branches to the long and medial heads of the triceps brachii.

During much of its course within the upper arm, it is accompanied by the deep branch of the brachial artery (Fig. 2.26).

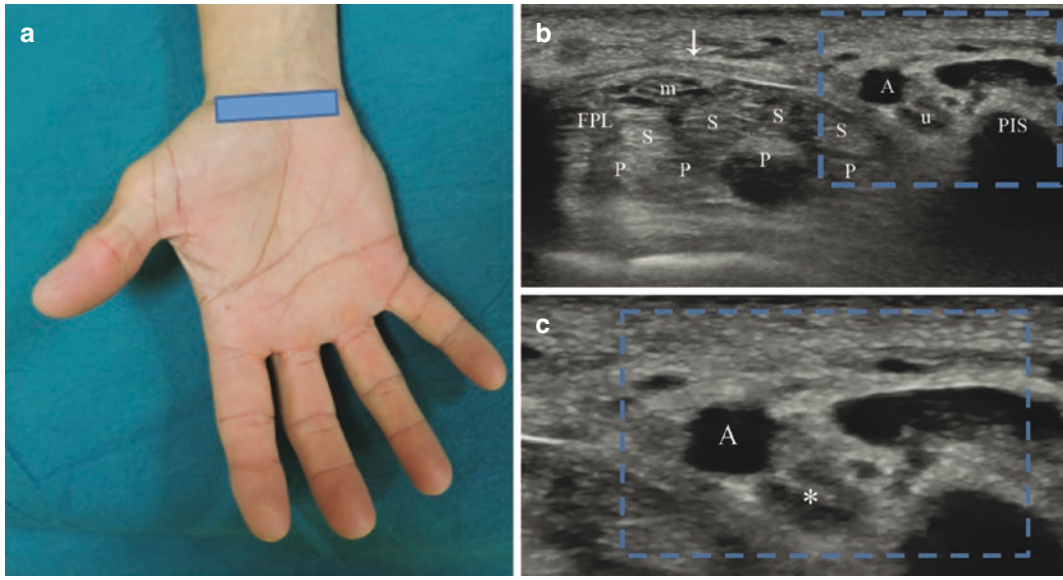

Fig. 2.25 (**a**) Positioning of the probe to analyze the ulnar nerve at the level of Guyon's canal; (**b**) *m* median nerve, *FPL* flexor pollicis longus muscle, *S* flexor digitorum superficialis tendons, *P* flexor digitorum profundus tendons, *A* ulnar artery, *u* ulnar nerve, *PIS* pisiform carpal

Table 2.3 The radial nerve

Roots	C5-C8 and T1
Cords	Posterior
Sensory innervation	Lower lateral cutaneous nerve of arm • Lateral side of the upper arm, under the deltoid muscle Posterior cutaneous nerve of arm • Skin of the posterior way of the upper arm Posterior cutaneous nerve of the forearm • Skin of the posterior forearm, in the middle Superficial branch • Dorsal and lateral side of the palm • I, II, III and half of the IV fingers, excluded the distal phalanges
Motor innervation	• The triceps brachii • Anconeus • Brachioradialis • Extensor carpi radialis longus • Extensor muscles of the posterior forearm
Branches	• Superficial (sensory) • Deep (motor)

After its course in the spiral groove of the humerus, the radial nerve divides into the deep branch and the superficial radial nerve (Fig. 2.27).

When the deep branch of the radial nerve penetrates the supinator muscle of the forearm, through the "arcade of Frohse," it becomes the posterior interosseous nerve (Fig. 2.28).

The superficial radial nerve descends along the lateral border of the forearm deep to the brachioradialis. Then, it passes between the brachioradialis and extensor carpi radialis longus (ECRL) and emerges from under the lateral border of the brachioradialis into the subcutaneous tissue.

At the level of the wrist, the superficial radial nerve pierces the fascia and overlies the anatomical "snuff-box," traversing the extensor tendons of the first compartment (Fig. 2.29).

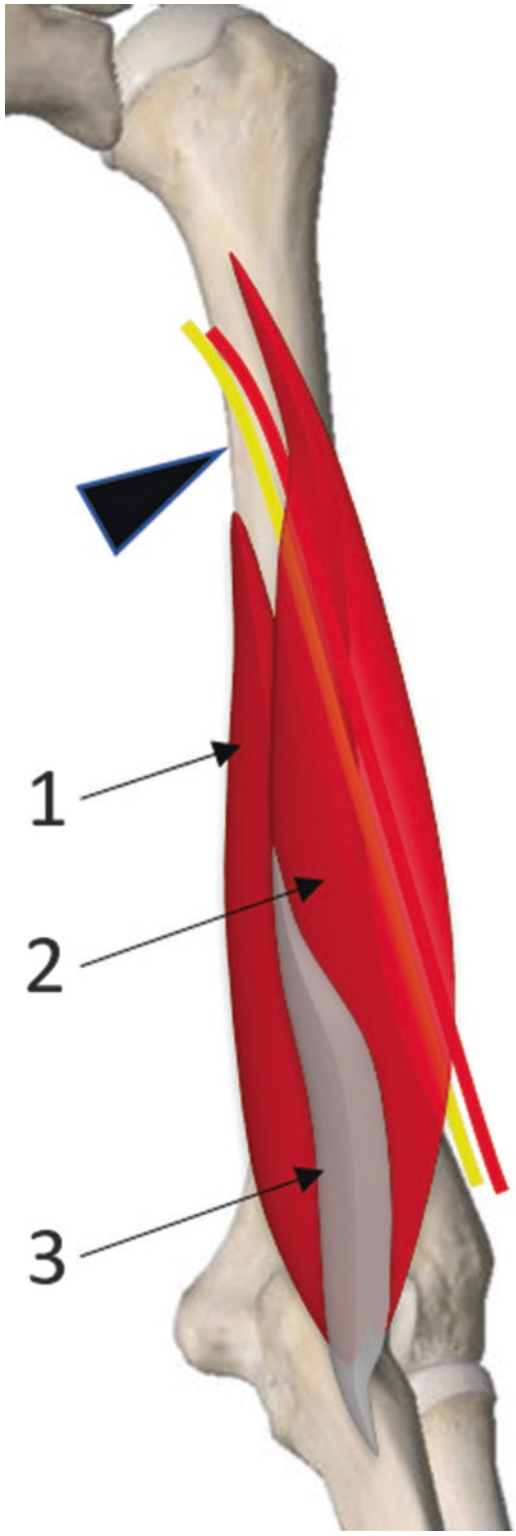

Fig. 2.26 Anatomical scheme of the radial nerve (arrowhead) at the level of the posterior aspect of the arm. *1* medial heads of the triceps muscle, *2* lateral heads of the triceps muscle, *3* triceps tendon

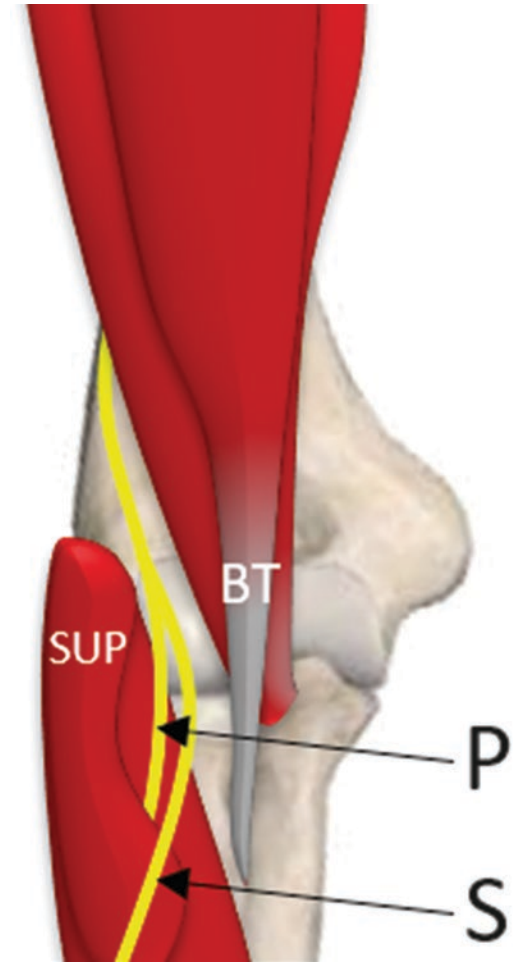

Fig. 2.27 Anatomical scheme of the radial nerve at the level of the elbow, with the division in the deep branch (P), passing through the supinator muscle (SUP), and the superficial branch, with a more superficial path. BT biceps brachialis tendon

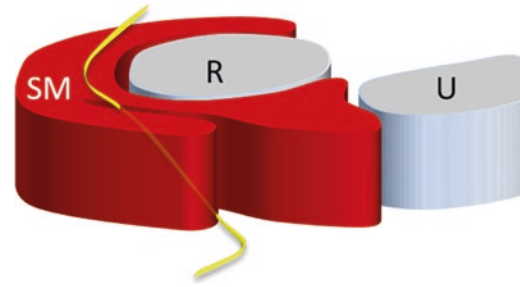

Fig. 2.28 Simplified 3D scheme of the proximal forearm, showing the passage of the deep branch of the radial nerve across the supinator muscle (SM)

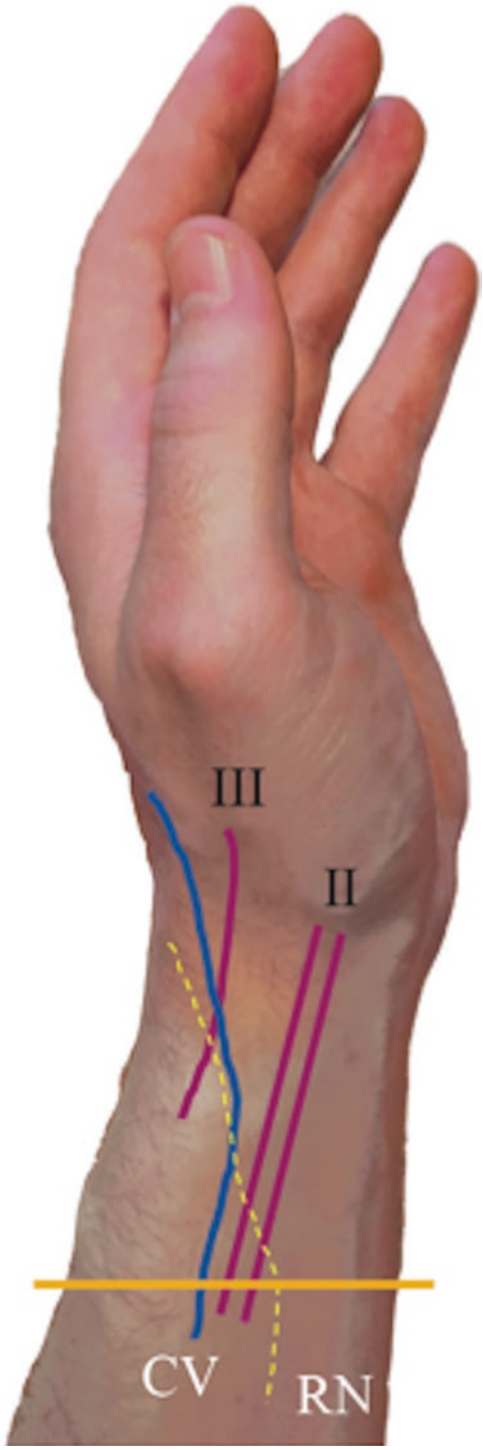

Fig. 2.29 Simplified scheme of the distal third of the forearm and the wrist, showing the passage of the superficial radial nerve over the extensor tendons of the first compartment

The nerve runs alongside the cephalic vein and divides into four or five digital branches to supply the skin of part of dorsum of the hand.

2.3.3.3 Radial Nerve: Technique

The echographic study of the radial nerve is conducted with a high-frequency linear transducer (9–17 MHz) with a thick layer of coupling gel.

Systematic scanning on short-axis planes of the nerve, following it proximally or distally throughout the limb, is essential to a correct approach.

Based on topographic anatomy, some anatomical regions can be identified when we want to study the course of the radial nerve:

- **Posterolateral side of the arm**
- **Lateral elbow**
- **Forearm**
- **Lateral side of the wrist**

2.3.3.4 Posterolateral Side of the Arm

The main landmarks that will help find the actual level of the radial nerve are:
- The brachial artery
- The medial and lateral heads of the triceps
- The humerus

The probe is positioned on the short axis of the radial nerve at the middle third of the humerus over the spiral groove (Fig. 2.30a).

The radial nerve and the deep brachial artery appear close to the surface of the bone, between the bellies of the triceps and the brachialis muscles (Fig. 2.30b).

Following the nerve proximally, the neurovascular complex runs through the medial, long, and lateral heads of the triceps (Fig. 2.30c).

2.3.3.5 Lateral Elbow

Landmarks:
- Capitulum humeri
- Radial head and neck

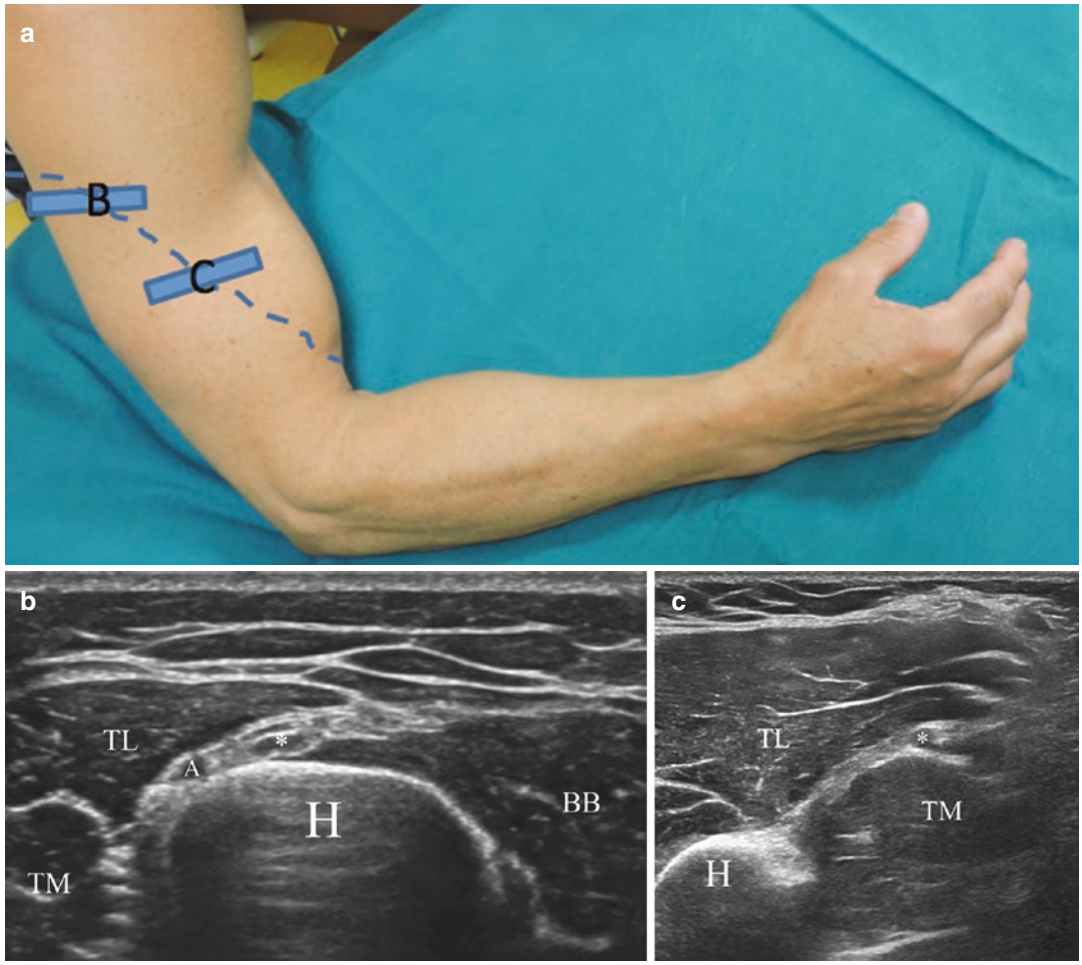

Fig. 2.30 (**a**) Positioning of the probe to analyze the radial nerve at posterolateral side of the arm, (**b**) *TL* triceps brachii lateral head, *TM* triceps brachii medial head, *BB* biceps brachii muscle, *asterisk* radial nerve, *A* brachial artery, (**c**) *TL* triceps brachii lateral head, *TM* triceps brachii medial head, asterisk radial nerve

Position the upper limb on a flat surface with the palm of the hand facing upward (Fig. 2.31a).

Distally, at the level of the proximal side of the lateral elbow, the radial nerve courses between the brachioradialis (posterolateral) and the brachialis (anteromedial).

Distal to the lateral epicondyle, the radial nerve passes over the radial head and divides into the posterior interosseous and superficial radial nerves. This division in two main branches can be seen over the supinator muscle (Fig. 2.31b).

The posterior interosseous nerve runs between the superficial and deep parts of the supinator muscle (Fig. 2.31c, d).

After leaving the supinator muscle, the posterior interosseous nerve enters the posterior compartment, close to the radial artery.

The superficial radial nerve continues into the anterior forearm, deep to the brachioradialis muscle, and close to the radial artery.

2.3.3.6 Forearm

Using the elevator technique, it is possible to study the course of the superficial sensory branch of the radial nerve, moving the transducer forward or backward through the volar compartment of the forearm.

The forearm is extended and the palm of the hand is facing upward.

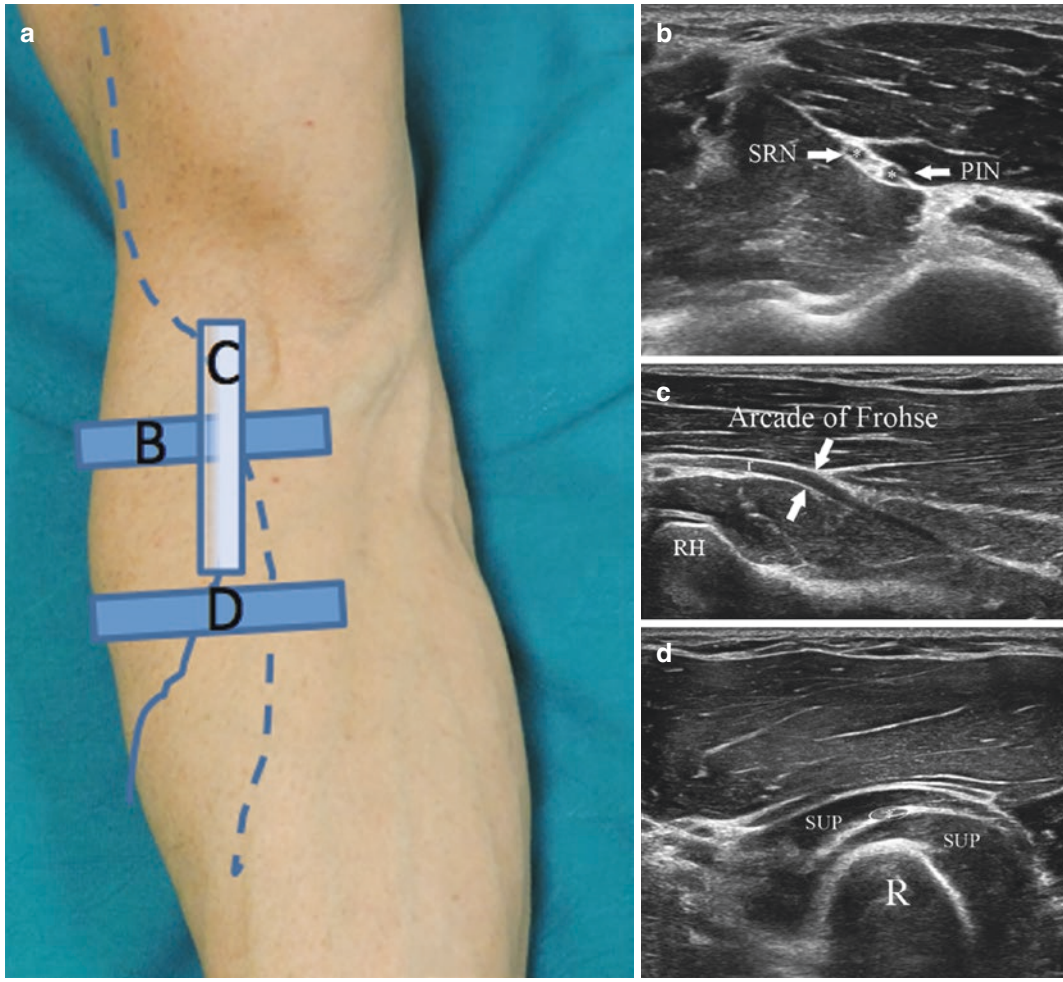

Fig. 2.31 (**a**) Positioning of the probe to analyze the radial nerve at lateral elbow; (**b**) *SRN* superficial radial nerve, *PIN* posterior interosseous nerve; (**c**) *RH* radial head bone; (**d**) *R* radial bone, *SUP* supinator muscle

In the distal part of the forearm, the superficial radial nerve and the radial artery run deep into the brachioradialis muscle.

At the distal forearm, it passes between the brachioradialis and the extensor carpi radialis longus (ECRL) muscles (Fig. 2.32a, b), and emerges from under the lateral border of the brachioradialis muscle into the subcutaneous tissue.

2.3.3.7 Lateral Side of the Wrist

At the lateral side of the wrist, the superficial radial nerve crosses the extensor tendons of the first compartment (abductor pollicis longus and extensor pollicis brevis tendons) to reach the dorsal aspect of the hand. The radial artery is lateral and superficial compared to nerve (Fig. 2.32c–f).

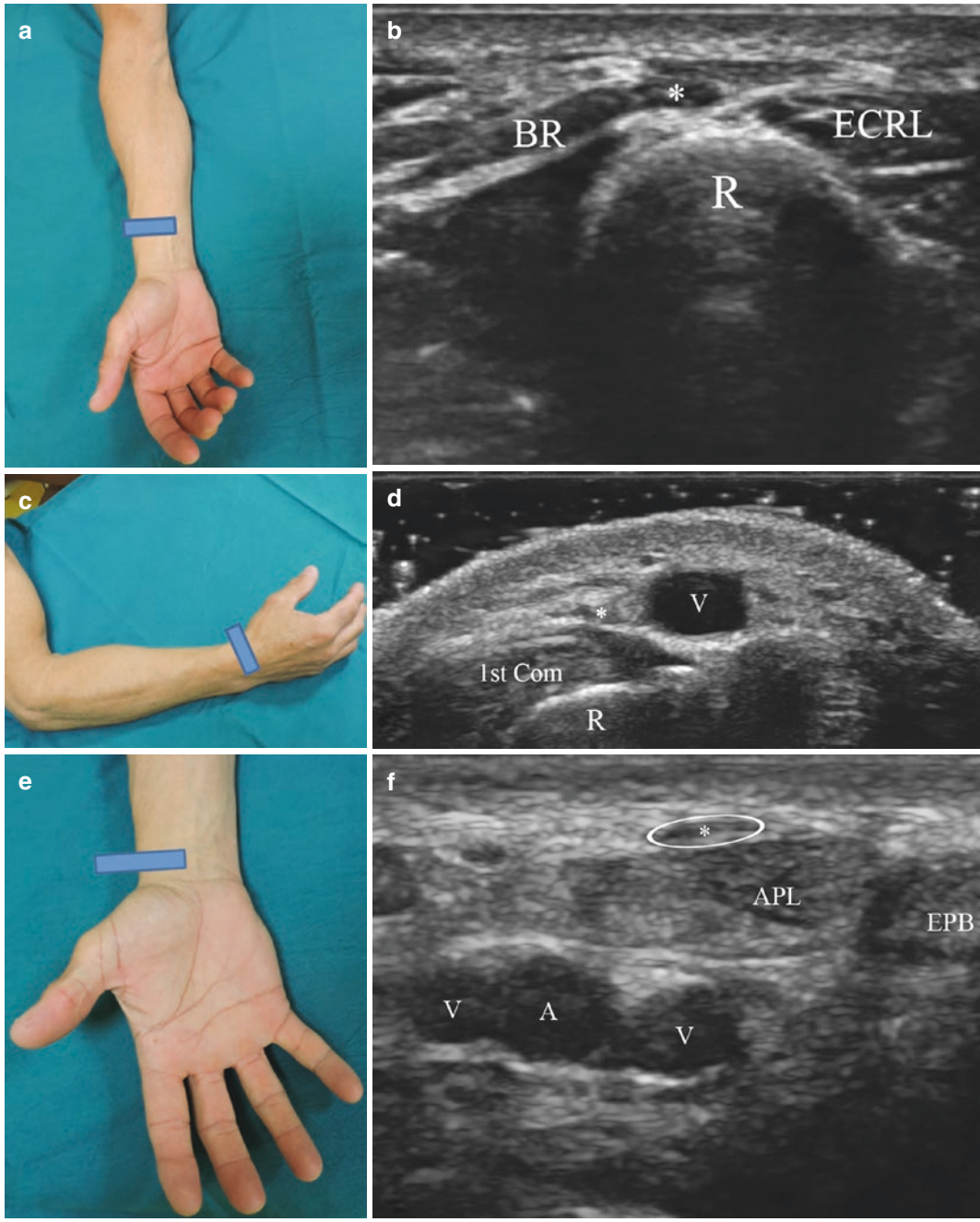

Fig. 2.32 (**a**–**e**) Positioning of the probe to analyze the radial nerve at forearm and lateral side of the wrist; (**b**) *B* brachio-radialis muscle, *ECRL* extensor carpi radialis longus muscle, *asterisk* radial nerve; (**d**) *asterisk* radial nerve, *First Com* first extensor compartment; (**f**) *APL* abductor pollicis longus, *EPB* extensor pollicis brevis, *asterisk* radial nerve, *A* radial artery, *V* radial vein

2.4 Lower Limb Peripheral Nerves

2.4.1 Lumbar Plexus

2.4.1.1 Anatomy

The lumbar plexus is localized in the lumbar region of the body and forms part of the lumbosacral plexus (which consist of the anterior divisions of the lumbar, sacral, and coccygeal nerves) (Fig. 2.33).

It is formed by the ventral divisions of the first four lumbar nerves (L1–L4) and by variable contributions from T12 (subcostal nerve, which is the last thoracic nerve) and L5.

This plexus lies in the posterior part of the psoas major muscle, in front of the transverse processes of the lumbar vertebrae, and projects laterally and caudally from the intervertebral foramina. Nerves of the lumbar plexus supply the skin and the muscles of the lower abdominal wall, thigh, and external genitals.

It differs from the brachial plexus because the nerves of distribution arise from one or more of the spinal nerves, in the following manner:

- The T12 and L1 nerves and the L2–L4 anterior primary divisions supply muscular branches to the psoas major and quadratus lumborum.
- The first lumbar nerve, which frequently receives a branch from the last thoracic nerve, splits into an upper and a lower branch: the upper branch is larger and is divided into the *iliohypogastric and ilioinguinal* nerves; the lower branch unites with a branch of the second lumbar to form the *genitofemoral* nerve.
- The remaining part of the second nerve, as well as the third and fourth nerves, divides into ventral and dorsal divisions. The ventral divisions of the second, third, and fourth nerves form the *obturator* nerve. The dorsal divisions of the second and third nerves divide into two branches; the smaller branches from each join to form the *lateral femoral cutaneous* nerve, while the larger branches from each merge with the dorsal division of the fourth nerve to form the *femoral* nerve. The accessory obturator nerve, when it exists, is formed by the fusion of two small branches arising from the third and fourth nerves.

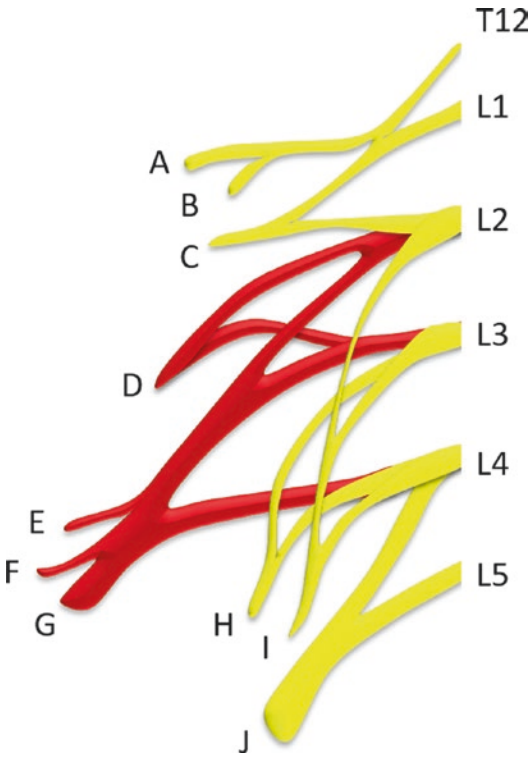

Fig. 2.33 Simplified scheme of the lumbar plexus, with the posterior nerves painted in red. *A* iliohypogastric nerve, *B* ilioinguinal nerve, *C* genitofemoral nerve, *D* lateral femoral cutaneous, *E* and *F* branches for psoas and iliacus muscles, *G* femoral nerve, *H* accessory obturator nerve, *I* obturator nerve, *J* lumbosacral trunk

2.4.1.2 US Exam

Landmarks:

- Sacrum
- Transverse processes of vertebrae
- Lower pole of the kidney

The patient is placed in the lateral position with the operative side up.

The operator should use a low-frequency curved transducer to optimize imaging at deep

locations and obtain a greater angular view, since the depth of the plexus makes visualization of the nerves difficult.

Place the probe approximately 3–4 cm lateral and parallel to the lumbar spine to produce a longitudinal scan of the lumbar paravertebral region. At this level the bone landmarks are the transverse processes of the vertebrae.

The technique to identify the vertebral transverse processes is the following: visualize the flat surface of the sacrum, and then move the probe cranially until the intervertebral space between L5 and S1, which is recognized as an interruption of the sacral line continuity. Cranially you can identify the transverse process of L4 and L3; in fact, the acoustic shadow of the transverse process has a characteristic appearance called "trident sign" (Fig. 2.34a, b).

As the transducer is progressively moved cranially, at the level of L2–L3, the lower pole of the kidney appears at approximately 5 cm depth as an oval structure that ascends and descends with respiration (Fig. 2.34c, d). The inferior vena cava (IVC), on the right, and the aorta, on the left, can be seen.

The psoas muscle is identified through the acoustic window of the transverse processes, with the typical hypoechoic appearance of muscle. The identification of the lumbar roots in a longitudinal scan is not easy: they appear as hyperechoic striations between the intervertebral space and the psoas muscle.

Next, rotate the probe by 90°, always positioned 3–4 cm lateral to lumbar spinous process at the L3–L4 level, to perform a transverse oblique scan.

2.4.2 Lateral Femoral Cutaneous Nerve

2.4.2.1 Anatomy

Lateral femoral cutaneous nerve (LFCN) is a small pure sensory nerve and originates directly

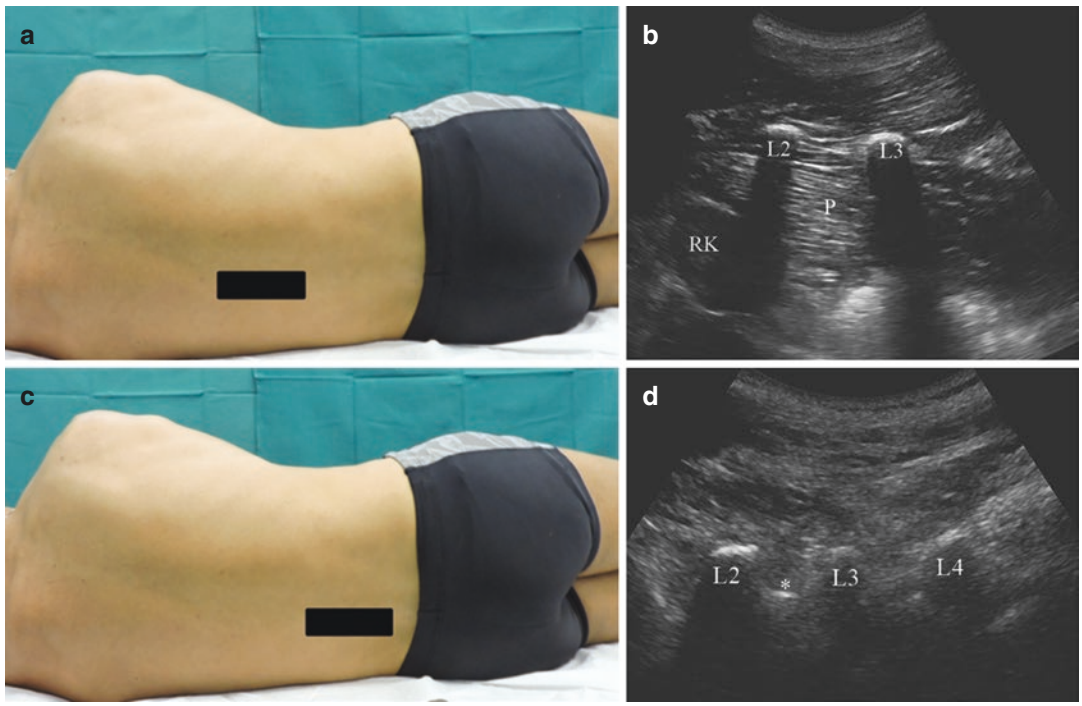

Fig. 2.34 (**a**, **b**) Probe position and ultrasound scan of the lumbar paravertebral space at the level of L2-L3. *RK* right kidney, *P* psoas, *L2* lumbar vertebra L2, *L3* lumbar vertebra L3. (**c**, **d**) Probe position and ultrasound scan of the lumbar paravertebral space at the level of L3-L4. *L2* lumbar vertebra L2, *L3* lumbar vertebra L3, *L4* lumbar vertebra L4, asterisk L2 nerve

from the lumbar plexus, from the L2 and L3 roots (Fig. 2.35).

The LFCN supplies sensation to the anterolateral aspect of the thigh.

It emerges from the side of the psoas muscle and passes the iliacus diagonally toward the ASIS.

It then runs under the inguinal ligament, crosses the sartorius muscle, and reaches the subcutaneous tissue of the femoral region.

The course of the LFCN is variable, but the most common one (about 30% cases) is medial and inferior to the ASIS. It has a diameter of about 2 mm that becomes smaller when it passes through the fascia, about 10 cm inferior to the inguinal ligament.

Then it divides into an anterior and a posterior branch: the anterior one controls the femoral region up to the knee, and the posterior branch controls the lateral femoral region up to the greater trochanter of femur.

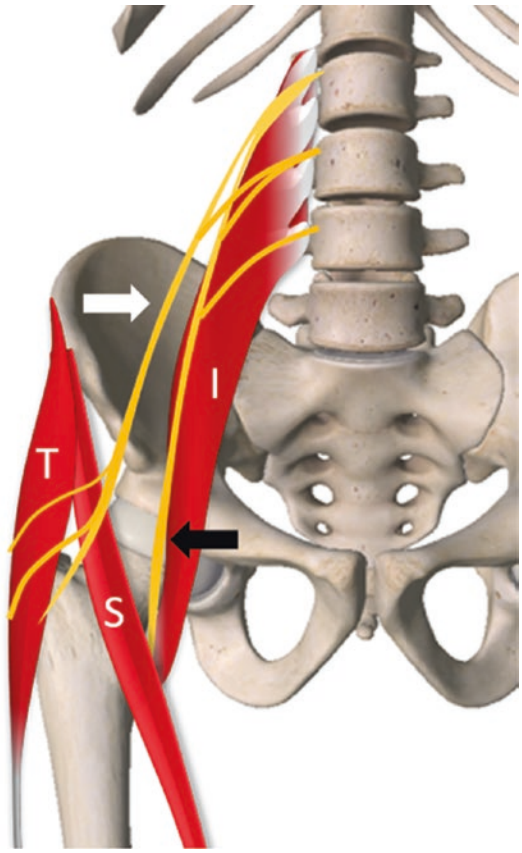

Fig. 2.35 Anatomical scheme of the lumbar plexus with the femoral nerve (black arrow) and the lateral femoral cutaneous nerve (white arrow). *T* Tensor fascia muscle, *S* sartorius muscle, *I* iliopsoas muscle

2.4.2.2 US Exams

Landmarks:
- ASIS (anterior superior iliac spine)
- Sartorius muscle

First of all the ASIS should be identified via palpation with the patient supine.

The end of the linear probe is applied perpendicular to the long axis of the limb, at the anterior superior iliac spine (ASIS) bony landmark.

Then move the probe in a transverse plane 2–3 cm distal and medial to the anterior superior iliac spine to confirm the course of LFCN, located above the sartorius and below the tensor fasciae latae, in the space between the two fascia layers (fascia lata and the fascia iliaca) (Fig. 2.36a–c).

Nerve morphology, cross-sectional area (CSA), and distance from the ASIS can be detected with US color Doppler can be used to prevent overestimation of the cross-sectional area by including blood vessels.

Turn the probe by 90° to visualize the LFCN in a longitudinal plane (Fig. 2.36d, e).

Focus on: Meralgia Paresthetica: *Meralgia paresthetica*, from the Greek words *meros* (thigh) and *algos* (pain), is characterized by pain and paresthesia along the LFCN course due to compression of the nerves.

It is exacerbated by conditions that increase intra-abdominal pressure such as obesity, pregnancy, metabolic disorders (diabetes), and alcohol.

LFCN could be also damaged from surgeries near the inguinal region (e.g., inguinal hernia repair; hip replacement).

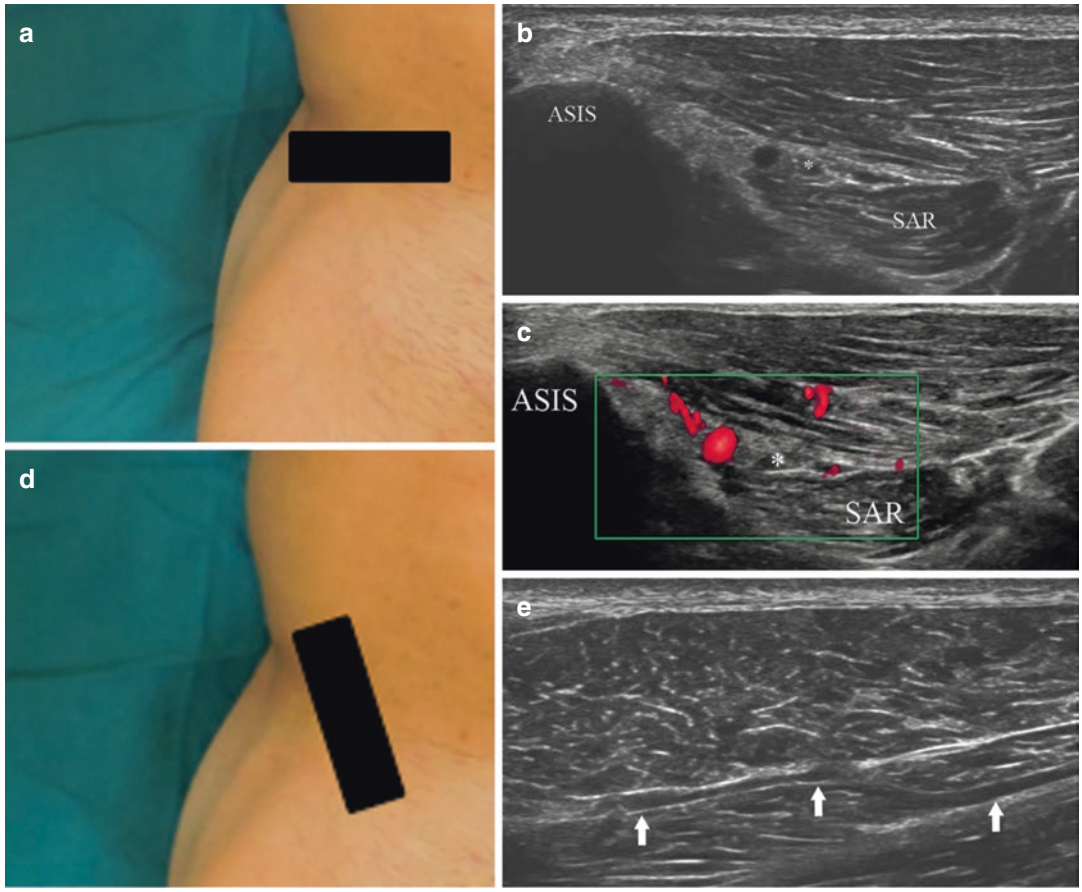

Fig. 2.36 (**a**) Probe position to evaluate the lateral femoral cutaneous nerve in a transverse plane; (**b**) ultrasound scan of the lateral femoral cutaneous nerve (asterisk) at the level of anterior superior iliac spine (ASIS). *SAR* sartorius muscle. (**c**) Power Doppler exam at the same level. (**d**) Probe position to evaluate the lateral femoral cutaneous nerve in a longitudinal plane. (**e**) Ultrasound longitudinal scan of the lateral femoral cutaneous nerve (arrows)

2.4.3 Ilioinguinal and Iliohypogastric Nerves

2.4.3.1 Anatomy

The ilioinguinal and iliohypogastric nerves (Figs. 2.37 and 2.38) are branches of the primary ventral ramus of L1, which immediately receives a branch from spinal nerve T12. They are parallel to the intercostal nerves (T1–T11), which run in the intercostal spaces, and subcostal nerve (T12), which is located below the twelfth rib.

The L1 primary ventral ramus, at the level of cranial end of the psoas major muscle, branches into the ilioinguinal and iliohypogastric nerves.

The iliohypogastric runs through the psoas muscle, extending diagonally along the anterior surface of the quadratus lumborum. It continues through the transversus abdominis, between the transversus and the internal oblique, and then, at the level of the anterosuperior iliac crest, it runs medially deep into the aponeurosis of the internal oblique and continues ventrally between the internal and external oblique.

At the level of the iliac crest, the iliohypogastric nerve divides into two terminal branches: the lateral cutaneous and the anterior cutaneous.

The ilioinguinal nerve is slightly thinner than the iliohypogastric and runs parallel to it although approximately 1 cm lower. It is divided into two branches: the lumbar and intermuscular one.

At the level of iliac crest, it perforates the lateral wall of the abdominal cavity, in particular the

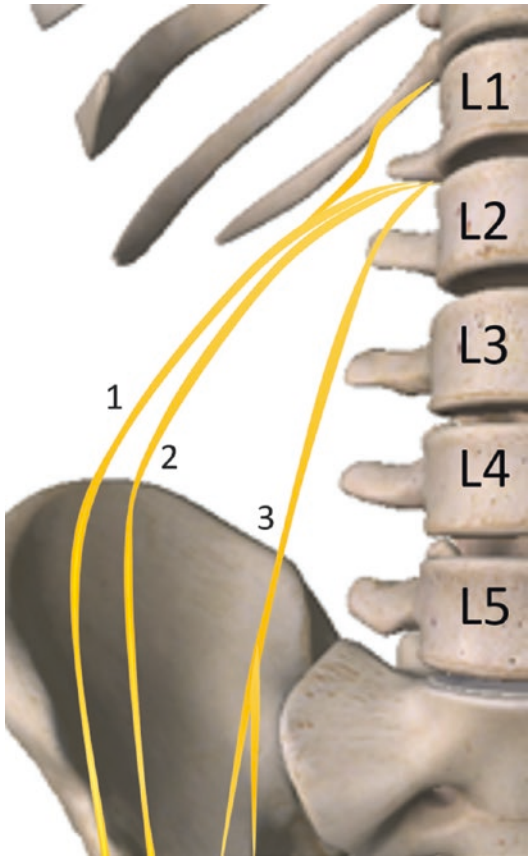

Fig. 2.37 Anatomical scheme of the lumbar plexus roots (L1 to L5: vertebral bodies), *1* iliohypogastric nerve, *2* ilioinguinal nerve, *3* lateral femoral cutaneous nerve

transversus abdominis, and runs anteromedially in the layer between the transverse abdominal and internal oblique muscles.

Then the ilioinguinal nerve pierces both the internal and external oblique muscles, toward the anterior superior iliac spine (ASIS), and then runs along the inguinal ligament, reaching the inguinal canal (near the lower border of the spermatic cord or the round ligament of the uterus) to pass through the superficial inguinal ring, where it gives off sensory end branches.

This nerve supplies the internal oblique, the skin of the upper medial part of the thigh, the upper part of the scrotum and of the penis in the males, or the skin covering the labium majus and the mons pubis in the females.

The ilioinguinal and iliohypogastric nerves innervate part of the structures in the inguinal

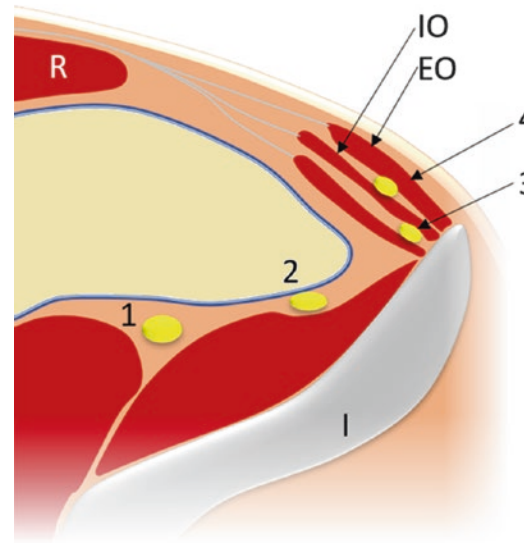

Fig. 2.38 Axial anatomical scheme of the iliac wing bone (I) that highlights the ilioinguinal nerve (4) and the iliohypogastric nerve (3). *2* Lateral femoral cutaneous nerve, *3* femoral nerve, *IO* internal oblique muscle, *EO* external oblique muscle, *R* rectus muscle

canal and lie on the anterior surface of the spermatic cord, while the genital branch of the genitofemoral nerve (L1, L2) lies on the posterior surface of the spermatic cord and provides motor and sensory innervation to the cremaster muscle and to the anterolateral aspect of the scrotum.

2.4.3.2 US Exams

Landmarks:
- ASIS (anterior superior iliac spine)
- Iliac crest
- Transverse abdominal muscle
- Internal oblique muscle
- External oblique muscle

The anterior superior iliac spine (ASIS) is a bony landmark that can be easily identified with palpation for the evaluation of the iliohypogastric and ilioinguinal nerves .

Place the linear probe on the ASIS, and move it approximately 5 cm cranially to scan the abdominal wall. This region is chosen because the nerves

have perforated the transverse abdominal muscle at this location with a probability of about 90%.

Both nerves can be found between the transverse abdominal and internal oblique muscle. At this location, all three muscles forming the abdominal wall, and we can see also the external oblique muscle.

Slightly rotate the transducer from a transversal to an oblique plane to be perpendicular to the nerves, with the lateral edge of the probe in contact with and perpendicular to the iliac crest and slightly lateral to the quadratus lumborum muscle (Fig. 2.39).

The ilioinguinal and iliohypogastric nerves appear as oval hypoechoic areas with hyperechoic spots inside, encircled by a hyperechoic layer.

Then move the probe caudally and medially along the course of the nerves, which still run between the internal oblique and transverse abdominal muscles. At this level in 50% of the cases, only two muscle layers can be identified because the external oblique abdominal muscle is only aponeurosis.

Ilioinguinal and iliohypogastric neuralgia: *Ilioinguinal and iliohypogastric neuralgia* is one of the most common causes of lower abdominal and pelvic pain and presents as paresthesias, burning pain, and occasionally numbness over the lower abdomen that radiates into the scrotum or labia majora. The pain can radiate to the inner upper thigh but not below the knee.

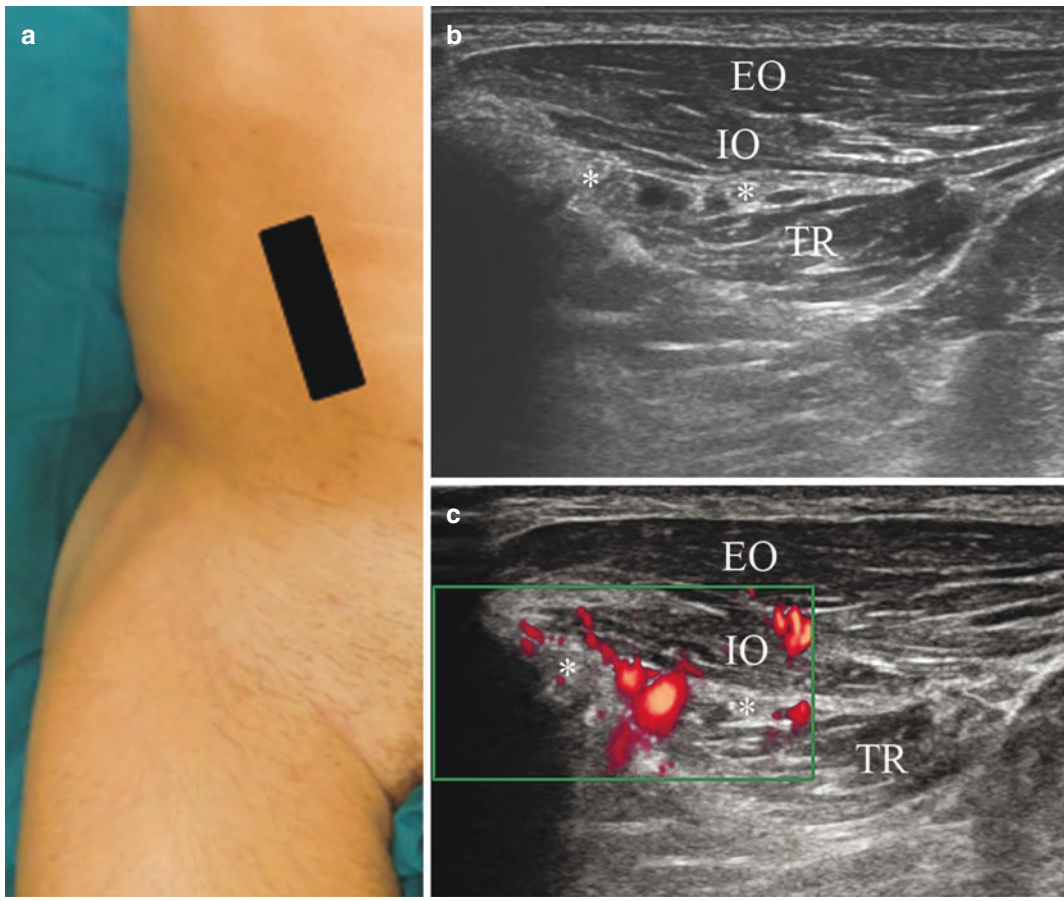

Fig. 2.39 (**a**) Probe position to evaluate the ilioinguinal and iliohypogastric nerves in a transverse plane; (**b**) ultrasound scan of the nerves (asterisks) and the corresponding power Doppler image (**c**). *EO* external oblique muscle, *IO* internal oblique muscle, *TR* transversus abdominis

It is caused by compression of the Ilioinguinal nerve as it passes through the transverse abdominis muscle at the level of the anterior superior iliac spine. The most common causes are trauma, including direct blunt trauma to the nerve, surgeries (inguinal herniorrhaphy and pelvic surgery), or during pregnancy, for the rapidly expanding abdomen in the third trimester.

Ilioinguinal neuralgia is also a cause of chronic groin pain in athletes, due to direct trauma or excessive training of the abdominal musculature.

2.4.4 Femoral Nerve

2.4.4.1 Anatomy

The femoral nerve, created by the dorsal divisions of the anterior rami of L2, L3, and L4, is the largest branch of the lumbar plexus.

It emerges at the inferolateral border of the psoas muscle to run caudally and laterally in the groove formed by the psoas and iliacus muscles. Then the nerve enters the thigh passing under the inguinal ligament, and, within a short distance, it divides into anterior and posterior branches.

At this level the femoral nerve is lateral and posterior to the femoral artery, deep to the fascia iliaca, and superficial to the iliopsoas muscle. Note that the inguinal ligament is a convergent point of the transversalis fascia (fascial layer of the deep surface of the anterior abdominal wall) and iliac fascia (fascia covering the posterior abdominal wall) (Fig. 2.40).

The anterior branch provides motor innervation to the sartorius and pectineus muscles and sensory innervation to the skin of the anterior and medial thigh from the inguinal ligament to the knee.

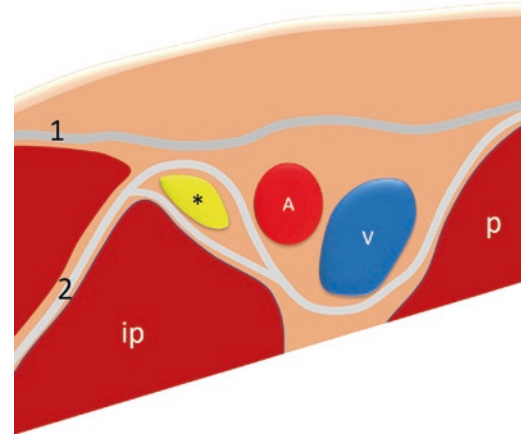

Fig. 2.40 Axial anatomical scheme of femoral nerve (*) and its relationships with the femoral artery (A) and vein (V), iliopsoas (ip) and pectineus (p) muscles. Femoral nerve is enveloped by two layers of fascia iliaca (2); *1* fascia lata

The posterior branch provides motor innervation to the quadriceps muscle and sensory innervation to the medial aspect of the lower leg from the knee to the internal malleolus via the saphenous nerve.

The anatomic location of the femoral nerve makes its identification simple because the landmarks are usually easy to find (except in cases of obesity) and the depth of the nerve is relatively superficial.

Focus on: Femoral neurovascular bundle

It is useful to think of the mnemonic "NAVEL" to remember the neurovascular structures that travel deep into the inguinal ligament and into the femoral triangle:

N = femoral nerve.

A = femoral arterv.

V = femoral vein.

EL = empty space (femoral canal) and lymphatics.

The **femoral triangle** is formed by the lateral border of the adductor longus, the medial border of the sartorius muscle, and the inguinal ligament, with the iliopsoas and pectineus muscles forming the floor (Fig. 2.41).

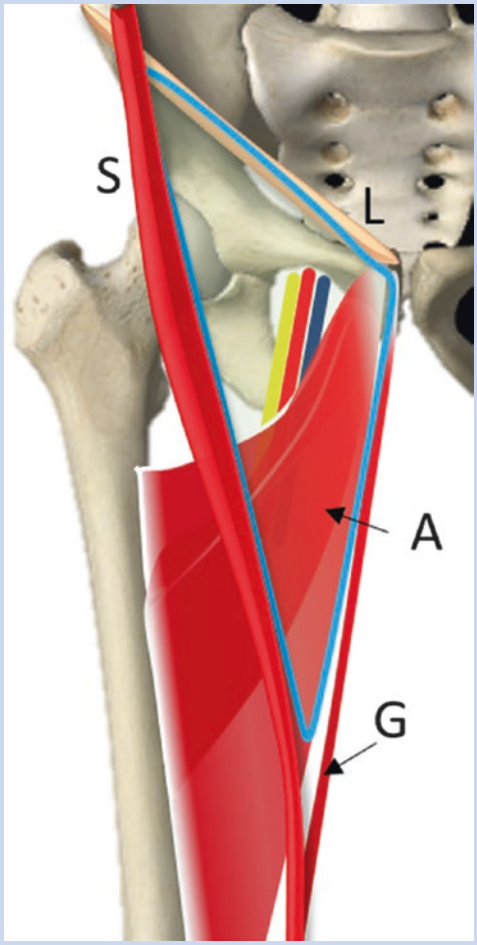

Fig. 2.41 Anatomical scheme of the femoral triangle. *L* inguinal ligament, *S* sartorius muscle, *A* adductor muscle, *G* gracilis muscle

The femoral nerve provides motor innervation to the muscles of the anterior compartment of the thigh, with some exceptions:

- The psoas portion of iliopsoas is innervated by muscular branches of the lumbar plexus.
- Tensor fasciae latae by the superior gluteal nerve.
- Pectineus occasionally can be innervated by the obturator nerve.

Injury to the femoral nerve determines weakness of hip flexion and of knee extension and sensory loss over the territories of the anterior and medial thigh and of the medial aspect of the lower leg.

2.4.4.2 US Exams

Landmarks:
- ASIS (anterior superior iliac spine)
- Femoral vessels
- Iliopsoas and pectineus muscles

Place the patient supine, with the leg extended and slightly externally rotated.

Identify the anterior superior iliac spine (ASIS) and the pubic symphysis, and draw an imaginary line between these two landmarks that represents the inguinal ligament.

Place the probe in the inguinal crease in a transverse plane, across the femoral region of the upper thigh, parallel to the inguinal ligament, to identify the femoral vein and artery. At this level the iliopsoas and pectineus muscles can be clearly recognized (Fig. 2.42a, b).

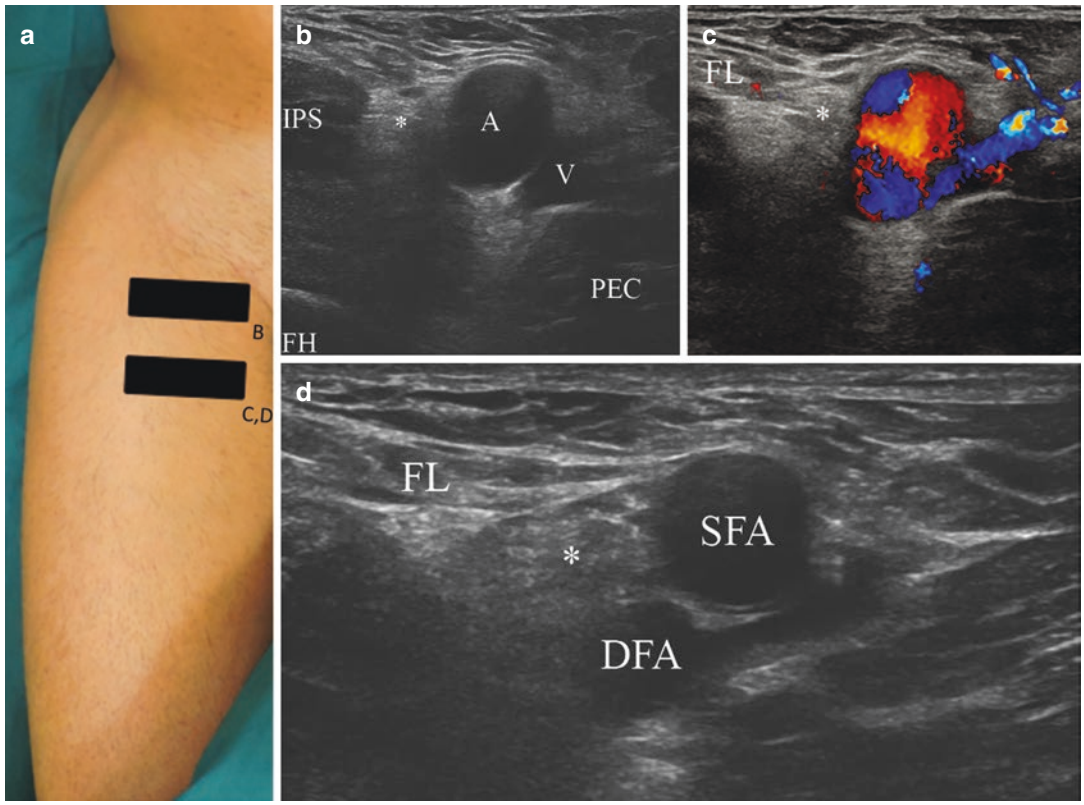

Fig. 2.42 (**a**) Probe position to evaluate the femoral nerve in a transverse plane; (**b**) ultrasound scan of the femoral nerve (asterisk). *IPS* iliopsoas muscle, *FH* head of femur, *PEC* pectineus, *A* femoral artery, *V* femoral vein. (**c**, **d**) Ultrasound scan and corresponding color Doppler image of the femoral nerve (asterisk). *FL* tensor fasciae latae, *SFA* superficial femoral artery, *DFA* deep femoral artery

If you cannot identify the vascular landmarks, slide the probe medial to lateral until the femoral vessels are seen.

Compression with the probe is useful to identify the femoral vein: in fact the vein (medial) collapses more easily than the artery (lateral). Color Doppler module can be used to confirm the identification of the femoral vessels (Fig. 2.42a, c and d).

The femoral nerve lies about 1–2 cm lateral to the artery, below fascia iliaca and lata and above the iliopsoas muscle, and appears as a triangular or oval honeycomb structure 3–10 mm in diameter covered anteriorly by the hyperechoic fascia iliaca.

If the femoral nerve appears hypoechoic due to anisotropy artifacts, slightly tilt the probe cranially or caudally to correctly visualize the nerve.

Then, turn the transducer by 90° to identify the nerve in a longitudinal plane.

2.4.5 Saphenous Nerve

2.4.5.1 Anatomy

The saphenous nerve is a purely sensory nerve, and it is the only nerve below the knee that is not derived from the sciatic nerve.

The cutaneous area of innervation of the saphenous nerve extends from the medial lower

leg, just distal to the knee, down to the medial malleolus, and in some patients as far down as the first metatarsal bone.

The saphenous nerve is the longest terminal branch of the posterior division of the femoral nerve, and it arises from the femoral nerve in the femoral triangle.

It descends laterally to the femoral vessels to enter the adductor or Hunter's canal, which is formed by a fibrous band spanning between the vastus medialis and the adductor magnus muscles and the adductor hiatus. At this level the saphenous nerve crosses over the femoral vessels to lie on their medial side at the distal third of the adductor magnus muscle. During its entire course in the thigh, the saphenous nerve runs deep to the sartorius muscle (Fig. 2.43).

In the adductor canal, just above the medial aspect of the knee, the saphenous nerve, with the saphenous branch of the descending genicular artery, pierces the roof of the subsartorial canal just proximal to the adductor hiatus between the sartorius and gracilis tendons (Fig. 2.44).

After exiting the subsartorial canal, the saphenous nerve splits into two terminal branches (Fig. 2.45):

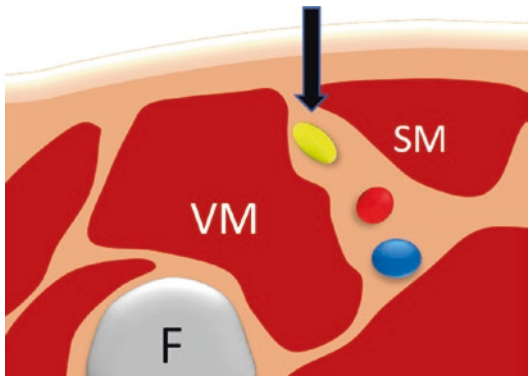

Fig. 2.43 Cross-sectional anatomy of the saphenous nerve (black arrow) at the level of the thigh. Saphenous nerve is positioned between the vastus medialis muscle (VM) and the sartorius muscle (SM) superficially to the femoral artery and vein. *F* femur

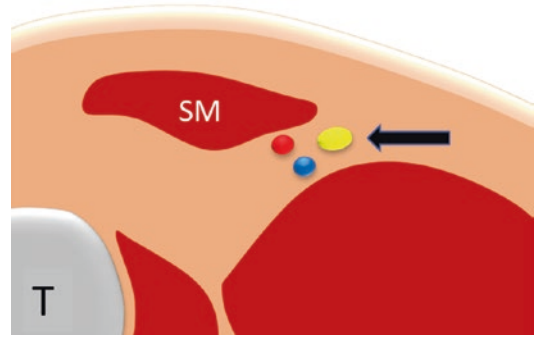

Fig. 2.44 Cross-sectional anatomy of the saphenous nerve (black arrow) at the level of the tibial tuberosity (T). *SM* sartorius muscle

- The *infrapatellar branch*, which pierces the sartorius muscle to reach the subcutaneous layer and innervates the infrapatellar fat pad and the anteromedial knee portion. At the level of the knee, the infrapatellar branch is susceptible to entrapment between the medial femoral condyle and the tendon of the sartorius muscle.
- The *descending branch*, which pierces the sartorius muscle or the superficial fascia between the gracilis and sartorius muscles to enter the subcutaneous tissue, travels distally in the leg providing articular branches to the knee and ankle and sensory innervations to the skin and fascia on the anteromedial aspect of the leg and foot to the first metatarsal.

Below the knee, the saphenous nerve follows the course of the greater saphenous vein to the medial side of the ankle and foot, ending as far as the medial aspect of the first metatarsal head.

At the level of ankle, the saphenous nerve is found between the medial malleolus and the anterior tibial tendon, just lateral to the saphenous vein.

Approximately 3 cm proximal to the tip of the medial malleolus, it divides into anterior and posterior branches, in relation to the saphenous vein. The nerve can communicate with branches of the

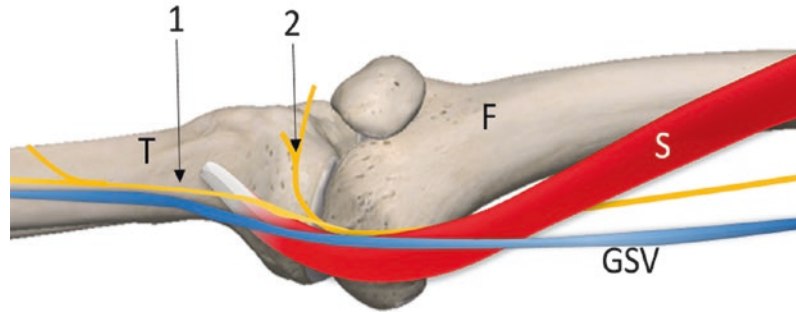

Fig. 2.45 Anatomical scheme at the level of the knee, showing the saphenous nerve (1) and its infrapatellar branch (2). *S* sartorius muscle, *GSV* great saphenous vein, *F* femur bone, *T* tibial bone

common fibular nerve. Both of these nerves supply sensitive innervation to the anterior surface of the leg.

Saphenous Nerve Entrapment Neuropathy at Adductor Canal Level

The *adductor canal, or Hunter's canal*, is an aponeurotic-fibromuscular tunnel delimited by the vastus medialis muscle anterolaterally, adductor longus and magnus muscles posteriorly, sartorius muscle medially, and a strong aponeurosis that extends between the adductors, over the vessels, to vastus medialis (vasto-adductor membrane) anteromedially.

This aponeurotic tunnel, located in the middle third of the thigh, runs from the apex of the femoral triangle (Scarpa's triangle) to a passage in the adductor magnus.

The femoral vessels leave the adductor canal to reach the popliteal fossa. The saphenous nerve passes through the adductor canal with the femoral artery and vein and can be entrapped, causing the following symptoms:

- Deep pain at level of the thigh
- Knee pain
- Loss of sensation over the medial aspect of the leg

Muscular hypertrophy may play an important role in the pathophysiological compressive mechanism.

2.4.5.2 US Exams

Landmarks in the thigh:
- Sartorius muscle
- Hunter's canal
- Femoral vessels

Landmarks in the leg:
- Tibial tuberosity
- Greater saphenous vein

Landmarks in the ankle:
- Medial malleolus
- Greater saphenous vein

Place the transducer in a transverse plane at the middle third of the medial aspect of the thigh, and identify the sartorius muscle as a superficial thin muscle belly.

The saphenous nerve is situated in the space between the vastus medialis muscle laterally and the sartorius muscle medially. At this level the saphenous nerve is accompanied by the femoral artery (Fig. 2.46). Use color Doppler modules to identify the femoral vessels.

If the saphenous nerve cannot be identified, start cranially from the femoral nerve, and then follow it caudally using the elevator technique.

Identify Hunter's canal: The Sartorius muscle forms the "roof" of the adductor canal in the middle third of the thigh and runs lateral to medial across the anterior thigh. The muscle appears as an oval shape under the subcutaneous layer of adipose tissue.

The sides of the triangular canal are formed by the vastus medialis laterally and adductor longus

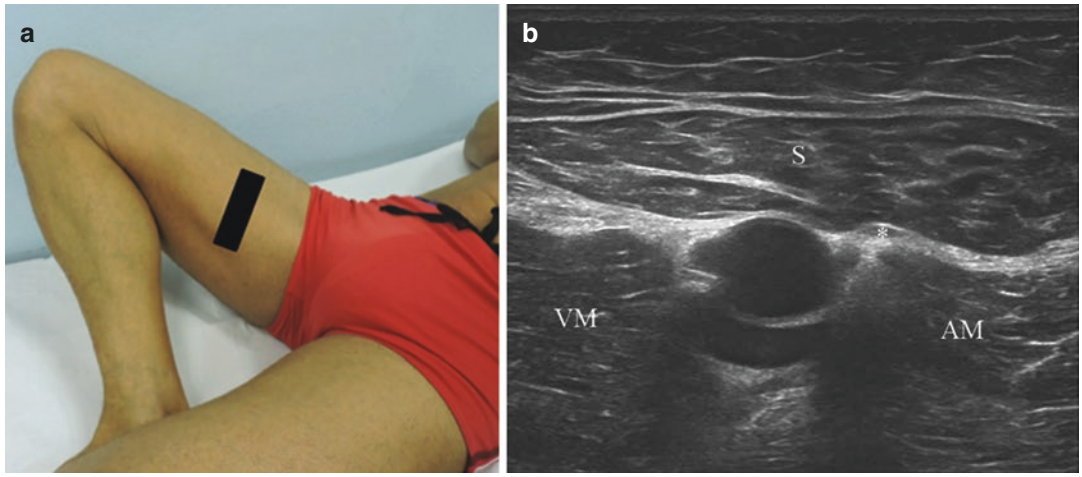

Fig. 2.46 (**a**) Probe position to evaluate the saphenous nerve at the level of Hunter's canal; (**b**) ultrasound scan of the saphenous nerve (asterisk). *S* sartorius, *VM* vastus medialis, *AM* adductor magnus

(proximally) and magnus (distally) medially. The saphenous nerve can be visualized as a small round hyperechoic structure medial to the femoral artery. A femoral vein accompanies the artery and saphenous nerve.

Move the probe caudally following the nerve: the saphenous nerve gradually runs toward the posteromedial aspect of the distal thigh and emerges from the fascia lata between sartorius and gracilis, becoming a subcutaneous nerve.

Place the transducer in a transverse plane on the anteromedial aspect of the knee at the level of the tibial tuberosity. The saphenous nerve runs along the tibial border with the greater saphenous vein. The nerve lies medial and posterior to the vein.

Below the knee, follow the nerve along the tibial side of the leg, adjacent to the great saphenous vein in the subcutaneous layer (Fig. 2.47a, b).

At this level, only a light pressure should be applied to the transducer, in order to avoid compression of the saphenous vein (SV), which is an important landmark for US examination of the saphenous nerve.

At the level of the ankle, place the probe in a transverse plane just anterior to the medial malleolus: the saphenous nerve is located medially next to the saphenous vein, which is positioned subcutaneously (Fig. 2.47a–c).

2.4.6 Obturator Nerve

2.4.6.1 Anatomy

The obturator nerve originates from the anterior primary rami of L2-L3-L4 roots and descends into the pelvis passing over the psoas major muscle at the level of the sacroiliac joint (Fig. 2.48).

In the pelvis, the obturator nerve runs close to the ureter and the internal iliac artery; then it exits the pelvis through the upper part of the obturator foramen and reaches the obturator groove where, in the majority of cases, it divides into an anterior and a posterior branch.

At the level of the femoral crease, the anterior branch lies between the fascia of pectineus and adductor brevis muscles and then runs between the adductor brevis and adductor magnus muscles posteriorly and the adductor longus anteriorly.

The anterior branch provides motor fibers to the adductor muscles and sensory innervation to the skin and fascia of the medial aspect of the mid-thigh.

The posterior branch pierces and innervates the obturator externus, then runs between the fascial planes of the adductor brevis and adductor magnus muscles, and splits into a motor branch, which innervates the deep adductor muscles (in particular the adductor magnus), and a sensory branch that innervates the knee joint (articular capsule, cruciate ligaments, and synovial

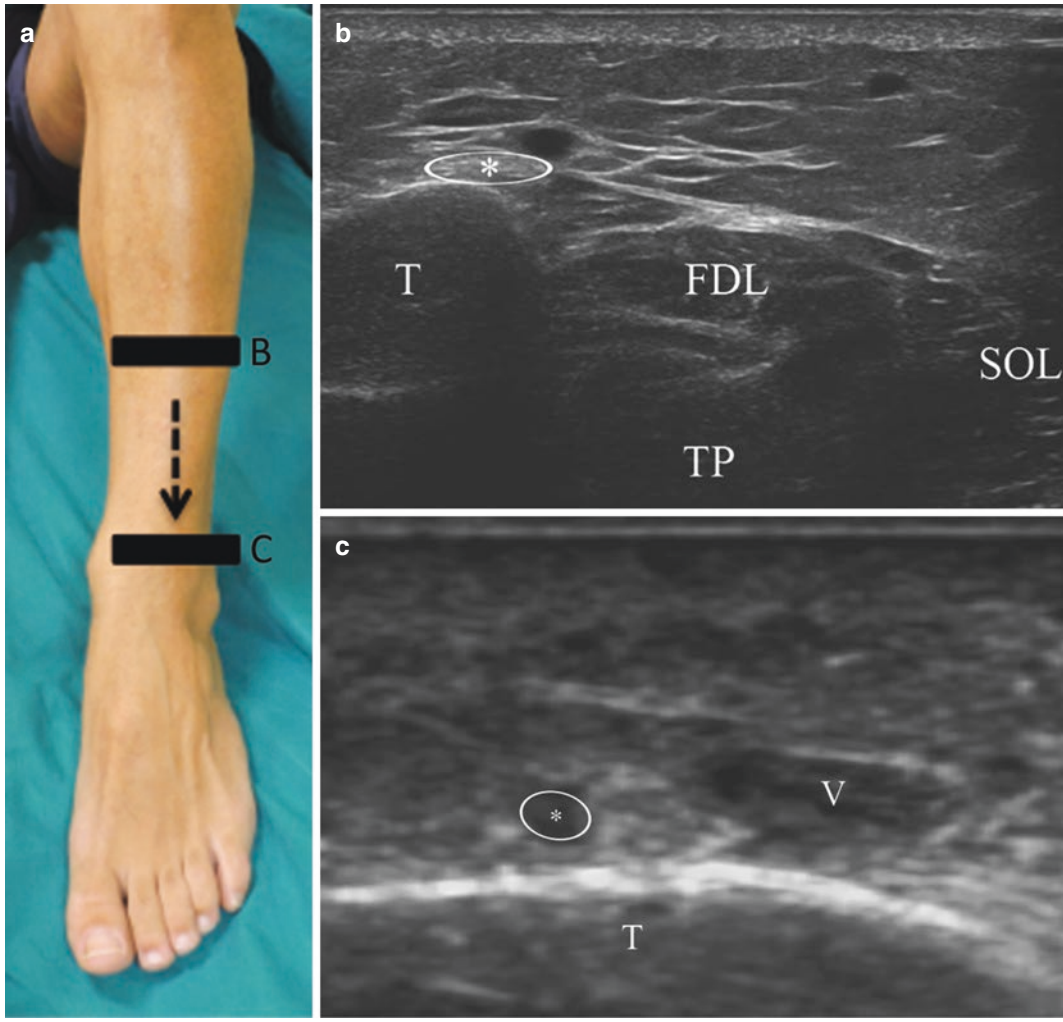

Fig. 2.47 (**a**) Probe path to evaluate the saphenous nerve below the knee; (**b**) ultrasound scan of the saphenous nerve (asterisk) at distal third of the leg; it runs along the tibial border with the great saphenous vein. *T* tibia, *FDL* flexor digitorum longus muscle, *TP* tibialis posterior, *SOL* soleus muscle. (**c**) ultrasound scan of the saphenous nerve (asterisk) at ankle level. *T* tibia, *V* great saphenous vein

membrane). The posterior branch occasionally innervates the adductor brevis (Fig. 2.49).

2.4.6.2 US Exams

Landmarks:
- Femoral vessels
- Adductor muscles (pectineus, adductor longus, adductor brevis, and adductor magnum)

The sonographic visualization of obturator nerve may not to be easy due to the fact that it is small in size, with a small deep course in the proximal thigh, and it lies between muscles. It is reported that the anterior and posterior rami are visible more often than the common nerve itself.

With the patient supine and the thigh slightly abducted and laterally rotated, place the ultrasound transducer in a transverse position on the anteromedial aspect of the thigh, at the level of the femoral crease, parallel to the inguinal ligament, to visualize the femoral vessels.

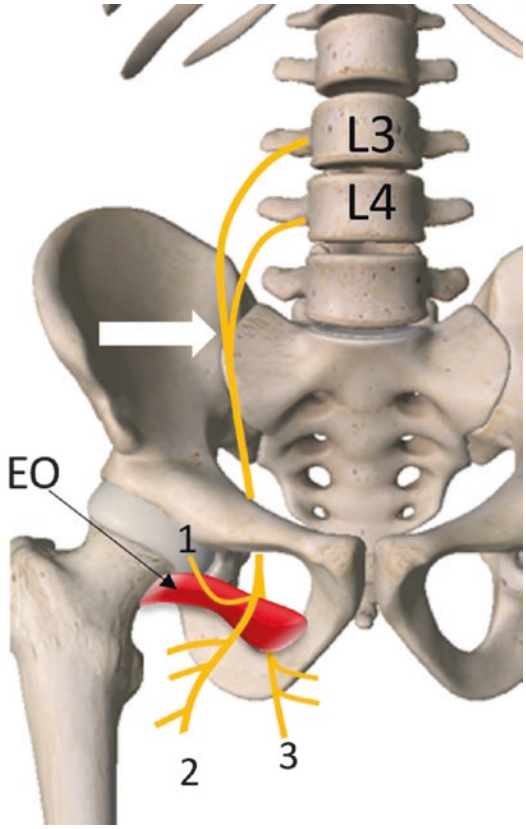

Fig. 2.48 Anatomical scheme of the obturator nerve (white arrow) with its branches: anterior branch (2) and posterior branch (3). *1* branch for hip joint, *EO* external obturator muscle

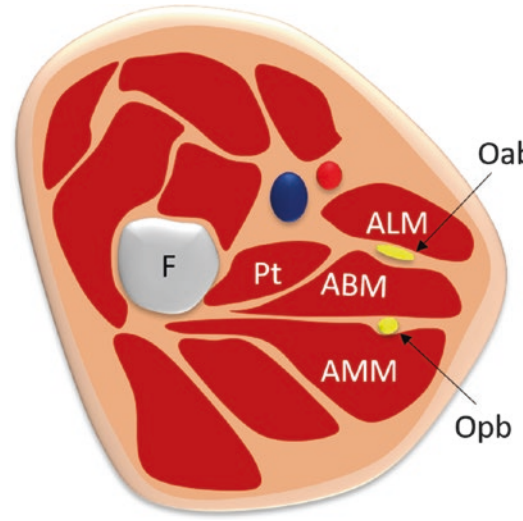

Fig. 2.49 Cross-sectional anatomy of the obturator nerve at the level of the diaphysis of the femur (F). *Oab* obturator anterior branch, *Opb* obturator posterior branch, *ALM* adductor longus muscle, *ABM* adductor Brevis muscle, *AMM* adductor magnus muscle, *Pt* pectineus muscle

The transducer is advanced medially, about 1 to 3 cm distal to the inguinal crease, to identify the adductor muscles and their fascia.

This approach gives the possibility to correctly visualize the structures of interest: the pectineus muscle, the adductor longus muscle, the adductor brevis muscle, and part of the adductor magnus muscle.

The anterior branch is located between the adductor longus and adductor brevis muscles, while the posterior branch is between the adductor brevis and adductor magnus muscles (Fig. 2.50).

At this level, identify the "spider net" image in the sonographic triangle formed by pectineus, adductor longus, and adductor brevis muscles. The image is formed by the fascial elements, the obturator nerve, the sigmoid-shaped ascending anterior division between adductor longus and adductor brevis muscles, and the posterior division.

Obturator nerve entrapment:

Obturator nerve entrapment and injury occur with pelvic trauma and associated fractures, during childbirth delivery as a result of compression of the nerve between the head of the fetus and the bony structures of the pelvis, or due to entrapment in the adductor muscles in athletes.

The clinical presentation includes difficulty in ambulation, exercise-related pain, or groin pain, deep ache in the region of the adductor origin at the pubic bone that could radiate down the medial aspect of the thigh toward the knee. The differential diagnosis includes adductor muscle strain, osteitis pubis, stress fracture of the pelvis, inguinal ligament enthesopathy, entrapment of the lateral cutaneous nerve of the thigh, and inguinal hernia.

Examination findings reveal externally rotated hip, weakness or wasting of the adductor muscles, and a decrease in hip adduction and internal rotation of the hip.

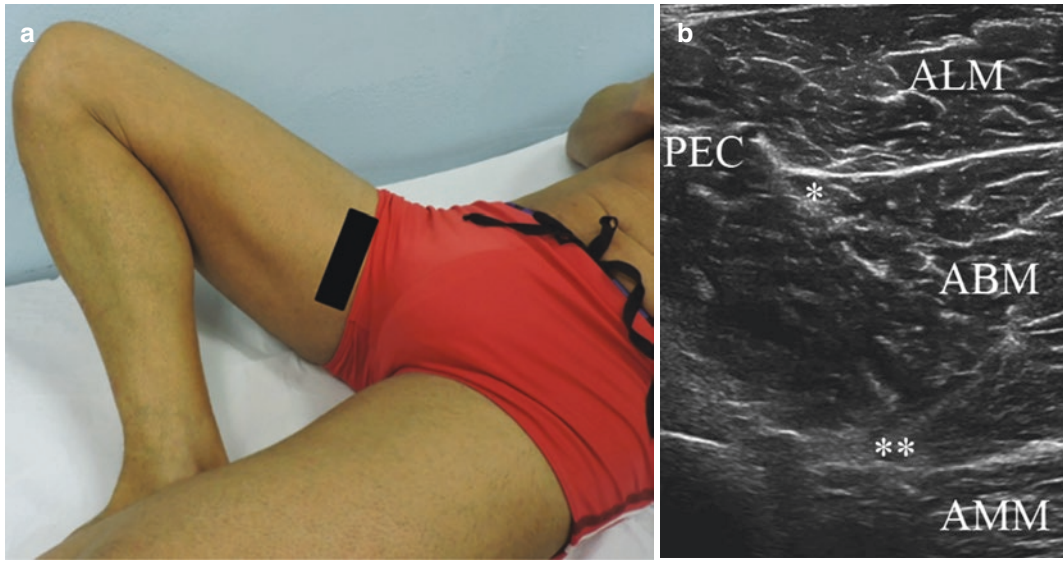

Fig. 2.50 (**a**) Probe position to evaluate the obturator nerve at the proximal third of medial compartment of thigh; (**b**) ultrasound scan of the obturator nerve branches. * Anterior branch of obturator nerve, ** posterior branch of obturator nerve, *PEC* pectineus, *ALM* adductor longus, *ABM* adductor brevis, *AMM* adductor magnus

2.4.7 Sciatic Nerve

2.4.7.1 Anatomy

The sciatic nerve is the longest and thickest peripheral nerve of the human body, with a diameter of about 2 cm. It supplies motor and sensory innervation to the posterior aspect of the thigh and of the whole lower leg, except for the medial aspect of the leg, which is supplied by the saphenous nerve (the terminal branch of the femoral nerve).

It originates from the ventral rami of spinal nerves L4–L5 and S1–S3: in fact the anterior ramus of L4 and L5 together with the first three sacral roots forms the sciatic nerve.

It leaves the lesser pelvis, where it is anterior to the piriformis muscle and posterior to the iliac vessels, through the greater sciatic foramen, emerging from beneath the piriformis muscle (in 85% of cases). In the other 15% of cases, the sciatic nerve either pierces the piriformis muscle or passes over it (Fig. 2.51).

In the upper part of its course, the nerve is accompanied on its medial side by the posterior femoral cutaneous nerve and the inferior gluteal artery, under the gluteus maximus muscle.

In the thigh it lies between the greater trochanter of the femur and the ischial tuberosity, always under the gluteal muscles. The belly of the quadratus femoris muscle separates the sciatic nerve from the femur's acetabular articular capsule.

The nerve runs distally in the thigh posteriorly to the adductor magnus muscle, and it is obliquely crossed by the long head of the biceps femoris muscle.

It then runs in the groove between the semimembranosus and biceps femoris muscles (Fig. 2.52).

Usually at lower third of the thigh, where the semimembranosus splits medially and the biceps femoris laterally (forming the superior angle of the popliteal fossa), it divides into two large branches, the tibial and common peroneal nerves.

The tibial nerve continues in the same direction of the main trunk, at the center of the popliteal fossa, while the common peroneal nerve turns laterally, medial to the biceps tendon.

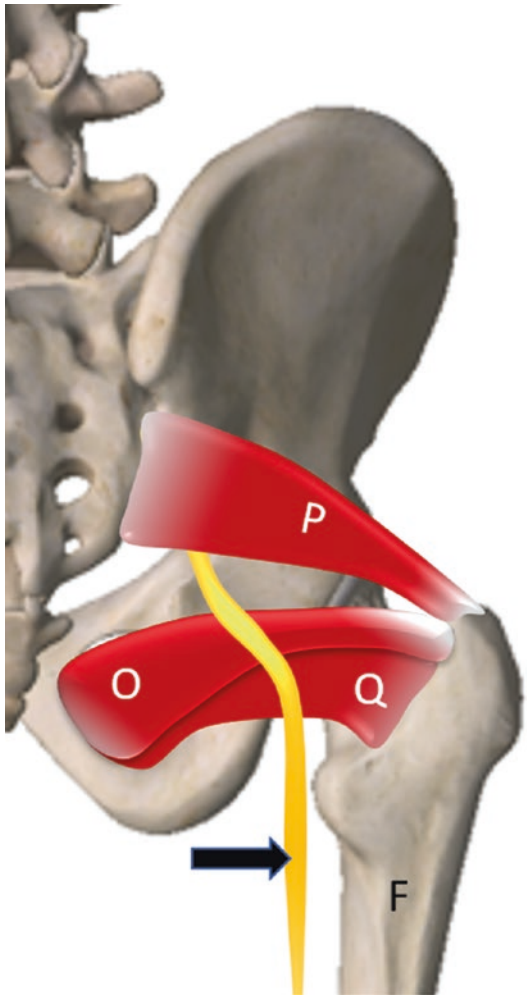

Fig. 2.51 Anatomical scheme of the sciatic nerve (black arrow) that highlights posterior course of the nerve in respect of the obturator internus (O) and quadratis femoris (Q) muscles. *P* piriformis muscle, *F* femur bone (F)

2.4.7.2 US Exams

Landmarks at the gluteal region:
- The gluteus maximum
- The ischial spine
- Pudendal vessels

Landmarks at the upper thigh:
- Greater trochanter of the femur
- Ischial tuberosity
- Common tendon of hamstring muscles

Landmarks at the popliteal fossa:
- Popliteal artery and vein

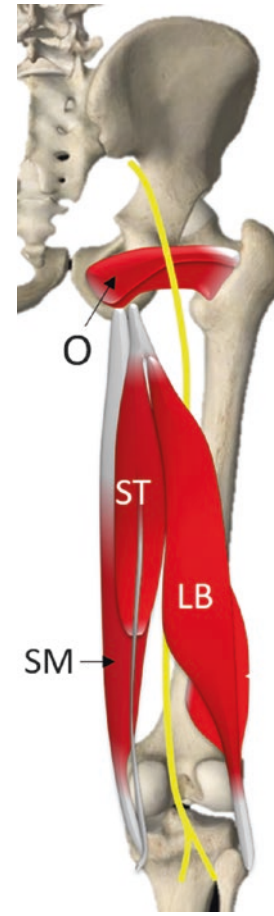

Fig. 2.52 Anatomical scheme of the posterior thigh for the sciatic nerve. *O* obturator internus muscle, *ST* semitendinosus muscle, *SM* semimembranosus muscle, *LB* long head of the biceps muscle

The patient is prone on the examination table.

Palpate the anatomical bony reference structures: the greater trochanter of the femur and the ischial tuberosity.

Then place the transducer in the transverse plane on the ischial tuberosity, where the common tendon of hamstring muscles can be seen. Then move the transducer laterally (between the ischial tuberosity and greater trochanter): the sciatic nerve is seen lateral to the ischial tuberosity overlying the quadratus femoris (a quadrilateral muscle which connects the ischial tuberosity and the intertrochanteric crest of the femur).

To easily identify the sciatic nerve, also in obese patients, use the low-frequency curved probe to identify both the greater trochanter and

ischial tuberosity, then use a high-frequency linear probe to increase resolution.

The ischial tuberosity (medial) and the greater trochanter (lateral) should be visible as hyperechoic curved structures on the right and left sides of the ultrasound screen.

The sciatic nerve is between these two landmarks and appears as a hyperechoic fasciculate oval structure. Follow the sciatic nerve in the posterior thigh: it descends between and deep to the biceps femoris (lateral) and semitendinosus and semimembranosus muscles (medial) and superficial to the adductor magnus muscle (Figs. 2.53 and 2.54).

Then the sciatic nerve reaches the proximal margin of the popliteal fossa, where it branches into the common peroneal and tibial nerves. Identify the point of bifurcation of the sciatic nerve and the popliteal artery and vein deep to the nerve (Fig. 2.55).

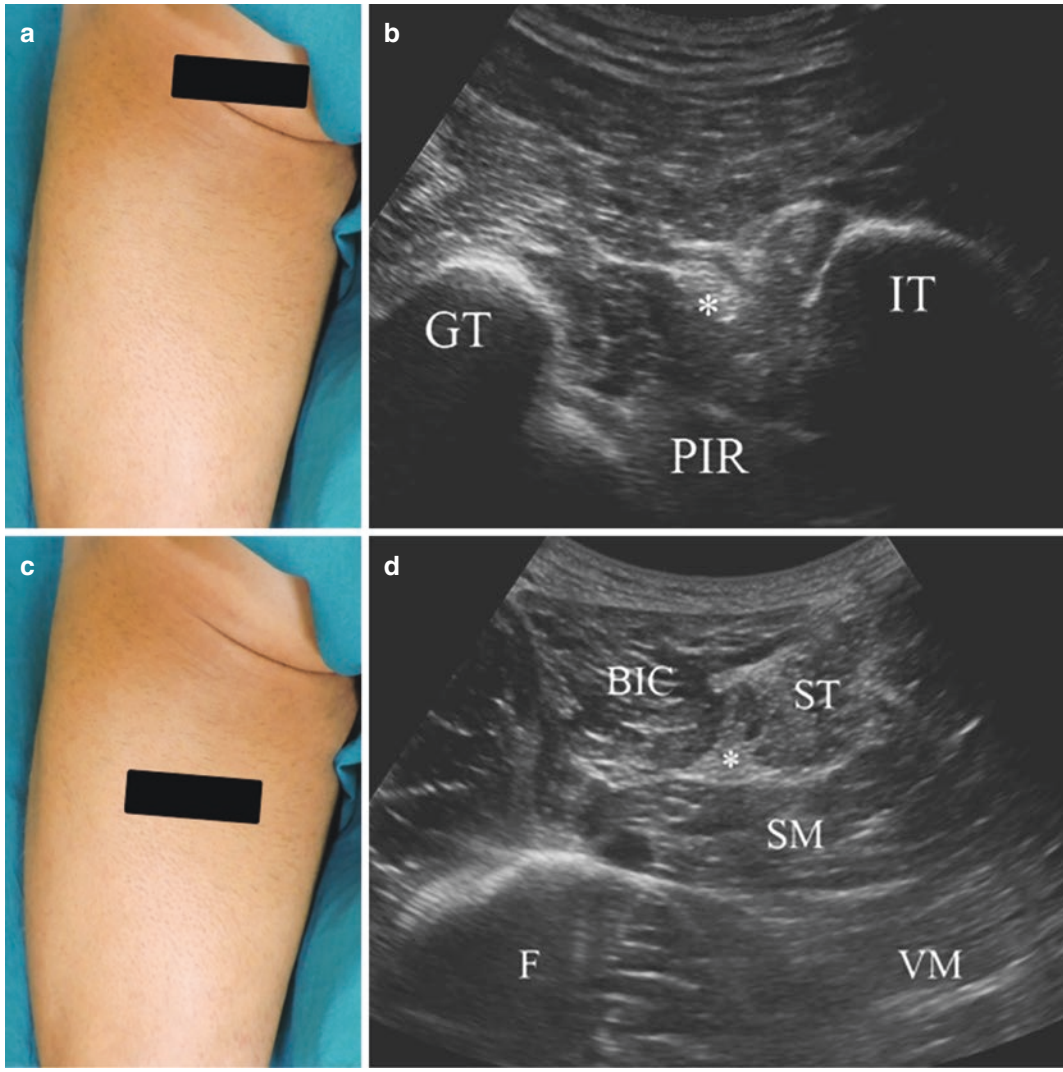

Fig. 2.53 (**a**, **b**) Probe position to evaluate the sciatic nerve (asterisk) at the mid-gluteal position and the corresponding ultrasound scan. *GT* great trochanter, *PIR* piriformis, *IT* ischial tuberosity. (**c**, **d**) Probe position to evaluate the sciatic nerve (asterisk) at the proximal third of posterior thigh and the corresponding ultrasound scan**.** *F* femur, *BIC* biceps femoris, *ST* semitendinosus, *SM* semimembranosus, *VM* vastus medialis

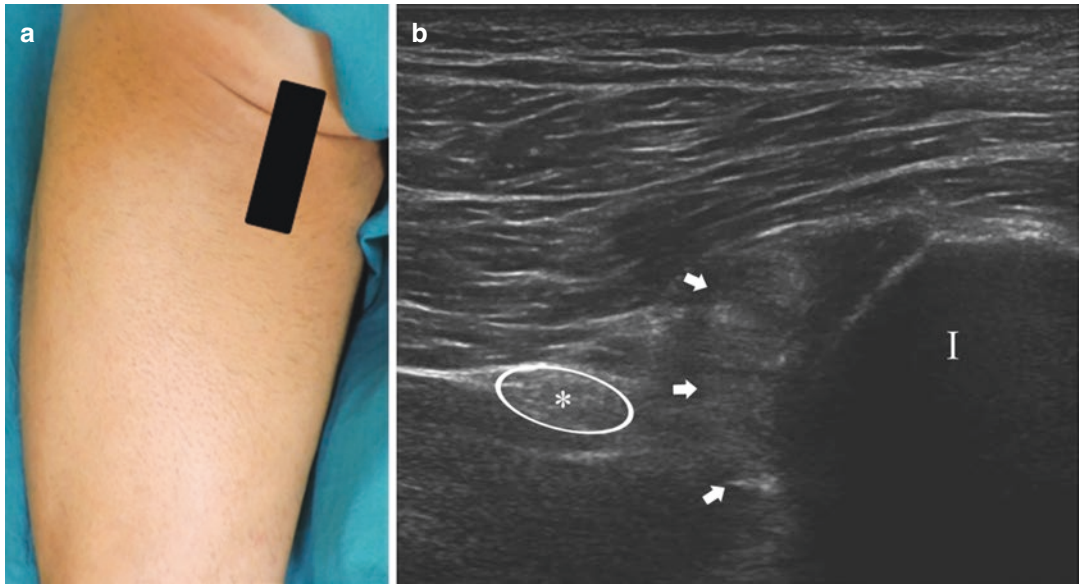

Fig. 2.54 (**a**) Probe position to evaluate the sciatic nerve (asterisk) at the level of ischial tuberosity (I). (**b**) Corresponding ultrasound scan of the sciatic nerve (asterisk). White arrows hamstring's tendon

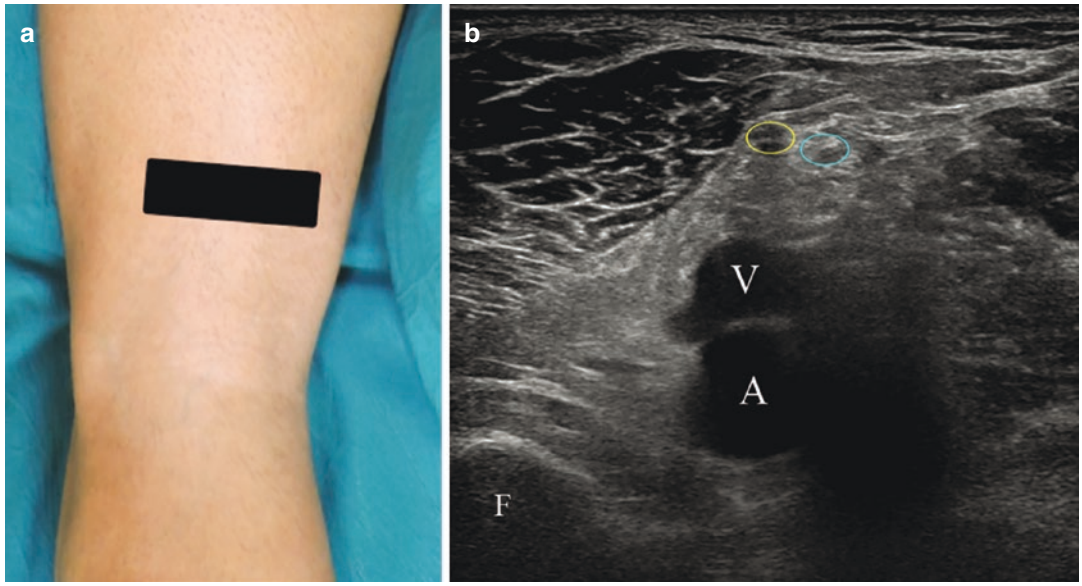

Fig. 2.55 (**a**) Probe position to evaluate the sciatic nerve (asterisk) at the level of popliteal fossa. (**b**) Corresponding ultrasound scan at the level of point of bifurcation of the sciatic nerve. Yellow circle tibial nerve, Ligth Blue Circle common peroneal nerve, *A* popliteal artery, *V* popliteal vein, *F* femur

Turn the probe by 90° to examine the sciatic nerve in long axis (longitudinal).

Due to its deep position, the sciatic nerve can be identified with a gluteal approach: it emerges from the greater sciatic foramen under the piriformis muscle and lies deep to the gluteus maximus muscle and superficial to the inner muscle layers. Always with the patient supine, palpate the posterior superior iliac spine, the sacral hiatus, and the greater

trochanter. Place the probe in a transverse axis in a mid-gluteal position (the midpoint of the line joining the sacral hiatus and the greater trochanter): the sciatic nerve is scanned in its short axis as a triangular hyperechoic bundle under the gluteus maximus; the ischial bone is identified as a continuous linear hyperechoic structure.

Move the probe caudally to identify the ischial spine, which is seen as a curved hyperechoic line, with the pudendal vessels above it. Use the color Doppler to help in the identification of the pudendal vessels.

Deep Gluteal Syndrome

Deep gluteal syndrome is characterized by pain and dysesthesias in the buttock area, hip, or posterior thigh due to a non-discogenic sciatic nerve entrapment in the subgluteal space.

It is caused by multiple pathologies: "piriformis syndrome," the presence of fibrous bands, obturator internus/gemellus syndrome, quadratus femoris/ischiofemoral pathology, hamstring pathology, and gluteal disorders.

The *subgluteal space* is delimitated posteriorly by the gluteus maximus muscle, anteriorly by the posterior surface of the femoral neck, laterally by the linea aspera and the iliotibial tract (the union of middle and deep gluteal aponeurosis and the tensor fasciae latae muscle), medially by the sacrotuberous and falciform fascia, superiorly by the inferior margin of the sciatic notch, and inferiorly by the hamstring tendons.

The subgluteal space contains superior and inferior gluteal nerves and vessels, sacrotuberous and sacrospinous ligaments, internal pudendal vessels, sciatic nerve, piriformis, obturator internus and externus, gemelli, quadratus femoris, and hamstrings.

Piriformis Syndrome

The piriformis muscle originates from the anterior surface of the sacrum and inserts on the upper surface of the greater trochanter, leaving the pelvis through the greater sciatic foramen.

The *piriformis syndrome* is characterized by a clinical presentation with sciatica-like symptoms. The etiology is not clearly known, but the entrapment and irritation of the sciatic nerve in the hip region could be influenced by the piriformis muscle (contracture of the piriformis muscle, anatomical abnormalities of the piriformis muscle, problem after spinal surgery, overuse of the piriformis muscle, trauma, or sports injury).

2.4.8 Common Peroneal Nerve

2.4.8.1 Anatomy

Common Peroneal Nerve

The common peroneal nerve, also known as the common fibular nerve or SPE (sciatic-popliteal externus), is the lateral terminal branch of the sciatic nerve and originates in the cranial part of the popliteal fossa (Fig. 2.56).

It supplies the motor innervation of the anterior and lateral compartments of the legs (muscles that assist with eversion and plantar flexion of the foot) and the sensory innervation of the skin of the anterolateral aspect of the leg and of the dorsum of the foot.

In the thigh, the peroneal division of the sciatic nerve supplies the short head of the biceps femoris muscle.

In the popliteal fossa, the common peroneal nerve runs obliquely passing along the medial border of biceps femoris muscle; then distally it lies between the tendon of the biceps femoris (medial) and the lateral head of the gastrocnemius muscle (lateral) until reaching the posterior surface of the head of the fibula and then passes over the peroneal head.

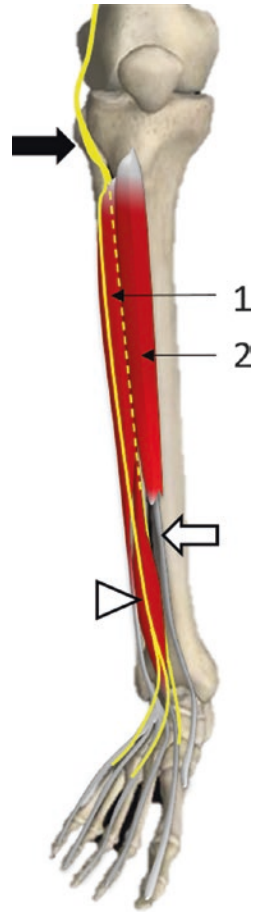

Fig. 2.56 Anatomical scheme of the peroneal nerve at the level of the leg. *1* peroneus longus muscle, *2* peroneus brevis muscle, Black Arrow common peroneal nerve, White Arrow deep peroneal nerve, Arrowhead superficial peroneal nerve

Then the common peroneal nerve moves anteriorly perforating the lateral intermuscular septum and enters in a tunnel between the long peroneal muscle and the proximal metaphysis of the fibula, passing in the anterior compartment of the leg.

At this location, the common peroneal divides into two terminal branches: the superficial and deep peroneal nerves.

The point of bifurcation usually is at the level of fibular neck but sometimes (10% cases) could be proximal or distal to the knee joint.

The common peroneal nerve has a smaller diameter than the tibial nerve (about one half).

In the popliteal fossa, the common peroneal nerve gives off articular branches and a small communicating branch, which, together with a reciprocal communicating branch from the tibial nerve, forms the sural nerve. The sural nerve supplies sensory innervation to the posterior and lateral surfaces of the distal third of the leg.

Common peroneal nerve entrapment
The *common peroneal nerve* can be entrapped during its passage through the fibular tunnel or the biceps femoris tunnel or during its superficial course around the knee. This clinical condition can present as foot drop, due to the denervation of the anterior compartment of the leg.

2.4.8.2 Deep Peroneal Nerve

The deep peroneal nerve is one of the two terminal branches of the common peroneal nerve and runs inferiorly, close to the fibular neck between the long peroneal muscle and the bony surface of the fibula, on the anterior aspect of the interosseous membrane of the leg.

It runs accompanied by the anterior tibial artery between the tibialis anterior and the extensor digitorum longus muscles and then, more distally, between the tibialis anterior and the extensor hallucis longus muscles.

At the level of the ankle joint (talocrural joint), it passes longitudinally through the anterior tarsal tunnel (the fibro-osseous tunnel between the inferior extensor retinaculum and the fascia over the talus and the navicular bones), beneath the extensor retinaculum. It crosses behind the tendon of the extensor hallucis longus and moves onto the dorsum of the foot between the extensor hallucis longus and extensor digitorum longus tendons. Here it passes from the lateral side to the medial side of the dorsalis pedis artery.

Approximately 1.5 cm above the ankle joint, in the dorsum of the foot, the deep peroneal nerve splits into a medial and a lateral branch. The point of bifurcation can be located under, above, or distal to the inferior extensor retinaculum (Fig. 2.57).

The lateral terminal branch runs beneath the extensor digitorum brevis and extensor hallucis brevis muscles and provides their motor innervation. It terminates into several thin divisions known as *dorsal interosseous nerves*

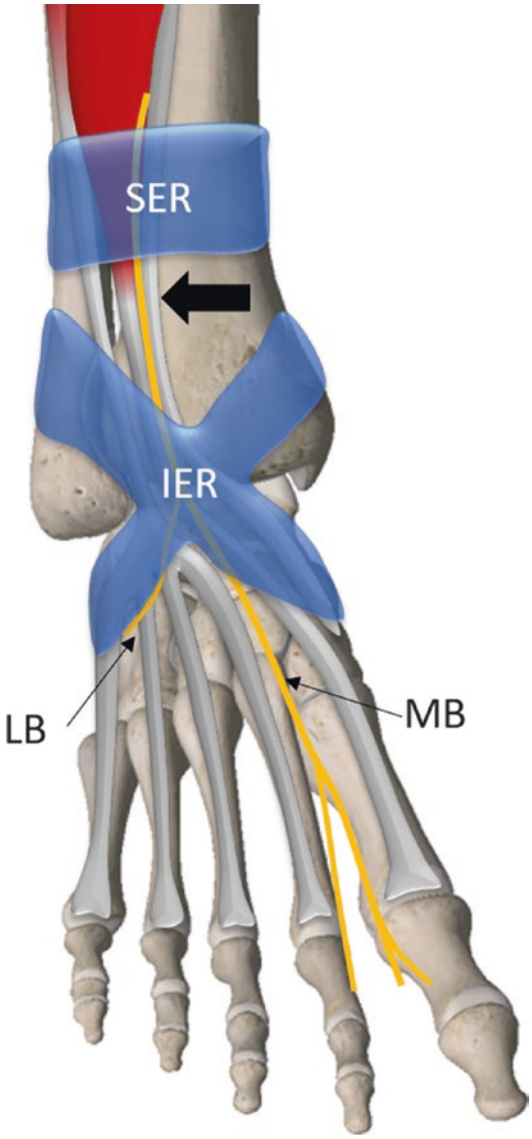

Fig. 2.57 Anatomical scheme at the level of the ankle, showing the deep peroneal nerve (black arrow) and its medial terminal branch (MB) and lateral terminal branch (LB) and its relationships with the superficial extensor retinaculum (SER) and inferior extensor retinaculum (IER)

(second, third, and fourth dorsal interosseous nerves). The lateral branch provides sensory innervation to the ankle and sinus tarsi.

The medial branch passes laterally along the dorsalis pedis artery toward the first interosseous space, where it divides into *dorsal digital nerves* and supplies the web space between the first and second toe.

The deep peroneal nerve supplies the muscles of the anterior compartment of the leg that allow dorsiflexion and inversion of the foot (tibialis anterior, extensor digitorum longus and brevis, extensor hallucis longus, and peroneus tertius muscles). It supplies sensory innervation to the first web space and the adjacent sides of the first two toes and the tarsal and metatarsophalangeal joints of the middle three toes. It provides sensation to the ankle joint and the sinus tarsi.

2.4.8.3 Superficial Peroneal Nerve

Deep peroneal nerve entrapment
Deep peroneal nerve palsy causes an inability to dorsiflex the ankle and loss of sensation in the first dorsal web space. The symptom is clinically described as "foot drop." Causes of compression or lesion of the deep peroneal nerve could be ganglion cyst, osteophytes from the talonavicular joint, subluxations or fractures, direct injury, an external pressure on the dorsum of the foot due to a long history of wearing shoes with tight laces, repeated extreme plantar flexion of the foot (e.g., in ballet dancers), and pes cavus.

The superficial peroneal (also called the musculocutaneous nerve of the leg) is the smaller of the two terminal branches of the common peroneal nerve.

It supplies motor innervation to the lateral compartment of the leg, innervating the peroneus longus and brevis muscles (these muscles assist with eversion and plantar flexion of the foot), which originate from the fibula. It also provides sensory innervation to the lateral compartment of the leg (above the sural nerve) and dorsum of the foot (excluding the first dorsal web space and fifth toe).

The superficial peroneal emerges at the bifurcation of the common peroneal nerve and runs between the peroneal muscles, supplying them with motor innervation.

Initially it runs along the peroneus brevis muscle, under the peroneus longus.

In the distal part of the leg, it runs underneath the fascia of the calf and descends between the peroneus muscles and the extensor digitorum longus.

In the lower third of the leg, it pierces the deep fascia through a short fibrous tunnel, to enter the subcutaneous tissue. This exit point is located at the level of a defect in the crural fascia, typically located about 10 cm above the ankle joint (Fig. 2.58).

More distally it divides into two cutaneous terminal branches: the *medial dorsal cutaneous nerve* and the *intermediate dorsal cutaneous* nerve, which supply the dorsal foot.

In fact, the **medial dorsal cutaneous nerve** and its branches run toward the medial border of the foot and great toe, reaching the dorsal surface of the second and third toes with the dorsal digital branches. The **intermediate dorsal cutaneous nerve** gives off dorsal digital branches to the third fourth and fifth toes.

Superficial peroneal nerve often divides into its terminal branches at the level of the ankle joint. The Superficial peroneal nerve is the only nerve in the human body that can be visible in the dorsum of the ankle.

Superficial peroneal nerve entrapment
Depending on the location of the entrapment or lesion, symptoms may vary:

- Proximal location in the lateral compartment of the leg: clinical examination reveals weak ankle eversion and dorsiflexion due to affected innervation of the peroneus longus and brevis muscles.
- At level of the crural fibrous tunnel, it causes pain in the anterolateral leg, hypo-sensation, or paresthesia over the dorsal foot, sparing the first web space.

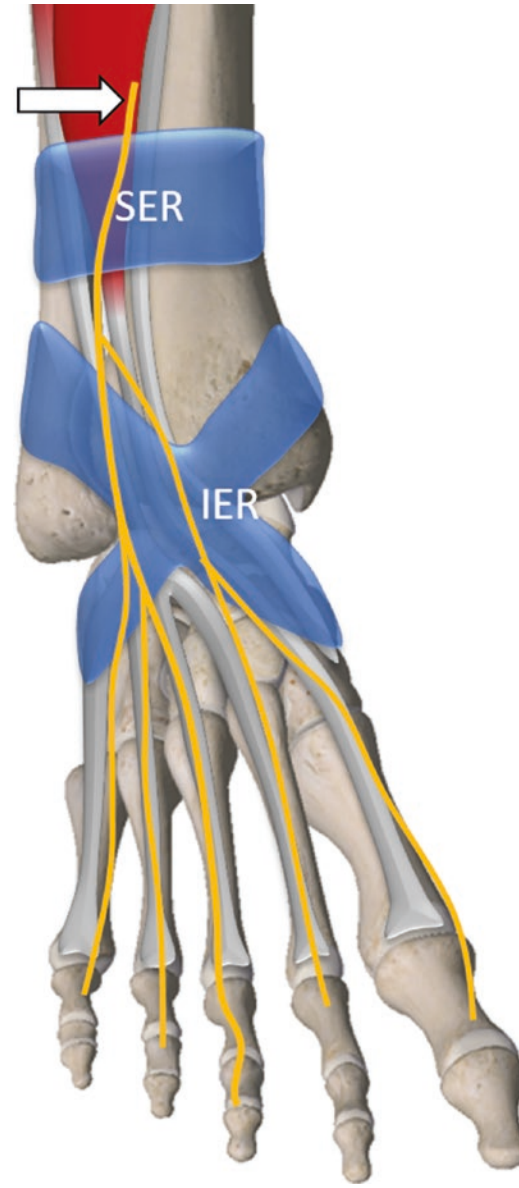

Fig. 2.58 Anatomical scheme at the level of the ankle, showing the superficial peroneal nerve (white arrow) and its relationships with the superficial extensor retinaculum (SER) and inferior extensor retinaculum (IER)

2.4.8.4 US Exam

Common Peroneal Nerve

Landmarks at the popliteal fossa:

- Popliteal vessels
- Biceps femoris and lateral head of the gastrocnemius

Landmarks at the leg:

- Lateral surface of the neck of the fibula
- Proximal end of the peroneus longus

With the patient supine, place the transducer in the transverse plane at the proximal popliteal fossa to visualize the distal part of the sciatic nerve, which branches into the common peroneal nerve laterally and the tibial nerve medially (Fig. 2.59a, b).

Follow the common peroneal nerve moving the probe along and lateral to the tendon of the biceps femoris. It passes between the biceps femoris and the lateral head of the gastrocnemius muscle and runs to the lateral aspect of the proximal third of the leg (Fig. 2.59c, d).

It then crosses the fibular head and passes under the proximal end of the peroneus longus.

Move the probe in a transverse plane caudally until the nerve divides into the superficial and deep peroneal nerves (Fig. 2.59e, f).

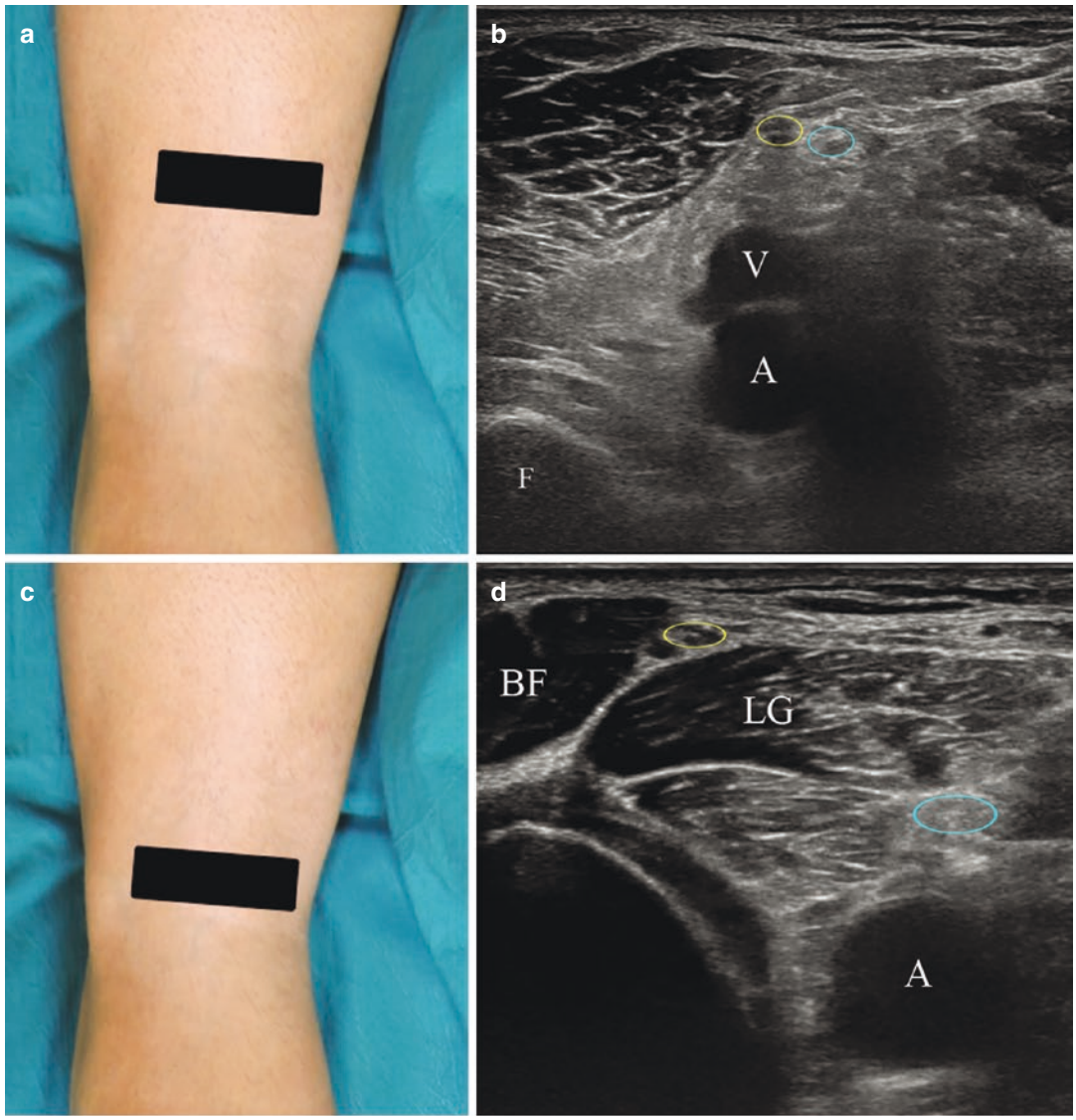

Fig. 2.59 (**a**, **b**) Probe position to evaluate the deep peroneal nerve in the popliteal fossa and the corresponding ultrasound scan. Yellow circle tibial nerve, Ligth Blue Circle common peroneal nerve, *A* popliteal artery, *V* popliteal vein, *F* femur. (**c**, **d**) Probe position to evaluate the deep peroneal nerve (asterisk) at the proximal third of posterior leg and the corresponding ultrasound scan**.** *BF* biceps femoris long head, *LG* gastrocnemius lateral head, *A* posterior tibial artery, Yellow Circle common peroneal nerve, Light Blue Circle tibial nerve. (**e**, **f**) Probe position to evaluate the deep peroneal nerve (asterisk) at the level of peroneal head (P). *LG* gastrocnemius lateral head

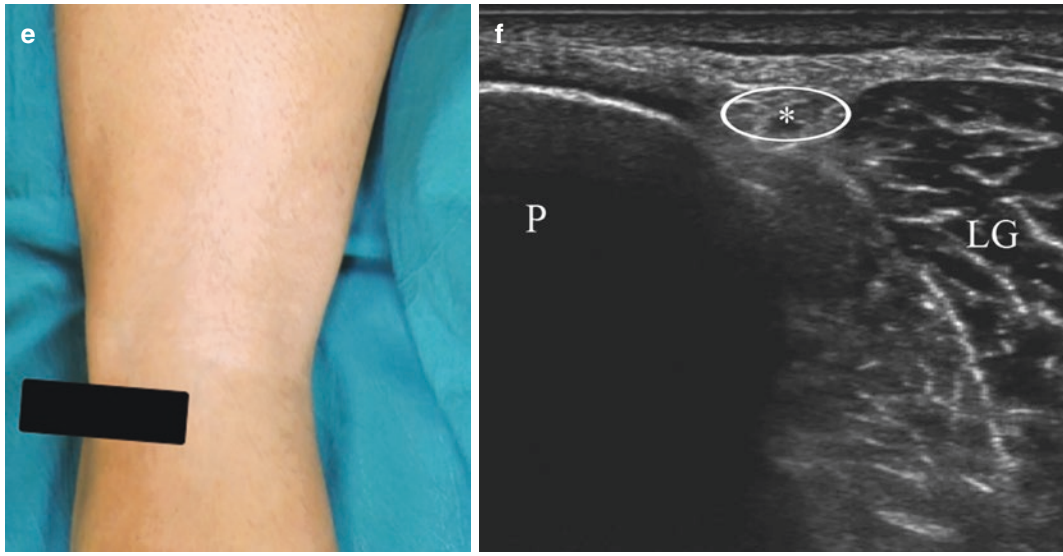

Fig. 2.59 (continued)

Turn the probe by 90° to examine the nerve in a longitudinal axis to evaluate the internal echo-structure.

The US exam can be also started placing the transducer on the lateral surface of the neck of the fibula, where the common fibular nerve lies on the bone surface, crossing anteriorly toward the anterior compartment of the leg. Because at this level it is very close to the bony surface, use a large amount of gel or a standoff pad.

Deep Peroneal Nerve

Landmarks in the leg:

- Fibular head
- Tibial artery
- Tibialis anterior, extensor digitorum longus, and extensor hallucis longus muscles

Landmarks in the ankle:

- Dorsalis pedis artery
- Extensor hallucis longus tendon

Start the US exam placing the probe on a transverse plane on the anterolateral aspect of the proximal leg, at the level of the fibular head, where the deep peroneal nerve arises with the superficial peroneal nerve. It is very close to the fibula, under the peroneus longus muscle.

Follow the nerve caudally in the leg.

The tibial artery is a very important landmark to identify the nerve course in the leg: in fact the neurovascular bundle runs superficial to the interosseous membrane and deep to the tibialis anterior, extensor digitorum longus, and extensor hallucis longus muscles (Fig. 2.60a, b).

In the distal third of the leg, proximal to the ankle joint, with the transducer placed in a transverse orientation at the level of the extensor retinaculum, the deep peroneal nerve crosses the anterior tibial artery from a medial to a lateral position. The nerve usually appears hyperechoic, lateral to the tibial artery, on the surface of the tibia (Fig. 2.60c, d).

At the level of the ankle, place the transducer at the anterior ankle joint in the transverse plane. The deep peroneal nerve is small and can be difficult to visualize: it lies, with the dorsalis pedis artery, lateral to the extensor hallucis longus tendon (Fig. 2.61). Use color Doppler to identify the dorsalis pedis artery.

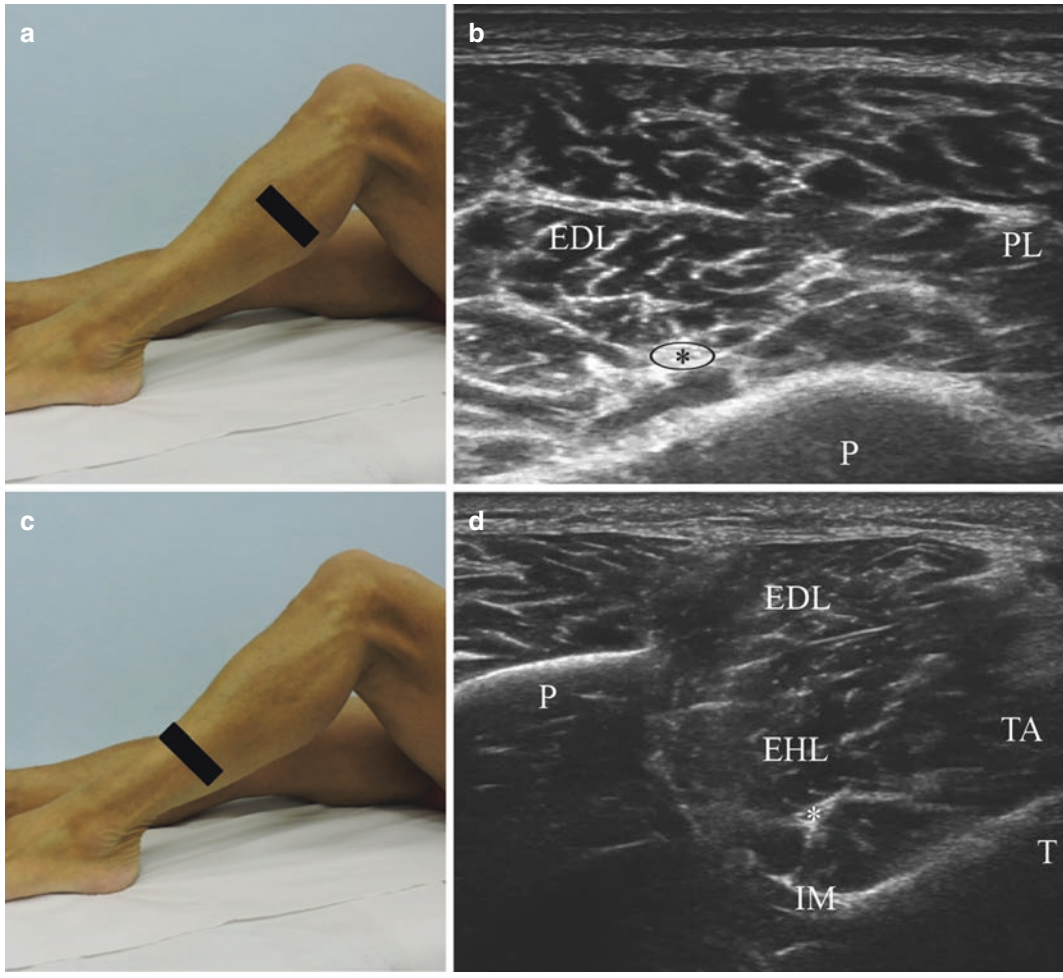

Fig. 2.60 (**a**, **b**) Probe position to evaluate the deep peroneal nerve (asterisk) at the proximal third of the leg and the corresponding ultrasound scan. *EDL* extensor digitorum longus, *PL* peroneus longus, *P* peroneal bone. (**c**, **d**) Probe position to evaluate the deep peroneal nerve (asterisk) at the distal third of the leg and the corresponding ultrasound scan. *P* peroneal bone, *EDL* extensor digitorum longus, *EHL* extensor hallucis longus, *TA* tibialis anterior, *IM* interosseous membrane, *T* tibia

Superficial Peroneal Nerve

Landmarks in the leg:

- Fibular head
- Peroneus longus and brevis muscles

Landmarks in the ankle:

- Lateral malleolus
- The extensor digitorum longus muscle
- Peroneus brevis muscle
- The tendon of peroneus longus

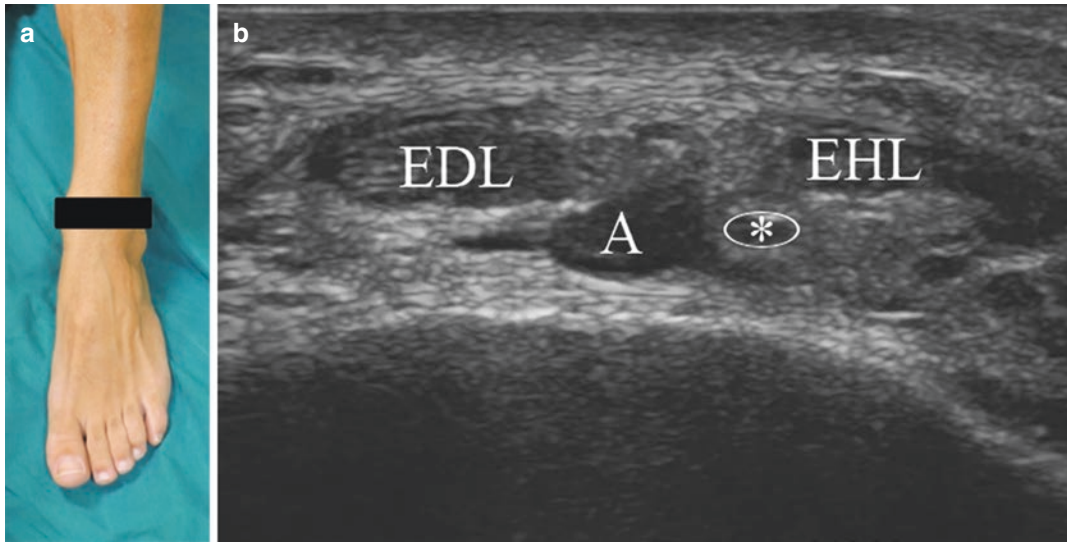

Fig. 2.61 (**a**) Probe position to evaluate the deep peroneal nerve at the level of the ankle. (**b**) Corresponding ultrasound scan of the deep peroneal nerve (asterisk). *EDL* extensor digitorum longus, *EHL* extensor hallucis longus, *A* anterior tibial artery

Place the probe in a transverse plane on the anterolateral aspect of the proximal leg, at the level of the fibular head, where the superficial peroneal nerve merges.

Follow the nerve until the proximal end of the peroneus brevis, where it passes between the fibula and the peroneus longus muscle. Distally it lies between the peroneus longus and brevis muscles (Fig. 2.62a, b).

At the level of the ankle, with the transducer placed on the anterior superior aspect of the lateral malleolus, the superficial peroneal nerve lies in a small groove between the extensor digitorum longus muscle anteriorly and peroneus brevis muscle posteriorly. Identify the tendon of the peroneus longus (not the muscle belly). Identify the hyperechoic structure that lies in the subcutaneous tissue immediately superficial to the fascia (Fig. 2.62c, d).

The nerve can then be followed more proximally, to the point where it pierces the fascia and enters the muscle.

At this level the extensor hallucis longus muscle is an excellent landmark for identifying the superficial peroneal nerve, which is located in this intermuscular septum, just deep to the fascia.

The US exam can also be started at the level of lateral malleolus following the superficial peroneal nerve proximally on its short axis.

2.4.9 Tibial Nerve

2.4.9.1 Anatomy

The posterior tibial nerve is the larger of the two terminal branches of the sciatic nerve (L4-S3).

It leaves the popliteal fossa between the heads of medial and lateral gastrocnemius muscles and then runs below the characteristic arch of the soleus muscle.

At this level the tibial nerve is lateral to popliteal vessels, while, proximally, it is close to the vessels and crosses to the medial side of the artery.

Then it descends in the median plane of the fibula, between soleus and deep ankle flexor muscles (tibialis posterior, flexor digitorum longus, and flexor hallucis longus).

At the ankle the tibial nerve runs posterior to the medial malleolus under the flexor retinaculum that forms the tarsal tunnel. At the level of

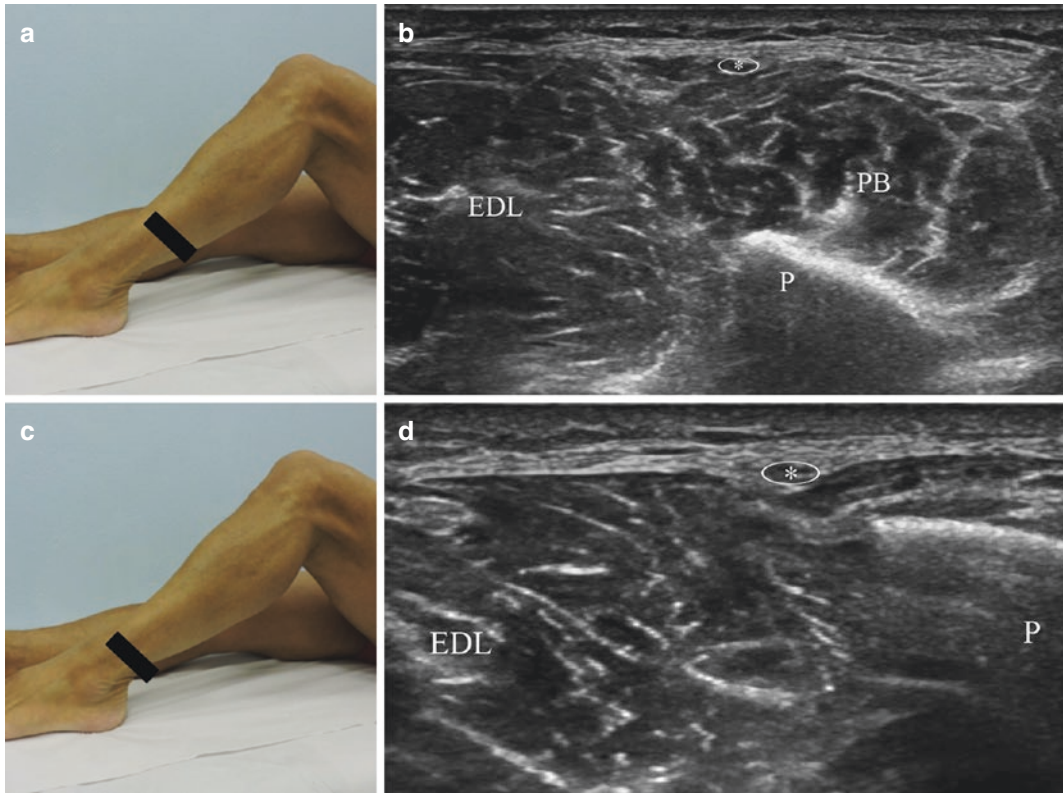

Fig. 2.62 (**a**, **b**) Probe position to evaluate the superficial peroneal nerve (asterisk) at the middle third of the leg and the corresponding ultrasound scan. *EDL* extensor digitorum longus, *PB* peroneus brevis, *P* peroneal bone. (**c**, **d**) Probe position to evaluate the superficial peroneal nerve (asterisk) at the distal third of the leg and the corresponding ultrasound scan. *P* peroneal bone, *EDL* extensor digitorum longus

the posterior aspect of medial malleolus, the tibial nerve is covered by the superficial and deep fascia of the leg and lies lateral and posterior to the posterior tibial artery, between the flexor digitorum and flexor hallucis muscles (Fig. 2.63).

The tarsal tunnel contains the tibial nerve, the tibial artery, the flexor hallucis longus tendon, the flexor digitorum longus tendon, and tibialis posterior tendon (Fig. 2.64).

Focus on: tibial neurovascular bundle

The mnemonic "Tom, Dick, and a Very Nervous Harry" is useful to remember the anatomical position of the tibialis posterior tendon, flexor digitorum longus tendon, vessels, nerves, and flexor hallucis longus tendon.

Once it has passed through the tunnel, the tibial nerve branches into the *lateral and medial plantar nerves*, which supplies all of the intrinsic muscles on the plantar side of the foot, providing sensitive innervation to the medial and lateral sole, respectively.

Tibial nerve bifurcation usually occurs distal to the medial malleolus tip, but anatomical variations are possible.

Before it division, the **tibial nerve** gives off cutaneous branches to the medial sural cutaneous nerve (which is continuous with the sural nerve), lateral calcaneal branches, medial calcaneal branches, and lateral dorsal cutaneous nerve. It also furnish articular branches for knee joint, providing the motor innervation of the gastrocnemius, soleus, plantaris, and deep ankle flexors muscles.

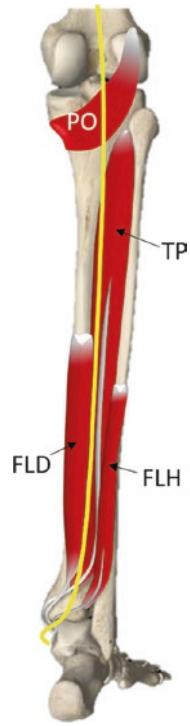

Fig. 2.63 Anatomical scheme of the tibial nerve. *PO* popliteal muscle, *TP* tibialis posterior muscle, *FLH* flexor longus hallucis muscle, *FLD* flexor longus digitorum muscle

The medial plantar nerve, the larger of the two terminal branches of the tibial nerve, crosses the lateral surface of the posterior tibial artery and courses anterior to the medial plantar artery.

Proximally, it runs between the quadratus plantae and abductor hallucis muscles. More distally, it is still located between these muscles but in proximity to the master knot of Henry (the crossover point of the flexor digitorum longus and flexor hallucis longus tendons at the level of the navicular bone), along the medial border of the flexor digitorum brevis muscle. At this level it gives off a proper digital plantar nerve which opposite the bases of the metatarsal bones divides into three common digital plantar nerves.

The medial plantar nerve supplies the cutaneous innervation of medial sole, first three toes, and sometimes the fourth toe and the motor innervation of the abductor hallucis, the flexor digitorum brevis, the flexor hallucis brevis, and the first lumbrical.

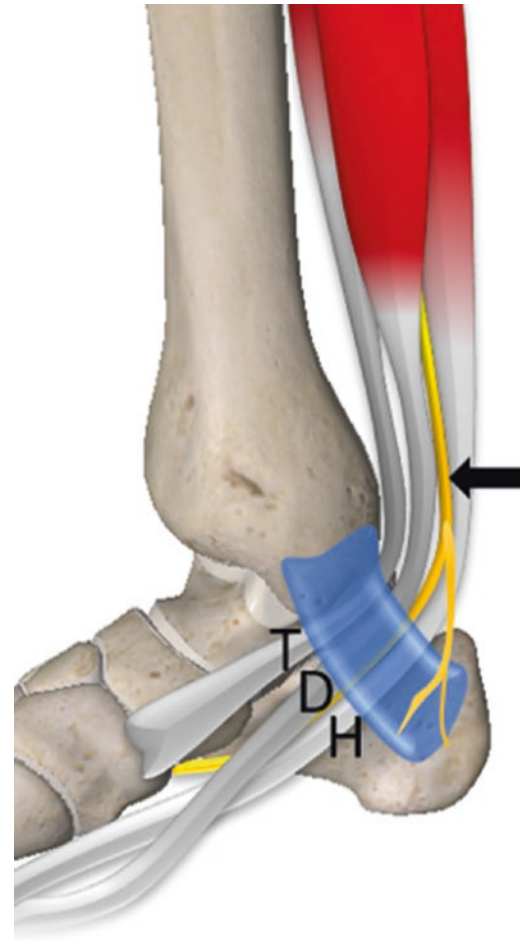

Fig. 2.64 Anatomical scheme at the level of the medial aspect of the ankle, showing the tibial nerve (black arrow) and its relationships with the tibialis posterior (T), flexor digitorum longus (D), and flexor hallucis longus (H) tendons

The lateral plantar nerve descends obliquely in the lateral side of foot, crossing the posterior tibial artery near its bifurcation in the proximal segment of the talocalcaneal canal. The nerve then courses between the medial and lateral plantar arteries.

It lies between the flexor digitorum brevis and quadratus plantae muscles in the middle plantar space.

More distally, it courses along the lateral border of the flexor digitorum brevis muscle, adjacent to the abductor digiti minimi muscle and, in proximity to the abductor digiti quinti, divides into a superficial and a deep branch.

The lateral plantar nerve supplies the cutaneous innervation of the lateral sole, fifth toe, and sometimes the fourth toe and the motor innervation of the quadratus plantae, the flexor digiti minimi, the adductor hallucis, the interossei, three lumbricals, and abductor digiti minimi.

2.4.9.2 US Exam

Landmarks at the popliteal fossa:

- Popliteal vessels

Landmarks at the leg:

- Soleus muscle
- Deep plantar flexor muscles (flexor hallucis longus, flexor digitorum longus, and tibialis posterior)

Landmarks at the ankle:

- Medial malleolus
- Posterior tibial artery
- Tibialis posterior and flexor digitorum longus tendons

The patient is supine with the foot externally rotated.

Place the probe in a transverse plane, cranial and posterior to the medial malleolus.

Identify the posterior tibial artery: the round, hypoechoic, pulsatile vessel.

Do not put too much pressure on the probe because the vessels are superficial and may be compressed. Color Doppler can be used to confirm the location of the artery if there is any doubt.

The posterior tibial nerve lies posterior to the artery and to the tibialis posterior and flexor digitorum longus tendons.

It appears like a round hyperechoic structure with a typical honeycomb appearance. Carefully tilt and rotate the US probe for the correct visualization of the nerve on its short axis (Fig. 2.65a–d).

Move the probe cranially to explore the nerve in the leg: the tibial nerve lies underneath the soleus muscle and superficial to the deep plantar flexor muscles (flexor hallucis longus, flexor digitorum longus, and tibialis posterior) (Fig. 2.66) until it merges with the common peroneal nerve in the popliteal fossa (Fig. 2.67).

Tibialis posterior and flexor digitorum longus tendons are also hyperechoic but with fibrillary echotexture, and they slide during ankle flexion (useful to distinguish from the tibial nerve).

Move the transducer distally to visualize the bifurcation point of the tibial nerve (located between the abductor hallucis brevis and quadratus plantae muscles) into the medial and lateral plantar nerves (Fig. 2.65e, f).

Tarsal Tunnel Syndrome

Tarsal tunnel syndrome is an entrapment syndrome caused by the compression of the tibial nerve or its terminal branches. Some authors introduced the term *proximal tarsal tunnel syndrome* to define entrapment of the posterior tibial nerve in the fibro-osseous tunnel behind the medial malleolus and the term *distal tarsal tunnel syndrome* to denote entrapment of the distal branches, that is, the medial and lateral plantar nerves.

This syndrome results in pain and sensory disturbances at the sole of the foot and hypoplasia of the intrinsic foot muscles.

Entrapments above the ankle have been reported in the popliteal fossa, where the nerve can be compressed by the tendinous arch of the soleus, a Baker's cyst, or other masses.

The causes of posterior tibial nerve compression could be fibrosis, ganglion cysts, lipomas, varicosities, other benign and malignant tumors, hypertrophic abductor hallucis, anomalous extra muscles (e.g., the flexor digitorum accessorius longus), tenosynovitis of the adjacent tendons, partial or complete rupture of the medial tendons, obesity, ankylosing spondylitis, acromegaly, and talocalcaneal coalition.

Tarsal tunnel syndrome could result also from nerve trauma related to tibial shaft or medial malleolus fractures.

Entrapment of the lateral plantar nerve usually occurs beneath the deep fascia of the abductor hallucis muscle or the medial edge of the quadratus plantae fascia, while the entrapment of the medial plantar nerve typically occurs in the areas of the master knot of Henry.

2.4.10 Sural Nerve

2.4.10.1 Anatomy

The sural nerve is a sensitive nerve formed by two branches tibial and peroneal one, respectively.

The medial sural cutaneous nerve (tibial branch) lies close to the small saphenous vein in the groove of the two heads of gastrocnemius and pierces the deep fascia proximally in the leg to join the lateral sural nerve (peroneal branch) in the middle third of the calf forming the distal sural nerve.

Then, the sural nerve courses anterolaterally to the Achilles tendon, following the course of the small saphenous vein (in variable proximity to it).

Finally, it anteriorly crosses the lateral edge of the foot, ending at the lateral side of the fifth toe in its distal branch (lateral dorsal cutaneous nerve).

On the dorsum of the foot it also joins with the intermediate dorsal cutaneous nerve, a branch of the superficial peroneal.

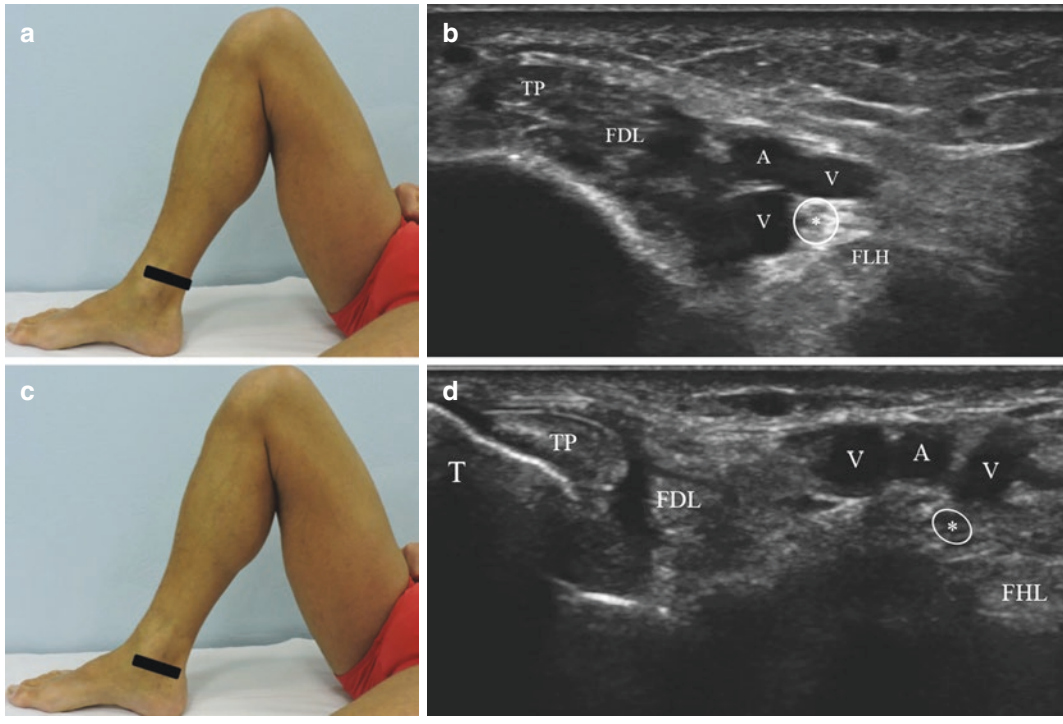

Fig. 2.65 (**a**, **b**) Probe position to evaluate the tibial nerve at the level of medial malleolus and the corresponding ultrasound scan. *T* tibia, *TP* tibialis posterior, *FDL* flexor digitorum longus, *FHL* flexor hallucis longus, *V* posterior tibial veins, *A* posterior tibial artery, asterisk tibial nerve. (**c**, **d**) Probe position to evaluate the tibial nerve in the tarsal tunnel and the corresponding ultrasound scan. *TP*, tibialis posterior, *FDL* flexor digitorum longus, *FHL* flexor hallucis longus, *V* posterior tibial veins, *A* posterior tibial artery, asterisk tibial nerve. (**e**, **f**) Probe position to evaluate the tibial nerve in the point of bifurcation and the corresponding ultrasound scan. Asterisks medial and lateral plantar nerves

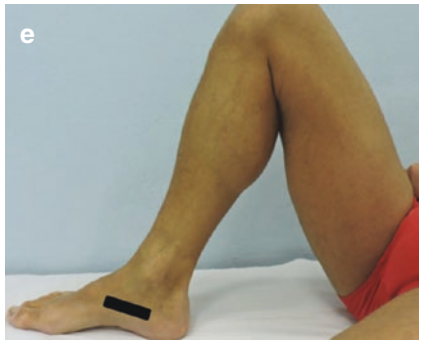

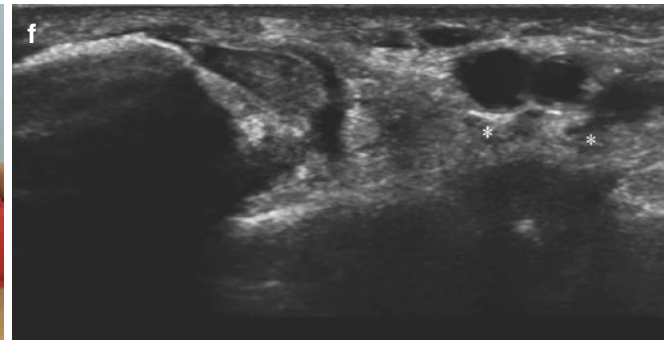

Fig. 2.65 (continued)

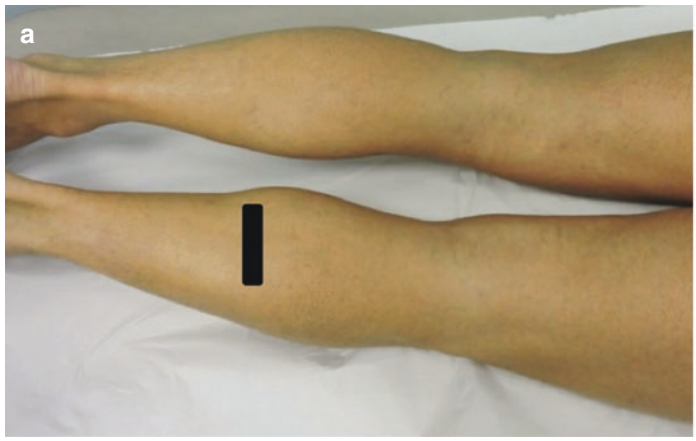

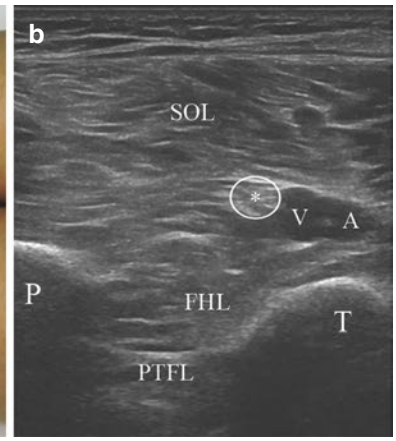

Fig. 2.66 (**a**) Probe position to evaluate the tibial nerve at the proximal third of the posterior leg. (**b**) Corresponding ultrasound scan of the tibial nerve (asterisk). *SOL* soleus, *FHL* flexor hallucis longus, *P* fibula, *T* tibia, *IM* interosseous membrane, *V* posterior tibial vein, *A* posterior tibial artery

The sural nerve provides cutaneous innervation to the posterior distal third of the calf and lateral ankle, lateral heel, and foot up to the tip of the fifth toe (Fig. 2.68).

Focus on: sural nerve

Because the *sural nerve* runs close to the small saphenous vein, it is at risk of injury during dissection, stripping, phlebotomy, and thermal ablation of the small saphenous vein. The clinical consequence is numbness, hypoesthesia, or anesthesia of posterolateral aspect of the leg and lateral aspect of the foot.

2.4.10.2 US Exam

Landmarks at the calf:

- Small saphenous vein

Landmarks at the ankle:

- Lateral malleolus
- Small saphenous vein

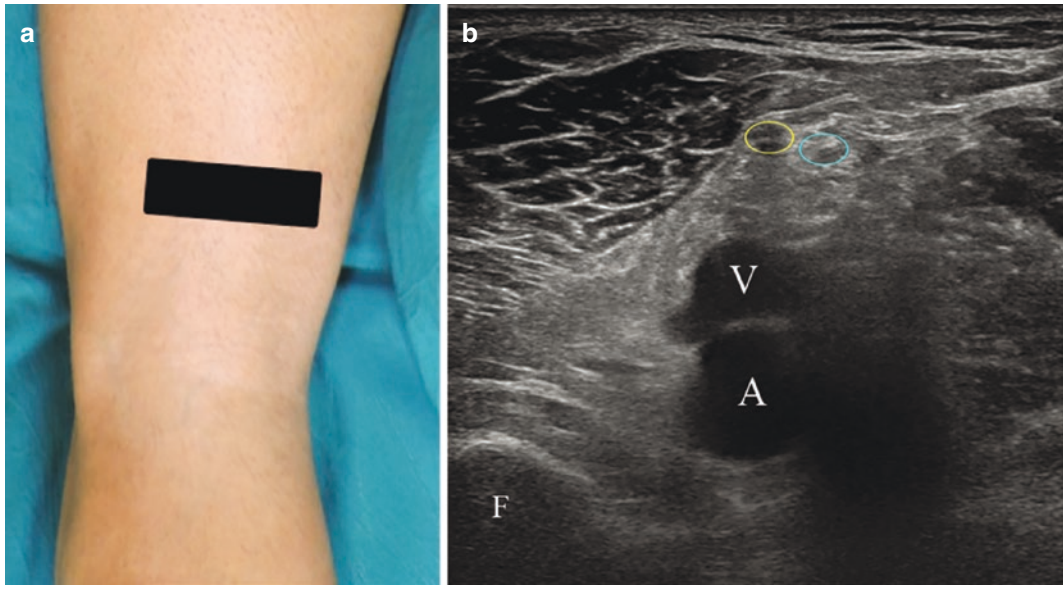

Fig. 2.67 (**a**) Probe position to evaluate the sciatic nerve (asterisk) at the level of popliteal fossa. (**b**) Corresponding ultrasound scan at the level of point of bifurcation of the sciatic nerve. *Yellow circle* tibial nerve, Light Blue Circle common peroneal nerve, *A* popliteal artery, *V* popliteal vein, *F* femur

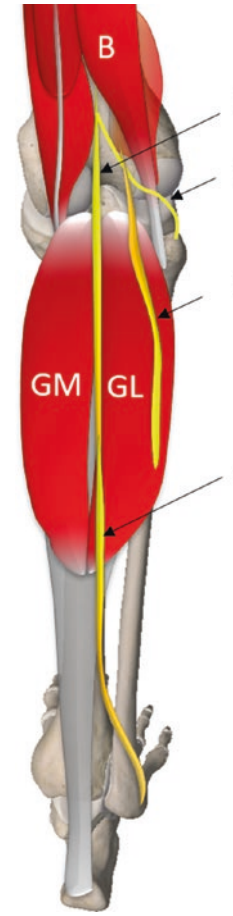

Fig. 2.68 Anatomical scheme of the posterior leg. *1* tibial nerve, *2* superficial peroneal nerve, *3* deep peroneal nerve, *4* sural nerve, *B* biceps muscle, GM gastrocnemius medialis muscle, GL gastrocnemius lateralis muscle

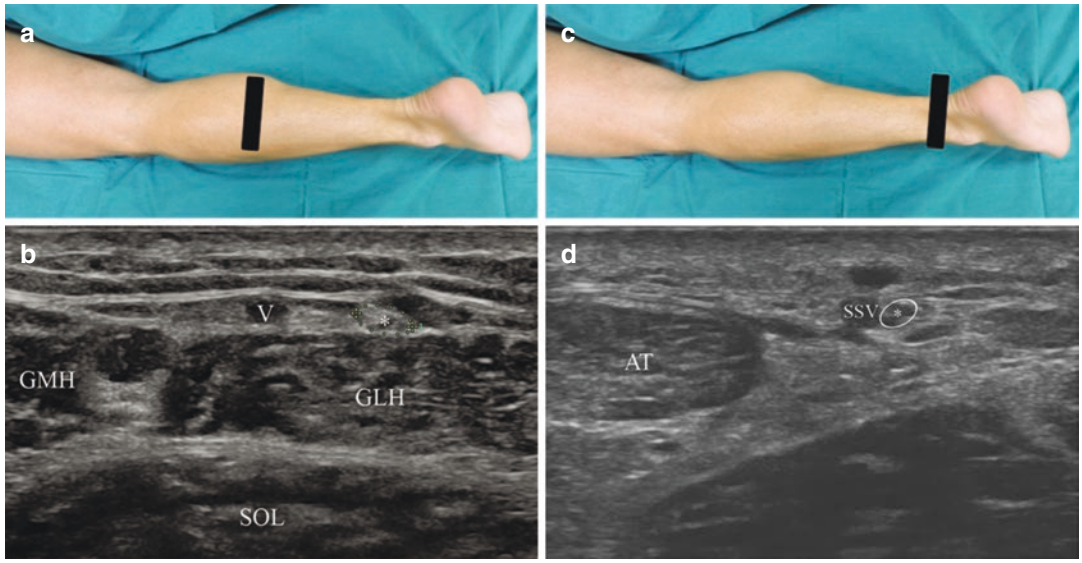

Fig. 2.69 (**a**, **b**) Probe position to evaluate the sural nerve at the level of middle third of the calf and the corresponding ultrasound scan. *GMH* gastrocnemius medial head, *GLH* gastrocnemius lateral head, *V* small saphenous vein, *SOL* soleus, asterisk sural nerve. (**c**, **d**) Probe position to evaluate the sural nerve at the level of Achilles tendon. *AT* Achilles tendon, *SSV* small saphenous vein, asterisk sural nerve

Place the probe in a transverse plane at the middle third of the calf and identify the small saphenous vein. The sural nerve could be seen closer and lateral to the vein as an ovoid hyperechoic honeycombing structure of 1–2 mm diameter (Fig. 2.69a, b).

Then, follow the sural nerve on its short axis with a transverse US scan along its course between the Achilles tendon and the lateral malleolus. At this level the sural nerve courses closer to the small saphenous vein which is easy to identify applying and releasing pressure with the transducer in order to detect the collapse of the vein. Use color Doppler if is necessary (Fig. 2.69c, d).

The sural nerve is the small oval hyperechoic structure located posterior to the vein, closer to peroneal malleolus.

2.4.11 Interdigital Nerve

2.4.11.1 Anatomy

At the dorsum of the foot, sensory branches of the deep peroneal nerve innervate the first interspace, while branches of the superficial peroneal nerve provide sensory innervation to the other spaces (Fig. 2.70).

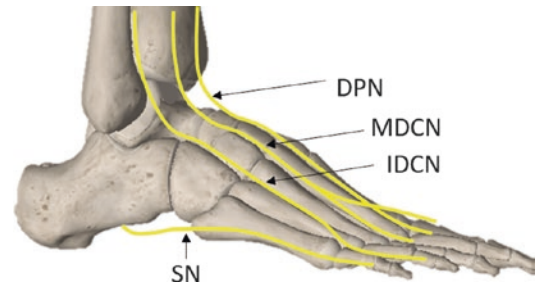

Fig. 2.70 Anatomical scheme of the dorso-lateral aspect of the foot showing the deep peroneal nerve (DPN); the medial dorsal cutaneous nerve (MDCN); the intermediate dorsal cutaneous nerve (IDCN) and the sural nerve (SN)

Medial plantar hallucis (from medial plantar nerve) and medial dorsal hallucis (from superficial peroneal nerve) nerves innervate the medial surface of the first toe. These nerves are located in the medial plantar aspect of the hallux adjacent to the medial sesamoid bone.

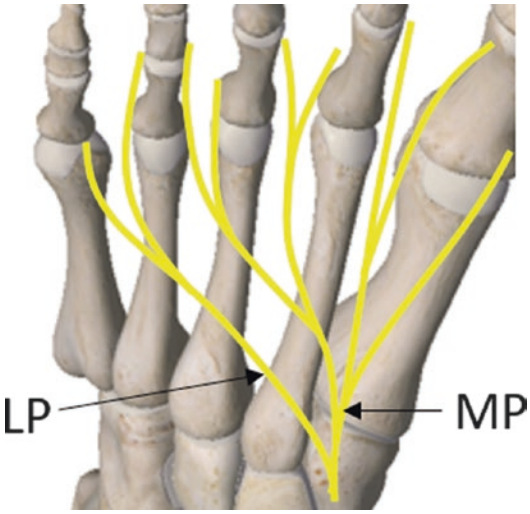

Fig. 2.71 Anatomical scheme of the plantar aspect of the foot showing the lateral plantar nerve (LP) and the medial plantar nerve (MP) and their branches

At the plantar aspect of the foot, the common digital nerves originate from the medial and lateral plantar nerves.

The medial plantar nerve divides into the first, second, and third common digital nerves, which supply cutaneous branches to the medial three digits.

The lateral plantar nerve divides into two common digital nerves, supplying cutaneous branches to the fifth toe and half of the fourth one.

The digital nerve of the third web space commonly receives fibers from both the medial and lateral plantar nerves (Fig. 2.71).

The interdigital nerves lie in the intermetatarsal space, deep to the interosseous muscle and distal to the intermetatarsal ligament, a fibrous band which forms the anterior portion of the deep plantar fascia.

The digital nerves, at the level of the web spaces, surround the intermetatarsal ligament and divide into medial and lateral digital branches, innervating the adjacent toes.

In the intermetatarsal space, the plantar digital artery runs parallel and close to the digital nerve covered by the same fascial sheath, and the intermetatarsal bursa lies dorsal to the intermetatarsal ligament.

Focus on: Morton's Neuroma

Morton's neuroma is the thickening of a digital nerve, resulting from compression and irritation of the nerve under the intermetatarsal ligament, particularly at the second and third web spaces.

Imaging is important to identify the neuroma and make a differential diagnosis with acute lesions of the metatarsophalangeal lateral collateral ligaments, metatarsophalangeal joint synovitis (e.g., second ray syndrome), and isolated tarsometatarsal bursitis.

Symptoms are burning or numbness, lancinating pain in the plantar aspect of the metatarsal interspace, particularly when walking, and a feeling that there is something in the shoe at level of intermetatarsal space.

Joplin's neuroma consists in a focal irritation of the medial plantar hallucis nerve.

2.4.11.2 US Exam

Place the probe on the plantar aspect of the foot in a coronal plane at the level of the metatarsal heads to study the anatomy of each web space.

Landmarks:

- Metatarsal heads
- Dorsal digital arteries

Identify the metatarsal heads as hyperechoic, curvilinear structures, which continue in the bony surface of the metaphysis and diaphysis of the metatarsal bone.

The web space is a uniform tissue, less echogenic than the adjacent bone, composed of muscles and fat.

Use color Doppler to visualize the plantar and dorsal digital arteries.

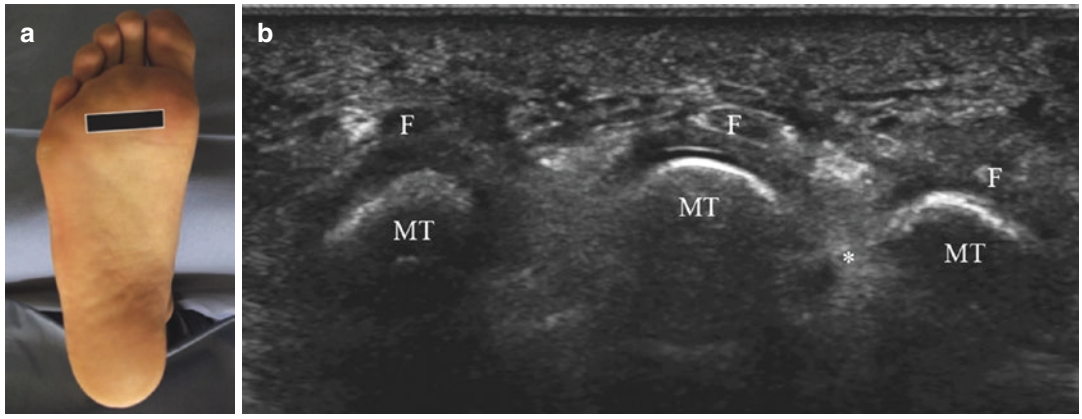

Fig. 2.72 (**a**) Probe position to evaluate the interdigital nerve on the plantar surface of the foot at the level of metatarsal heads. (**b**) Corresponding ultrasound scan. *MT* metatarsal, *F* flexor digitorum tendons, asterisk interdigital nerve

The digital nerve can be identified closer to the interdigital vessels and, at the level of the metatarsal heads, normally measures 2 mm in diameter.

Turn the probe by 90° to evaluate the web space on an axial plane at the level of the metatarsal heads (Fig. 2.72).

Also place the probe on the dorsal surface of the foot to evaluate the interdigital nerve in axial and longitudinal planes.

At this level with the probe in a longitudinal plane, we can do a dynamic scan to evaluate the "snake sign": with the transducer in a dorsal longitudinal approach, applying a plantar pressure with the finger in the web space.

It can be useful to perform the sonographic *Mulder's maneuver* to identify a neuroma and make a differential diagnosis with bursitis. With the probe positioned on the plantar surface of the foot, squeeze the dorsum of the foot from medial to lateral. Morton's neuroma will pop-out in the plantar surface of the foot through the metatarsal interspace, while the bursa is typically compressible during dynamic imaging.

Suggested Readings

Ahmed A, Arora D, Kochhar AK. Ultrasound-guided alcohol neurolysis of lateral femoral cutaneous nerve for intractable meralgia paresthetica: a case series. Br J Pain. 2016;10(4):232.

Beaudoin FL, Nagdev A, Merchant RC, Becker BM. Ultrasound-guided femoral nerve blocks in elderly patients with hip fractures. Am J Emerg Med. 2010;28(1):76–81.

Bianchi S, Martinoli C, editors. Ultrasound of the musculoskeletal system. Milan, Italy: Springer Verlag; 2009.

Chiou HJ, Chou YH, Chiou SY, Liu JB, Chang CY. Peripheral nerve lesions: role of high-resolution US. Radiographics. 2003;23:15.8.

Fornage BD. Peripheral nerves of the extremities: imaging with US. Radiology. 1988;167:179–82.

Gray H. Anatomy descriptive and applied. London: Longman's, Green and CO; 1935.

Gray AT. Atlas of ultrasound-guided regional anesthesia. 2nd ed. Philadelphia: Saunders; 2013.

Huelke DF. The origin of the peroneal communicating nerve in adult man. Anat Rec. 1958;132:81–92.

Kele H. Ultrasonography of the peripheral nervous system. Pers Med. 2012;1:417–21.

Kosinski C. The course, mutual relations and distribution of the cutaneous nerves of the metazonal region of leg and foot. J Anat. 1926;60:274–97.

Kowalska B, Sudoł-Szopińska I. Normal and sonographic anatomy of selected peripheral nerves. Part

III: peripheral nerves of the lower limb. J Ultrason. 2012a;12:148–63.

Kowalska B, Sudoł-Szopińska I. Normal and sonographic anatomy of selected peripheral nerves. Part II: peripheral nerves of the upper limb. J Ultrason. 2012b;12(49):131–47.

Lapegue F, Faruch-Bilfeld M, Demondion X, et al. Ultrasonography of the brachial plexus, normal appearance and practical applications. Diagn Interv Imaging. 2014;95(3):259–75.

Martinoli C. Imaging of the peripheral nerves. Semin Musculoskelet Radiol. 2010;14:461–2.

Mentzel M, Fleischmann W, Bauer G, Kinzl L. Ankle joint denervation. Part 1. Anatomy: the sensory innervation of the ankle joint. Foot Ankle Surg. 1999;5:15–20.

Mercer D, Morrell NT, Fitzpatrick J, et al. The course of the distal saphenous nerve: a cadaveric investigation and clinical implications. Iowa Orthop J. 2011;31:231–5.

Merga H, Nega D, Leulayehu A. Practice of regional anesthesia and analgesia in Ethiopian hospital. International Journal of Medicine and Medical Sciences. 2015;7:8–130.

Mian A, Chaudhry I, Huang R, Rizk E, Tubbs RS, Loukas M. Brachial plexus anesthesia: a review of the relevant anatomy, complications, and anatomical variations. Clin Anat. 2014;27(2):210–21.

Mikityansky I, Zager EL, Yousem DM, Loevner LA. MR imaging of the brachial plexus. Magn Reson Imaging Clin N Am. 2012;20(4):791–826.

Miller R, Eriksson L, Fleisher L, Wiener-Kronish J, Youn W. Millers anesthesia. 7th ed. London: Churchill Livingstone; 2010.

Peer S, Kovacs P, Harpf C, Bodner G. High-resolution sonography of lower extremity peripheral nerves: anatomic correlation and spectrum of disease. J Ultrasound Med. 2002;21:315–22.

Peng P, Tumber P. Ultrasound-guided interventional procedures for patients with chronic pelvic pain – a description of techniques and review of literature. Pain Physician. 2008;11:215–24.

Philip WH. Peng ultrasound-guided interventional procedures for patients with chronic pelvic pain — a description of techniques and review of literature. Pain Physician. 2008;11:215–24.

Tsui BC, Dillane D, Pillay J, et al. Cadaveric ultrasound imaging for training in ultrasound-guided peripheral nerve blocks: lower extremity. Can J Anaesth. 2007;54:475–80.

Wedel D. Nerve blocks. In: Miller R, editor. Anesthesia. 5th ed. New York: Churchill Livingstone; 2010. p. 1521–47.

US Pathologic Findings

3

Enzo Silvestri, Ernesto La Paglia, Angelo Corazza, and Gianluigi Martino

In the recent years, high-resolution US has been established as an effective diagnostic modality for the assessment of peripheral nerve pathology, in addition to clinical evaluation and electrophysiological studies.

Due to its intrinsic features (such as cost-effectiveness, possibility to perform dynamic maneuvers, lack of contraindications, and noninvasiveness), US can be used for the assessment of patients with traumatic, neoplastic, infective, or compressive nerve injury.

Careful examination with a proper scanning technique, combined with good knowledge of ultrasonographic anatomy and semeiotics, might provide the correct diagnosis and useful presurgical information. Moreover, a comparison with the healthy contralateral side can often be very helpful and should always be considered as part of the US examination.

E. Silvestri, M.D. (✉)
Department of Radiology, Ospedale Evangelico Internazionale, Genova, Italy

E. La Paglia, M.D.
Department of Radiology, Ospedale di Alessandria, Alessandria, Italy

A. Corazza, M.D.
Department of Diagnostic and Interventional Radiology, IRCCS Istituto Ortopedico Galeazzi, Milano, Italy

G. Martino, M.D.
Department of Radiology, Ospedale di Venere, Bari, Italy

3.1 Compressive/Entrapment Syndromes

Nerve compressive syndromes are relatively common pathologies. They can occur acutely or chronically anywhere in the body; however, they develop more frequently at certain anatomic sites where the nerve passes through fibro-osseous tunnels or at the level of anomalous bony, muscular, or connective structures.

Nerve conduction study and US examination provide complementary assessment in evaluating nerve entrapment syndromes; in particular, US can be very helpful for the detection of the site of compression and for the identification of abnormal findings in the nerve surroundings.

Ultrasound can directly demonstrate morphologic changes in the nerve appearance, and, sometimes, it can identify secondary causes (i.e., accessory muscle, thickened fibrous band, cyst, bony prominence, vascular or neoplastic mass, foreign body, orthopedic implants, etc.); this is especially true for larger and more superficial nerves.

In case of nerve compression, a focal flattening with reduction of nerve cross-sectional area (CSA) at the compression point can be appreciated. Proximal to the level of compression, a fusiform enlargement of the nerve could be observed: it usually extends 2–4 cm in length and presents maximum diameter immediately before the compression point, where the nerve suddenly flattens.

E. Silvestri et al. (eds.), *Ultrasound-Guided Peripheral Nerve Blocks*,
https://doi.org/10.1007/978-3-319-71020-4_3

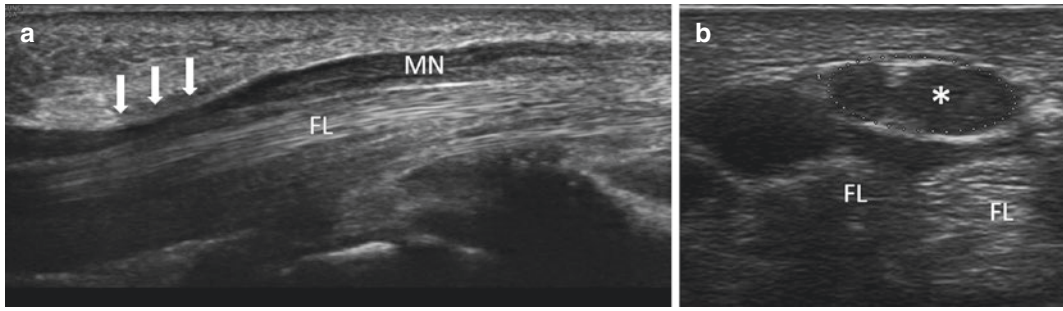

Fig. 3.1 Carpal tunnel syndrome. (**a**) Longitudinal view, flattened (arrows) median nerve (MN); (**b**) axial view, median nerve (dots) with hypoechoic appearance and loss of the typical fascicular pattern; flexor tendons (FL)

In combination to such morphologic changes, also the normal US echotexture is altered: the nerve appears homogeneously hypoechoic with loss of the typical fascicular pattern, reflecting the sub-standing venous congestion and consecutive epi-/endoneural edema; consequently the outer lining of the nerve becomes well delineated from the hyperechoic perineural fat.

Furthermore, intraneural microcirculation can be assessed with color or power Doppler US examination: in cases of acute compression, a local interruption in the microcirculation can occur with possible venous congestion; on the other hand, an increase in intraneural blood flow signals can be appreciated in chronic compressive neuropathies.

Long-standing nerve compression leads to fibrosis and eventually to damage to the myelin sheath and to axonal degeneration. At this stage, a diffuse hyperechogenicity and reduction of volume of the innervated muscles can be assessed because of muscular atrophy.

Carpal tunnel syndrome is the most common entrapment neuropathy. It results from the compression of the median nerve in the fibro-osseous tunnel between the carpal bones and flexor retinaculum (or carpal transverse ligament). US may demonstrate the homogeneously hypoechoic enlargement of the median nerve proximal to the carpal tunnel, with sudden flattening through the fibro-osseous tunnel; palmar bowing of the flexor retinaculum and hypomobility of the nerve during dynamic maneuvers (opening and closing of fingers) may be associated. However, in few cases, the median nerve may appear normal even in presence of positive clinical and electrophysiological findings (Fig. 3.1, Table 3.1).

Table 3.1 Most common entrapment syndromes

Syndrome	Nerve
Carpal tunnel	Median
Cubital tunnel	Ulnar
Spiral groove	Radial
Peroneal neuropathy	Common peroneal (deep & superficial)
Guyon tunnel	Ulnar
Tarsal tunnel	Tibial
Posterior interosseous sy	Posterior interosseous nerve (radial)
Kiloh-Nevin sy	Anterior interosseous nerve (median)
Morton's neuroma	Interdigital (foot)
Meralgia paresthetica	Lateral femoral cutaneous
Sciatalgia	Ischiatic
Suprascapular neuropathy	Suprascapular
Pronator teres	Median
Wartenberg sy	Superficial branch of radial nerve at distal forearm
Quadrilateral space sy	Axillary

3.2 Traumatic Injuries

Three different types of traumatic or iatrogenic nerve damage have been described based on the mechanism of injury: traction, contusion, and

penetrating trauma (multiple mechanisms may coexist), which could result in neurapraxia, axonotmesis, or neurotmesis.

Ultrasound examination, being able to evaluate and differentiate fascicles, perinevrium, epinevrium, and surrounding tissues, can be used to assess the site of injury, discriminate nerve injury in continuity from nerve transection, and identify foreign bodies, neuroma, and scarring. It is very useful in the case of traumatic nerve injury and could help clinical examination and nerve conduction studies to provide information about the condition of the injured nerve and, consequently, possible surgical indications.

Nerve stretching syndromes can occur from sprain or strain injuries and, less frequently, from overuse. A typical injury is the avulsion of the nerve roots of the brachial plexus during motor vehicle accidents. Another typical injury is the peroneal nerve traction at the popliteal fossa during high-grade sprain traumas.

Neurapraxic injury can be appreciated as a swollen nerve with hypoechoic appearance. The outer nerve sheath may be intact. In cases of partial nerve tear, a so-called traction neuroma can be seen along the course of the stretched nerve without discontinuity: it appears as an irregular focal thickening of hypoechoic tissue (Fig. 3.2). In mild traumas, the neuroma may involve only one or few fascicles without resulting in nerve cross-sectional enlargement.

In complete nerve lesions, US demonstrates the retraction of the fascicles with a wavy appearance of the nerve ends.

Contusion traumas typically occur where nerves run in proximity of bony surfaces. In most cases, they do not cause morphologic changes detectable with US, and the pathologic process is self-resolving. Nevertheless, in some cases repeated minor traumas could lead to a focal fusiform thickening of the nerve at the site of repetitive contusions (i.e., peroneal nerve neuritis in soccer players and ulnar nerve friction neuritis in cubital tunnel instability).

In penetrating wounds, US can detect a partial tear or a complete transection of the nerve fascicles. In both cases, the regenerative process leads to the formation of a hypoechoic fibrous mass in the attempt to restore the continuity of the nerve, but in different ways.

In partial tears, the hypoechoic neuroma may develop from the resected fascicles preserving the healthy fascicles, and its size would be smaller than the CSA of the nerve, or it may encase both the resected and the unaffected fascicles determining a fusiform swelling of the nerve.

In complete tears, the so-called stump neuromas or terminal neuromas appear as hypoechoic mass-like lesions at the resected nerve edges with a CSA slightly larger than the nerve itself. The detection of terminal neuromas is of additional help when the resected nerve ends are retracted from the site of injury (Fig. 3.3).

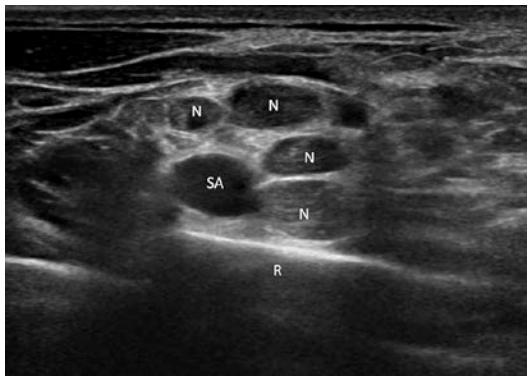

Fig. 3.2 Brachial plexus stretching. Supraclavicular region, oblique view: subclavian artery (SA), enlarged cords (N), rib (R)

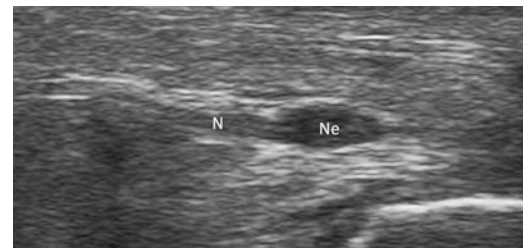

Fig. 3.3 Terminal traumatic neuroma. Longitudinal view of a digital nerve (N) and traumatic neuroma (Ne)

3.3 Tumors and Tumor-like Conditions

The most common nerve tumors are nerve sheath tumors; they include two benign forms (schwannoma (or neurinoma) and the neurofibroma) and a malignant form which is often a sarcomatous degeneration of neurofibromas. Less frequently, other types of tumors may develop within the nerve, such as ganglion cysts, hemangiomas, and lymphomas. Furthermore, two kinds of tumor-like masses could be encountered in peripheral nerves: the Morton's neuroma and the fibrolipomatous hamartoma (or neural lipoma, lipofibroma, fibrolipoma of the nerve).

Ultrasound evaluation, in addition to clinical evaluation and anamnestic data, may differentiate neoplastic masses from other peripheral nerve syndromes, and, secondarily, it may discriminate between intrinsic and extrinsic nerve tumors. It may contribute to the surgical planning, assessing the extent of the disease, and could represent a guidance for the biopsy of the mass.

It may not always be possible to differentiate between schwannomas, neurofibromas, and malignant transformation, despite some slight but distinct different features.

Peripheral nerve sheath tumors derive from Schwann cells. On ultrasound evaluation, a well-defined ovoid solid hypoechoic mass, in direct continuity with a nerve at its proximal and distal poles, is depicted. Schwannomas are eccentric to the axis of the nerve with some nerve fascicles seen separately (they may even develop from an individual fascicle) and posterior acoustic enhancement; often the proximal nerve portion, which enters into the tumor, could have a thickened hypoechoic appearance with loss of the typical fascicular pattern. Occasionally, a myxoid matrix may develop within the tumor giving the mass a cystic appearance. Rarely some calcifications may be depicted into the mass.

Neurofibromas are spindle-shaped with loss of normal fascicular pattern. They appear as fusiform hypoechoic masses in continuity with nerve contours; as they grow, they may spread into the surrounding tissues. They are subdivided into three types: a more common localized form (accounting for approximately 90% of cases), a diffuse form involving the skin and the subcutaneous tissue, and a plexiform form associated with type 1 neurofibromatosis.

At color or power Doppler evaluation, nerve sheath tumors have a hypervascular pattern; in particular, schwannomas are extremely vascularized, while neurofibromas are less.

Sudden increase in the size of a nodule, ill-defined margins, and absence of cleavage from the surrounding tissue represent signs of malignant transformation and indicate the need for immediate biopsy, especially in the case of type I neurofibromatosis (Fig. 3.4).

Intraneural ganglia are relatively rare entities, affecting most frequently the common peroneal nerve at the level where the small recurrent branch of the deep peroneal nerve courses around the fibular neck, serving as a conduit for synovial fluid to pass from the tibiofibular joint into the nerve. At ultrasound examination, they appear as anechoic cystic masses contained within the nerve sheath.

Nerve hemangiomas are extremely rare, mostly identified in children and young patients, with a predilection for the median nerve because of the presence of a persistent median artery. US depicts a swollen nerve with fluid intraneural, compressible, anechoic structures separating the fascicles; color and power Doppler imaging show slow-flowing blood within them.

Lymphomas affect peripheral nerves in rare cases, especially as the result of direct spread from adjacent tumors or as a paraneoplastic involvement. US reveals a heterogeneous hypoechoic mass with thickening and distortion of the nervous fascicular pattern.

Fibrolipomatous hamartoma is a benign proliferation of mature adipocytes between axons, with a strong predilection for the median nerve. It presents with a pathognomonic cable-like US appearance, reflecting the morphology of the lesion, with fusiform swelling of the nerve and hyperechoic adipose tissue interposed between hypoechoic preserved normal fascicles.

Morton's neuromas are tumor-like masses, which develop as a result of perineural fibrosis and thickening of plantar digital nerves caused by the chronic rubbing of the nerve in a narrowed web space. They are associated with chronic microtrauma and have a typical location at the II and III web spaces at the level of the metatarsal heads.

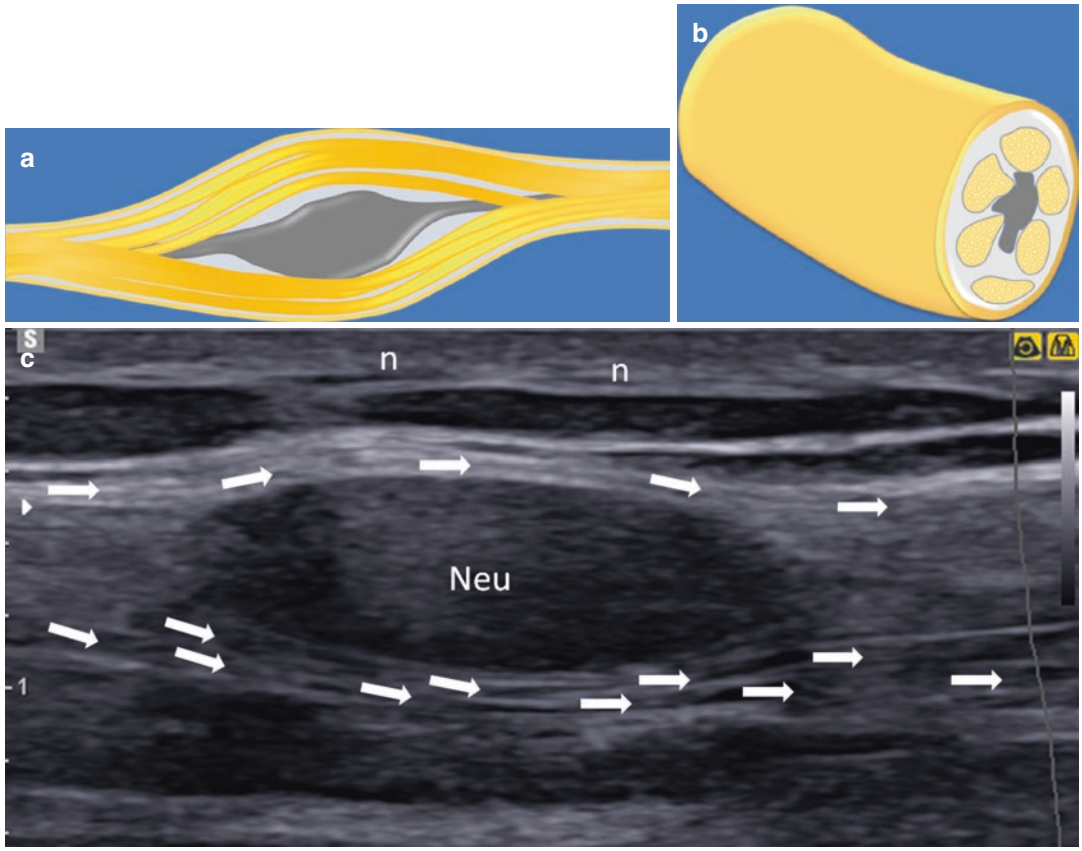

Fig. 3.4 Neurofibroma. (**a**) Long axis view; central neurofibroma (Neu) in continuity with a nerve bundle; nerve bundles (arrows). (**b**, **c**) Anatomical schemes

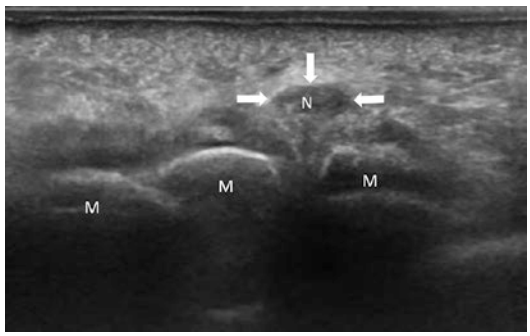

Fig. 3.5 Morton's neuroma. Axial scan of foot of plantar aspect at the metatarsal heads level: neuroma (N, arrows), metatarsal heads (M)

At US evaluation, Morton's neuroma appears as a hypoechoic lesion replacing the normal hyperechoic fat in the web space, often associated with intermetatarsal bursitis; performing the Mulder's clinical test during US examination increases diagnostic confidence (Fig. 3.5).

Suggested Readings

Bianchi S, Martinoli C. Ultrasound of the musculoskeletal system. Berlin, Germany: Springer-Verlag; 2007.

Brown JM, Yablon CM, Morag Y, Brandon CJ, Jacobson JA. US of the peripheral nerves of the upper extremity: a landmark approach. Radiographics. 2016;36(2):452–63.

Chiou HJ, Chou YH, Chiou SY, Liu JB, Chang CY. Peripheral nerve lesions: role of high-resolution US. Radiographics. 2003;23(6):e15.

Jacobson JA, Wilson TJ, Yang LJ. Sonography of common peripheral nerve disorders with clinical correlation. J Ultrasound Med. 2016;35(4):683–93.

Peer S, Bodner G. High-resolution sonography of the peripheral nervous system. Berlin: Springer-Verlag; 2007.

Yablon CM, Hammer MR, Morag Y, Brandon CJ, Fessell DP, Jacobson JA. US of the peripheral nerves of the lower extremity: a landmark approach. Radiographics. 2016;36(2):464–78.

Nerve Entrapment Syndromes

4

Filomena Puntillo and Laura Bertini

4.1 Physiopathologic Findings

4.1.1 Definition

Entrapment neuropathy (EN) is the most frequent mononeuropathy encountered in clinical practice. It is defined as a pressure-induced injury to a peripheral nerve usually by fibrous bands and ligaments at the level of fibro-osseous canals where the nerve runs. EN can be also due to soft tissue tumors (lipoma or fibroma), cysts, vascular changes (aneurysm, anatomic variants), or bony spurs.

4.1.2 Pathophysiology

Nerve entrapment syndromes share a unique common pathophysiology and pathogenesis. Mechanisms of nerve injury include direct pressure, repetitive microtrauma, and stretching or compression-induced ischemia. As a matter of fact, EN can be acute, caused by trauma, or chronic due to overuse with dynamic compression or to a space-occupying lesion.

Risk factors for EN include a superficial position of the nerve, a long course through an area at high risk of trauma, and a narrow path through a bony canal. Also metabolic diseases, such as diabetes, are risk factors for EN.

Mechanical forces on the nerve can result in block of venous outflow, which leads to hyperemia and edema of the nerve. The obstruction of venous outflow may cause blood accumulation and increased pressure in the region of entrapment, which results in decreased arterial supply by the vasa nervorum followed by ischemia of the nerve. The blood-nerve barrier breaks and dysfunction of the intraneural circulation occurs. At this point, injury can be reversible with treatment, but as ischemia persists, the damage of the myelin sheath and axonal disruption results in irreversible nerve damage with epineural fibrosis and thickening of the nerve.

Nerve injuries can be classified in three categories: neurapraxia, axonotmesis, and neurotmesis. Neurapraxia consists in a focal damage of the myelin fibers around the axon sparing the axon and the connective tissue sheath. Axonotmesis, more severe, involves injury to the axon itself; regeneration of the nerve is possible even if usually with no complete recovery. Neurotmesis involves complete disruption of the axon, with little likelihood of normal regrowth or clinical

F. Puntillo (✉)
Assistant Professor of Anaesthesia and Pain Therapy, Department of Emergency and Organ Transplantation, University of Bari, Bari, Italy
e-mail: filomena.puntillo@uniba.it

L. Bertini
Anaethesia and Pain Unit, Santa Caterina Hospital, Rome, Italy

E. Silvestri et al. (eds.), *Ultrasound-Guided Peripheral Nerve Blocks*,
https://doi.org/10.1007/978-3-319-71020-4_4

recovery. The later consequence is function impairment with altered conduction of the impulse distally to the compression site and neuropathic pain.

4.2 Clinical and Sonographic Considerations

Peripheral entrapment neuropathies usually present with pain, numbness, tingling, weakness, and muscle wasting with a peripheral nerve distribution.

Accurate diagnosis is paramount, as these presentations can be very similar to radiculopathy or systemic neuropathy. Clinical evaluation of signs and symptoms is helpful to understand the nerves commonly involved and to localize the site of pathology; neurophysiological and/or radiographic studies can confirm it.

Nerve conduction velocity (NCV) studies assess the integrity of sensory and motor nerves: areas of nerve injury or demyelination appear as slowing of conduction velocity along the nerve segment in question. Electromyography (EMG) records the electrical activity of a muscle looking for signs of denervation. The combination of NCV studies and EMG can help distinguish peripheral from central nerve injuries.

Magnetic resonance imaging (MRI) already plays an important role in the diagnosis of peripheral nerve disorders such as in trauma and tumors, but with improved nerve visualization, this modality can play an even larger role in entrapments. Indirect signs of chronic nerve injury may be abnormal signal patterns on MRI, of the muscles involved. A normal MRI finding does not rule out nerve injury. Newer techniques, such as gadofluorine M-enhanced MRI, may ultimately be able to assess nerve regeneration.

High-resolution ultrasound (US) is playing an increasingly important role in the study of the nerves thanks to several advantages over MRI:

- Lower costs and widespread availability.
- Superior spatial resolution compared to MRI.
- Faster examination using axial scans (elevator technique).
- Dynamic and comparative studies.
- The patients can be studied in the standing position.
- Positive US Tinel sign can be detected using the probe.
- Color/power Doppler US, particularly useful in patients with vascular disorders.

However, unlike MRI, US imaging cannot detect muscle edema caused by denervation. Diagnosis of atrophy and fatty infiltration of the muscles is more difficult on US than MRI. Furthermore, although ultrasonography is a noninvasive and less expensive modality to define anatomic entrapment, its use is limited by lack of standardization of technique and interpretation.

Nonetheless high-resolution ultrasonography (US), with high-frequency transducers (7–18 MHz or more), can satisfactorily depict subtle details of the peripheral nerves (fascicles, epineurium, and perineurium). It is capable of depicting real-time static and dynamic morphological alteration concerning the peripheral nerves and their surrounding tissues. Ultrasound can be precious for the diagnosis also because it is the only exam that can be done dynamically (during arm movement). Ultrasound is more versatile so multiple nerve segments can be imaged in one examination. It also allows quick comparison to the contralateral nerve and dynamic capability to view nerve subluxation or impingement in real time.

The most common US finding of compression neuropathies concern fibrillar echotexture alterations and nerve thickness modifications, both due to the edema, inflammation with hypervascularization, secondary remyelination, and fibrosis. The structural changes of entrapped nerves include a hypoechoic appearance with the normal striated neuronal structure rarefied or completely lost (Fig. 4.1a, b).

The nerve thickness alterations include a fusiform swelling (pseudoneuroma) above the site of the entrapment (2–4 cm) and an abrupt flattening at point of compression (Fig. 4.2). Reduced mobility can be replicated on dynamic imaging. Because nerve enlargement is the most important diagnostic

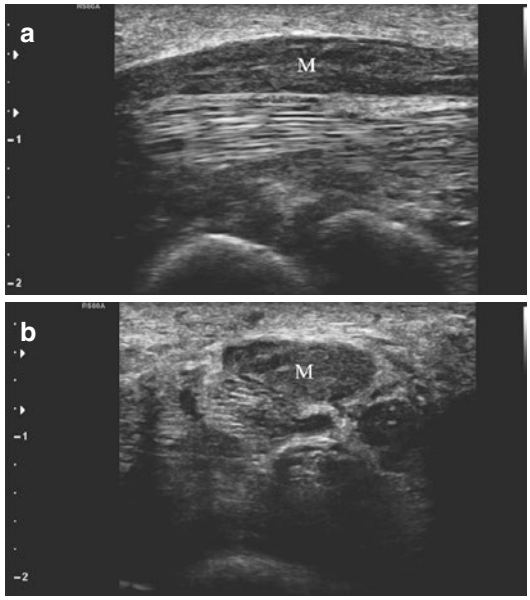

Fig. 4.1 Patient with nerve conduction studies and surgically proven carpal tunnel syndrome. Sonogram in sagittal (**a**) and coronal (**b**) plane reveals significative alterations of fibrillar echotexture and inhomogeneously decreased echogenicity. *M* median nerve

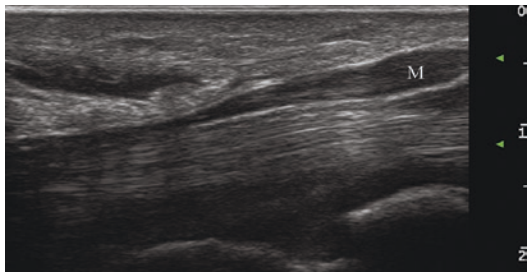

Fig. 4.2 Longitudinal view of the median nerve showing relevant enlargement as it enters the carpal tunnel and distal flattening in patient with CTS. *M* median nerve

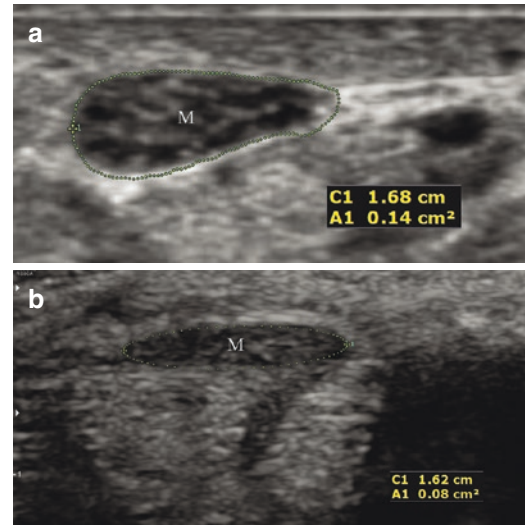

Fig. 4.3 Carpal tunnel syndrome. (**a**) Proximal transverse sonogram of carpal tunnel showing thickened median nerve (outlined). The CSA is 14 mm2. (**b**) Distal transverse sonogram reveals a flattened median nerve (outlined). *M* median nerve

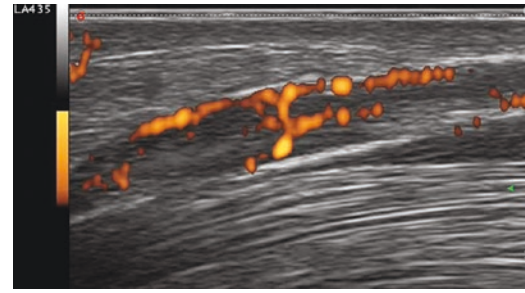

Fig. 4.4 Carpal tunnel syndrome in same patient as in Fig. 4.2. The power Doppler sonogram at carpal tunnel inlet reveals intraneural abnormal vasculature

marker of an abnormal nerve, quantification of nerve size is essential. The maximum cross-sectional area (CSA) and swelling ratio allow the quantitative assessment of nerve thickening and can be measured on transverse images. The CSA is measured by tracing along the hyperechoic rim of the nerve using the continuous trace function on the ultrasound device (Fig. 4.3a, b). The swelling ratio is the ratio between the cross-sectional area of the nerve at the site of maximal enlargement (CSA) and that at an unaffected site. Another potentially useful parameter for evaluating focal nerve compression is the flattening ratio, which is defined as the ratio between the largest and smallest diameters of nerves. The diameter of the fusiform nerve swelling can be measured on longitudinal images. For correct measurement, the transducer should be held perpendicular to the nerve, with minimal pressure. The nerve returns to normal size after entrapment area.

Someone argues that Doppler sonography may be more sensitive than other techniques in diagnosing EN especially during the early stages, showing intraneural hypervascularization (Fig. 4.4).

In fact, intraneural vascularity has been proposed as an additional diagnostic parameter in patients with carpal tunnel syndrome (CTS) and can increase sensitivity and specificity compared with measurements of cross-sectional area alone.

Finally, ultrasound can guide conservative therapy with nerve blocks.

Surgical decompression is indicated in case of intractable pain or progressive neurologic deficit.

4.3 Entrapment Syndromes: The Upper Limb

4.3.1 Brachial Plexus Injuries

Landmarks:
The brachial plexus originates from the ventral primary rami of spinal nerves C5–T1 and provides sensory and motor innervation to the upper limb.

C5 and C6 rami unite near the medial border of the middle scalene muscle to form the superior trunk of the plexus.

C7 ramus becomes the middle trunk.

C8 and T1 rami unite to form the inferior trunk.

At the lateral border of the first rib, the three trunks divide into anterior and posterior divisions.

The posterior divisions of all three trunks form the posterior cord.

The anterior divisions of the superior and middle trunks form the lateral cord of the plexus.

The anterior division of the inferior trunk forms the medial cord.

The three cords divide and give rise to the terminal branches of the plexus.

The lateral cord contributes the musculocutaneous nerve and the lateral component of the median nerve.

The posterior cord gives rise to the radial and axillary nerves.

The medial cord contributes the ulnar nerve and the medial component of the median nerve.

Roots, trunks, divisions, cords, and terminal branches of the brachial plexus are shown in Fig. 4.5.

Figure 4.6 shows the upper limb cutaneous innervation of the brachial plexus' terminal branches, while Fig. 4.7 shows upper limb dermatomes.

Brachial plexus injury is common after a trauma involving the spine or the shoulder. Risk factors for injury/entrapment are stretch injury at neck and shoulder regions with traction in abduction.

The classic presentation is acute onset of paresthesias in the upper arm with weakness in many movements of the shoulder or upper arm.

A circumferential pattern of paresthesias is the landmark of brachial plexus injury, while an individual nerve root injury shows a dermatomal anesthesia or paresthesia.

Brachial plexus lesions can cause the following syndromes: the upper (Duchenne-Erb), the lower (Dejerine-Klumpke), the intermediate palsy, and the total type (Table 4.1). Usually a Bernard-Horner syndrome is associated to the total type brachial plexus lesion due to a lesion of

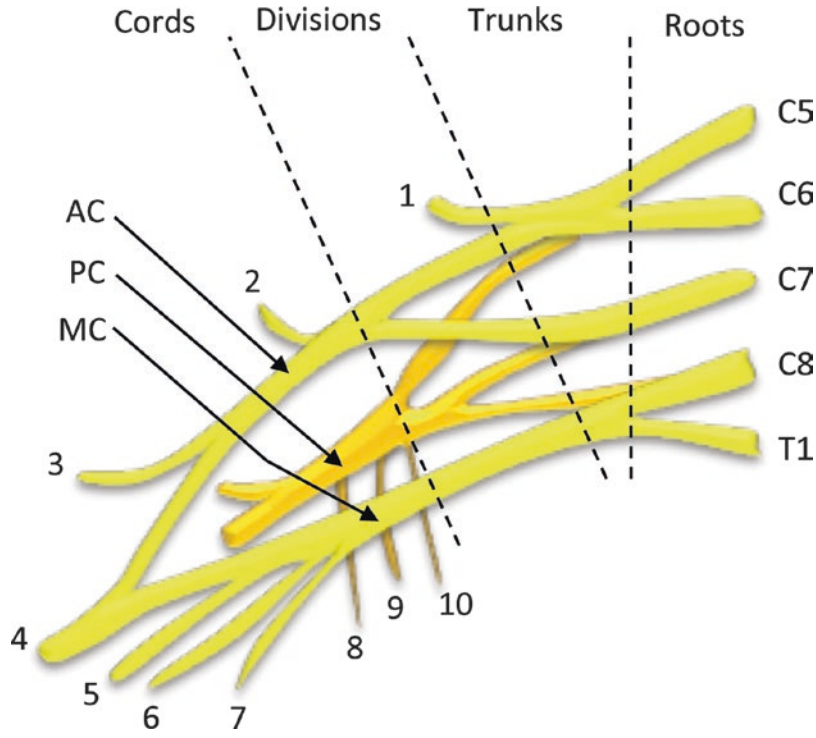

Fig. 4.5 Brachial plexus anatomy: AC lateral cord (fron anterior divisions), PC posterior cord (from posterior divisions), MC medial cord (from anterior divisions). 1 suprascapular nerve, 2 lateral pectoral nerve, 3 muscolocutaneous nerve, 4 median nerve, 5 ulnar nerve, 6 medial cutaneous nerve of the foream, 7 medial cutaneous nerve of the arm, 8 lower subscapular nerve, 9 thoraco dorsal nerve, 10 medial pectoral nerve

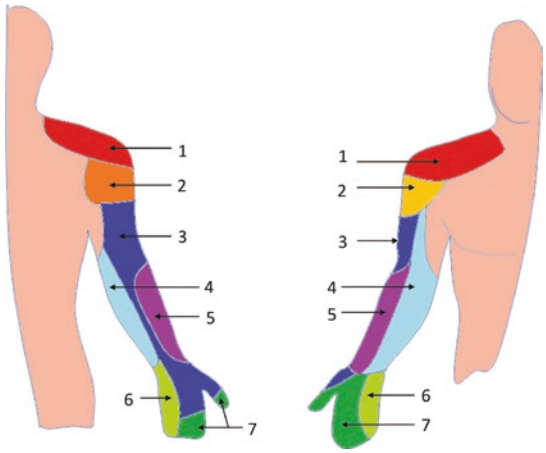

Fig. 4.6 Upper limb cutaneous innervations. 1 supraclavicular nerve, 2 axillary nerve, 3 radial nerve, 4 cutaneus medialis nerve, 5 terminal part of muscolocutaneous nerve, 6 ulnar nerve, 7 medial nerve.

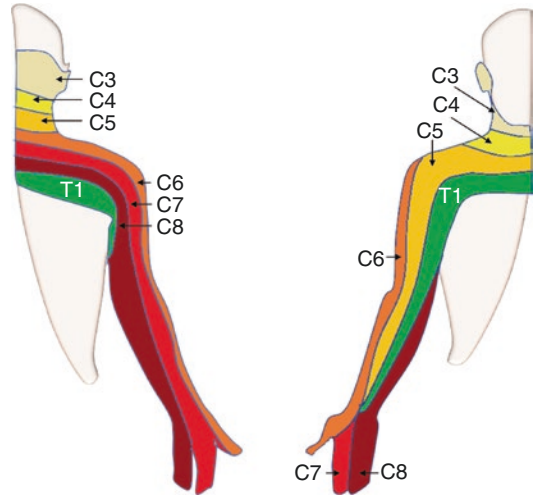

Fig. 4.7 Upper limb dermatomes

the sympathetic fibers coming from T1 to T2 and directed toward stellate ganglion.

For the diagnosis of brachial plexus injury, a systematic and comprehensive electrodiagnostic evaluation can provide the maximum precision for localization, extent of involvement, and severity of injury. EMG potentials can notice the status of individual muscles: denervated, reinnervating, etc. Imaging gives valuable information about the lesion as also about the associated injuries: MR

Table 4.1 Brachial plexus lesions

Syndrome	Level of lesion	Motor muscles	Sensory	Symptoms	Signs	Reflexes absent/ reduced
Upper trunk (Erb's palsy)	C5–C6	Infraspinatus, supraspinatus, biceps, brachialis, brachioradialis deltoid	C5–C6 dermatomes	Weakness in many movements of the shoulder and upper arm and atrophy of muscle involved	"Waiter tip position" arm adducted and internally rotated, forearm extended and pronated, the palm of the hand is facing backward and outward Hypoesthesia on the shoulder and on the radial aspect of the forearm and hand	Biceps and radio-flexor
Middle trunk (intermediate palsy)	C7	Triceps and extensor muscles of wrist and fingers	C7 dermatome	Weakness of muscle involved	Muscle atrophy and hypoesthesia on the dorsal aspect of the forearm and hand. Muscle long supinator is saved unlike the radial nerve palsy	Triceps
Lower trunk (Dejerine-Klumpke)	C8-T1	Carpal and finger flexor, intrinsic muscle of the hand	C8-T1 dermatomes	Impossibility to hand prehension movements	Attitude "en griffe" of the hand associated with hypoesthesia on the inner aspect of the arm, forearm, and hand	Radial pronator and cubital pronator

neurography is currently the most valuable tool for visualizing the plexus.

4.3.2 Thoracic Outlet Syndrome (TOS)

TOS is a controversial entrapment syndrome characterized by different neurovascular signs and symptoms due to compression of neurovascular bundle passing through the thoracic outlet, proximally or at the first rib. Compression may occur in different segments of the brachial plexus, trunks, or cords: the interscalene triangle is the most frequent. TOS is usually classified into vascular type and neurogenic type. Neurogenic TOS can be "true or classic" and "disputed or common." True neurogenic TOS is caused by structural anomalies at the base of the neck like a prominent C7 transverse process or a rudimentary cervical rib with associated fibrous bands extending to the first thoracic rib that may compress the lower roots and/or trunks of the brachial plexus. In this case, neurologic symptoms are typically confined to the anatomic distribution of the C8 and T1 spinal nerves. Instead, in disputed neurogenic TOS, the pain may or may not follow a confined dermatomal pattern.

EMG and NCV studies are most useful for the diagnosis of true neurogenic TOS, while in disputed neurogenic TOS, electrophysiological studies are usually normal.

US is unable to show nerve changes at the costoclavicular space. MRI may occasionally depict fibrous bands causing nerve distortion or compression.

4.3.3 Axillary Nerve: Quadrilateral Space Syndrome

Anatomy (Fig. 4.8): The axillary nerve arises from brachial plexus and passes inferiorly to the shoulder joint, exiting the axilla through the quadrangular space, with the posterior circum-

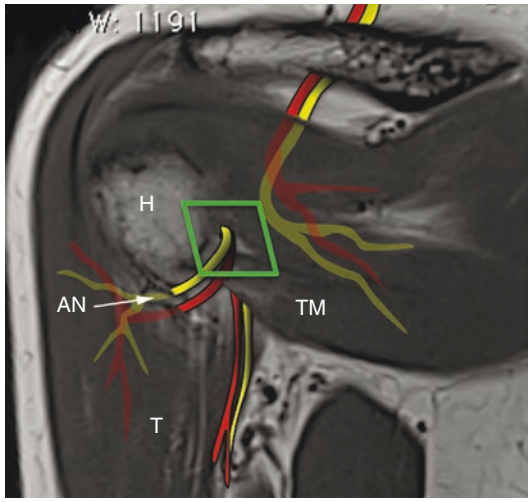

Fig. 4.8 Quadrilateral space (green square). TM teres minor muscle, T triceps, AN Axillary nerve, H humerus

flex humeral artery. It gives off anterior, posterior, and articular terminal branches.

Quadrilateral space syndrome: Involves compression of the axillary nerve and/or the posterior circumflex artery within the quadrilateral space. This space is defined by the teres minor muscle superiorly, the long head of the triceps brachii muscle medially, the humerus laterally, and the teres major inferiorly (Fig. 4.8).

Function: *Motor*, deltoid muscle by the anterior branch and teres minor muscle by the posterior one. *Sensory*, skin of lower half of the deltoid.

Risk factor for injury/entrapment: Shoulder dislocation, proximal humeral fractures, repetitive overload activities with extreme abduction, and arthroscopy or rotator cuff repair.

Symptoms: Weakness with overhead activity is the typical symptom. Pain is usually dull, burning, or described as a deep ache localized to the lateral and posterior portion of the shoulder. It usually is worsened with activity. There may be associated paresthesias of the lateral and posterior upper arm.

Signs: Weak lateral abduction and external rotation of the arm.

Strumental studies: Plain radiographs can be sought to evaluate for fractures and confirm reduction. EMG/NCV studies are helpful to confirm the diagnosis and stage severity and recovery. MRI and US may demonstrate a space-occupying lesion in the quadrilateral space or show signal alteration or atrophy of the teres minor or deltoid.

4.3.4 Long Thoracic Nerve

Anatomy: It is a long nerve (20–22 cm) that emerges from C5 to C7 and travels subcutaneously along the chest wall to innervate the serratus anterior muscle.

Function: *Motor*, serratus anterior muscle. *Sensory*, none.

Risk factor for injury/entrapment: Prolonged compression (backpackers' palsy), a sudden upper extremity traction, or activities that involve chronic repetitive traction on the nerve. LTN palsy has been seen in archery, bodybuilding, tennis, swimming, and baseball players.

Symptoms: Diffuse shoulder or neck pain that worsens with overhead activities.

Signs: Scapular winging and weakness with forward elevation of the arm.

Strumental studies: NCV studies can be challenging, but EMG is generally helpful in detecting problems in the serratus anterior. Plain films may be helpful to look for a cervical rib.

4.3.5 Spinal Accessory Nerve

Anatomy: After leaving the jugular foramen, the nerve has a subcutaneous course until reaching the trapezius muscle.

Function: *Motor*, trapezius muscle. *Sensory*, none.

Risk factor for injury/entrapment: Trapezius trauma or shoulder dislocation. Radical neck dissection, carotid endarterectomy, and cervical node biopsy.

Symptoms: Generalized shoulder pain and weakness.

Signs: Asymmetry of the shoulders with a drooping shoulder and neckline asymmetry for

atrophy of the trapezius. Associated weakness of forward arm elevation above the horizontal plane is common.

There may be a winging of the scapula. Classically there is no winging with forward flexion, differentiating it from a long thoracic nerve (LTN) injury.

Strumental studies: EMG is helpful to confirm the diagnosis of trapezius dysfunction. Imaging is useful not helpful.

4.3.6 Suprascapular Nerve

Anatomy: After branching from the brachial plexus, the suprascapular nerve accompanies the suprascapular artery and vein laterally and posteriorly deep to the trapezius muscle to the superior margin of the scapula, where it passes through the suprascapular notch inferior to the superior transverse scapular ligament to enter the supraspinous fossa.

Function: *Motor*, supraspinatus and infraspinatus muscles. *Sensory*, acromioclavicular and glenohumeral joints.

Risk factor for injury/entrapment: The suprascapular and the spinoglenoid notch are sites of nerve entrapment. Narrow notches and pathologic transverse scapular or spinoglenoid ligaments can be causes of compression. Repetitive overhead loading and shoulder pathologies; cyst formation at the suprascapular notch, from a labral tear.

Symptoms: Deep, dull, chronic pain localized usually to the superior, posterior, and lateral aspects of the shoulder. It worsens with adduction, abduction, and movements of the shoulder across the body.

Signs: Weak external rotation of the arm (infraspinatus involvement) and/or weak arm elevation, which is most pronounced in the range of 90 to 180 degrees (supraspinatus involvement).

Strumental studies: Electrodiagnostic studies can help confirm the diagnosis and differentiate other painful shoulder pathology. Suprascapular nerve injury and rotator cuff tear both lead to supraspinatus and infraspinatus weakness. Differentiating the two injuries may require MRI or US.

4.3.7 Median Nerve at the Elbow: Pronator Syndrome and AIN (Anterior Interosseous Nerve) Syndrome

Anatomy: The median nerve arises from contributions of the lateral and medial cords and travels with the brachial artery and vein in the medial aspect of the arm.

At antecubital fossa, the median nerve continues between the heads of the pronator teres before it dives deep to the fibrous arch of the flexor digitorum superficialis (FDS) muscle origin. At this point, the AIN branches off, whereas the rest of the median nerve continues deep to the FDS muscle toward the carpal tunnel.

Function: *Motor*, muscles of the superficial forearm compartment, which include the pronator teres, the palmaris longus, the flexor digitorum superficialis (FDS), and the flexor carpi radialis.

AIN provides motor innervation to the flexor pollicis longus (FPL), the FDP of the index and the long fingers, and the pronator quadratus. *Sensory*, the inner face of the hand, thenar eminence, and first three fingers and the medial aspect of the ring finger. AIN has no cutaneous sensory component.

Risk factor for injury/entrapment: Potential entrapment sites of the median nerve in the forearm include Struthers' ligament, the biceps brachii aponeurosis (lacertus fibrosus), and the FDS aponeurotic arch (Figs. 4.9 and 4.10).

The pronator syndrome is an entrapment disorder in which the median nerve is compressed between the superficial and deep heads of the pronator teres muscle. The AIN syndrome is a compression of the motor branch of the median nerve. Compression may occur at the FDS origin and flexor carpi radialis origin or by an accessory head of the FPL (Gantzer's muscle). The AIN syndrome is purely motor, so there is no sensory loss.

Symptoms: Proximal volar forearm pain with numbness and/or paresthesias in the distribution of the median nerve in the hand. Sensory loss over the thenar eminence may help distinguish pronator syndrome from carpal tunnel syndrome (CTS) and from AIN syndrome because the pal-

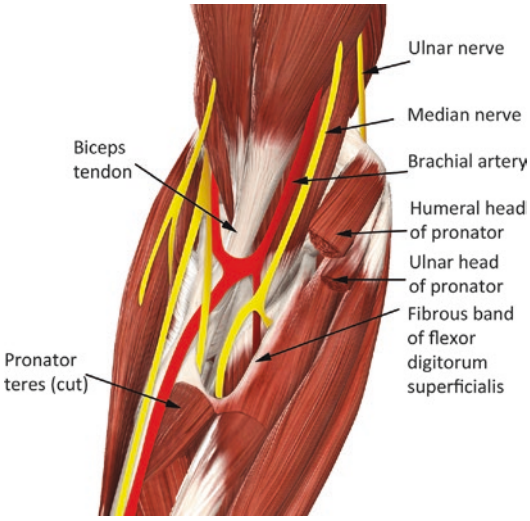

Fig. 4.10 Illustration showing the median nerve passing deep to the fibrous arch of the flexor digitorum superficialis, which is a potential site of compression

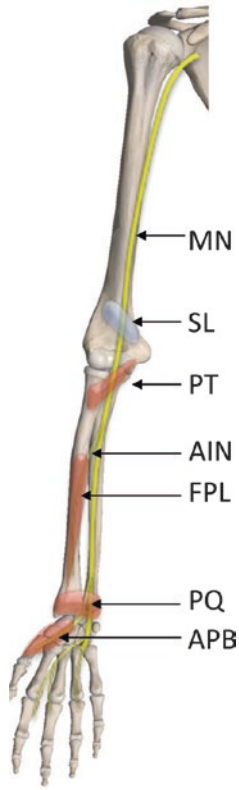

Fig. 4.9 Illustration showing the median innervated muscles and potential sites of compression, which include the ligament of Struthers SL (if present) and the pronator teres *PT*, *MN* Median Nerve, *AIN* Anterior Interosseus Nerve, *FPL* Fllexor pollicis longus, *PQ* Pronator Quadratus, *APB* Abductor Pollicis Brevis

mar cutaneous branch arises proximal to the carpal tunnel.

Signs: Weak wrist flexion, no interphalangeal flexion of the thumb, index, and long digit. The patient is unable to make the OK sign and may have tenderness over the pronator teres muscle. The Tinel sign over the wrist or a Phalen sign is not present as well as nocturnal component of pain.

Strumental studies: Seldom detectable using electrophysiological techniques, EMG may demonstrate abnormality in the flexor carpi radialis, pronator teres, or any other median innervated musculature. US and MR imaging of the median nerve within the pronator teres muscle are typically not helpful unless the nerve is significantly thickened.

4.3.8 Ulnar Nerve at the Elbow: Cubital Tunnel Syndrome

Cubital tunnel syndrome is the second most common entrapment neuropathy, after carpal tunnel syndrome. It is caused by compression and traction of the ulnar nerve.

Anatomy (Fig. 4.11): After arising from the brachial plexus, the ulnar nerve descends in the arm on the medial side, and then, just above medial epicondyle, it passes to the posterior compartment and into a osteofibrous canal, the cubital tunnel. Distal to the condylar groove, the ulnar nerve enters in a tunnel formed between the ulnar and humeral heads of the flexor carpi ulnaris muscle, the Guyon canal, which is connected by the arcuate ligament and travels alongside the

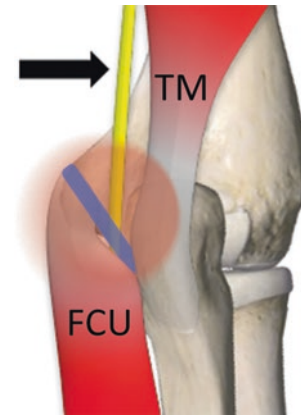

Fig. 4.11 Posterior vision of the elbow where the ulnar nerve (black arrow) can be entrapped in the cubital tunnel. *TM* triceps muscle, *FCU* flexor carpi ulnaris muscle

ulna. Finally, it splits into deep (motor) and superficial (sensory) branches.

Function: *Motor*, in the forearm, it serves the flexor carpi ulnaris and the flexor digitorum profundus. It innervates the muscles of the hand (apart from the thenar muscles and two lateral lumbricals), flexor carpi ulnaris, and medial half of flexor digitorum profundus. *Sensory*, ulnar side of forearm and ulnar digits.

Risk factors for injury/entrapment: It can occur in baseball, football, bodybuilding, and wrestling. Compression can occur at the arcade of Struthers (present in 70% of patients), medial intermuscular septum, medial epicondyle, cubital tunnel, anconeus, and fibrous bands in the flexor carpi ulnaris.

Symptoms: Nocturnal paresthesias of the fourth and fifth digits. There may be elbow pain radiating to the hand, and symptoms may be worse with prolonged or repetitive elbow flexion. Paresthesias precede clinical examination findings of sensory loss.

Signs: Weakness may occur, but is a late symptom. When present, motor findings are weak digit abduction, weak thumb abduction, and weak thumb-index finger pinch. The Wartenberg sign is the inability to fully adduct the small finger with the finger held slightly abducted and extended. With Froment sign, patients are asked to perform a pinch, with a positive test being flexion of the interphalangeal joint of the thumb to compensate for weakness of the adductor pollicis by using the FPL (median nerve innervated).

Stumental studies: Electrodiagnostic testing is usually very helpful. EMG and NCS can be used to determine the precise site of the neuropathy and confirm localization.

4.3.9 Radial Nerve at the Elbow: Radial Tunnel and Posterior Interosseous Nerve Syndromes

Anatomy (Fig. 4.12): The radial nerve goes down in the posterior arm until it circles toward the anterior arm at spiral groove of the humerus and

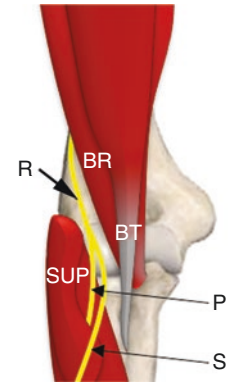

Fig. 4.12 Illustration showing the radial nerve and posterior interosseous nerve. The radial nerve R lies lateral to the brachialis muscle BR and then divides into its terminal branches, the posterior interosseous nerve P and the superficial sensory branch S. The posterior interosseous nerve passes between the bellies of the supinator muscle SUP, reaching the posterior compartment of the elbow

enters radial tunnel just above the lateral epicondyle. The radial nerve divides into a superficial branch (sensory only) and a deep branch (posterior interosseous nerve, PIN) at the lateral elbow. The PIN is the terminal motor branch of the radial nerve.

Function: *Motor*, it innervates the triceps brachii (extends at the elbow) and the majority of the extensor muscles in the forearm (extends the wrist and fingers and supinates the forearm).

Sensory, it innervates most of the skin of the posterior side of the forearm and the dorsal surface of the lateral side of the palm and lateral three and a half digits.

Risk factors for injury/entrapment: Radial nerve can be compressed in the radial tunnel (radial tunnel syndrome, RTS), a potential space located anterior to the proximal radius, or at the elbow, the arcade of Frohse, the medial edge of the extensor carpi radialis brevis, the radial recurrent blood vessels, and the inferior margin of the supinator muscle (PIN syndrome). PIN syndrome has been reported in tennis players, bodybuilders, swimmers, and gymnasts.

Symptoms: Forearm pain that is exacerbated by repetitive forearm pronation is the presenting symptom of radial tunnel syndrome, which involves injury to the superficial branch of the radial nerve. Symptoms of radial tunnel syn-

drome are almost identical to those of tennis elbow (i.e., lateral epicondylitis), and distinguishing the two can be difficult because physical examination maneuvers that aggravate radial tunnel syndrome may also be positive in patients with tennis elbow (e.g., supination against resistance with the elbow and wrist extended and resisted extension of the middle finger). A differentiating factor is the point of maximal tenderness. In radial tunnel syndrome, this point is over the anterior radial neck; in tennis elbow, it is at the origin of the extensor carpi radialis brevis muscle.

Signs: PIN syndrome has clear motor loss and neurodiagnostic findings. Patients present with dropped fingers and lack of thumb extension. Extensor carpi radialis longus is usually preserved (due to innervation proximal to PIN branching), so wrist extension and radial deviation will be present still.

*Stumental studie*s: Electrodiagnostic studies are frequently not helpful. NCS are usually normal. EMG can be helpful if positive for denervation changes in muscles. Posterior interosseous nerve syndrome is usually caused by compression by the tight tendinous arcade of Frohse. Researchers suggested a 15-mm cutoff value of the PIN diameter for the diagnostic criteria of PIN syndrome by comparison with a contralateral normal control. Rarely, space-occupying lesions causing PIN compression can be found with ultrasound. In addition, the sonography may reveal an echo difference of the dorsal extensor muscles caused by denervation, as compared to the contralateral side.

4.3.10 Median Nerve at the Wrist: Carpal Tunnel Syndrome

Carpal tunnel syndrome is the most common nerve entrapment injury in the normal population as well as sports. Incidence rates are very high in wheelchair athletes, in cyclists, in wrestlers, and in football from blocking technique.

Risk factors for injury/entrapment: It is due to compression of the median nerve, which is deep into the transverse retinacular ligament.

Symptoms: Paresthesias and pain of the thumb, index digit, and long digit (sparing the thenar eminence). The paresthesias are worsened usually at night. Some patients also have forearm pain.

Sign: The sensory examination is normal initially, although late findings include sensory loss in the median nerve distribution. Phalen sign (symptom reproduction with bilateral wrist flexion) and Tinel sign at the wrist have been used as physical examination findings for diagnosing CTS, with Phalen's being the most reliable clinical test. Later in the disease course, there may be thenar atrophy and weakness of the grip or pinch.

*Stumental studie*s: Electrodiagnostic testing can be useful and quantitates the severity of entrapment, although false negatives and false positives may occur.

Based on the electrophysiological studies, the wrists were classified into one of the five stages of severity:

1. Minimal CTS, abnormal comparative test
2. Mild CTS, slowing of median digit-wrist segment, and normal distal motor latency (DML)
3. Moderate CTS, slowing of median digit-wrist segment, and abnormal DML
4. Severe CTS, the absence of median SNAPs (digit-wrist segment), and abnormal DML
5. Extreme CTS, the absence of thenar motor (and sensory) response

The most common ultrasound finding of carpal tunnel syndrome is the swelling of the median nerve, and this is usually most prominent at the scaphoid-pisiform level. By using the ellipse formula, the most appropriate cutoff value of the median nerve cross-sectional area ranges between 9 and 10 mm^2 at the scaphoid-pisiform level as the diagnostic criteria of carpal tunnel syndrome with acceptable sensitivity and specificity.

4.3.11 Ulnar Nerve at the Wrist: Cyclist's Palsy

Ulnar tunnel syndrome refers to compression of the ulnar nerve in Guyon canal at the level of the wrist. Guyon canal is bordered by the volar carpal liga-

ment, by the transverse retinacular ligament, by pisiform, and laterally by the hook of the hamate. In sports, it is most seen commonly in cyclists.

Risk factors for injury/entrapment: Compression may occur from space-occupying lesions such as ganglion cysts, hook of the hamate and pisiform fractures, ulnar artery aneurysms, and deviant hypothenar muscles.

Symptoms: Presentation may include pure motor, sensory, or mixed findings, depending on the area of compression. Proximal compression before any nerve bifurcation causes motor weakness of ulnar innervated intrinsic muscles and sensory deficits over the hypothenar eminence and small and ring finger. Compression deep in Guyon canal causes pure muscle weakness, as the superficial sensory branch is spared. Pure sensory symptoms occur from compression of the superficial branch of the ulnar nerve.

Signs: Examination should include good motor testing, paying attention to intrinsic muscles, and any potential atrophy, as well as a good sensory examination. Tinel and Phalen tests are used often as provocative tests, but their effectiveness has not been verified. The inability to cross fingers or abducted positioning of the little finger, which is known as the Wartenberg sign, suggests motor branch involvement. Attempted pinch between the thumb and the index finger may lead to compensatory thumb interphalangeal flexion (Froment sign) and, occasionally, hyperextension of the thumb metacarpophalangeal joint (Jeanne sign), which occur secondary to paralysis of the adductor pollicis muscle.

Stumental studies: EMG can be helpful for confirmation and localization of the area of compression. Ultrasound can identify the cause of Guyon's canal syndrome and the morphologic change of the ulnar nerve.

4.3.12 Radial Nerve at the Wrist: Handcuff Neuropathy

The superficial branch of the radial nerve crosses the volar wrist on top of the flexor retinaculum of the carpal tunnel.

Risk factors for injury/entrapment: It is vulnerable to compression by anything wound tightly around the wrist. Historically, this is an area easily injured by tight handcuffs, thus the name "handcuff neuropathy."

Symptoms: Numbness on the back of the hand, mostly on the radial side.

Sign: Decreased sensation to soft touch and pinprick over the dorsoradial hand, dorsal thumb, and index digit. Motor function is typically intact.

4.4 Entrapment Syndromes: The Lower Limb

4.4.1 Lower Limb Cutaneous Innervation

Lower limb cutaneous innervation origins from lumbar plexus nerve branches (Figs. 4.13 and 4.14).

4.4.2 Lateral Femoral Cutaneous Nerve

4.4.2.1 Meralgia Paresthetica

Anatomy (Fig. 4.15): Lateral femoral cutaneous nerve (LFCN) arises from the L2 and L3 spinal nerve roots, travels downward lateral to the psoas muscle, and then crosses the iliacus muscle. Close to the anterior superior iliac spine (ASIS), the nerve courses in contact with the lateral aspect of the inguinal ligament.

Function: LFCN is a purely sensory nerve. It innervates the skin on the lateral part of the thigh.

Risk factor for entrapment: Entrapment of the lateral femoral cutaneous nerve as it passes under the inguinal ligament (Fig. 4.15). The most frequent associated conditions are obesity, diabetes mellitus, older age, tight belts or garments around the waist, scar tissue near the lateral aspect of the inguinal ligament, and pregnancy.

Symptoms: Paresthesia, numbness, burning sensation, dysesthesia, and pain over the anterolateral aspects of the thigh. These complaints may be worsened by walking or prolonged standing and typically disappear after weight loss, abdominal muscle strengthening, or elimination of the underlying cause.

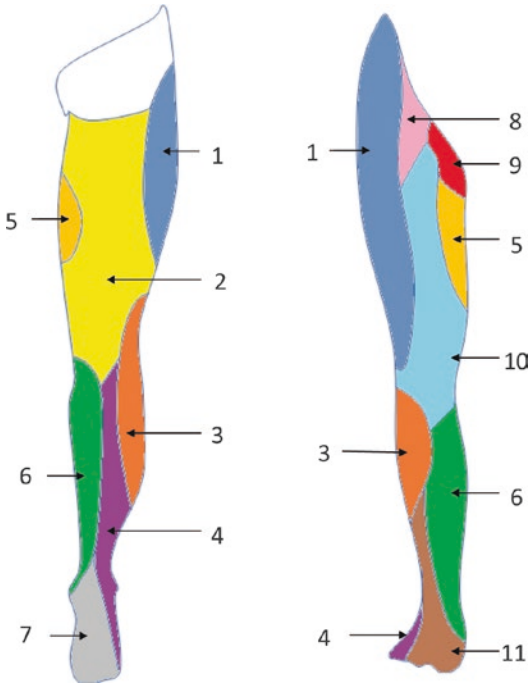

Fig. 4.13 Lower limb cutaneous innervations. 1 lateral femoral cutaneous nerve, 2 posterior femoral cutaneous nerve, 3 common peroneal nerve, 4 sural nerve, 5 obturator nerve, 6 saphenous nerve, 7 tibial posterior nerve, 8 genito femoral nerve, 9 ileoinguinal nerve, 10 anterior femoral cutaneous nerve, 11 superficial peroneal nerve

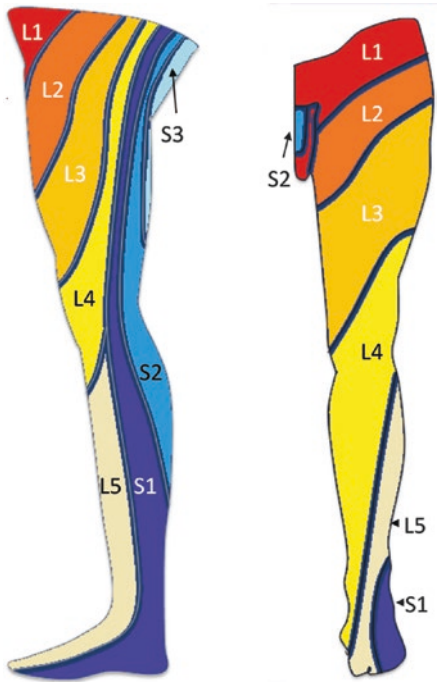

Fig. 4.14 Lower limb dermatomes

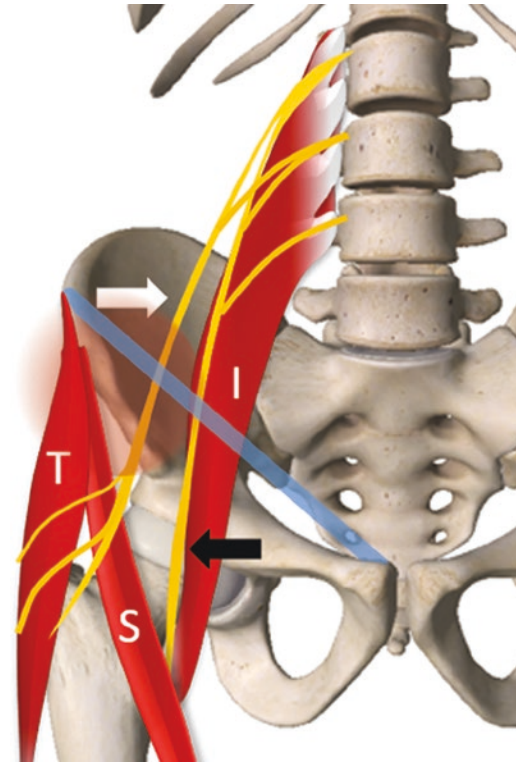

Fig. 4.15 The lateral femoral cutaneous nerve (white arrow) can be entrapped by the inguinal ligament (in blue). *I* iliopsoas muscle, *S* sartorius muscle, *T* tensor fasciae latae muscle. Black arrow: femoral nerve

Sign: Sensory changes in the nerve distribution.

Strumental studies: MP is often diagnosed using neurophysiological studies such as somatosensory evoked potentials (81.3% sensitivity) and sensory nerve conduction (65.2% sensitivity). But there are limitations to nerve conduction studies examining the LCNT. One limitation is increased adipose tissue which makes this type of study difficult to perform.

4.4.3 Iliohypogastric Nerve

Anatomy: Iliohypogastric nerve (IHN) originates from the T12 to L2 spinal nerve roots and emerges from the lateral border of the psoas major muscle traveling anteriorly to the rectus border and emerging superficially at a point about 2–3 cm medial to the anterior superior iliac spine.

Function: It supplies the skin over the abdomen and inguinal region. The motor portion of

the nerve innervates the lowest portions of the transverse abdominis and internal oblique muscles.

Risk factor for entrapment: The IHN is commonly trapped at the rectus border, the iliac crest, and the paravertebral area or after open and laparoscopic surgery, primarily hernia repairs and Pfannenstiel incisions.

Symptoms: Depending on the location of the entrapment, the clinical picture may vary, often pain originating in the iliac fossa and radiating into the ipsilateral groin and anteromedial thigh, sometimes accompanied by sensory changes such as dysesthesia or hypoesthesia in the nerve distribution.

Sign: Sensory changes in nerve distribution.

Strumental studies: MRI and electrodiagnostic studies are not useful.

4.4.4 Obturator Nerve

Anatomy (Fig. 4.16): The obturator nerve is formed from the L2 to 4 nerve roots. It forms within the psoas and runs anterior to the sacroiliac joint. The nerve then passes into the obturator foramen and it divided into the anterior branch of the obturator nerve traveling in the inguinal region, placed between the pectineus muscle and the adductor longus and brevis and posterior one.

Function: Anterior branch supplies the adductor longus, adductor brevis, and gracilis muscles and the medial aspect of the thigh. Posterior branch supplies the external obturator muscle and the adductor magnus muscle and the knee capsule, cruciate ligaments, and synovial membranes.

Risk factor for entrapment: Prolonged, acute hip flexion (urologic and gynecologic surgery), fascial entrapment of the obturator in the adductor compartment induced by exercise.

Symptoms: Paresthesias, sensory loss, or pain, from the hip to the knee along the medial aspect of the thigh (and occasionally to the calf); sensory loss or a deep ache in the medial thigh from the pubis to the medial knee, occasionally to the ipsilateral ASIS; numbness of the inner thigh.

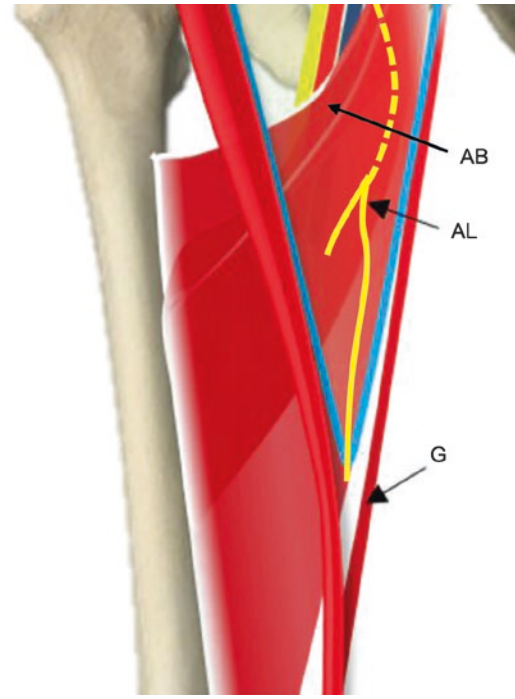

Fig. 4.16 Obturator nerve (in yellow) in the adductor compartment in the medial aspect of the thigh. *AB* adductor brevis, *AL* adductor longus, *G* gracilis

Sign: Sometimes weakness of the leg, especially after exercise, an abnormal walking pattern and posture, and the inability to adduce the affected leg close to the other leg.

Strumental studies: Needle electromyography is helpful in confirming suspected obturator neuropathy with abnormalities in the adductor muscles. If evaluating the adductor magnus, it is important to recognize that the sciatic nerve also contributes to its motor innervation. Assessment of femoral-innervated muscles and paraspinal muscles should be performed to rule out plexus injury or radiculopathy.

4.4.5 Pudendal Nerve

Anatomy (Fig. 4.17): The pudendal nerve arises from the sacral plexus and comprises the S2, S3, and S4 segments. The nerve exits through the greater sciatic foramen, crossing the ischial

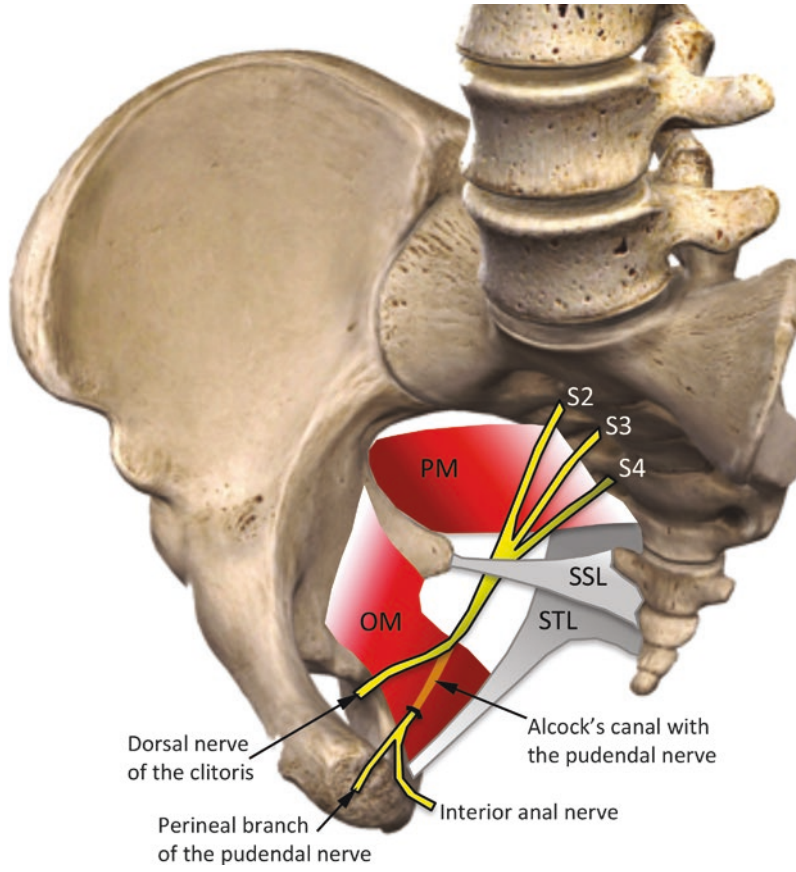

Fig. 4.17 Sites of pudendal nerve entrapment. OM obturator muscle, PM piriformis muscle, SSL sacro-spinous ligament, STL sacro-tuberous ligament

spine, the sacrospinous ligament, and the sacrotuberous ligaments.

Function: As sensitive nerve it supplies genitalia (penis, scrotum, clitoris, and labia) and innervates muscles of the perineum and pelvic floor.

Risk factor for entrapment: There are three common locations of nerve entrapment, between the sacrotuberous and sacrospinous ligaments, within the pudendal canal (Alcock canal), and while crossing the falciform process of the sacrotuberous ligament.

Symptoms: Perineal pain. Nantes criteria to facilitate diagnosis of pudendal neuralgia include (1) pain in the anatomical territory of the pudendal nerve, (2) worsened by sitting, (3) pain that does not wake the patient at night, (4) no objective sensory loss on clinical examination, and (5) pain relieved by pudendal nerve block. Other symptoms such as sexual dysfunction, defecation difficulty, and/or urinary impairment may be present.

Strumental studies: Electroneuromyographic (ENMG) investigation is often performed in this context, based on needle electromyography and the study of sacral reflex and pudendal nerve motor latencies. These two neurophysiologic techniques have been suggested: (1) concentric needle electromyography (EMG), performed bilaterally in both bulbocavernosus and external anal sphincter muscles for comparative analysis, and (2) pudendal nerve motor conduction studies, including transrectal stimulation of the pudendal nerves at the ischiatic spines to measure pudendal nerve terminal motor latencies and superficial stimulation of the dorsal nerve of the penis/clitoris to determine sacral reflex latencies. The diagnosis of pudendal neuralgia is therefore essentially clinical, in which the patient's clinical history plays a major role

because of the limited sensitivity and specificity of ENMG. Imaging studies such as color duplex scanning and magnetic resonance neurography should be done to reach a confirmatory diagnosis.

4.4.6 Sciatic Nerve

Anatomy (Fig. 4.18): The sciatic nerve arises from the lumbosacral plexus (L4–5 and S1–3) and providing sensory and motor innervation to the lower extremity. Within the deep gluteal region, the nerve passes between the ischial tuberosity and the greater trochanter of the femur lying close to the posterior capsule of the hip joint and is covered at that point by the gluteus maximus muscle. The nerve trunk passes distally deep in the thigh to the popliteal fossa where it divides into the tibial and peroneal nerves.

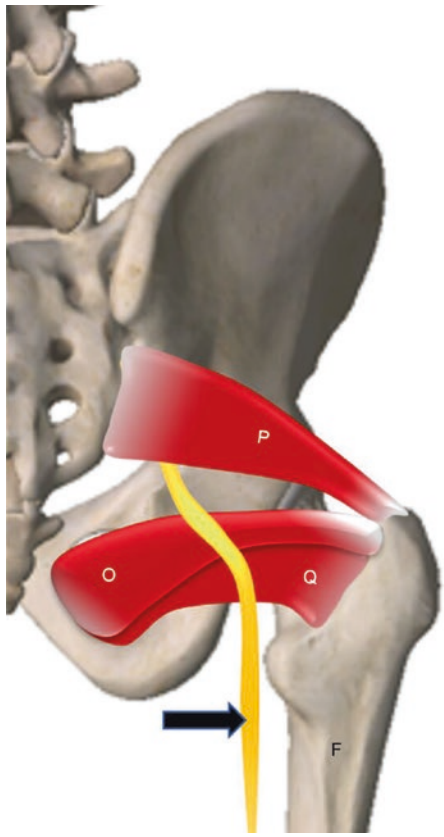

Fig. 4.18 Sciatic nerve (black arrow) compression by piriformis muscle (P). *O* obturator internus, *Q* quadratus femoris

Function: The sciatic nerve does directly innervate the muscles in the posterior compartment of the thigh and the hamstring portion of the adductor magnus. The sciatic nerve does not have any direct cutaneous functions. It also does provide indirect motor and sensory innervation via its terminal branches.

Risk factors for entrapment: Sciatic nerve entrapment may occur in the hip region and less commonly in the thigh, and clinical presentations are based upon the level of injury. Sciatic neuropathy may result from fibrous or muscular entrapment, vascular compression, scarring related to trauma or radiation, tumors, and hypertrophic neuropathy. Piriformis syndrome is a discussed entity often thought to be related to sciatic nerve compression or irritation related to the piriformis muscle.

Symptoms: Inability to sit; buttock, lateral hip, and groin pain; paresthesia in the lower limb.

Sign: Sciatic neuropathy affects hamstring muscles, with weakness of hip extension and knee flexion and weakness of muscles in the peroneal and tibial nerve distribution, with a diffusely weak foot and ankle.

Strumental studies: ENMG in sciatic neuropathy will yield reduced amplitudes of the superficial peroneal sensory and sural sensory responses; it could be helpful in localizing the lesion. MR imaging is not only a sensitive technique in identifying and characterizing the causative abnormalities but also can provide useful information for surgical planning. High-resolution and high-field magnetic resonance neurography (MR neurography, MRN) has shown to have excellent anatomic capability to identify sciatic neuritis.

4.4.7 Common Peroneal Nerve

Anatomy (Fig. 4.19): It runs with tibial nerve as part of sciatic nerve in the posterior thigh. The popliteal fossa diverges to wrap around the fibula head, and then it divides into the terminal branches and superficial and deep peroneal nerves.

Function: It supplies muscular branches to biceps femoris, peroneus longus and brevis, anterior tibialis, extensor hallucis longus, peroneus tertius, and extensor digitorum brevis and sen-

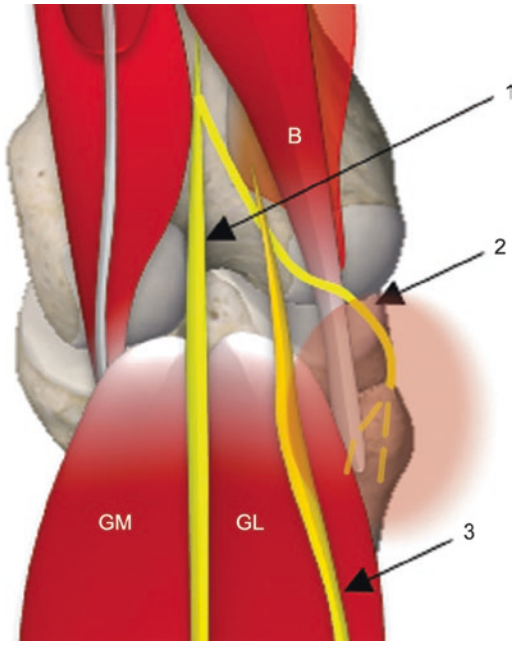

Fig. 4.19 View of the popliteal fossa. *1* tibial nerve, *2* common peroneal nerve. *GM* gastrocnemius medial head, *GL* gastrocnemius lateral head, *B* biceps femoris

sory innervation to the lower two-thirds of the lateral leg and the dorsum of the foot.

Risk factors for entrapment: Peroneal mononeuropathies are the most common mononeuropathy in the lower extremity. The most common cause of peroneal neuropathy is external compression of the nerve at the fibular head.

Symptoms: Patients may experience pain at the site of entrapment.

Sign: Foot drop and a slapping gait.

Strumental studies: ENMG can be helpful in localizing a peroneal lesion; reduction of the superficial peroneal sensory response indicates a lesion distal to the dorsal root ganglia. Tibial motor, F-response, and sural nerve studies are useful in ruling out a peripheral neuropathy or a more widespread lesion, such as a plexopathy or sciatic injury. MR imaging is superior in depicting the location and cause of compression and assessing the stage of the neuropathy, indicated by early muscle denervation or later changes such as atrophy. The sonographic appearance of the entire common peroneal nerve is best depicted in the short axis. In this plane, the relationship of the nerve with adjacent known anatomic structures is readily depicted, since the nerve has a distinctive honeycomb pattern and can be readily followed. When scanned in the long axis, the nerve is more difficult to image because of its curvilinear course. However, once an abnormality is detected, the longitudinal scan best shows the relationship of the nerve with adjacent structures, the length of involvement, and the etiology. Although the common peroneal nerve may be entrapped at any location along its course, it is most common at the fibular neck because of its superficial location and fixed position.

4.4.8 Tibial Nerve

Anatomy (Fig. 4.20): As a terminal branch of sciatic nerve, the tibial nerve descends into the posterior compartment of the lower leg deep to the soleus, plantaris, and gastrocnemius muscles, it crosses the ankle behind the medial malleolus, and

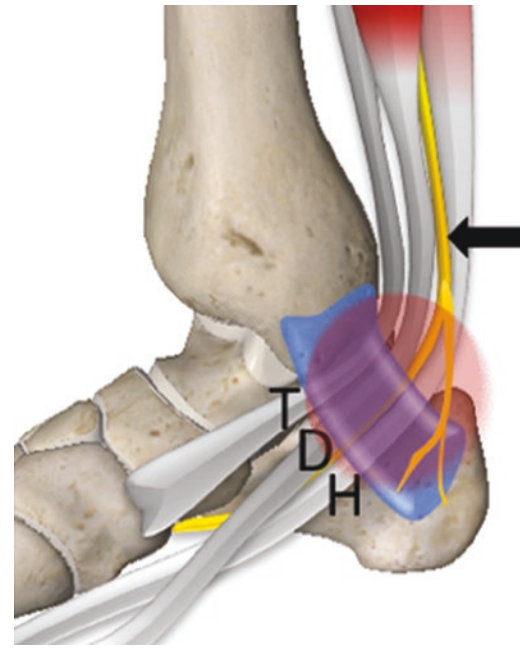

Fig. 4.20 Tibial nerve (black arrow) in the tarsal tunnel. Flexor retinaculum in light blue. *T* tibial posterior tendon, *D* flexor digitorum longus tendon, *H* flexor hallucis longus tendon

it divides into its terminal branches, the medial calcaneal nerve, and medial and lateral plantar nerves.

Function: Supplies all of the hamstring muscles with the exception of the short head of the biceps femoris, partial innervation to the adductor magnus, and the muscles of the posterior compartment of the lower leg.

Risk of entrapment: The most frequent cause of entrapment is located at the tarsal tunnel fibro-osseous canal in the medial aspect of the ankle with the flexor retinaculum as the roof.

Symptoms: Pain and sensory loss can be seen in the sole of the foot and the posterolateral lower leg and foot in the sural distribution.

Sign: Weakness of plantar flexion and inversion of the ankle and loss of toe flexion strength with accompanying atrophy of the calf. A Tinel sign can be elicited by tapping over the flexor retinaculum at the medial malleolus.

Strumental studies: ENMG evaluation of suspected tibial lesions should include sural sensory responses; reduction in tibial motor responses to the abductor hallucis will be seen. MR imaging is useful for localizing pathologies within the tarsal tunnel and depicting the lesion extent and relationship to the nerve and branches. US imaging generally permits a reliable study of the tarsal tunnel and can detect neuropathy and/or US Tinel sign, which may confirm clinical diagnosis. A well-known advantage of US technique is the possibility to study patients during limb loading, which is very useful in the diagnosis of varicose plantar veins and in the investigation of pain due to nerve injury associated with static foot disorders.

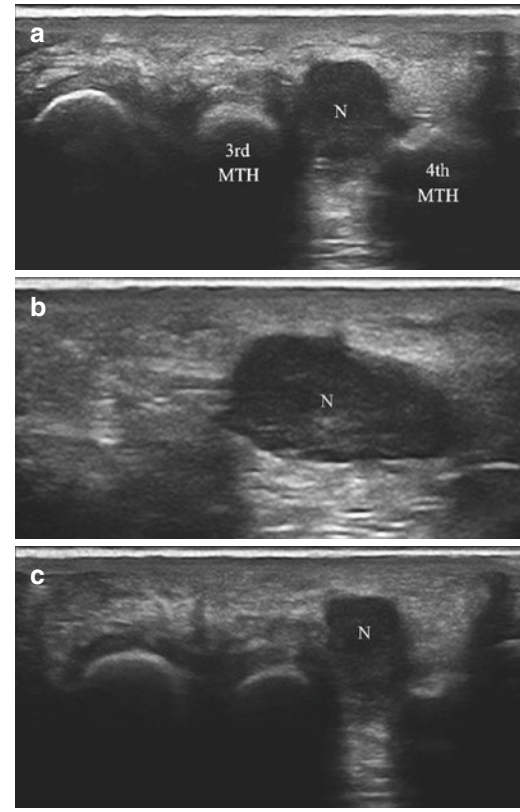

Fig. 4.21 Morton's neuroma (N). Sonogram in coronal (**a**) and sagittal (**b**) plane reveals characteristic spindle-shaped hypoechoic nodule, with mass effect at the third and fourth intermetatarsal space. (**c**) Squeezing the metatarsal heads together (foot squeeze test) causes the Morton's neuroma to "pop" out. *N* Morton's neuroma, *MTH* metatarsal head

4.4.9 Interdigital Nerve

Anatomy: Terminal branches of the tibial nerve divide into interdigital nerves at the level of metatarsal bases, and they pass deep to the transverse intermetatarsal ligament into a relatively small space between the metatarsal heads.

Function: They innervate lumbrical muscles and skin of the foot finger.

Risk of entrapment: The most direct cause of interdigital nerve entrapment is compression of the nerve as it passes under the transverse intermetatarsal ligament. Repeated trauma leads to reactive overgrowth and scarring that disrupt the nerves and the arteries causing the development of Morton's neuroma in which common locations are in the second and third webspace.

Symptoms: Intermittent dull ache or cramping sensation on the plantar aspect of either the second or the third interspace with numbness or burning, with occasional shooting pain, exacerbated by walking.

Sign: Dorsoplantar compression of the second or third intermetatarsal space reproduces pain that may radiate to the toes or proximally along the course of the affected nerve.

Strumental studies: The diagnosis of interdigital neuritis is based primarily on clinical findings.

MR and ultrasound imaging provide very helpful information in localization and accurate size assessment of Morton's neuroma (Fig. 4.21a–c). A local anesthetic block proximal to the involved area below the intermetatarsal ligament can confirm the diagnosis.

Suggested Readings

Ali ZS, Pisapia JM, Ma TS, Zager EL, Heuer GG, Khoury V. Ultrasonographic evaluation of peripheral nerves. World Neurosurg. 2016;85:333–9.

Hussain A, Winterton RIS. Peripheral nerve entrapment syndromes of the upper limb. Surgery. 2016;34(3):134–8.

Bendszus M, Wessig C, Schultz A, et al. Assessment of nerve degeneration by gadofluorine M-enhanced magnetic resonance imaging. Ann Neurol. 2005;57(3):388–95.

Brown JM, Yablon CM, Morag Y, Brandon CJ, Jacobson JA. US of the peripheral nerves of the upper extremity: a landmark approach. Radiographics. 2016;36(2):452–63.

Caliandro P, La Torre G, Padua R, Giannini F, Padua L. Treatment for ulnar neuropathy at the elbow. Cochrane Database Syst Rev. 2016;11:CD006839.

Cass S. Upper extremity nerve entrapment syndromes in sports: an update. Curr Sports Med Rep. 2014;13(1):16–21.

Cheatham SW, Kolber MJ, Salamh PA. Meralgia paresthetica: a review of the literature. Int J Sports Phys Ther. 2013;8(6):883–93.

Craig A. Entrapment neuropathies of the lower extremity. PMR. 2013;5(5 Suppl):S31–40.

Dahlin LB. Aspects on pathophysiology of nerve entrapments and nerve compression injuries. Neurosurg Clin N Am. 1991;2(1):21–9.

Ferkel E, Davis WH, Ellington JK. Entrapment neuropathies of the foot and ankle. Clin Sports Med. 2015;34(4):791–801.

Ferrante MA, Ferrante ND. The thoracic outlet syndromes: part 1. Overview of the thoracic outlet syndromes and review of true neurogenic thoracic outlet syndrome. Muscle Nerve. 2017 Jun;55(6):782–93.

Hobson-Webb LD, Juel VC. Common entrapment neuropathies. Continuum. 2017;23(2):487–511.

Kutlar N, et al. Diagnosing carpal tunnel syndrome with Doppler ultrasonography: a comparison of ultrasonographic measurements and electrophysiological severity. Neurol Res. 2017;39(2):126–32.

Martinoli C, Tagliafico A, Bianchi S, et al. Peripheral nerve abnormalities, ultrasound clinics. Musculoskelet Ultrasound. 2007;2(4):655–67.

Neal S, Fields KB. Peripheral nerve entrapment and injury in the upper extremity. Am Fam Physician. 2010;81(2):147–55.

Padua L, Coraci D, Erra C, Pazzaglia C, Paolasso I, Loreti C, Caliandro P, Hobson-Webb LD. Carpal tunnel syndrome: clinical features, diagnosis, and management. Lancet Neurol. 2016;15(12):1273–84.

Strohl AB, Zelouf DS. Ulnar Tunnel Syndrome, Radial Tunnel Syndrome, Anterior Interosseous Nerve Syndrome, and Pronator Syndrome. J Am Acad Orthop Surg. 2017;25(1):e1–e10.

US-Guided Nerve Blocks: Procedure Technique

5

Filomena Puntillo, Laura Bertini, Mario Bosco, Mario Tedesco, and Marco Baciarello

5.1 General Considerations

The principles underlying ultrasound (US)-guided regional anesthesia practice do not differ significantly from established practice.

The addition of US imaging poses few additional problems when organizing one's practice and when approaching specific patients.

5.1.1 Ergonomics

When setting up a US-guided nerve block, care should be taken to ensure that the machine's screen can be viewed without exerting too much stress on the operator, who is normally facing the patient. Ideally, the machine's controls should be within their reach too, as image setup is best carried during preprocedural scans, using the same approach as will be used for the block.

5.1.2 Sterility

Whether full sterile barrier precautions are needed for single-shot and/or regional catheter placement has been the object of debate and a full analysis is beyond the scope of this chapter. However, adequate precautions to prevent contamination of the equipment should always be employed.

Several approaches have been proposed to protect US transducers. Historically, these have included the creative use of sterile surgical gloves and sterile dressing. As the use of US guidance becomes standard practice in more and more institutions throughout the world, the choice not to use proper sterile sheaths and sonographic gel seems all the more untenable.

Care should be taken to avoid (cross-)contamination of patients even before the field is prepped. Precautions should be taken when performing both diagnostic and preprocedural scans. In these cases, wound dressings can be more practical to use; tissue wipes soaked with specific, noncorrosive disinfectant are also available.

F. Puntillo (✉)
Assistant Professor of Anaethesia and Pain Therapy, Department of Emergency and Organ Transplantation, University of Bari, Bari, Italy
e-mail: filomena.puntillo@uniba.it

L. Bertini
Anaethesia and Pain Unit, Santa Caterina Hospital, Rome, Italy

M. Bosco
Anaesthesia and Intensive Care Unit, Santo Spirito Hospital, Rome, Italy

M. Tedesco
Pain Therapy Unit, Mater Day Hospital, Bari, Italy

M. Baciarello
Assistant Professor of Anaethesia and Pain Therapy, Department of Medicine and Surgery, University of Parma, Parma, Italy

E. Silvestri et al. (eds.), *Ultrasound-Guided Peripheral Nerve Blocks*,
https://doi.org/10.1007/978-3-319-71020-4_5

Alcohols may gradually wear down the conducive surface of US transducers. Disinfection should include all external surfaces of the US machine; as keyboards are notoriously difficult to sanitize, it has been proposed that touchscreen interfaces may be more easily decontaminated.

5.2 Indications and Contraindications

The choice whether to implement regional anesthesia and specifically peripheral nerve blocks (PNB) into a patient's clinical pathway will only seldom be based strictly on evidence. In fact, there are but few settings where it has been indisputably demonstrated that PNBs improve outcomes—and, even then, the choice of the outcome variables may vary greatly depending on the setting.

Evidence-based medicine, however, is mostly based on results obtained on selected populations, by investigators employing predetermined techniques and sharing a common goal. While rigorous methodology guarantees internal validity, generalization of results depends on inclusion criteria and should always be interpreted at the population level. In other words, while evidence-based medicine is useful in guiding population-level decision-making in healthcare policy (e.g., whether to offer femoral nerve blocks to all patients undergoing total knee replacement at one's hospital), it is not necessarily the preferred approach when discussing options with an individual patient.

Furthermore, other steps in an institution's clinical pathway may limit the applicability of available evidence in the given context. For example, differences in mobilization policies and physical therapy availability between a randomized controlled trial and a given institution may negate the advantages of femoral nerve blocks in terms of joint range of motion at 3 months; or again, variations in patterns of perioperative opioid use may affect the prevalence of chronic pain after surgery. To summarize, general indications to PNBs should always begin at the evidence base and then be adapted in the context of the individual patient.

The main purposes of a PNB may be summarized in two items: analgesia, both intraoperative and postoperative, and anesthesia. The former term refers to the utilization of the technique as the sole anesthetic technique, as opposed to the combination of general anesthesia or central blocks as complements. While it is empirically known that many kinds of surgery may be carried out with PNBs as the main anesthetic in the context of monitored anesthesia care (MAC), little evidence is available to demonstrate the possible outcome differences when compared to general anesthesia or central blocks, either alone or in combinations with PNBs.

In some countries, anesthetic management may be influenced by reimbursement practices, encouraging the addition of general anesthesia or central blocks to PNBs. When this is not an issue, the *need* for an additional anesthetic technique should be evaluated on the basis of block effectiveness, surgical technique, patient preference, and practical considerations. However, the need for MAC (i.e., the continued presence of dedicated personnel trained in anesthesia) should never be questioned but for the simplest surgical procedures performed with distal nerve blocks.

In the setting of chronic pain medicine, PNBs can be considered to have two primary indications: pain relief in the short-to-medium term and differential diagnosis. In specific settings, results obtained after a PNB may influence subsequent management, although this is usually practical evidence. For example, significant pain relief after a suprascapular nerve block for rotator cuff syndrome may suggest that a patient will benefit from pulsed radiofrequency treatment of the nerve; absence of pain relief despite a successful block (as evidenced by skin sensory testing) may, conversely, advise against such procedure. In the latter case, the pain generator could be assumed to be innervated by a different nerve. However, it is unclear whether diagnostic blocks are predictive of outcome after radiofrequency treatment in cases where the pain generator is clearly identified (e.g., intercostal nerves, knee, hip, etc.), as one should always consider the possibility of technical failure of the diagnostic block.

Table 5.1 Pharmacokinetic characteristics of local anesthetics

Anesthetic	Concentration (%)	Onset	Duration (hours)	Toxicity	Usual dose (mL; 70-kg patient)
Lidocaine	1–2	Rapid	1.5–3	Moderate	20–40
Mepivacaine	1–2	Moderate	3–5	Moderate	20–40
Bupivacaine	0.25–0.5	Slow	6–12	High	30–40
Ropivacaine	0.5	Slow	5–8	Moderate	30–40

A search of the literature will reveal a growing number of case reports for niche indications for PNBs, including:

- Acute limb ischemia/vasospasm
- Limb replantation/salvage procedures
- Chronic regional pain syndromes

The underlying theory, demonstrated in part in animal models, is that blockade of sympathetic efferents will favorably affect these conditions.

5.3 Setting and Patient Preparation

The ideal environment for the execution of a nerve block is a preparation room, where the anesthetist can have the material and the time required for the execution of the block and where the patient can be monitored and treated in case of adverse events. However, the execution of a nerve block does not require a specific setting, as it can be performed even directly in the operating room.

Beyond the specific setting, the patient should be positioned in the most favorable posture for the execution of the block itself, as described in each chapter.

The anesthetist should ensure the patient's monitoring (electrocardiographic trace and peripheral O_2 saturation are usually enough), prepare a sterile field, and proceed with the ultrasound scan and with the nerve block.

In some cases, it may be appropriate to consider the need for a mild sedation or analgesia before the execution of the block, in order to make the procedure easier and better tolerated by the patient.

5.4 Drug and Material Requirements

The only required materials are an ultrasound machine with a linear and a convex transducer (depending on the block, as described in each chapter), ultrasound gel, a needle whose length depends on the target depth, syringes, sterile gloves, disinfectant, and local anesthetic.

One of the most important choice in the execution of a nerve block is obviously of the local anesthetic and its concentration. This choice depends on the desired effect in terms of the type of block (anesthetic or analgesic) and in terms of duration of the block itself.

An in-depth dissertation on local anesthetics is not the goal of this manual; therefore we report a simple summary in Table 5.1.

5.5 US Guidance and Navigation Systems

The introduction of ultrasound guidance has been a marked advance in the practice of regional anesthesia and has gained popularity as an adjunct or alternative to the nerve stimulation technique. Ultrasound-guided nerve blocks consist of the identification of the target nerve, visualization of the surrounding anatomy (such as blood vessels, lymph nodes, and other important structures), needle tip, and real-time observation of the local anesthetic spread. Peripheral nerves can be identified and traced to alternative sites where local anesthetic can be safely injected without the risk of neurovascular injury. Direct visualization of the target nerve and deposition of local anesthetic have been shown to improve block operating efficiency while decreasing placement complications and patient discomfort.

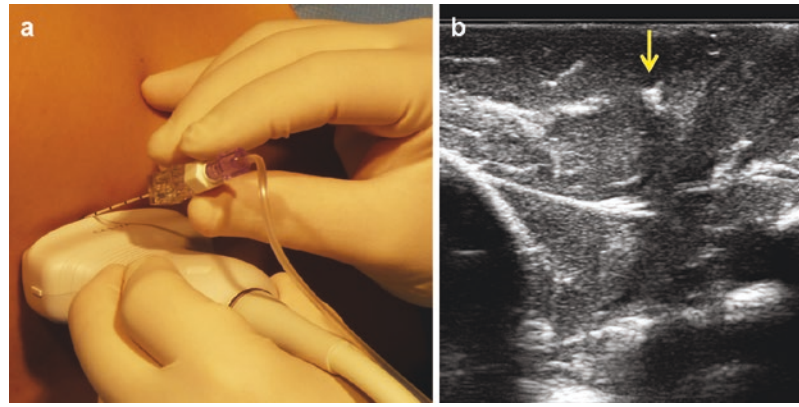

Fig. 5.1 (**a**) The needle is inserted using an out-of-plane approach. (**b**) It is relatively easy to confuse the shaft that appears as an echogenic dot (indicated by yellow arrow)

Variations in limb anatomy are commonly identified by ultrasonography and may, in part, explain the documented high incidence of block failure using traditional methods. Regional anesthesia performed with bedside ultrasound guidance compared to peripheral nerve stimulation has been shown to have a significant decrease in the risk of vascular puncture, an increase in the nerve block duration, and a faster onset time. Ultrasound has already transformed the practice of peripheral nerve and plexus blockade, and its wider availability is likely to ensure even greater use in the future.

For evaluation of the superficial nerves, such as those in the forearm, the brachial plexus, and femoral nerves, a high-frequency (10–15 MHz) linear transducer is required which provides better resolution. A lower-frequency convex probe (4–7 MHz), which provides better penetration, is recommended for deeper targets such as the sciatic nerve or for more obese patients. The availability of color flow Doppler is useful for differentiating vascular structures. Needle visualization during US-guided regional anesthesia is likely essential for safety and efficacy.

However, accurate and consistent needle tip visualization is hampered by several factors, including the difficulty of needle-beam alignment, and the poor echogenicity of commonly available block needles in the clinical setting. There are two methods of orienting the needle relative to the US beam in US-guided peripheral nerve block: the in-plane and out-of-plane approaches. In the out-of-plane needle approach, the longitudinal axis of the needle is inserted in a plane perpendicular to that of the US beam, and the needle tip crosses the plane of imaging as an echogenic dot (Fig. 5.1a, b).

This approach has a shorter needle trajectory and mirrors the landmark-based technique, but with the additional benefits of ultrasound guidance. However, the block needle, usually 22 gauge and 5 cm in length, is viewed in cross section only, and the precise location of the needle tip can be uncertain. If the needle tip crosses the scan plane without recognition, it may be advanced into undesired structures. In general, the out-of-plane approach provides less-consistent needle visualization when compared to the in-plane approach and is typically used for superficial injections with minimal surrounding soft tissues. Using the in-plane approach the entire length of the needle is held within the plane of the ultrasound beam and is visible as a bright hyperechoic line (Fig. 5.2a, b). The needle can be viewed continuously throughout the procedure and the tip accurately placed while avoiding vital structures. The angle at which the needle shaft and US beam intersect (needle-beam angle) greatly affects needle visibility. Needle tip and shaft visibility are better at larger needle-beam angles when using an in-plane needle approach; the optimal angle appears to be >55°, and a needle-beam angle close to 90° offers the best needle visibility (Fig. 5.3a, b).

However, difficulties in aligning the needle and the transducer can lead to incorrect identification of the needle tip, possibly damaging

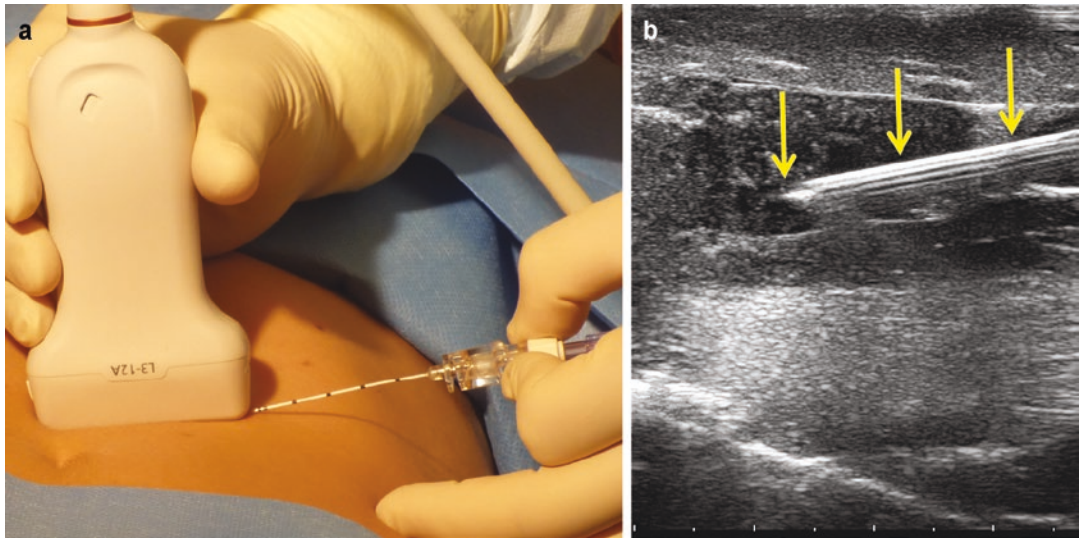

Fig. 5.2 (**a**) The needle is inserted using an in-plane approach (the needle-beam angle is almost 90°) in a shallow trajectory. (**b**) Both the shaft and tip (yellow arrows) are clearly visible, with maximal reflection back to the transducer

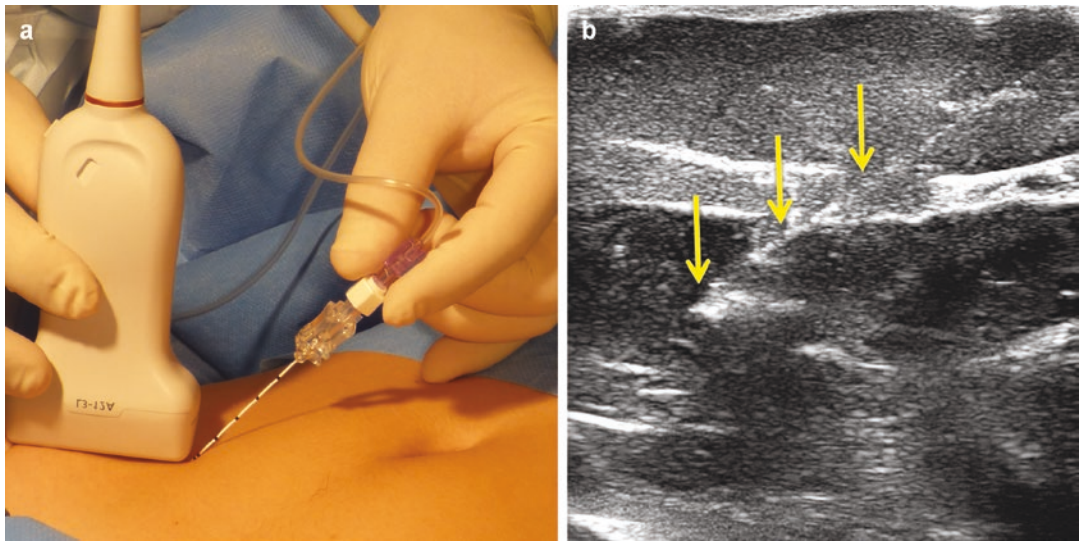

Fig. 5.3 (**a**) The needle is inserted in a steep trajectory (small needle-beam angle). (**b**) The needle shaft and tip (yellow arrows) become less echogenic and are poorly visible

structures not visible on the ultrasound screen. Additional techniques specifically developed to aid alignment of needle and probe or identification of the needle tip are now available, such as needle guides; three- and four-dimensional ultrasound; magnetism, electromagnetic, or GPS systems; optical tracking; augmented (virtual) reality; robotic assistance; and automated (computerized) needle detection.

For the fusion imaging technique, a variety of tracking methods are available, including optical, image-based, and electromagnetic tracking. Electromagnetic tracking is most widely used for US-guided interventions. There are three

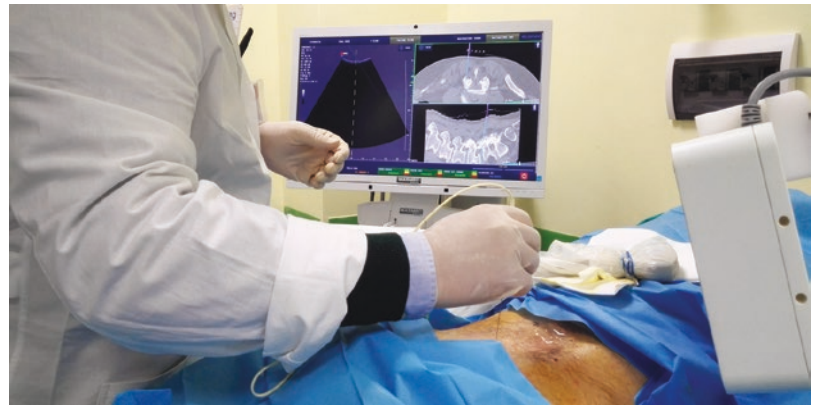

Fig. 5.4 CT fusion-assisted US-guided injection of facet joints in patients suffering from back pain. The needle is inserted using a "navigation system" with virtual needle tracking, provided by an electromagnetic position sensor embedded in the needle tip

components of the electromagnetic tracking-based fusion imaging technique: the magnetic field generator, position sensor, and position sensor unit. The first step of image fusion is uploading the data set to be fused with real-time US to the US machine. This technique involves the co-registered display of real-time ultrasound with a reference series from another modality, such as CT or MRI. As the ultrasound exam is performed, the fusion system continuously generates reformatted planes from the reference series matching the oblique imaging planes of the ultrasound transducer.

Virtual needle tracking (navigation system) can be provided by the fusion imaging system with the use of the electromagnetic position sensor embedded in the distal tip of a needle or attached to the hilt of the needle. A needle with a position sensor at the distal tip of the needle can provide a more accurate expected electrode path than that with a position sensor attached to the hilt of the needle. US needle guidance with CT fusion assistance allows for safe and effective injection of degenerative facet joint disease in patients suffering from back pain (Fig. 5.4). This technique may be readily translated also to other applications in which spinal needles are used.

5.6 Interscalene Block

The brachial plexus (Fig. 5.5) that provides sensory and motor innervation to the upper limb can be blocked at four levels: at trunks level (interscalene block), at divisions level (supraclavicular block), at cords level (infraclavicular block), and at terminal branches level (axillary block).

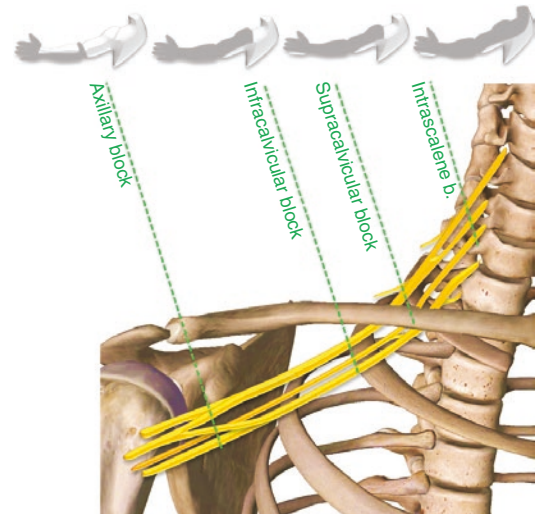

Fig. 5.5 Brachial plexus anatomy and blocks' sites

Anatomy (Fig. 5.6)**:** At this level the trunks, surrounded by a connective sheath, are located in the interscalene groove (defined by the anterior and middle scalene muscles) deep to the sternocleidomastoid muscle.

Indications: Anesthesia or analgesia for shoulder surgery as this approach targets the proximal roots of the plexus (C4–C7). The more distal roots of the plexus (C8–T1) are usually spared by this approach.

Patient position: The patient is positioned supine or with the head elevated 45° with a pillow under the shoulder. The head is turned 45° to the contralateral side.

What you need: A high-frequency (10–15 MHz) linear probe and a 22G atraumatic echogenic needle, 50 mm of length. 15 mL of local anesthetic.

Sonoanatomy (Fig. 5.7)**:** When the probe is in the right position, you can see the interscalene groove that is located under the sternocleidomastoid muscle, lateral to the carotid artery and internal jugular vein. Between the anterior and the middle scalene muscles, you can see the three trunks of the brachial plexus: they appear hypoechoic, with a round or oval cross section and with a hyperechoic labrum, aligned one above the other like a "traffic light."

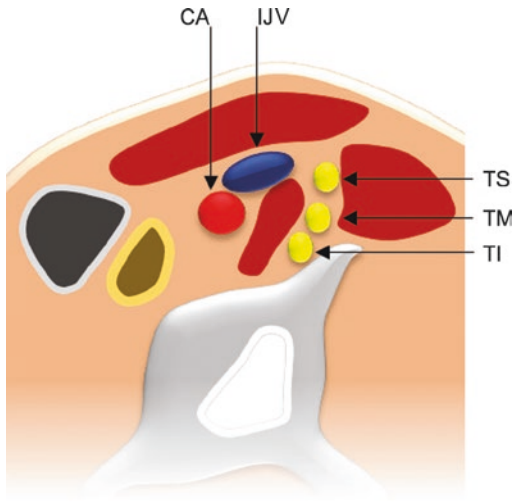

Fig. 5.6 The interscalene groove in a trans-sectional view of the neck. *TS* superior trunk, *TM* middle trunk, *TI* inferior trunk, *CA* carotid artery, *IJV* internal jugular vein

How to do it (Fig. 5.7)**:** We suggest the "traceback method." The probe is initially positioned above the clavicle to search the subclavian artery and the secondary trunk of the plexus lateral and above the artery. Afterward, the probe is withdrawn along the sternocleidomastoid muscle: the secondary trunks become primary trunks, and a transverse image of the plexus roots in the interscalene area is obtained on the lateral aspect of the neck in an axial oblique plane.

The needle is inserted in-plane with the skin entry point 1–2 cm away from the probe. The tip of the needle must be between the superior and the middle trunks of the plexus. The anesthetic spread will be inside the connective sheath surrounding the brachial plexus in order to provide an adequate anesthesia/analgesia with the lowest volume of anesthetic.

Tips and tricks: Be aware of anatomical variants of the brachial plexus. One of the most common, concerns the root of C5 that gives rise to the superior trunk. The C5 ventral ramus can pass through or upon the anterior scalene muscle, and this can be a cause of failure of the blind interscalene approach of the brachial plexus.

Before the injection of the anesthetic solution, use the power Doppler to detect vessels near the tip of the needle.

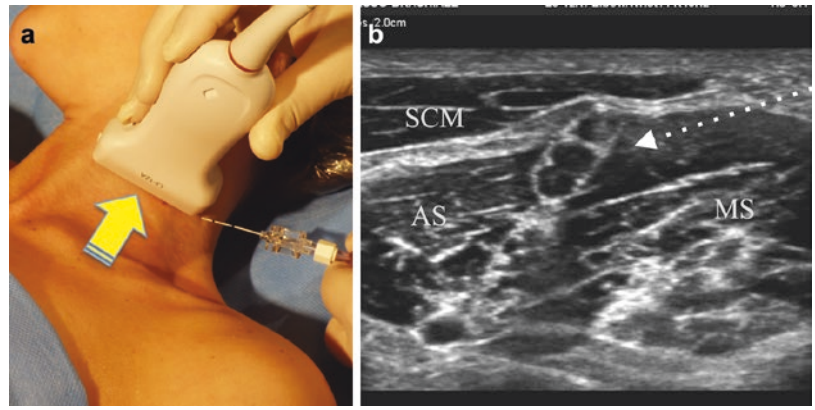

Fig. 5.7 (**a**) Patient position and needle entry point. The yellow arrow shows the trajectory of "traceback method" scanning. (**b**) Sonoanatomy. *SCM* sternocleidomastoid muscle, *AS* anterior scalene muscle, *MS* middle scalene muscle, Long white arrow needle direction and target point

Complications: One of the most common side effects of interscalene block is hemidiaphragmatic paresis secondary to phrenic nerve palsy. Using low volume of anesthetic can mitigate it.

Unintentional epidural or spinal anesthesia and spinal cord injury are very rare complications of interscalene block.

5.7 Supraclavicular Block

Anatomy (Fig. 5.8)**:** In the supraclavicular area, the brachial plexus (the trunks and/or their respective anterior and posterior divisions) is located lateral and posterior to the subclavian artery. They both lie over the first rib and under the clavicle.

Indications: Surgeries of the arm, forearm, or hand.

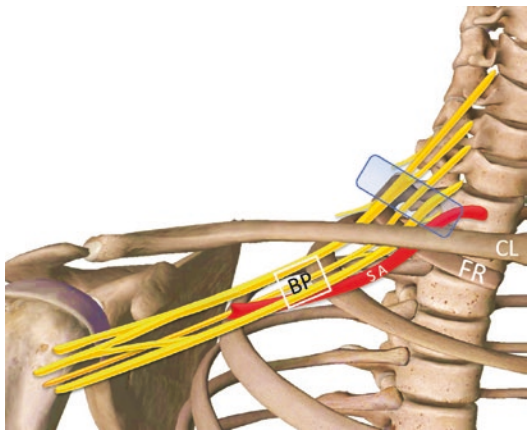

Fig. 5.8 Topography of brachial plexus in the supraclavicular area. *CL* clavicle, *FR* first rib, *BP* brachial plexus trunk's divisions, *SA* subclavian artery. The blue box shows the echographic supraclavicular window

Patient position: Supine position with a pillow under the shoulder. The head is turned 45° to the contralateral side.

What you need: A high-frequency (10–15 MHz) linear probe and a 22G atraumatic echogenic needle, 50 mm of length. 15 mL of local anesthetic.

Sonoanatomy (Fig. 5.9)**:** In the supraclavicular area, the plexus appears most commonly as a group of several hypoechoic structures with a round or oval cross section and with a hyperechoic labrum that has been compared to a "bunch of grapes" lateral to a round pulsatile uncompressible structure that is the subclavian artery. Under the plexus you can see a hyperechoic structure with the acoustic shadowing below the first rib. Over the plexus you can see a light hyperechoic line that is the superficial cervical fascia.

How to do it (Fig. 5.9)**:** We suggest scanning over the supraclavicular fossa in a coronal oblique plane. From medial to lateral you can find the trachea, the carotid artery, the jugular vein, and finally the subclavian artery with the plexus. Tilt the probe to check the right window.

In order to facilitate the entry of the needle, just before inserting it, move the lateral part of the probe away from the clavicle. In this way the humeral head will not be an obstacle for the physician.

The needle is inserted in-plane with the skin entry point 1–2 cm away from the probe.

The "corner pocket," the angle between the subclavian artery and the first rib, is traditionally the site of local anesthetic injection, but it has been demonstrated that a multiple injection between the plexus nerves, a so-called "targeted intra-cluster injection," can allow a rapid onset of the block.

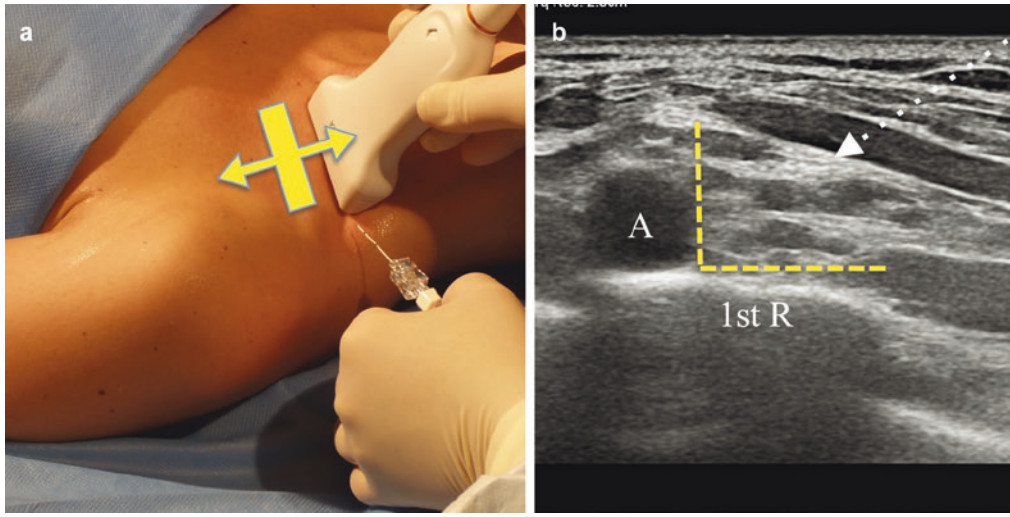

Fig. 5.9 (**a**) Patient position and needle entry point. Probe tilting (yellow arrows). (**b**) Sonoanatomy. *1st R* first rib, *A* subclavian artery. Corner pocket (yellow dashed lines). Long white arrow needle direction and target point

Tips and tricks: Be aware of intra-grape vessel of the brachial plexus, and use the power Doppler before the injection (Fig. 5.10).

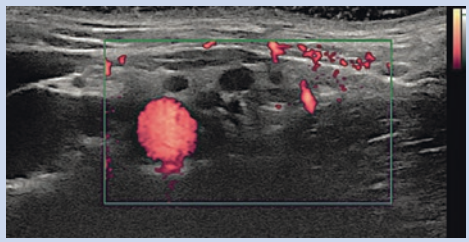

Fig. 5.10 Power Doppler showing an intra-grape vessel

During the injection of local anesthetic in the pocket corner, look at the movement of the subclavian artery away from the first rib to be sure to anesthetize the divisions that will generate the radial nerve.

Complications: The risk of pneumothorax is greatly reduced with the use of ultrasound-guided block. Other rare complications can be hemidiaphragmatic paresis (1%), Horner syndrome (1%), and vascular puncture (0.4%).

5.8 Infraclavicular Block

Anatomy (Fig. 5.11)**:** In the infraclavicular area, the cords of the brachial plexus are located posterior to major and minor pectoralis muscles, around the second part of the axillary artery. The lateral cord of the plexus lies superior and lateral, the posterior cord lies posterior, and the medial cord lies posterior and medial to the axillary artery.

Indications: Surgeries of the arm, forearm, or hand. This approach is the preferred one for catheter positioning thanks to better stability of the catheter.

Patient position: the patient is positioned supine with the arm on the side abducted 90°. In this way the artery becomes more superficial and more distant from the pleura, while the three cords become all lateral and posterior to the artery (Fig. 5.12).

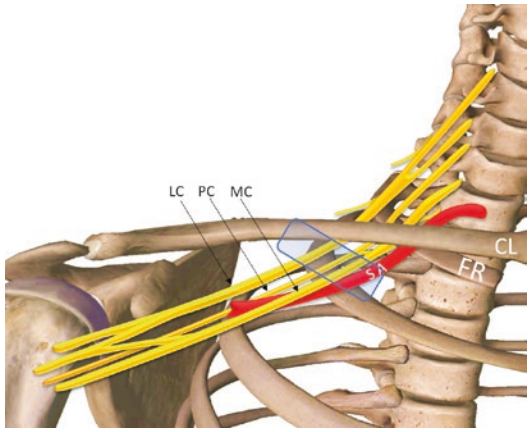

Fig. 5.11 Anatomy of infraclavear cords of brachial plexus (arrowed). *LC* lateral cord, *PC* posterior cord, *MC* medial cord, *CL* clavicle, *FR* first rib, *BP* brachial plexus trunk's divisions, *SA* subclavian artery. The blue box shows the echographic infraclavicular window

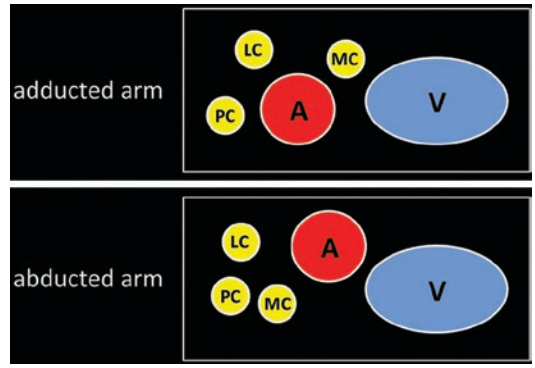

Fig. 5.12 The abduction of the arm shifts the three cords of the brachial plexus lateral and posterior to the artery MC medial cord, LC lateral cord, PC posterior cord

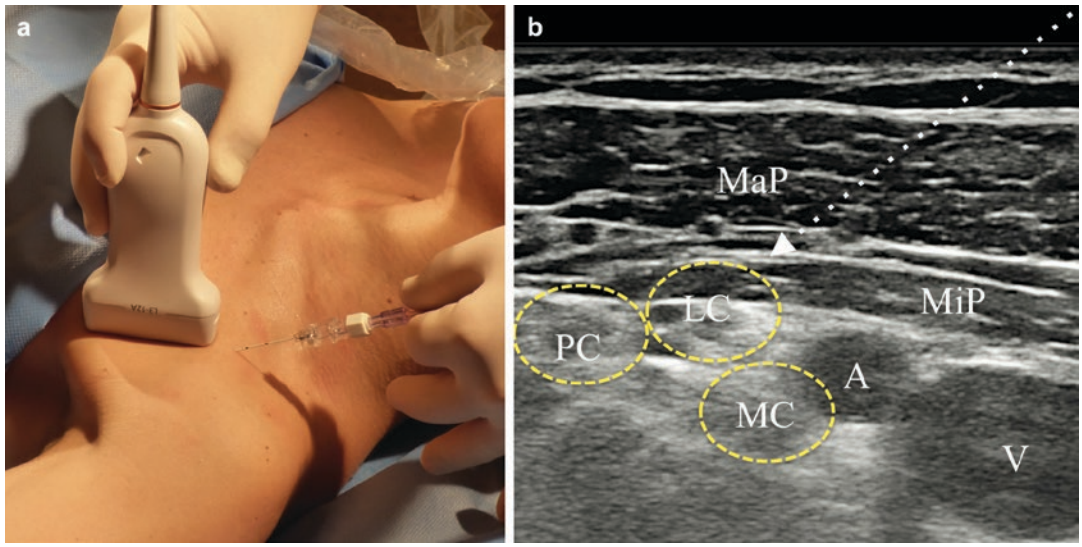

Fig. 5.13 (**a**) Patient position and needle entry point, with abducted arm. (**b**) Sonoanatomy. *MaP* major pectoralis muscle, *MiP* minor pectoralis muscle, *A* axillary artery, *V* axillary vein, *MC* medial cord (yellow outlined), *LC* lateral cord (yellow outlined), *PC* posterior cord (yellow outlined), Long white arrow needle direction and target point

What you need: A high-frequency (6–13 MHz) linear probe. A 22G atraumatic echogenic needle, 80 mm of length. Local anesthetic: 30 mL.

Sonoanatomy (Fig. 5.13)**:** In the upper part of the screen, we can see the pectoralis muscles with their fasciae (hyperechoic lines), two vascular structures, the axillary vein (oval shape, bigger, squeezable), and the axillary artery (smaller, round shape, pulsing, and incompressible). More deeply you can see the pleura and the three cords as hyperechoic structures like a "honeycomb" (Fig. 3).

How to do it (Fig. 5.13)**:** Put the probe on the deltoid pectoral sulcus with a transverse view scanning in a parasagittal plane.

The needle is inserted in-plane with the ultrasound beam in a cephalo-to-caudad orientation and with a lateral direction to avoid the pneumothorax.

The tip of the needle must be posterior to the artery: we suggest to inject here 20 mL of local anesthetic and 10 mL during the drawing back of the needle before crossing to deeper fascia of the pectoralis muscle.

Tips and tricks: Use a small linear probe (<2.5 cm) in order to have a skin entry point 2–3 cm far away from the probe, to facilitate needle visibility.

Sometimes the cords are not very visible; in this case you can use ENS guide together with ultrasound guide to find the posterior cord. The anesthetic injection will produce an anechoic bubble like the artery one with the so-called "double bubble sign."

Be aware of the possibility to find two axillary arteries or a lot of thoracic veins: in this case it is better to avoid this approach in order to avoid intravascular injection or vascular complications.

Complications: Pneumothorax remains the most feared complication of this block. Vascular injection is also possible but rare.

5.9 Axillary Block

Anatomy (Fig. 5.14)**:** The axillary approach to the brachial plexus targets three terminal branches of the plexus: the median, the ulnar, and the radial nerve. The musculocutaneous nerve often departs from the lateral cord in the proximal axilla and is commonly spared by the axillary approach (Fig. 1).

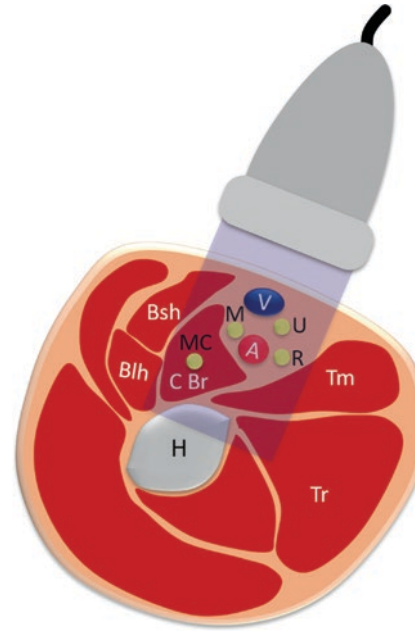

Fig. 5.14 Anatomic slice of axillary area. *Bsh* biceps short-head muscle, *Blh* biceps long-head muscle, *CBr* coracobrachialis muscle, *H* humerus, *Tm* teres major muscle, *Tr* triceps muscle, *A* axillary artery, *V* axillary vein, *MC* musculocutaneous nerve, *M* median nerve, *U* ulnar nerve, *R* radial nerve

Indication: Axillary brachial plexus block is usually indicated for distal upper limb surgery (hand and wrist).

Patient position: The patient is positioned supine with the arm on the side abducted 90° and the elbow flexed or extended.

What you need: A high-frequency (6–13 MHz) linear probe. A 22G atraumatic echogenic needle, 50 mm of length. Local anesthetic: 20, 5 mL for nerve.

Sonoanatomy (Fig. 5.15)**:** With the probe in the right position, you can see in the deeper area of the screen the humerus (a curved hyperechoic image with acoustic shadowing below it) and three muscles, the triceps (posterior), the biceps, and the coracobrachialis (anterior), that create a triangular area in which you can find the axillary artery and the three nerves. The median nerve is commonly anteromedial to the artery, the ulnar nerve medial to the artery, and the radial nerve posteromedial to it.

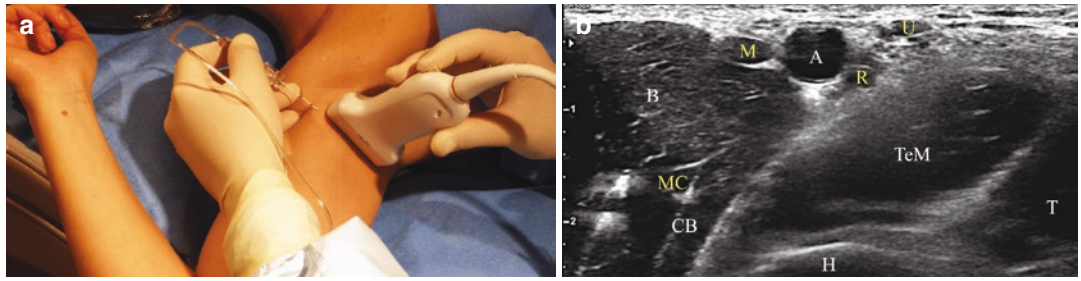

Fig. 5.15 (**a**) Patient position and needle entry point. (**b**) Ultrasound view of axillary area. *A* axillary artery, *MC* musculocutaneous nerve, *M* median nerve, *U* ulnar nerve, *R* radial nerve, *B* biceps muscle, *CB* coracobrachialis muscle, *TeM* teres major muscle, *T* triceps muscle, *H* humerus

The musculocutaneous nerve can be found in the coracobrachialis muscle or between it and the triceps muscle.

Nerves in the axilla have mixed echogenicity and a "honeycomb" appearance (representing a mixture of hypoechoic nerve fascicles and hyperechoic non neural fibers).

How to do it (Fig. 5.15)**:** The transducer is placed along the axillary crease, perpendicular to the long axis of the arm. The needle is inserted in-plane 1 cm away from the probe.

We suggest to scan the axilla beginning from lateral to medial in order to find the best site for the block: one in which you can block the four nerves with a unique skin entry point.

The first nerve to be blocked is the musculocutaneous nerve; afterward, draw back the tip of the needle and go to the front of the axillary artery. When a loss of resistance is felt, you can switch on the ENS to be sure to be close to the median nerve. Afterward, draw back the tip of the needle and go under the artery; at this point the ENS will elicit the ulnar nerve. Finally put the tip of the needle at the back of the artery and find the radial nerve with the ENS. This technique is called "perineural technique" (Fig.5.16a–c).

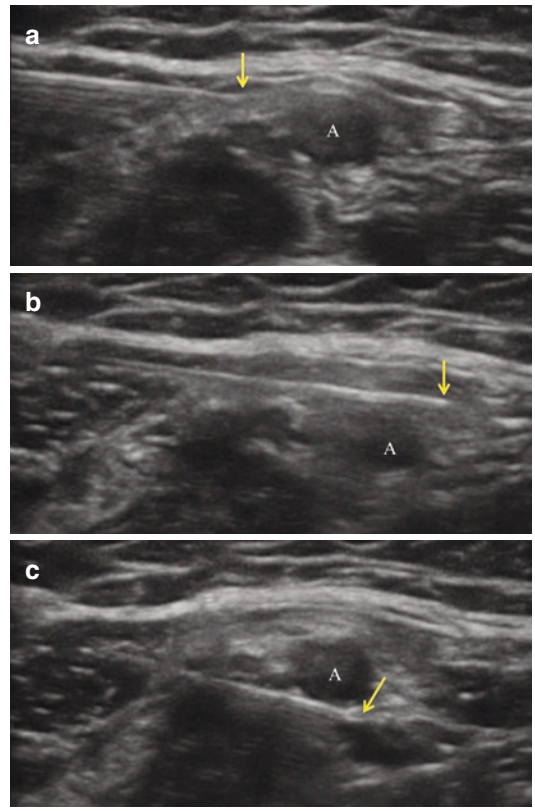

Fig. 5.16 (**a–c**) The yellow arrows indicate the needle around the axillary artery (A) near to the terminal branches of the brachial plexus

Tips and tricks: The classical disposition of nerves around the axillary artery can be found in 65% of people. However you can obtain an axillary block using the so-called "perivascular technique" putting the local anesthetic just around the artery without localizing the nerves, except for the musculocutaneous nerve.

Watch out to see the "black cloud" when you inject the local anesthetic in order to avoid intravascular injection.

Complications: The most common complication is axillary artery puncture or intravascular injection. Nerve injury is also possible.

5.10 Median Nerve Block

Anatomy (Fig. 5.17)**:** Median nerve can be located just proximal to the elbow crease, medial to the brachial artery, or at the forearm among the tendons of flexor muscles.

Patient position: The patient is positioned supine with the arm on the side abducted 90° with the elbow extended.

What you need: A high-frequency (6–13 MHz) linear probe. A 22G atraumatic echogenic needle, 50 mm of length. 5 mL of local anesthetic solution is generally sufficient to block any of the terminal nerves individually.

Sonoanatomy (Figs. 5.18 and 5.19)**:** You have to look for the typical "honeycomb" aspect. In distal arm, the medial nerve can be found superficially, medial to the brachial artery. Just below the median nerve, you can see the brachialis muscle and deeper the humerus.

In the forearm the median nerve can be found among the flexor muscles.

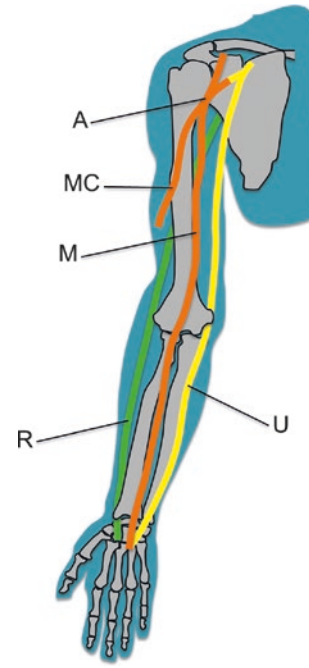

Fig. 5.17 Terminal branches of the brachial plexus in the upper limb. *A* axillary nerve, *MC* musculocutaneous nerve, *M* median nerve, *U* ulnar nerve, *R* radial nerve

How to do it (Figs. 5.18 and 5.19)**:** The transducer is placed perpendicular to the long axis of the arm. The needle is inserted in-plane.

Tips and tricks: As the nerve is always lateral to the artery, put yourself by the side of the nerve to block, in order to facilitate it and avoid arterial puncture.

Be careful to paresthesia and/or high pressure of injection that are warning signs of intraneural injection.

Complications: Arterial puncture and intraneural injection.

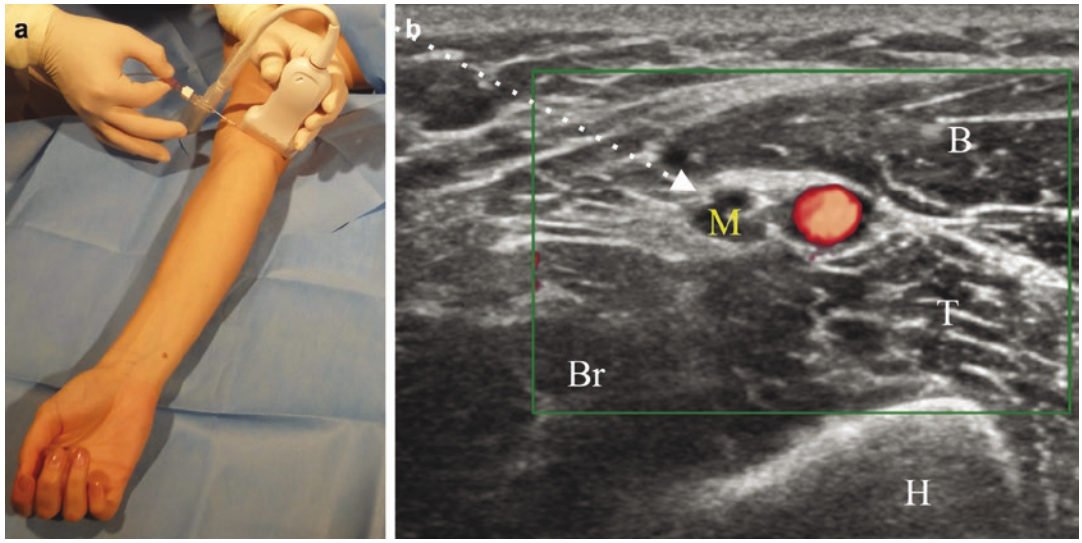

Fig. 5.18 (**a**) Patient position and needle entry point. (**b**) Sonoanatomy of median nerve in distal arm. *M* medial nerve close to brachial artery, *B* biceps muscle, *T* triceps muscle, *Br* brachialis muscle, *H* humerus, Long white arrow needle direction and target point

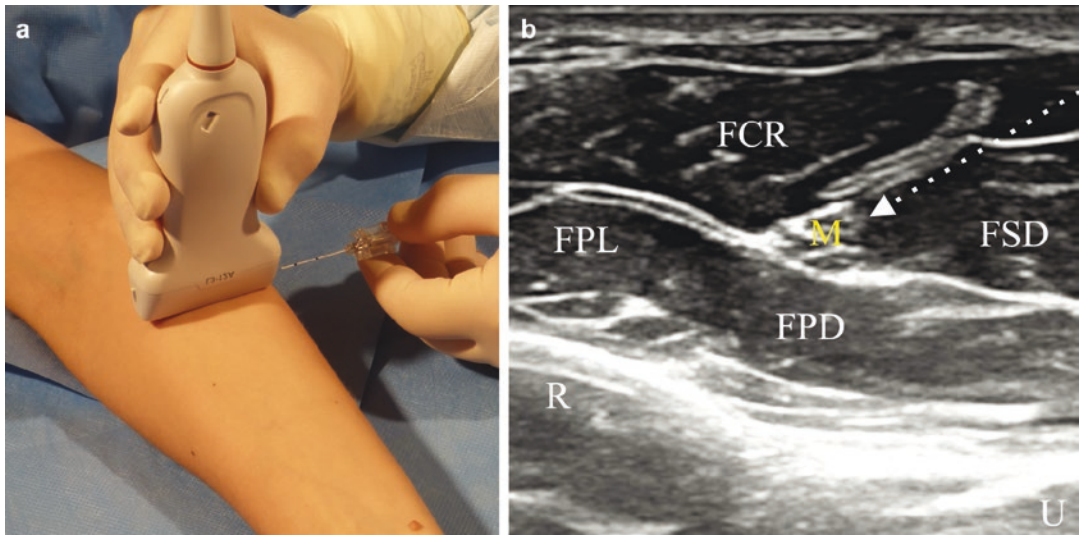

Fig. 5.19 (**a**) Patient position and needle entry point. (**b**) Sonoanatomy of median nerve in the forearm. *M* median nerve, *FCR* flexor carpi radialis muscle, *FPL* flexor pollicis longus muscle, *FPD* flexor profundus digitorum muscle, *FSD* flexor superficialis digitorum muscle, *R* radius, *U* ulna, Long white arrow needle direction and target point

5.11 Ulnar Nerve Block

Anatomy (Fig. 5.20)**:** The ulnar nerve is superficially located in the arm. It may be safely blocked proximal to the ulnar groove or at the forearm.

Patient position: The patient is positioned supine with the arm on the side abducted 90° with the elbow extended.

What you need: A high-frequency (6–13 MHz) linear probe. A 22G atraumatic

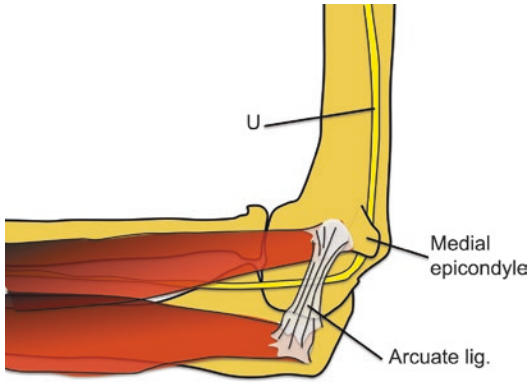

Fig. 5.20 Anatomic schema of ulnar nerve at the elbow. *U* ulnar nerve

echogenic needle, 50 mm of length. 5 mL of local anesthetic.

Sonoanatomy (Figs. 5.21 and 5.22)**:** In the arm you can see the ulnar nerve superficially, above the brachialis and the triceps muscles. In the forearm, the ulnar nerve is close to the ulnar artery.

How to do it (Figs. 5.21 and 5.22)**:** The transducer is placed perpendicular to the long axis of the arm to see the nerve in short axis. The needle is inserted in-plane.

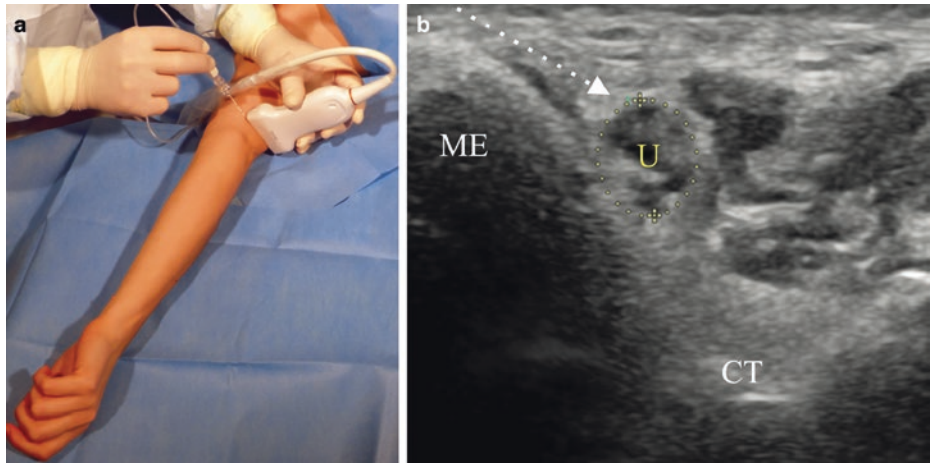

Fig. 5.21 (**a**) Patient position and needle entry point. (**b**) Sonoanatomy of ulnar nerve in cubital tunnel. *U* ulnar nerve (outlined), *ME* medial epicondyle, *CT* cubital tunnel, Long white arrow needle direction and target point

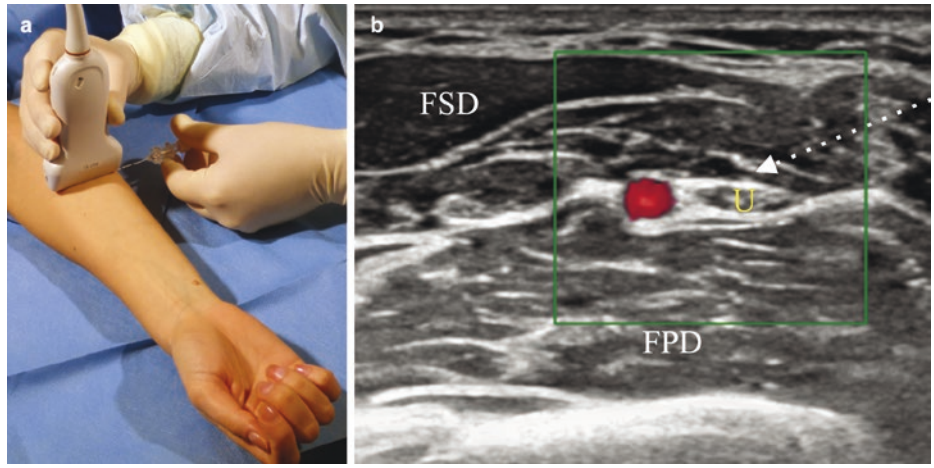

Fig. 5.22 (**a**) Patient position and needle entry point. (**b**) Sonoanatomy of ulnar nerve in distal arm. *U* ulnar nerve close to the ulnar artery, *FSD* flexor superficialis digitorum muscle, *FPD* flexor profundus digitorum muscle, Long white arrow needle direction and target point

For the forearm block, begin the scanning at the wrist and after go cephalic. The right site for the block is where the nerve runs from the artery.

Tips and tricks: As the ulnar nerve is close to the ulnar artery, use the power Doppler to detect it. Avoid to block at the wrist as the risk of arterial puncture or hematoma is higher. Both blockade of the ulnar nerve at the elbow (ulnar groove) is traditionally discouraged as the nerve is circumscribed by rigid structures (bones and ligaments) and there is the potential for entrapment.

5.12 Radial Nerve Block

Anatomy (Fig. 5.23)**:** The radial nerve can be located in the lateral aspect of the distal part of the arm, deep to the brachialis and brachioradialis muscles and superficial to the humerus. In the forearm, the radial nerve runs laterally to the radial artery.

Patient position: For the proximal block, the arm is adducted and the elbow is flexed 90°.

For the block at the forearm, the patient is positioned supine with the arm on the side abducted 90° with the elbow.

What you need: A high-frequency (6–13 MHz) linear probe. A 22G atraumatic echogenic needle, 50 mm of length. 5 mL of local anesthetic.

Sonoanatomy (Figs. 5.24 and 5.25)**:** In the arm the radial nerve with his honeycomb aspect is between the brachialis and brachioradialis muscles. In the forearm, the radial nerve is next to the radial artery.

How to do it: The transducer is placed perpendicular to the long axis of the arm to see the nerve in short axis. The needle is inserted in-plane.

For the forearm block begin the scanning at the wrist and after go cephalic. The right site for the block is where the nerve runs from the artery.

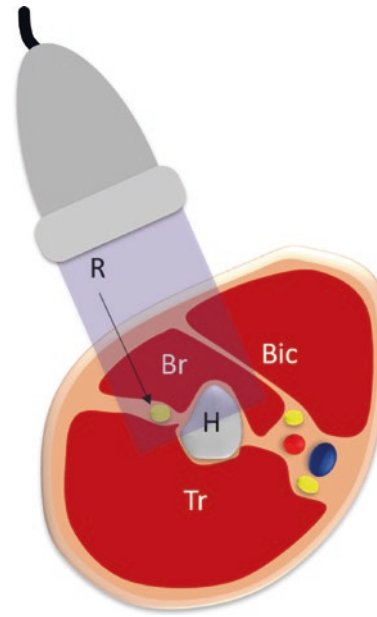

Fig. 5.23 Anatomic slice of distal arm. *Bic* biceps muscle, *Br* brachialis muscle, *H* humerus, *Tr* triceps muscle, *R with* black arrow radial nerve

Tips and tricks: As the nerve is always lateral to the artery, put yourself by the side of the nerve to block, in order to facilitate it and avoid arterial puncture.

Be careful to the warning signs of intraneural injection: paresthesia and/or high pressure of injection.

Complications: Arterial puncture and intraneural injection.

5.13 Thoracic Paravertebral Block

Anatomy (Figs. 5.26 and 5.27)**:** The paravertebral space (PVS) is a wedge-shaped area positioned between the heads and necks of the ribs. The anterolateral boundary is formed by the parietal pleura. The medial boundary is formed by the posterolateral aspect of the vertebral body, the intervertebral discs, the intervertebral foramen, the

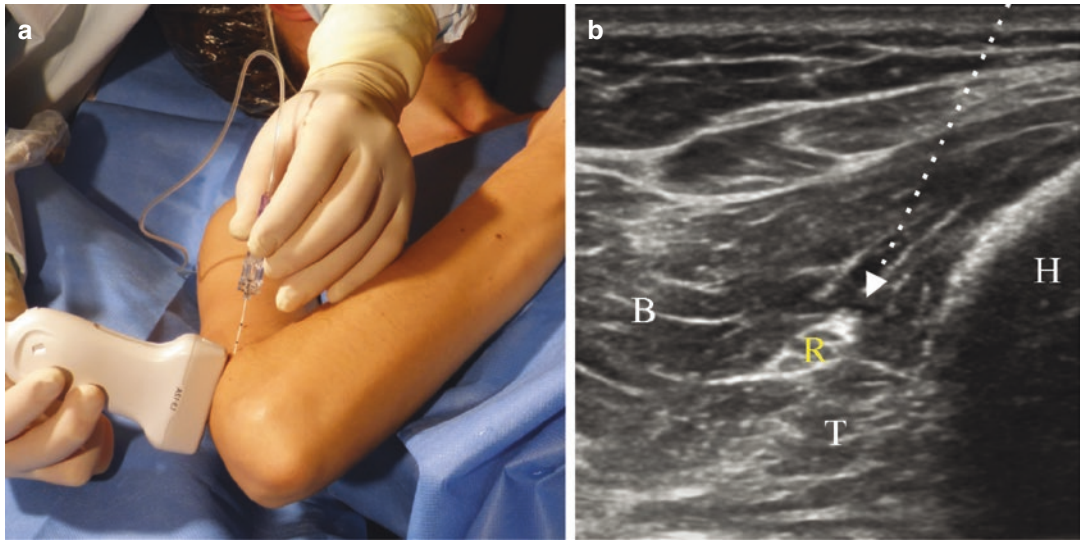

Fig. 5.24 (**a**) Patient position and needle entry point. (**b**) Sonoanatomy of radial nerve in distal arm. *R* radial nerve, *B* brachialis muscle, *T* triceps muscle, *H* humerus, long white arrow needle direction and target point

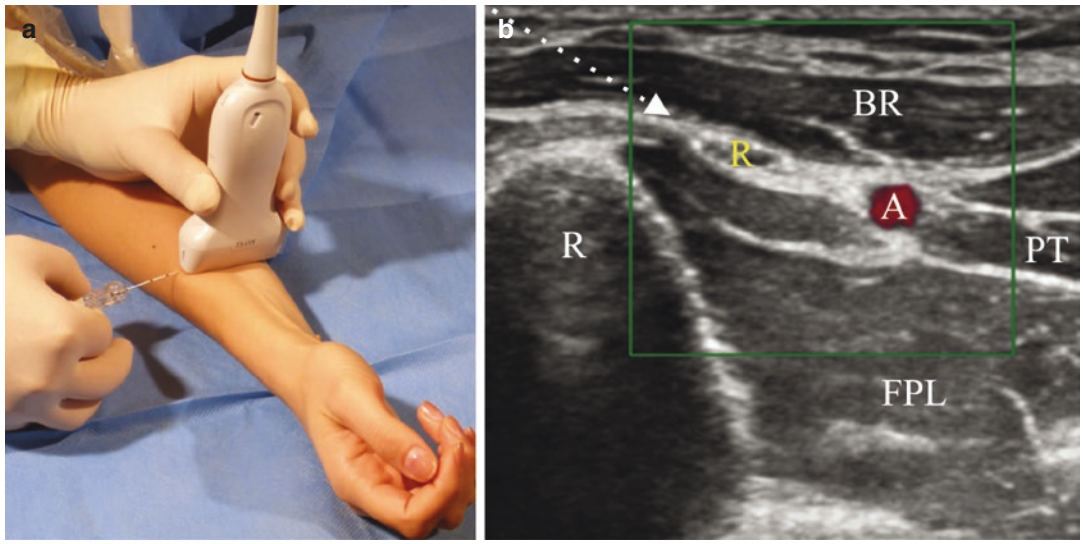

Fig. 5.25 (**a**) Patient position and needle entry point. (**b**) Sonoanatomy of radial nerve at forearm. *R* ulnar nerve close to the radial artery, *BR* brachioradialis muscle, *PT* pronator teres muscle, *FPL* flexor pollicis longus muscle, long white arrow needle direction and target point

spinal nerves, and connective tissue. The posterior boundary is formed by the superior costotransverse ligament which extends from the inferior aspect of each transverse process to the superior aspect of the rib below. The superior costotransverse ligament is continuous laterally with the internal intercostal membrane, which is the aponeurosis of the internal intercostal muscle and attaches medially to the upper and lower borders of the ribs.

Indications: Analgesia for unilateral surgical procedures or painful conditions of the thorax and abdomen.

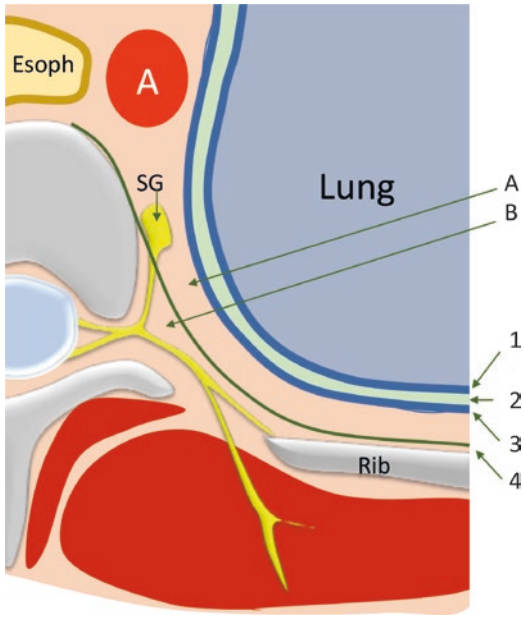

Fig. 5.26 Paravertebral space between the extrapleural (**a**) and the subendothoracic (**b**) spaces. *1* visceral pleura, *2* interpleural space, *3* parietal pleura, *4* endothoracic fascia. *SG* sympathetic ganglion, *A* aorta

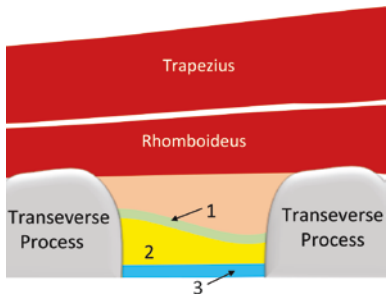

Fig. 5.27 Schematic representation of the ultrasound view of the paravertebral space in a paramedian longitudinal plane. *1* superior costotransverse ligament, *2* paravertebral space, *3* pleura

Patient position: Sitting position with neck and back flexed or prone position with a pillow under the thorax.

What you need: A high-frequency (10–15 MHz) linear probe and a 22G atraumatic echogenic needle, 50 mm of length. 10–20 mL of local anesthetic.

Sonoanatomy (Figs. 5.28 and 5.29)**:** The transverse processes and ribs are visualized as hyperechoic structures with acoustic shadowing below them. The PVS appears as a wedge-shaped hypoechoic layer demarcated by the hyperechoic reflections of the pleura below and the internal intercostal membrane above.

How to do it: There are two different approaches to the paravertebral space: the paramedian sagittal approach and the transverse one.

Paramedian sagittal approach (Fig. 5.28)**:** The probe is placed in a longitudinal paramedian plane between two transverse processes, 5–6 cm lateral to the midline. Both transverse processes should be visualized, with the superior costotransverse ligament and the pleura visible in between. The needle is inserted in-plane under direct visualization until it pierces the superior costotransverse ligament. When the needle tip is located immediately above the pleura, you can inject the local anesthetic. Look at the downward displacement of the pleura, indicating proper spread of the local anesthetic. The extent of local anesthetic spread should be evaluated by moving the ultrasound probe superiorly and inferiorly.

Transverse approach (Fig. 5.29)**:** The probe is placed in a transverse position and is moved superiorly and inferiorly to confirm the correct position. The transverse process is visualized medially with the pleura dipping under the inferolateral aspect. The needle is inserted in-plane until the PVS; inject local anesthetic, resulting in downward displacement of the pleura, indicating proper spread of the local anesthetic.

Tips and tricks: Inject slowly the local anesthetic avoiding forceful high-pressure injection to reduce the risk of bilateral epidural spread.

Complications: Unintentional injection in unwanted locations (pleura, neuraxial space) resulting in pneumothorax and spinal anesthesia.

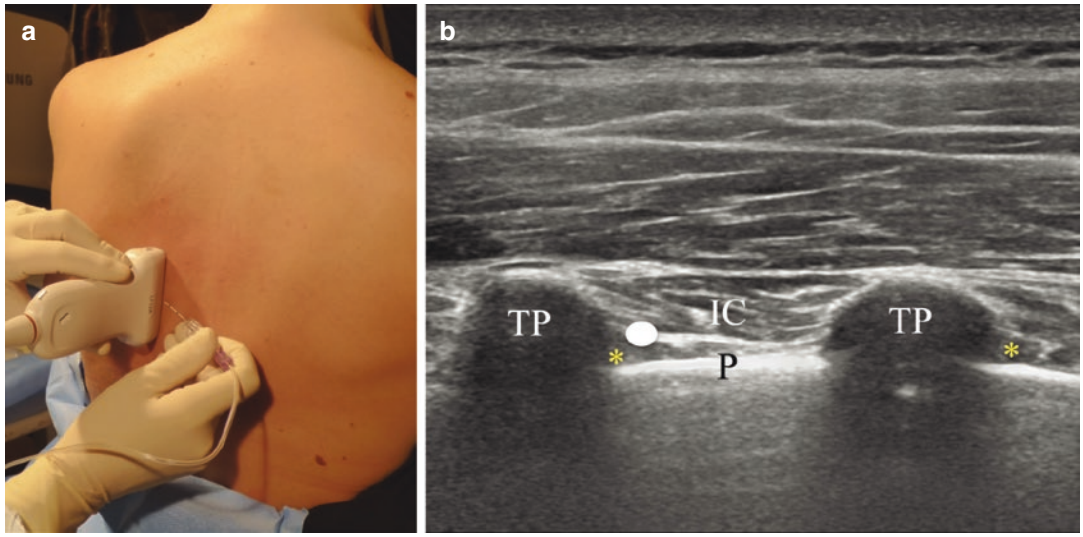

Fig. 5.28 (**a**) Patient position and needle entry point for paramedian sagittal approach. (**b**) Sonoanatomy. *TP* transverse process, *IC* intercostal muscles, *P* pleura, Yellow asterisk paravertebral space, White dot needle position in target point

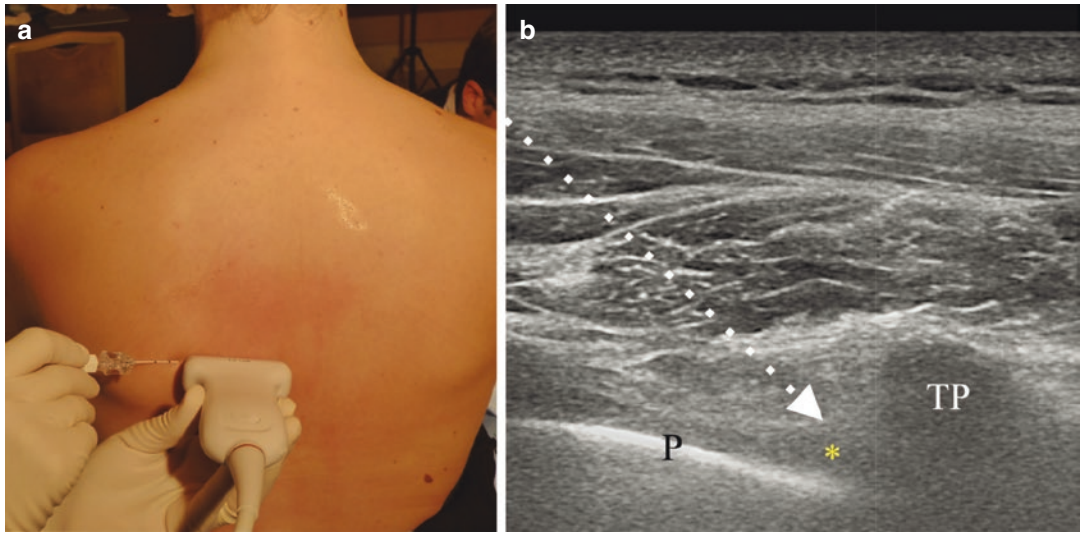

Fig. 5.29 (**a**) Patient position and needle entry point for transverse approach. (**b**) Sonoanatomy. *TP* transverse process, *P* pleura, Yellow asterisk paravertebral space, Long white arrow needle direction and target point

5.14 Transversus Abdominis Plane (TAP) Block

Anatomy (Fig. 5.30)**:** the anterior abdominal wall is innervated by the anterior rami of the lower thoracic nerves (T7–T12) and by the first lumbar nerve (L1). The terminal branches of these somatic nerves run in a neurovascular plane between the internal oblique and the transversus abdominis muscles. This plane is called transversus abdominis plane (TAP).

Indications: Postoperative analgesia for laparotomy, appendicectomy, abdominoplasty, open-prostatectomy, cesarean section, and laparoscopic

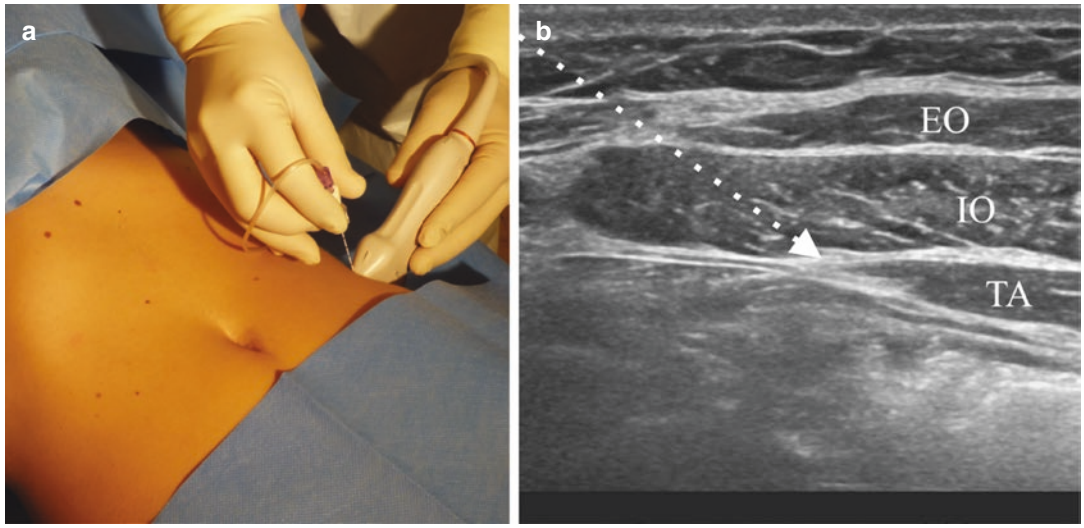

Fig. 5.30 (**a**) Patient position and needle entry point. (**b**) Sonoanatomy. *EO* external oblique muscle, *IO* internal oblique muscle, *TA* transverse abdominis muscle, *IH* iliohypogastric nerve, *II* ilioinguinal nerve, Long white arrow needle direction and target point

surgery; alternative technique to epidural anesthesia/analgesia for surgery on abdomen; chronic abdominal pain.

Patient position: Supine position.

What you need: High-frequency (10–15 MHz) linear probe, 50–100-mm and 20–21-gauge needle; two 20-mL syringes of local anesthetic.

Sonoanatomy (Fig. 5.30)**:** From the surface into the depth, the abdominal wall between the costal margin and the iliac crest is composed of these different layers: skin, subcutaneous tissue, and three muscle layers separated by hyperechoic fascia (external oblique, internal oblique, transversus abdominis), peritoneum, and abdominal cavity with bowel.

How to do it (Fig. 5.30): With the transducer transverse on the abdomen, at the anterior axillary line between the costal margin and the iliac crest, move slightly caudal or cephalic to identify the three muscle layers.

Once the TAP is identified, insert the needle with the in-plane approach from medial to lateral. A "pop" may be felt when the needle tip enters the plane between two muscles. When the TAP is reached, after gentle aspiration, inject a small amount of LA to verify the position of the tip. Not infrequently, the LA will spread *within*, rather then *between* muscle bellies; when this happens, the needle should be advanced or withdrawn and a test injection performed again. When dissection of the correct plane by injectate is achieved (Fig. 4), 15–20 mL of LA (different concentration, depending on the indication) can then be administered, with frequent aspirations. The goal is to visualize the LA spread between the transversus abdominis and the internal oblique muscle plane.

Tips and tricks: Usually the appropriate depth of the ultrasound field is about 3–4 cm. In obese patients the exact identification of TAP can be challenging. In these cases remember that the internal oblique muscle is always the thickest, while the transversus abdominis the thinnest. During the LA injection, scan the abdomen caudal and cephalic to determine the extent of longitudinal spread. Make sure the transversus muscle and the underlying peritoneum and bowel are clearly identified at the bottom of the image**.** If prolonged analgesia is needed, consider the insertion of a catheter.

Complications: LA toxicity, intravascular injection, nerve wound, block failure, hepatic puncture, bowel wound, hematoma, and transient paralysis of femoral nerve.

5.15 Rectus Sheath Block

Anatomy (Fig. 5.31)**:** Innervation of the anterolateral abdominal wall arises from the anterior rami of spinal nerves from T7 to L1. They are located in the plane between the internal oblique and the transversus abdominis muscles. Thoracic nerves (T7–T11) pierce the posterior wall of the rectus sheath as anterior cutaneous branches, and they provide sensory innervation to the rectus muscle and the overlying skin. In particular, nerves T7–T9 supply the skin superior to the umbilicus, T10 the umbilicus, and T11 the skin inferior to the umbilicus.

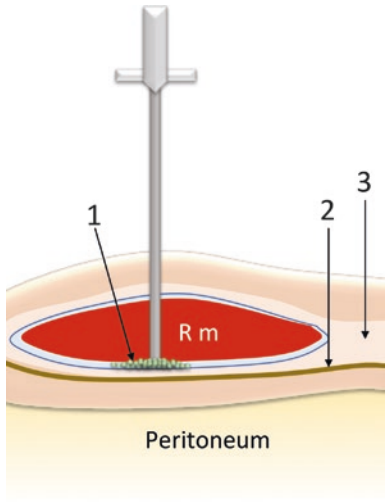

Fig. 5.31 Anatomy of rectus muscle (Rm). *1* Site of local anesthetic injection, *2* fascia transversalis, *3* linea alba

Indication: Postoperative analgesia for umbilical hernia repair and other umbilical surgery, analgesia for the middle anterior wall from xiphoid process to the symphysis pubis.

Patient position: Supine position.

What you need: High-frequency (10–15 MHz) linear probe, 50–100-mm 22-gauge needle; local anesthetic 15–30 mL.

Sonoanatomy (Fig. 5.32)**:** The rectus abdominis muscle is an oval-shaped structure under the superficial fascia of the abdomen. The muscle is surrounded by an aponeurotic sheath which splits into two layers, which merge near the midline and conjoin with the contralateral fascia to form the linea alba. Color Doppler imaging may reveal small epigastric arteries deep in the muscle belly. More deeply, one can see pre-peritoneal fat, the peritoneum, and bowel.

How to do it (Fig. 5.32)**:** Put the transducer transverse on abdomen lateral to the umbilicus;

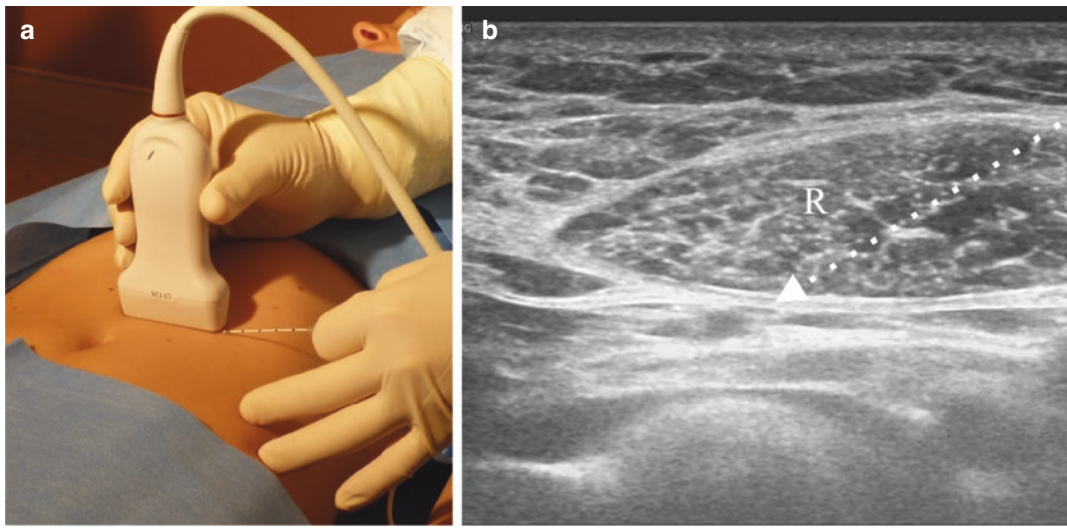

Fig. 5.32 (**a**) Patient position and needle entry point. (**b**) Sonoanatomy. *R*: rectus muscle, Long white arrow needle direction and target point

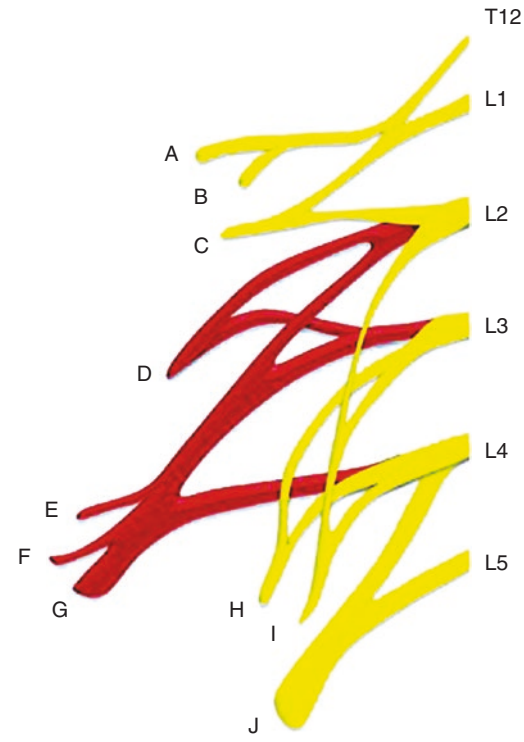

Fig. 5.33 Simplified schema of lumbar plexus anatomy (posterior nerves red painted). *A* iliohypogastric nerve, *B* ilioinguinal nerve, *C* genitofemoral nerve, *D* lateral femoral cutaneous nerve, *E* and *F* branches for psoas and iliacus muscles, *G* femoral nerve, *H* accessory obturator nerve, *I* obturator nerve, *J* lumbosacral trunk

insert the needle with an in-plane approach with lateral to medial direction. Advance the needle until the posterior rectus sheath. Inject first a small amount of LA to confirm the right position of the tip. Then inject the total dose of AL (about 10–20 mL per side in adults). The goal is to visualize an adequate LA spread between rectus muscle and posterior rectus sheath.

Complications: Rare. Bleeding, infection, LA systemic toxicity, intravascular injection, rectus sheath hematoma, peritoneal and bowel perforation.

Tips and tricks: Use color Doppler to avoid the puncture of epigastric arteries.

If prolonged analgesia is needed, consider the insertion of a catheter.

5.16 Lumbar Plexus Block

The lumbar plexus (LP) consists of a group of six nerves that supply the lower abdomen and lower leg. Combined with a sciatic nerve block, the lumbar plexus block can provide complete analgesia to the lower extremity. The complete lumbar plexus can be blocked from a posterior approach (also known as the psoas compartment block), and with other new ultrasound-guided approaches.

Anatomy (Fig. 5.33)**:** The lumbar plexus is formed from the ventral rami of L1–L4 with variable contributions from T12 and L5 (Fig. 1). The peripheral branches of the lumbar plexus include the iliohypogastric, ilioinguinal, genitofemoral, lateral femoral cutaneous, femoral, and obturator nerves. The plexus forms within the body of the psoas muscle.

Indications: Anesthesia or analgesia for lower limb surgery, enclosed hip surgery, in association with proximal sciatic block.

What you need: A low-frequency (6–8 MHz) convex probe and a 22G atraumatic echogenic needle, 100 mm of length. 20–30 mL of local anesthetic.

Sonoanatomy (Figs. 5.34 and 5.35)**:** The transverse processes are closely related to the plexus and therefore are used as the main landmark during LPB. A scan for the LPB can be performed in the transverse or longitudinal axis. The ultrasound transducer is positioned 3–4 cm lateral to the lumbar spine for either orientation.

Using a transverse oblique view, you can see lumbar plexus root just below the lamina and above the vertebral body. Quadratus lumborum muscle and psoas major muscle are lateral to the root.

Using a longitudinal view the acoustic shadow of the transverse processes has a characteristic appearance called the "trident sign." Lumbar plexus roots look like linear hyperechoic structures between the transverse processes above the psoas muscle.

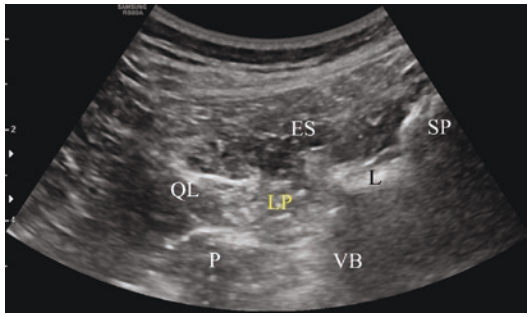

Fig. 5.34 Ultrasound anatomy of the lumbar paravertebral space using transverse oblique view. *ES* erectors spinae muscle, *QL* quadratus lumborum muscle, *P* psoas major muscle, *LP* lumbar plexus, *VB* vertebral body, *L* lamina, *SP* spinal process

Patient position: The patient is placed in the lateral decubitus position with the operative side up.

How to do it: Lumbar plexus block can be done using different techniques. We suggest two methods.

Karmakar's approach (Fig. 5.35)**:** Put the transducer longitudinally on the lumbar paravertebral region, and scan gradually from caudal to cephalad in order to find the transverse processes and the "trident sign." Insert the needle out-of-plane.

The goal of the technique is to guide the needle between the transverse processes (between the "teeth of the trident") of L3–L4 or L2–L3 into the posterior part of the psoas major muscle containing the roots of the lumbar plexus. Use nerve stimulation to confirm the correct position (ipsilateral quadriceps muscle contractions) before the injection of the anesthetic solution.

Shamrock's method (Fig. 5.36)**:** Another method of ultrasound-guided lumbar plexus block is scanning the patient's flank, immediately cranial to the iliac crest, in a transverse plane and inserting the needle 4–5 cm later to the midline

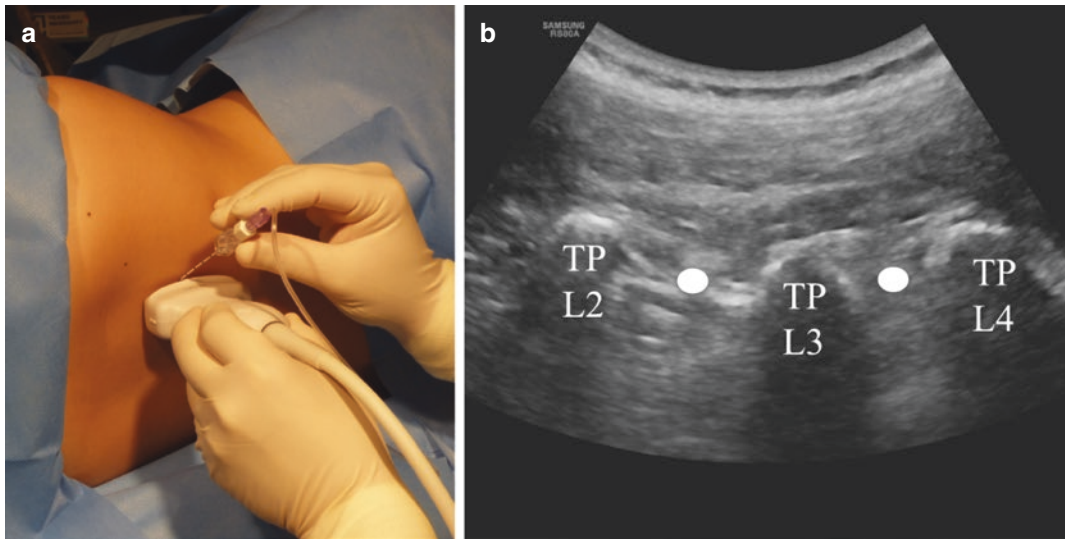

Fig. 5.35 Patient position (**a**) and sonoanatomy (**b**) in Karmakar's approach. The tip of the needle (white dots) is between the "teeth of the trident." *TP* transverse process

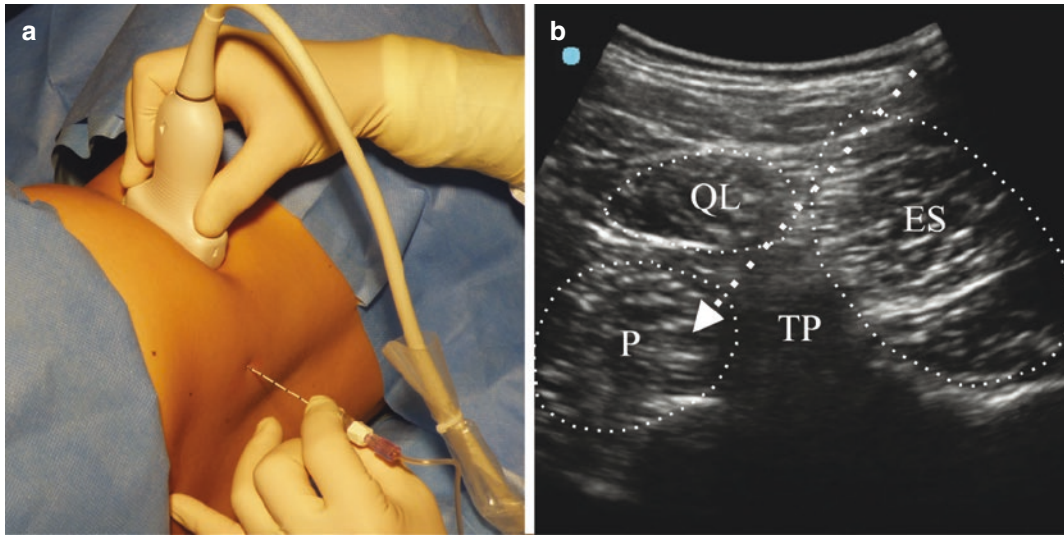

Fig. 5.36 Patient position (**a**) and sonoanatomy (**b**) in Shamrock's method. *P* psoas muscle, *ES* erector spinae muscle, *QL* quadratus lumborum muscle, *TP* transverse process, *L4* represents the pattern of a shamrock with three leaves. The nerve (arrowed in target point) is found in the medial and posterior part of the psoas muscle. Long white arrow needle direction and target point

in-plane and perpendicular to the ultrasound beam. In this way the anatomical structures surrounding the lumbar plexus give a recognizable ultrasonographic pattern like a shamrock with three leaves. Hyperechoic round oval structures representing the nerves of the lumbar plexus are found in the medial and posterior part of the psoas muscle, typically within a distance of two centimeters from the transverse process. The needle tip can be visualized clearly and positioned precisely beside the target nerves. Nerve stimulation with ipsilateral quadriceps muscle contractions can confirm it.

Tips and Tricks: Dual guidance with neurostimulator is recommended because at such deep location nerve roots can be indistinguishable from tendons or muscle septa, in a longitudinal view.

Local anesthetic must be administered in fractionated doses of 5 mL every minute to identify LA toxicity phenomena.

Complications: Unintentional epidural or spinal anesthesia, retroperitoneal hematoma, and renal injury are the rare complications of lumbar plexus block.

5.17 Iliohypogastric and Ilioinguinal Nerve Block

Anatomy (Fig. 5.37)**:** Ilioinguinal (ILIN) and iliohypogastric (ILHN) nerves both emanate from the first lumbar spinal root. As they emerge from the lateral border of the psoas major, they pass obliquely across the quadratus lumborum and iliacus and finally perforate the transverse muscle above the iliac crest. The ILHN lies medial to the ILIN. The ILHN pierces the internal oblique muscle distributing filaments to it and lies between the external and internal oblique muscles. It descends medially and caudally accompanying the spermatic cord through the subcutaneous inguinal ring. The ILHN supplies the skin over the inguinal region. The ILIN runs anteroinferiorly to the superficial inguinal ring, where it emerges to

supply the skin on the superomedial aspect of the thigh.

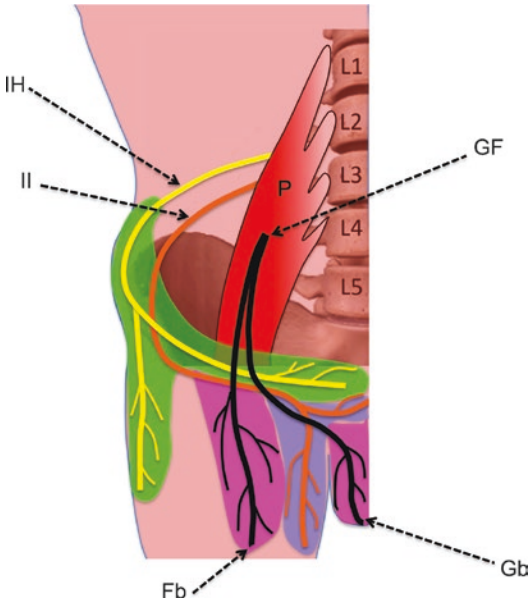

Fig. 5.37 The anatomy of iliohypogastric (IH) and ilioinguinal (II) nerves. *GF* genitofemoral nerve, *Gb* genital branch, *Fb* femoral branch, *P* psoas muscle

Indications: Anesthesia for any somatic procedure involving the lower abdominal wall/inguinal region such as inguinal herniorrhaphy and for analgesia after surgical procedures using a Pfannenstiel incision. These blocks do not provide visceral anesthesia.

Patient position: Supine.

What you need: A high-frequency (10–15 MHz) linear probe, 50–80-mm and 20–21-gauge needle, 20-mL syringe, sterile gloves, disinfectant, local anesthetic 5–10 mL.

Sonoanatomy (Fig. 5.38)**:** The anterior superior iliac spine (ASIS) is the standard starting position from which the transducer should be slowly moved along the ASIS-umbilicus line. The adult ILIN can be visualized between the internal oblique and transverse or external oblique muscles and within 1–3 cm from the ASIS. The ILHN lies immediately adjacent or somewhat medial to it**.**

How to do it (Fig. 5.38)**:** Put the probe perpendicular to the inguinal ligament so that the lateral aspect of the probe lies on top of the iliac crest. The ASIS is the standard starting position from which the transducer was moved slowly

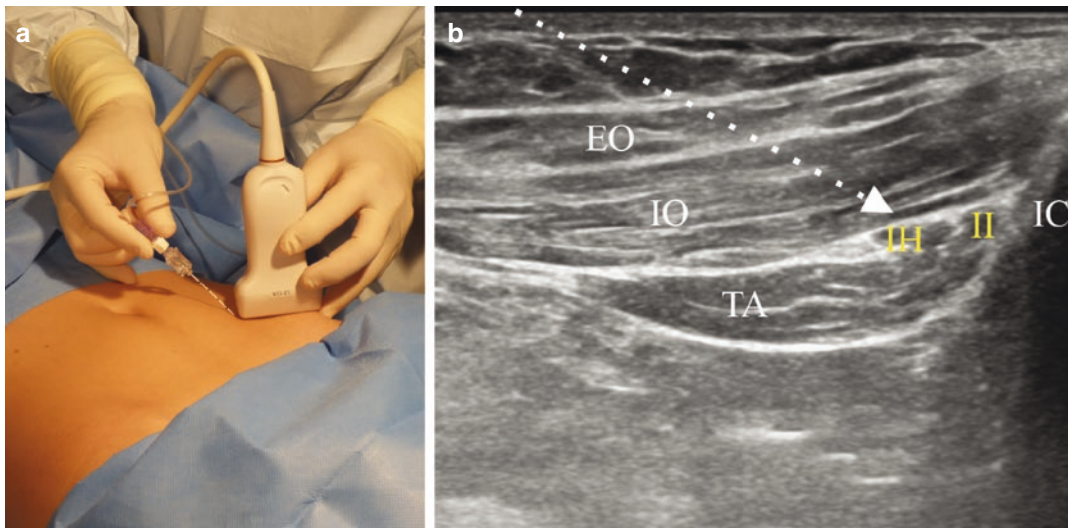

Fig. 5.38 (**a**) Patient position and needle entry point. (**b**) Sonoanatomy. *EO* external oblique muscle, *IO* internal oblique muscle, *TA* transverse abdominis muscle *IH* iliohypogastric nerve, *II* ilioinguinal nerve IC Iliac Crest. Long white arrow needle direction and target point

along the ASIS-umbilicus line. Ilioinguinal and iliohypogastric nerves are sought in the fascial plane between the external oblique and internal oblique and between internal oblique and transverse abdominis muscle. The ilioinguinal nerve is usually found close to the iliac crest, and the iliohypogastric nerve lies medial to it.

Complications: Perforation of both the small and large bowels and creation of a pelvic hematoma have been reported after ilioinguinal/iliohypogastric blocks without ultrasound guide.

5.18 Lateral Femoral Cutaneous Nerve Block

Anatomy (Fig. 5.39)**:** The lateral femoral cutaneous nerve (LFCN), arises from the dorsal divisions of L2–L3. After emerging from the lateral border of the psoas major muscle, it courses inferiorly and laterally toward the anterior superior iliac spine (ASIS). The nerve passes under the inguinal ligament and over the sartorius muscle into the thigh, where it divides into two branches (anterior and posterior).

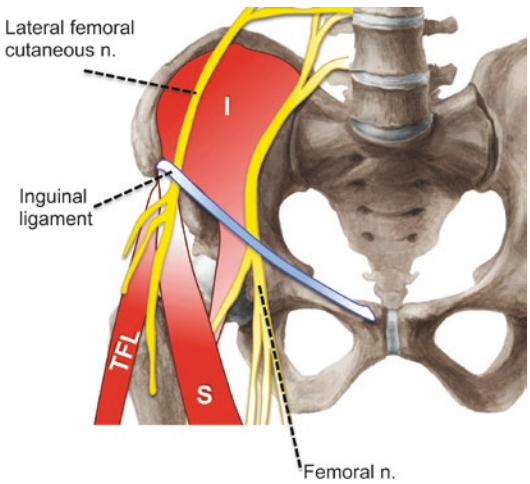

Fig. 5.39 Anatomy of the lateral femoral cutaneous nerve. *I* iliacus muscle, *S* sartorius muscle, *TFL* tensor fasciae latae muscle

Indications: LCFN provides sensory innervation of the lateral thigh. Anesthesia of this nerve is useful for head neck surgery in older people. It is also used in the management of meralgia paresthetica caused by the entrapment of the nerve. The ultrasound-guided techniques showed a higher success rate because of a high variability in the course of the nerve.

Patient position: Supine position with the leg in a neutral position.

What you need: A high-frequency (10–15 MHz) linear probe and a reflective atraumatic 22G ultrasound needle, 50 mm of length. 4–5 mL of local anesthetic.

Sonoanatomy (Fig. 5.40)**:** The LFCN is identified as a hypoechoic structure generally founded in the interfascial plane above the sartorius muscle medially and the tensor fascia lata muscle laterally. It looks like an "eye" with a hyperechoic circle inside of an almond-shaped structure.

How to do it (Fig. 5.41)**:** We suggest to identify the ASIS and then move the linear probe

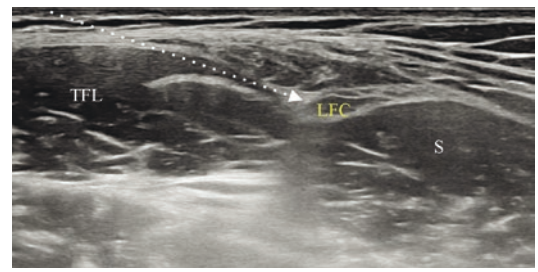

Fig. 5.40 Sonoanatomy. *S* sartorius muscle, *TLF* tensor fascia lata, *LFC* lateral femoral cutaneous nerve, Long white arrow needle direction and target point

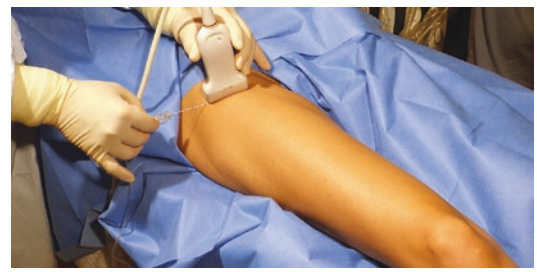

Fig. 5.41 Patient position and needle entry point

medially and inferiorly to locate the fascia lata and the sartorius muscle. Look for the "eye sign" above the sartorius muscle. Insert the needle in-plane. The injection should be done below the fascia lata.

Tips and tricks: Insert the needle with a shallow angle to reach the plane just below the fascia lata immediately medial and inferior to the ASIS.

Complications: Intraneural or intravascular injection.

5.19 Femoral Nerve Block

Anatomy (Fig. 5.42)**:** The femoral nerve is the largest branch of the lumbar plexus, arising from the second, third, and fourth lumbar nerves. The femoral nerve passes underneath the inguinal ligament into the thigh. As it passes beneath the inguinal ligament, the nerve is positioned lateral and slightly deeper than the femoral artery between the psoas and iliac muscles.

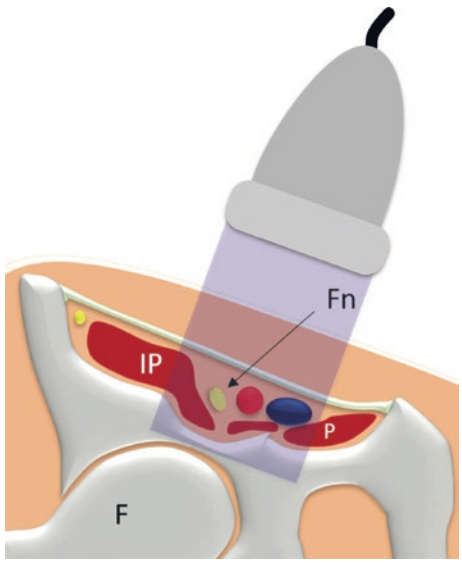

Fig. 5.42 A trans-sectional view of the thigh showing the adductor canal. *IP* biceps muscle, *P* brachialis muscle, *F* femur, *Fn with* black arrow femoral nerve close to femoral artery and vein

Indications: Anesthesia and analgesia for anterior thigh, femur, and knee surgery.

Patient position: The patient is in supine position with the leg slightly externally rotated.

What you need: A high-frequency (10–15 MHz) linear probe and a reflective atraumatic 22G ultrasound needle. 10–20 mL of local anesthetic.

Sonoanatomy (Fig. 5.43)**:** The nerve lies about 1–2 cm lateral to the artery, positioned below fascia iliaca and lata and above the iliopsoas muscle and is contained within a triangular-shaped sheath of fascia by the ligamentum iliopectineus. The nerve itself can have a triangular or oval shape and is often not clearly visualized. Because of this, the triangle created by the femoral artery medially, fascial planes anteriorly, and the iliopsoas muscle posteriorly is used as the target for the block. The nerve becomes visualized after injection.

How to do it (Fig. 5.43): The probe is placed in the inguinal crease, parallel to the inguinal ligament and transverse to femoral vein and artery with the indicator toward the patient's right. The probe is slid medial to lateral until the femoral vessels are seen. Insert the needle in-plane (Fig. 3) until the needle tip is witnessed adjacent (either above, below, or lateral) to the nerve; after inject the anesthetic solution.

Tips and tricks: To confirm the proper needle placement, inject 1–2 mL of local anesthetic. When injection of the local anesthetic does not appear to result in a spread close to the femoral nerve, additional needle repositions and injections may be necessary.

Complications: Intraneural or intravascular injection.

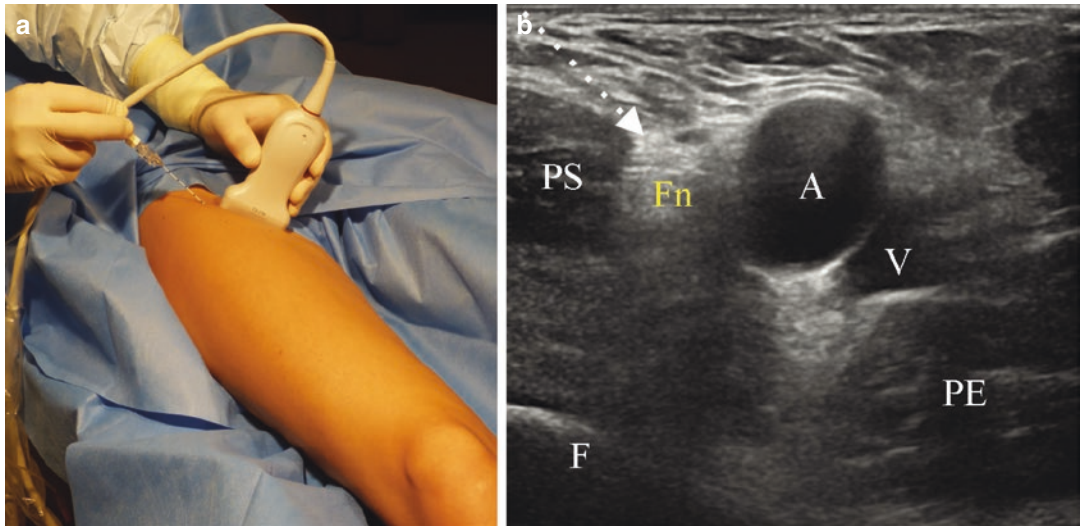

Fig. 5.43 (**a**) Patient position and needle entry point. (**b**) Sonoanatomy of the inguinal area. *Fn* femoral nerve, *PS* iliopsoas muscle, *PE* pectineus muscle, *A* femoral artery, *V* femoral vein, *F* femur

5.20 Saphenous Nerve Block

Anatomy (Fig. 5.44): The saphenous nerve is the largest cutaneous branch of the femoral nerve. The saphenous nerve often lies anterior to the femoral artery as this vessel passes beneath the sartorius muscle and posterior to the aponeurotic covering of the adductor canal. It descends along the medial side of the knee posterior to the sartorius muscle. It is a sensory nerve covering the medial aspect of the calf, ankle, foot, and great toe.

Indications: Anesthesia and analgesia of anterior aspect of the knee and leg.

Patient Position: Supine position with the leg externally rotated (frog position).

What you need: a high-frequency (10–15 MHz) linear probe and a reflective atraumatic 22G ultrasound needle. 5–10 mL of local anesthetic.

Sonoanatomy (Fig. 5.45)**:** The adductor canal in the lower half of the thigh is covered by the sartorial muscle in its descent laterally to medially across the anterior thigh. The sides of the triangular canal are formed by the vastus medialis laterally and adductor longus or magnus medially. The femoral artery passes beneath the muscle. The saphenous nerve is infrequently seen on the ultrasound image; however, sometimes it is visualized as a small round hyperechoic structure medial to the artery. A femoral vein accompanies the artery and saphenous nerve, which are all typically visualized at 2–3 cm depth.

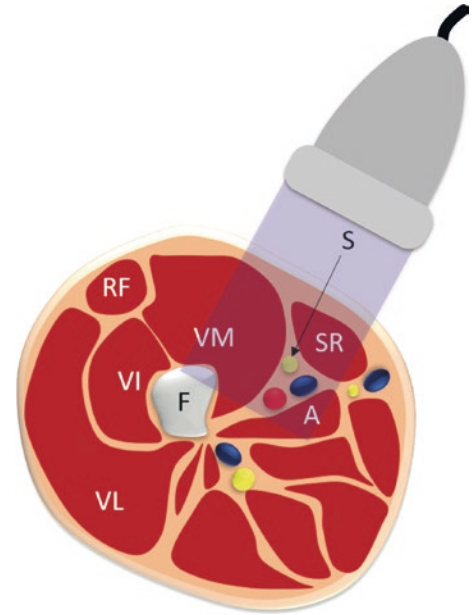

Fig. 5.44 A trans-sectional view of the thigh showing the adductor canal. *RF* rectus femoris muscle, *VL* vastus lateralis muscle, *VI* vastus intermedius muscle, *VM* vastus medialis muscle, *SR* sartorius muscle, *A* adductor longus muscle, *S with* black arrow saphenous nerve

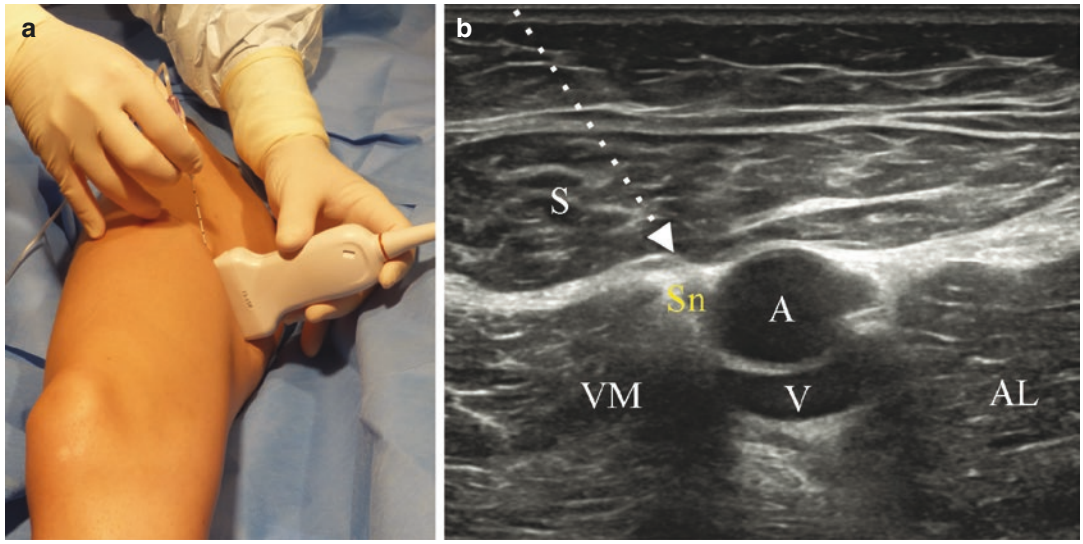

Fig. 5.45 (**a**) Patient position and needle entry point. (**b**) Sonoanatomy of the adductor canal. *S* sartorius muscle, *VM* vastus medialis muscle, *AL* adductor longus muscle, *Sn* saphenous nerve, *A* femoral artery, *V* femoral vein, Long white arrow needle direction and target point

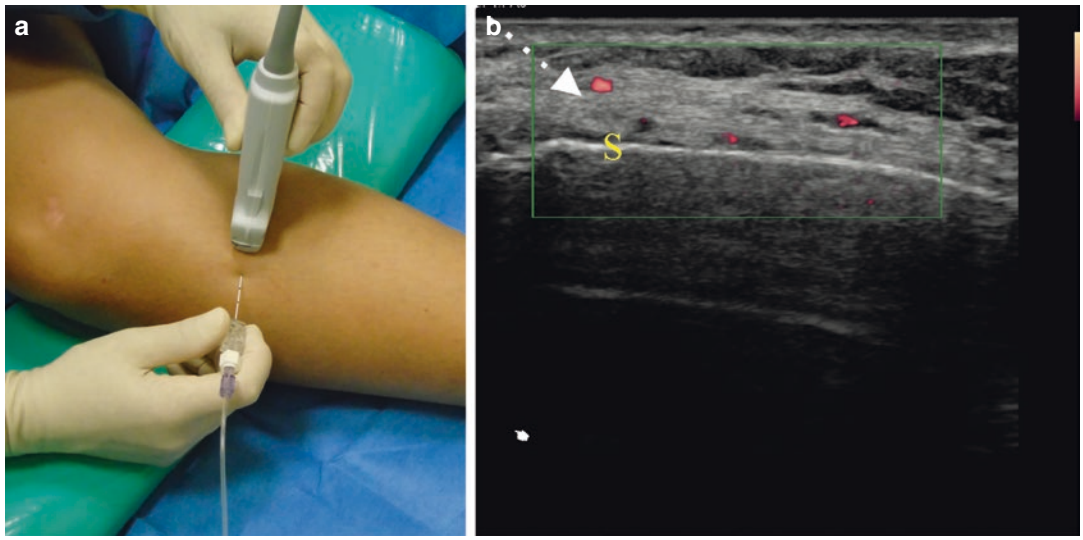

Fig. 5.46 (**a**) Patient position and needle entry point. (**b**) Sonoanatomy of a transverse section at tibial level. *S*: saphenous nerve, Long white arrow needle direction and target point

How to do it— block at the adductor canal (Fig. 5.45)**:** Put the probe transverse to the longitudinal axis and scan the medial aspect of the thigh. Identify the femoral artery, the sartorius muscle, and the saphenous nerve below it. Insert the needle in-plane. The aim is to insert the needle deep to the sartorius and depositing the local anesthetic medial to the artery.

Block at tibial level (Fig. 5.46): Put the probe in a transverse plane at the level of tibial tuberosity; insert the needle in-plane. Here the nerve pierces the fascia lata between the sartorius and the gracilis

tendons and joins the saphenous vein. The aim is to insert the needle near the saphenous vein.

Tips and tricks: Visualization of the nerve, at the abductor canal, is not necessary for this block. Administration of 5–10 mL of local anesthetic next to the artery should suffice without confirming the nerve position.

Also at the tibial level the saphenous nerve is difficult to visualize, but the block is easily performed with an ultrasound-guided perivenous injection of local anesthetic.

Complications: Intraneural or intravascular injection.

5.21 Obturator Nerve Block

Anatomy (Fig. 5.47)**:** The obturator nerve arises from the anterior rami of the second, third, and fourth lumbar nerves. The obturator nerve then runs along the lateral wall of the lesser pelvis and extends to the anterior thigh after passing through the obturator canal. During its course, the obturator nerve divides into anterior and posterior branches that run between the pectineus and obturator externus muscles.

Indications: Analgesia/anesthesia of the medial aspect of thigh and knee. Relief of painful adductor muscle contractions or to prevent adduction of thigh during transurethral bladder surgery.

Patient position: The patient is in supine position. The thigh is slightly abducted and laterally rotated.

What you need: A high-frequency (10–15 MHz) linear probe and a reflective atraumatic 22G ultrasound needle. 3–5 mL of local anesthetic for each branch.

Sonoanatomy (Fig. 5.48)**:** The two branches of the obturator nerve appear as hyperechoic lip-shaped structures contained in the fascia of adductor muscles. The anterior branch of the obturator nerve lies in a fascial layer between the pectineus, adductor longus, and adductor brevis muscles. The posterior branch lies between the adductor brevis and the adductor magnus muscles. Often the anterior and the posterior branches

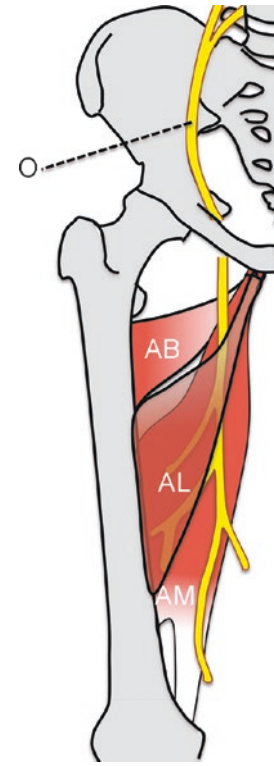

Fig. 5.47 Schema of obturator nerve anatomy *AB* Adductor brevis, *AL* Adductor longus, *AM* Adductor magnus

of the obturator nerve are not visible like hyperechoic structures, and only the fascial planes can be distinguished.

How to do it (Fig. 5.48)**.** Put the probe horizontal, 1–3 cm inferior to the inguinal crease on the medial aspect (adductor compartment) of the thigh. Identify the three adductor muscles (pectineus, adductor longus, and brevis); insert the needle in-plane to reach the fascial plane and the anterior branch between pectineus and adductor

Tips and tricks: A low-current nerve stimulation that elicits adductor muscle contraction can be used to aid localization of the obturator nerve.

When the obturator nerve branches are not visible, perform the block just putting the anesthetic solution into the appropriate interfascial planes.

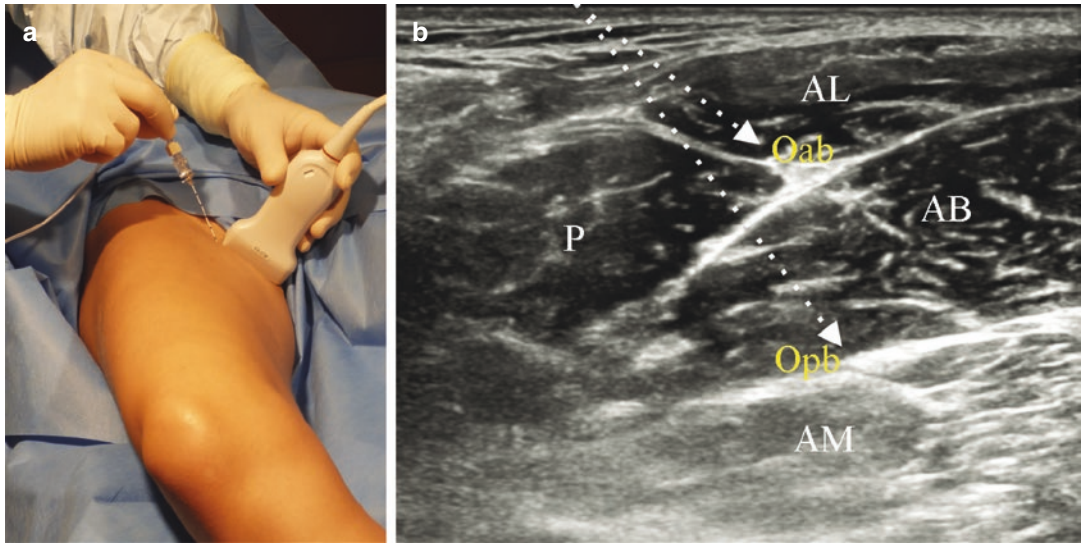

Fig. 5.48 (**a**) Patient position and needle entry point. (**b**) Sonoanatomy of medial aspect of upper thigh showing adductor longus *AL*, brevis *AB*, and magnus muscles *AM* in a transverse view *P* pettineus, *OAB* Obturator anterior branch, *OPB* Obturtor Posterior branch. Long white arrows needle direction and target points

longus and the posterior one between adductor longus and magnus.

Complications: Intraneural and intravascular injection.

5.22 Sciatic Nerve Block

Anatomy (Fig. 5.49)**:** The sciatic nerve is the largest nerve in the human body, originating from the lumbosacral plexus (L4–5 and S1–3) and providing sensory and motor innervation to the lower extremity.

The sciatic nerve exits the pelvis via the greater sciatic foramen below the piriformis muscle. In the gluteal region, the sciatic nerve courses between muscle layers. The sciatic nerve anterior (deep) to the gluteus maximus muscle is found just lateral to the origin of the biceps femoris muscle at the ischial tuberosity.

The sciatic nerve lies medial to the greater trochanter.

In the subgluteal region, the sciatic nerve is more accessible for the block, even in obese patients, because it is more superficial than in the gluteal region and it lies within a palpable groove in this location.

Indications: With femoral nerve block for knee and lower limb surgery and foot surgery.

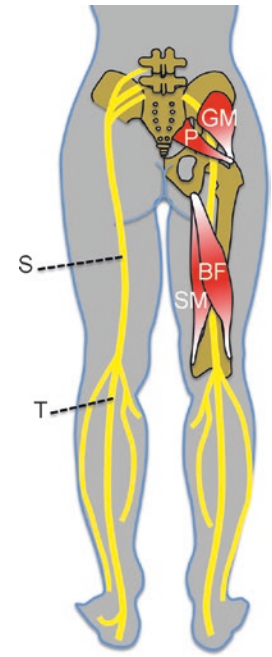

Fig. 5.49 Schema of sciatic nerve anatomy *S* sciatic nerve, *T* tibial nerve, *GM* gluteus maximus muscle, *P* piriformis muscle, *BF* Biceps femoris muscle, *SM* semitendinosus muscle

Patient position: The patient is in a position between the lateral decubitus and prone position (Sim's position). The leg to be blocked is up, with the hip and knee flexed.

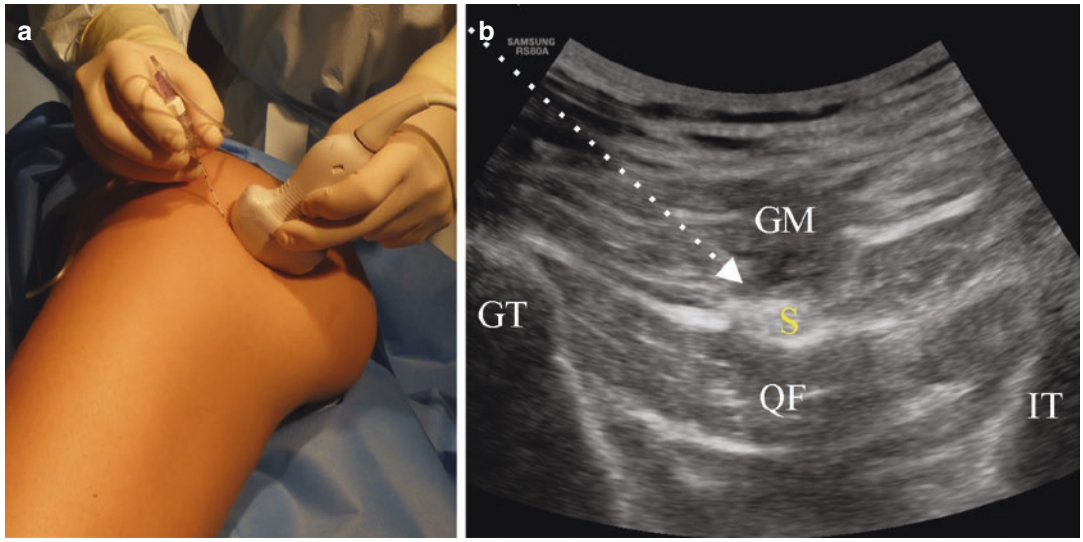

Fig. 5.50 (**a**) Patient position and needle entry point. (**b**) Sonoanatomy. *S* sciatic nerve, *GT* greater trochanter, *GM* gluteus maximus muscle, *QF* quadratus femoris muscle, *IT* ischial tuberosity, *Long white arrow* needle direction and target point

What you need: A low-frequency (4–6 MHz) convex probe and a reflective atraumatic 22G ultrasound needle. 15–20 mL of local anesthetic.

Sonoanatomy (Fig. 5.50)**:** In the subgluteal region, the sciatic nerve usually appears as a wedge-shaped hyperechoic structure between the two hyperechoic bony prominences of the ischial tuberosity and the greater trochanter of the femur. The sciatic nerve is located immediately deep to the gluteus muscles, superficial to the quadratus femoris muscle.

How to do it (Fig. 5.50)**:** For the subgluteal approach, place the probe over the subgluteal region in a transverse plane.

Move the probe from lateral (great trochanter area) to medial (ischial tuberosity) until the sciatic nerve is visible in a sling between the two hyperechoic bony shadows. Insert the needle in-plane. The angle of approach of the needle is often close to perpendicular to the skin.

This makes visualization of the entire needle shaft using the in-plane approach more difficult.

Performing this block with nerve stimulation guidance is very helpful to identify the sciatic nerve when it is not clearly visible. The goal is to see circumferential spread of hypoechoic local anesthetic solution around the nerve.

Tips and tricks: It is often easier to identify the sciatic nerve from its surrounding structures by decreasing the gain on the US machine.

As imaging of the needle tip can be problematic for the deep location, its position is often inferred by injections of small volumes of saline solution, local anesthetic, or air.

Never inject against high resistance to injection (>15 psi) because this may signal an intraneural injection.

Complications: Intraneural injection is the more feasible. Intravascular injection is more unlikely for the lack of adjacent vascular structures.

5.23 Popliteus Nerve Block

Anatomy (Fig. 5.51)**:** Sciatic nerve, after emerging from the pelvis, travels deep in the posterior thigh. Proximal to the popliteal fossa, the sciatic nerve lies more superficial, between the long head of the biceps femoris laterally and the semimembranosus muscles medially. In this location, the nerve generally bifurcates into the common peroneal and tibial nerves. These nerves continue into the popliteal fossa where they lie superficial and lateral to the popliteal vessels. The tibial nerve provides innervation to the majority of the posterior lower extremity, knee joint, and plantar surface of the foot. The common peroneal nerve provides sensory innervation to the dorsal lateral foot and ankle and posterolateral portion of the distal lower extremity via its branches.

Indications: Anesthesia and analgesia of ankle and foot with saphenous nerve block.

Patient position: Prone position with a roller pillow under the ankle.

What you need: A high-frequency (10–15 MHz) linear probe and a reflective atraumatic 22G ultrasound needle. 15–20 mL of local anesthetic.

Sonoanatomy (Fig. 5.52)**:** In the popliteal fossa, at the popliteal crease, the femur is identified as characteristic hyperechoic stripe and dense posterior shadowing; the pulsatile popliteal artery and corresponding vein are located superficial and medial to the femur. At this level, the

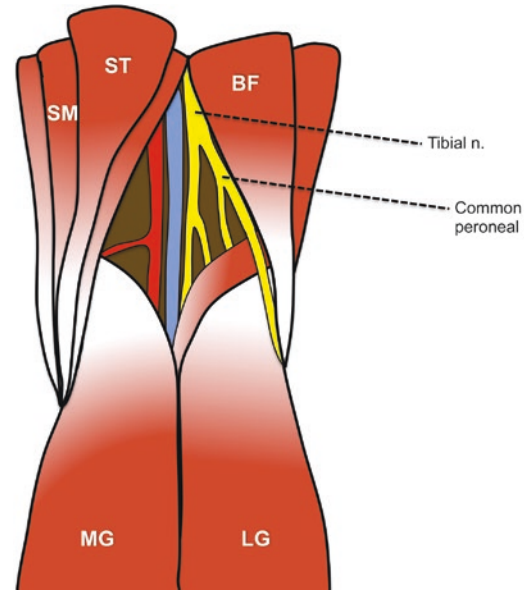

Fig. 5.51 Schema of popliteal fossa anatomy BF Biceps femoris muscle, *ST* Semitendinosus muscle, *SM* semimembranosus muscle, *LG* Gastrocnemius lateral head, *MG* Gastrocnemius medial head

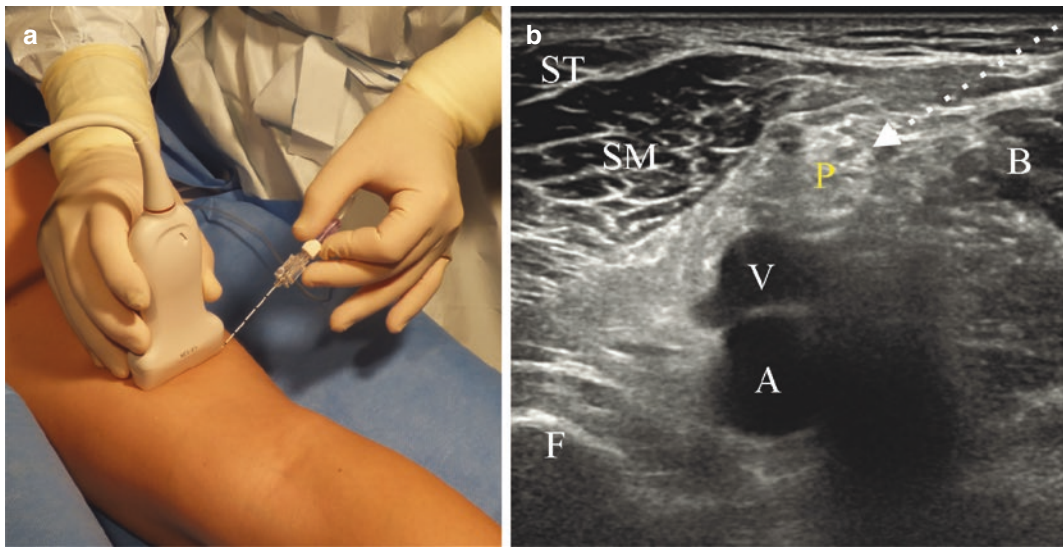

Fig. 5.52 (**a**) Patient position and needle entry point. (**b**) Sonoanatomy in a transverse section of popliteal region showing popliteal nerve, vein, and artery. *F* femur, *ST* semitendonosus muscle, *SM* semimembranosus muscle. Long white arrow needle direction and target point

sciatic nerve has generally bifurcated into the tibial and common peroneal nerves. The tibial is found superficial and lateral to the artery. The common peroneal nerve is found lateral to the tibial nerve at a similar depth.

How to do it (Fig. 5.52)**:** The probe is placed transversely across the popliteal fossa at the popliteal crease. The needle is inserted in an in-plane approach from the side of the probe; it is advanced to the deep border of the sciatic nerve. The goal is to surround the nerve(s) with local anesthetic.

Tips and tricks: If nerve visualization is difficult, ask the patient to plantar flex and dorsiflex the foot. This will cause the "see-saw" sign: tibial and peroneal components move during foot movement.

If blocking the tibial and common peroneal nerves after the bifurcation, the nerve farther from the needle entry site is blocked before blocking the closer one.

Complications: Intraneural or intravascular injection.

5.24 Ankle Block

Anatomy (Fig. 5.53)**:** Five nerves provide sensory innervation to the foot at or below the level of the ankle. These are posterior tibial, sural, deep, and superficial peroneal nerves (terminal branches of sciatic nerve) and saphenous nerve (branch from the femoral nerve).

Indications: Acute pain management in trauma as ankle block results in anesthesia of the entire foot. Foot surgery without the need of tourniquet and for postoperative pain relief as it causes no motor blockade of the foot.

Patient position: Supine position with a footrest underneath the calf facilitates access to the ankle, especially for the tibial and sural nerve blocks.

What you need: A small (25 mm) high-frequency (10–15 MHz) linear probe or a hockey probe and a 22–25-gauge ultrasound needle, 4–5 cm of length. 3–5 cc of local anesthetic for each nerve.

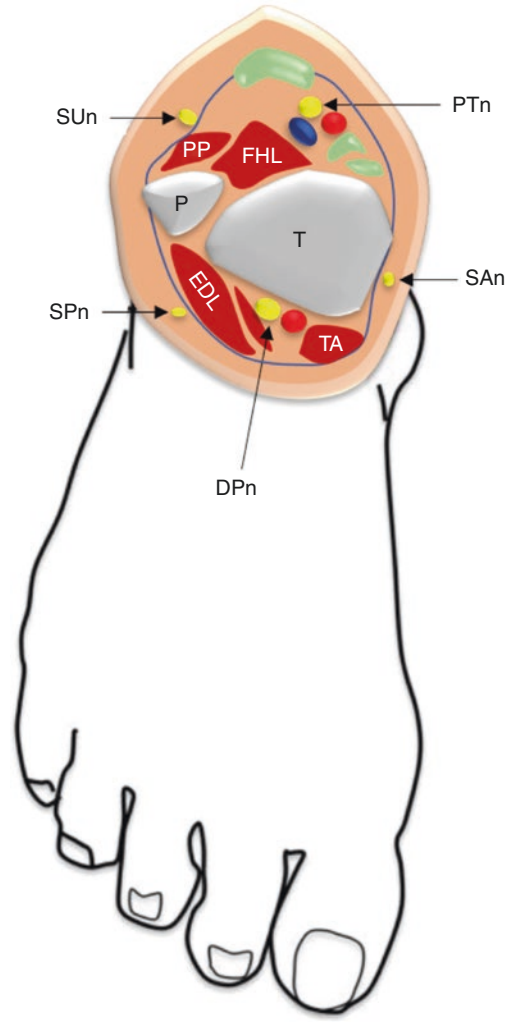

Fig. 5.53 Schema of ankle nerves anatomy *PTn* posterior tibial nerve, *SAn* saphenous nerve, *DPn* deep peroneal nerve, *SPn* superficial peroneal nerve, *SUn* surak nerve. *T* tibia, *P* Fibula, *EDL* extensor digitorum longus muscle, *TA* tibial anterior muscle, *FHL* flexor hallucis longus, *PP* peroneus muscles

Sonoanatomy: Tibial nerve passes posterior to the medial malleolus and posterior to the posterior tibial artery at the ankle (Fig. 5.54). A transducer placed in the transverse orientation at the level of the extensor retinaculum will show the deep peroneal nerve lying immediately lateral to the artery, on the surface of the tibia (Fig. 5.55). A transducer placed transversely on the leg,

approximately 5 cm proximal and anterior to the lateral malleolus, will identify the superficial peroneal nerve lying in the subcutaneous tissue over the fascia (Fig. 5.56). Near to the lateral malleolus, the sural nerve can be visualized as a small hyperechoic structure that is intimately associated with the small saphenous vein (Fig. 5.57). The saphenous nerve is a small nerve; it is best visualized 10–15 cm proximal to the medial malleolus, using the saphenous vein as a landmark (Fig. 5.58).

How to do it. For all blocks put the probe in a transverse plane. Insert the needle in-plane or out-of-plane.

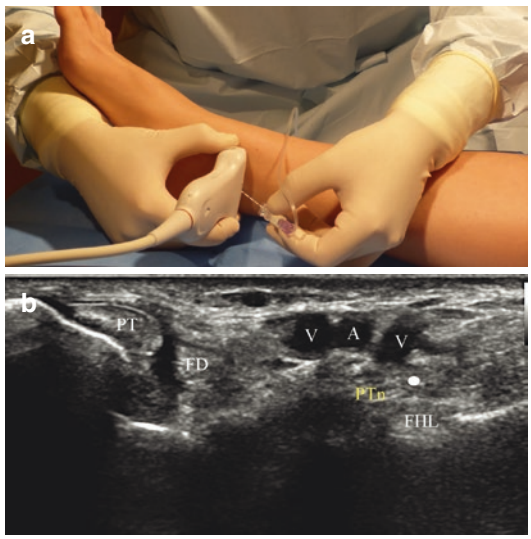

Fig. 5.54 (**a**) Patient position and needle entry point. (**b**) Sonoanatomy of the tibial nerve at the ankle. *PTn* posterior tibial nerve, *A* tibial artery, *V* tibial vein, *FHL* flexor hallucis longus, White dot needle target point

Tips and tricks: The nerves at the ankle are so small that it is difficult to detect them. The simpler method is to look for the vessel.

Do not press the probe in order to not squeeze vessels.

Complications: Intraneural and intravascular injection.

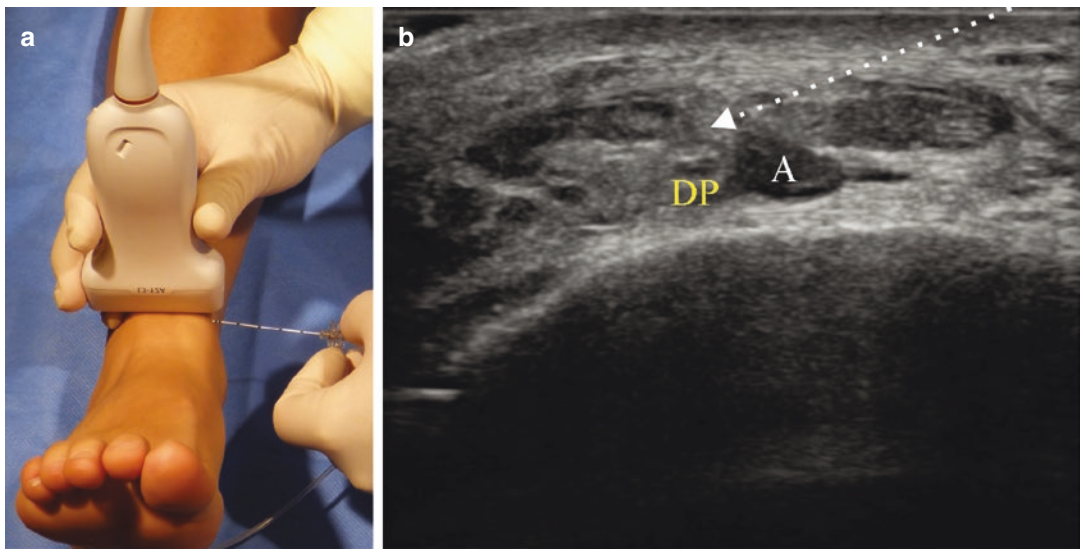

Fig. 5.55 (**a**) Patient position and needle entry point. (**b**) Sonoanatomy. *DP* deep peroneal nerve, *A* anterior tibial artery, Long white arrow needle direction and target point

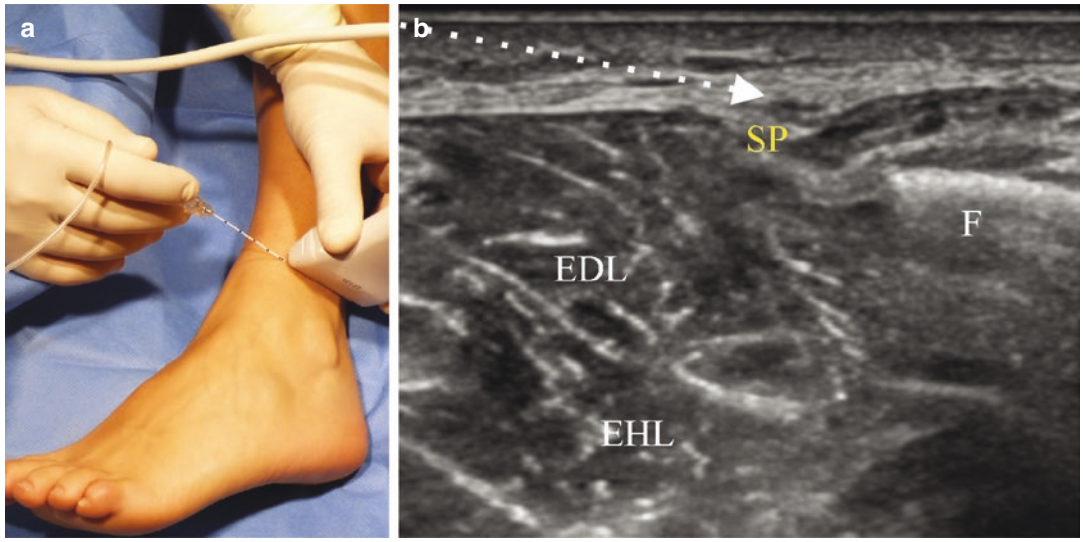

Fig. 5.56 (**a**) Patient position and needle entry point. (**b**) Sonoanatomy. *SP* superficial peroneal nerve, *F* fibula, *EDL* extensor digitorum longus muscle, *EHL* Extensor hallucis longus. Long white arrow needle direction and target point

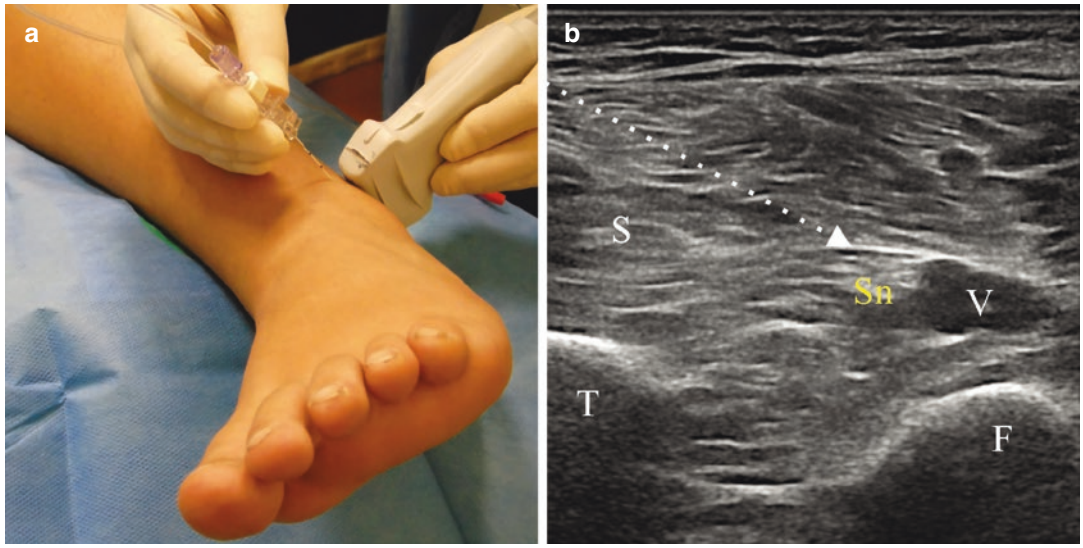

Fig. 5.57 (**a**) Patient position and needle entry point. (**b**) Sonoanatomy. *Sn* sural nerve, *V* small saphenous vein, *F* fibula, *T* tibia. Long white arrow needle direction and target point

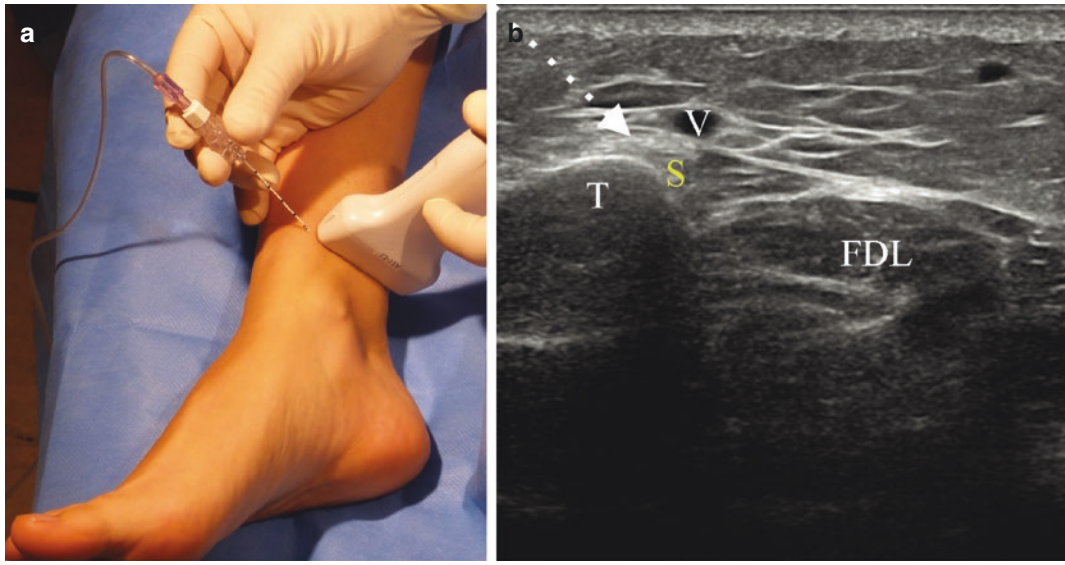

Fig. 5.58 (**a**) Patient position and needle entry point. (**b**) Sonoanatomy. *S* saphenous nerve, *V* saphenous vein, *T* tibia, *FDL* flexor digitorum longus. Long white arrow needle direction and target point

Suggested Readings

Beaudoin FL, Nagdev A, Merchant RC, Becker BM. Ultrasound-guided femoral nerve blocks in elderly patients with hip fractures. Am J Emerg Med. 2010;28(1):76–81.

Ben-Ari A, Moreno M, Chelly JE, Bigeleisen PE. Ultrasound-guided paravertebral block using an intercostal approach. Anesth Analg. 2009;109:1691–4.

Casati A, Baciarello M, Di Cianni S, Danelli G, De Marco G, Leone S, Rossi M, Fanelli G. Effects of ultrasound guidance on the minimal effective anaesthetic volume required to block the femoral nerve. Br J Anaesth. 2007;98:823–7.

Demirelli G, Baskan S, Karabeyoglu I, Aytac I, Ornek DH, Erdogmus A, Baydar M. Comparison of ultrasound and ultrasound plus nerve stimulator guidance axillary plexus block. J Pak Med Assoc. 2017;67(4):508–12.

Dufour E, Toussaint A, Liu N, Fischler M, Nourry G, Vercoutère M. Ultrasound-guided perineural circumferential median nerve block in carpal tunnel syndrome. Anaesthesia. 2013;68(4):434–6.

Falyar CR. Ultrasound-guided ankle blocks: a review of current practices. AANA J. 2015;83(5):357–64.

Franco CD, Williams JM. Ultrasound-guided interscalene block: reevaluation of the "stoplight" sign and clinical implications. Reg Anesth Pain Med. 2016;41(4):452–9.

Guirguis MN, Abd-Elsayed AA, Girgis G, Soliman LM. Ultrasound-guided transversus abdominis plane catheter for chronic abdominal pain. Pain Pract. 2013;13(3):235–8.

Gurnaney H, Ganesh A. Incidence and effects of unintentional intraneural injection during ultrasound-guided subgluteal sciatic nerve block. Reg Anesth Pain Med. 2013;38:72.

Hara K, Sakura S, Nomura T, Saito Y. Ultrasound guided thoracic paravertebral block in breast surgeries. Anesthesia. 2009;64:223–5.

Hara K, Sakura S, Shido A. Ultrasound-guided lateral femoral cutaneous nerve block: comparison of two techniques. Anaesth Intensive Care. 2011;39:69–72.

Henshaw DS, Kittner SL, Jaffe JD. Ultrasound-guided continuous superficial radial nerve block for complex regional pain syndrome. J Pain Palliat Care Pharmacother. 2016;30(2):118–23.

Herring AA, Stone MB. The accuracy of a handheld ultrasound machine in locating the sciatic nerve in the popliteal fossa. Reg Anesth Pain Med. 2004;29:413–6.

Herring AA, Stone MB, Fischer J, Frenkel O, Chiles K, Teismann N, Nagdev A. Ultrasound-guided distal popliteal sciatic nerve block for ED anesthesia. Am J Emerg Med. 2011;29(6):697.e3–5.

Honnannavar KA, Mudakanagoudar MS. Comparison between conventional and ultrasound-guided supraclavicular brachial plexus block in upper limb surgeries. Anesth Essays Res. 2017;11(2):467–71.

Ilfeld BM. Continuous peripheral nerve blocks: an update of the published evidence and comparison with novel, alternative analgesic modalities. Anesth Analg. 2017;124(1):308–35.

Jenstrup MT, et al. Effects of adductor-canal-blockade on pain and ambulation after total knee arthroplasty: a randomized study. ActaAnaesthesiol Scand. 2012;56(3):357–64.

Kim BG, Han JU, Song JH, Yang C, Lee BW, Baek JS. A comparison of ultrasound-guided interscalene and supraclavicular blocks for post-operative analgesia after shoulder surgery. Acta Anaesthesiol Scand. 2017;61(4):427–35.

Moritz T, Prosch H, Berzaczy D, Happak W, Lieba-Samal D, Bernathova M, Auff E, Bodner G. Common anatomical variation in patients with idiopathic meralgia paresthetica: a high resolution ultrasound case-control study. Pain Physician. 2013;16:E287–93.

Nwawka OK, Miller TT, Jawetz ST, Saboeiro GR. Ultrasound-guided perineural injection for nerve blockade: does a single-sided injection produce circumferential nerve coverage? J Clin Ultrasound. 2016;44(8):465–9.

O Riain SC, Donnell BO, Cuffe T, Harmon DC, Fraher JP, Shorten G. Thoracic paravertebral block using real-time ultrasound guidance. Anesth Analg. 2010;110:248–51.

Rahiri J, Tuhoe J, Svirskis D, Lightfoot NJ, Lirk PB, Hill AG. Systematic review of the systemic concentrations of local anaesthetic after transversus abdominis plane block and rectus sheath block. Br J Anaesth. 2017;118(4):517–26.

Redborg KE. Ultrasound improves the success rate of a tibial nerve block at the ankle. Reg Anesth Pain Med. 2009;34(3):256–60.

Shteynberg A, Riina LH, Glickman LT, Meringolo JN, Simpson RL. Ultrasound guided lateral femoral cutaneous nerve (LFCN) block: safe and simple anesthesia for harvesting skin grafts. Burns. 2013;39:146–9.

Strakowski JA. Ultrasound-guided peripheral nerve procedures. Phys Med Rehabil Clin N Am. 2016;27(3):687–715.

Tammam TF. Ultrasound-guided infragluteal sciatic nerve block: a comparison between four different techniques. Acta Anaesthesiol Scand. 2013;57:243–8.

Tumber PS, Bhatia A, Chan VW. Ultrasound-guided lateral femoral cutaneous nerve block for meralgia paresthetica. Anesth Analg. 2008;106:1021–2.

Turner AL, Stevenson MD, Cross KP. Impact of ultrasound-guided femoral nerve blocks in the pediatric emergency department. Pediatr Emerg Care. 2014;30(4):227–9.

Ueshima H, Otake H, Lin JA. Ultrasound-guided quadratus lumborum block: an updated review of anatomy and techniques. Biomed Res Int. 2017;2017:2752876.

Yoshida T, Nakamoto T, Kamibayashi T. Ultrasound-guided Obturator nerve block: a focused review on anatomy and updated techniques. Biomed Res Int. 2017;2017:7023750.

Index

E. Silvestri et al. (eds.), *Ultrasound-Guided Peripheral Nerve Blocks*,
https://doi.org/10.1007/978-3-319-71020-4